NASA CONTRACTOR REPORT

NASA CR-347

NASA CR-347

DEVELOPMENT OF THE DRY TAPE BATTERY CONCEPT

by Bernard A. Gruber, Joseph J. Byrne, Ralph Kafesjian, Kurt W. Klunder, Elizabeth A. McElhill, Wilson H. Power, Theodore J. Wolanski, and Louis I. Zirin

Prepared under Contract No. NAS 3-4168 *by*
MONSANTO RESEARCH CORPORATION
Everett, Mass.
for Lewis Research Center

NATIONAL AERONAUTICS AND SPACE ADMINISTRATION - WASHINGTON, D. C. - DECEMBER 1965

NASA CR-347

DEVELOPMENT OF THE DRY TAPE BATTERY CONCEPT

By Bernard A. Gruber, Joseph J. Byrne, Ralph Kafesjian, Kurt W. Klunder, Elizabeth A. McElhill, Wilson H. Power, Theodore J. Wolanski, and Louis I. Zirin

Prepared under Contract No. NAS 3-4168 by
MONSANTO RESEARCH CORPORATION
Everett, Mass.

for Lewis Research Center

NATIONAL AERONAUTICS AND SPACE ADMINISTRATION

For sale by the Clearinghouse for Federal Scientific and Technical Information
Springfield, Virginia 22151 – Price $6.00

FOREWORD

The research described herein was conducted at the Boston Laboratory of the Monsanto Research Corporation under contract to NASA and at the Southwest Research Institute under subcontract to Monsanto. This work was done under the technical management of William J. Nagle of the NASA Lewis Research Center.

ABSTRACT

Several new high energy couples were discharged efficiently at high voltages in a moving single-tape configuration. The constant potential and power output due to continuous supply of fresh reactants and removal of reaction products from the current collector zone were demonstrated.

Couples not suitable for conventional battery operation were discharged efficiently in the tape configuration. Magnesium was successfully discharged versus potassium periodate, organic nitro compounds (picric acid, m-dinitrobenzene) and organic N-chlorine compounds in both strong acid and neutral electrolyte.

Macroincapsulation of electrolytes in Kel-F 81 tubing was achieved with payloads greater than 80%. Microincapsulation of both aqueous and organic electrolytes was achieved with lower payloads.

A lightweight demonstration conversion unit was designed and constructed.

TABLE OF CONTENTS

SUMMARY

A. OBJECTIVES

The primary objective of this contract was to incorporate previously unused high energy electrochemical couples into a single tape configuration, deliver the available energy in an efficient and practical manner, and demonstrate those features of a dry tape battery system that distinguish it from conventional battery configurations.

B. STATUS

1. A magnesium-potassium periodate cell (Mg/2M $AlCl_3$, 1M HCl/KIO_4) was discharged at high rate (65-75% at 450 ma/in.^{2}) and cell voltage (1.95 to 2.00 v) in a moving tape configuration. The moving tape consisted of anode, cathode and separator with electrolyte being fed from a continuous segmented tube to a point just ahead of the cathode current collectors. Power densities of 1 watt/in.^{2} of collector area were attained at slightly lower efficiencies.

2. Magnesium was successfully used as an anode material in strong acid electrolyte (e.g., 2M $AlCl_3$, 1M HCl). Anode corrosion was relatively light and gassing did not interfere with cell operation. Organic nitro compounds (picric acid, dinitrobenzene), which had not been previously discharged successfully at high current densities, were discharged (50-60%, 1.0-1.2 v vs. Mg) at current densities of 500 ma/in. using a combination of acid electrolyte and thin tape configuration.

3. The constant potential and power output due to continuous supply of fresh reactants and removal of reaction products from the current collector zone were demonstrated.

4. Of the couples investigated, potassium periodate was the most suitable depolarizer found for tape configuration studies. Energy densities, determined experimentally from dynamic tests, for the potassium periodate-magnesium couple in acid electrolyte were 50-75 watt-hours per pound of complete tape and electrolyte weight. Single cell tests gave energy densities of 80-90 watt-hr/lb. Using the technology acquired here, the incorporation of more energetic couples has begun. Organic N-halogen compounds (trichlorotriazinetrione and hexachloro-melamine), which have energy capacities substantially higher than the periodate system, have been successfully discharged vs magnesium in aqueous electrolyte in a tape

configuration. In addition, work on a lithium tape anode has begun.

5. Methods for delivering dry tape energy in a weight optimized device were developed. A continuous manufacturing process for cathode tape preparation involving metering cathode mix onto nylon separator tape and compressing between steel rolls has been developed. Cathode tapes made with this equipment have suitable physical uniformity and adherence for use in the tape device. Rolled and perforated magnesium ribbon and macroincapsulated electrolyte were combined with the potassium periodate cathode tape and separator to make the complete dry tape battery.

6. A permanent magnet 4-vdc gear motor was selected for driving the 12- to 16-watt demonstration unit. The unit will drive four tapes connected in series to provide 8 v at a current of 1.5 to 2 amp using the magnesium-potassium periodate system. The device will provide speed variation from 0.1 to 0.25 in./min and will weigh about 2.4 lb with capacity for approximately 75 feet of tape. The power requirement for parasitic drive is approximately 0.3 watt or 2 to 3% of the power output.

7. Macroincapsulation of electrolytes in Kel-F 81 tubing was achieved with payloads greater than 80%. Measured loss rates were about 1% per year at ambient conditions. Permeability coefficients (2.4×10^{-4} g-mm/24 hr-m^2-cm Hg) agree reasonably well with literature values. An activation energy of about 12 kcal/mole was found for the permeation process. This value allows estimation of loss rates over a temperature range.

8. Microincapsulation studies, subcontracted to the Southwest Research Institute, have shown that aqueous solutions can be contained in capsules about 1000 microns in diameter, but the loss rate of water is high (0.3 to 4.0%/day), and initial payloads range from 40 to 75%. Two nonaqueous electrolyte solvents have also been incapsulated.

INTRODUCTION

A. OBJECTIVES

The particular objectives of this program were to develop (1) methods of utilizing high energy anodes and cathodes on tapes and to combine these couples onto a single tape, (2) methods of electrolyte incapsulation and tape activation, (3) a weight-optimized tape energy conversion device capable of unattended operation by start-stop parasitic power, and (4) methods of supplying multiple cell voltages from the dry tape system.

B. DRY TAPE CONCEPT

A "dry tape" battery uses a thin separator tape with dry anode and cathode coatings of the active components of a battery system and incapsulated electrolyte. This tape can be fed continuously or intermittently to a set of current collectors after releasing the electrolyte to wet the separator and electrodes. Electrolyte is released by crushing microcapsules between rolls or by slitting macrocapsules just prior to discharging a section of the tape.

In addition to having extended shelf life, a dry tape device can be designed to minimize some of the common limitations of conventional batteries such as reactant depletion and reaction product build-up during discharge as well as separator deterioration. Because of the continuous supply of fresh reactants and the removal of reaction products from the current collector area, a constant potential and power output should be maintained. Relatively heavy separators are required by conventional batteries to prevent shorting and intercontamination of oxidant and reductant. Such separators usually limit the battery to low-rate applications. By using a compact electrode spacing with minimum separator thickness, the dry tape can be designed for high-rate discharges of the small activated section.

Since the duration of discharge of a specific tape section is only a few minutes, long-term parasitic deterioration is not a problem. The tape can use electrolyte-reactant combinations that have high energy potential but that cannot be used in conventional batteries because of self discharge that would consume the reactants during extended contact of electrodes and electrolyte.

Since the tape moves between permanent current collectors, the conventional grid supports for active materials are not required and the weight can be eliminated.

A summary of the features of the dry tape battery is given in Figure 1.

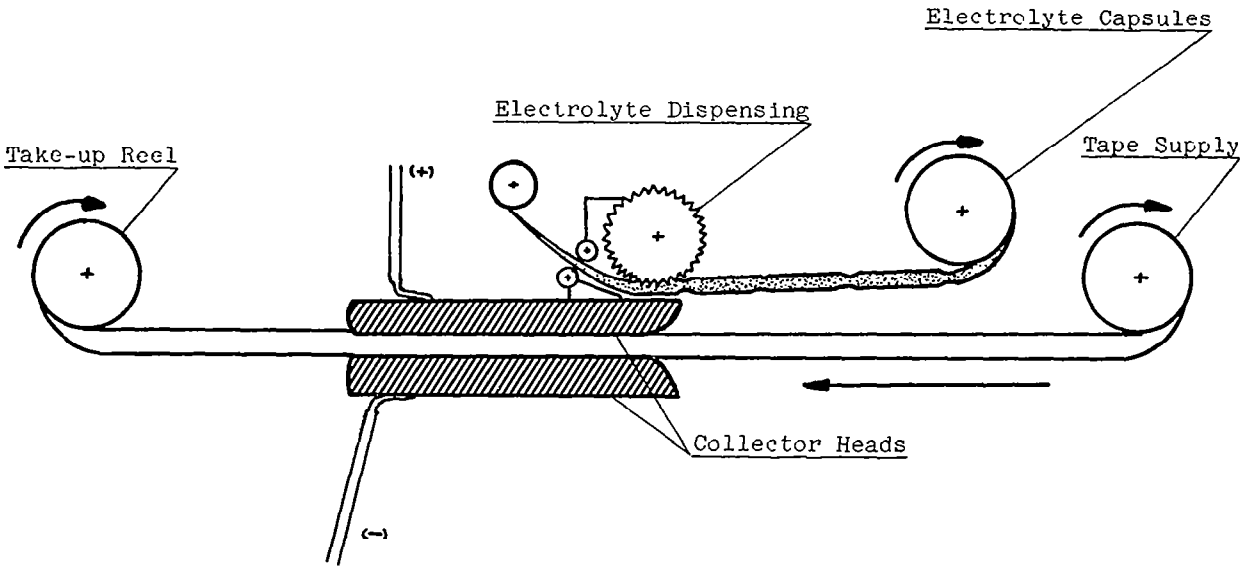

Design Attribute	Beneficial Effect	Resultant Advantage
Use of thin electrode structures	Minimized (electrolyte) concentration polarization	Higher watt-hr/lb
	Elimination of metallic grid support	
Continuous feed of anode and cathode	Continuous removal of discharged products	Low internal impedance maintained
	Continuous refreshment with unused active materials	Constant potential maintained
	Both of above	Separator shoring, if occurring, is only temporary problem
Continuous electrolyte wet-out only as required	Unused electrode sections remain dry	Reserve capability maintained even under stop-start conditions
	Use of incompatible couples	Higher watt-hr/lb
Adjustable motor drive speed	Control over feed rate of reactants	Programmed power or self adjustment through voltage monitor and feedback
Separation of active material from auxiliary components	Renewable tape reels for each unit	Logistic storage and transport advantage

Figure 1. Features of the Dry Tape Battery

C. PREVIOUS WORK

During our previous NASA contract (ref. 1), the feasibility of the dry tape battery concept was demonstrated using the silver peroxide/zinc system. Tapes coated with silver peroxide were discharged efficiently (85%) at high current density (1000 ma/in.^{2}) against a zinc block anode. Tape speed, electrolyte feed rate, and other operating parameters were investigated. Four spring-driven devices were constructed and used to demonstrate the dry tape concept. Discharge was accomplished by drawing the tape between current collectors, one of which also served as the zinc anode. Electrolyte was supplied by a second prewet tape that contacted the coated tape ahead of the current collectors. Current densities up to 850 ma/in.^{2} at tape speeds of 0.2 to 1.5 in./min and electrolyte feed rates of 0.15 to 0.3 ml/min were attained.

D. SCOPE OF THIS REPORT

A research program leading to the demonstration of a dry tape unit is described in this report. The fabrication and testing of anode and cathode materials, the effect of many electrolytes on current efficiencies, macro- and microincapsulation of electrolytes, electrolyte loss rates during storage, and methods of electrolyte release during tape operation are discussed. A process for continuously manufacturing tape electrodes is given. The fabrication of dry tape, incapsulated electrolyte packets, and a weight-optimized energy conversion device for the complete dry tape demonstration unit are described. Results of a brief investigation of a nonaqueous system are discussed.

PHASE 1. SINGLE COMPONENT CONFIGURATION DEVELOPMENT

A. HIGH ENERGY ANODE DEVELOPMENT

1. Background

The objective of the electrode component research portion of the overall dry tape battery program was the development of high energy density couples that could be discharged efficiently at high current drains (0.5 to 1.0 amp/in.^{2}) in a practical tape configuration. Magnesium (2.2 amp-hr/g), aluminum (2.98 amp-hr/g), and lithium (3.86 amp-hr/g) were the prime anode candidates because of their potentially high energy density. None of these has been used to any significant extent in conventional battery systems primarily because of compatibility problems leading to electrode corrosion and unsatisfactory shelf life. However, the dry tape electrodes, which are discharged soon after the initial electrode-electrolyte contact, are not dissipated by minor spontaneous reactions with the electrolyte.

To achieve the objective of a working electrode system within the contract period, work on the better characterized magnesium- and aluminum-aqueous electrolyte systems rather than the less well known lithium-nonaqueous electrolyte systems was emphasized. Attention could be concentrated on electrode design and operating technique development; such technology was applicable to any future electrode system. The ability to use couples considered unsuitable for conventional batteries would be demonstrated. In addition, effort duplication with existing lithium anode research programs would be avoided.

Recent developments now make examination of lithium as a tape anode more desirable. A limited research program was initiated. Preliminary results are reported in Section II-D dealing solely with nonaqueous systems.

2. Method

Three anode configurations were studied: (1) solid block or foil; (2) pressed porous powder; and (3) flame-sprayed films on tape backing. Commercial solid stock was used, and the flame sprayed tapes were made by a local vendor. The pressed porous powder electrodes were prepared using a die mold as illustrated in Figure 2.

Table 1 summarizes the various sheet forms of magnesium. For the preliminary configuration studies 20-mil primary and alloyed (AZ31B) magnesium and 1-mil aluminum foil were used. The flame-sprayed stock included magnesium, and aluminum on nylon, dynel fabric and polypropylene. The pressed powder (20-100 mesh) anodes

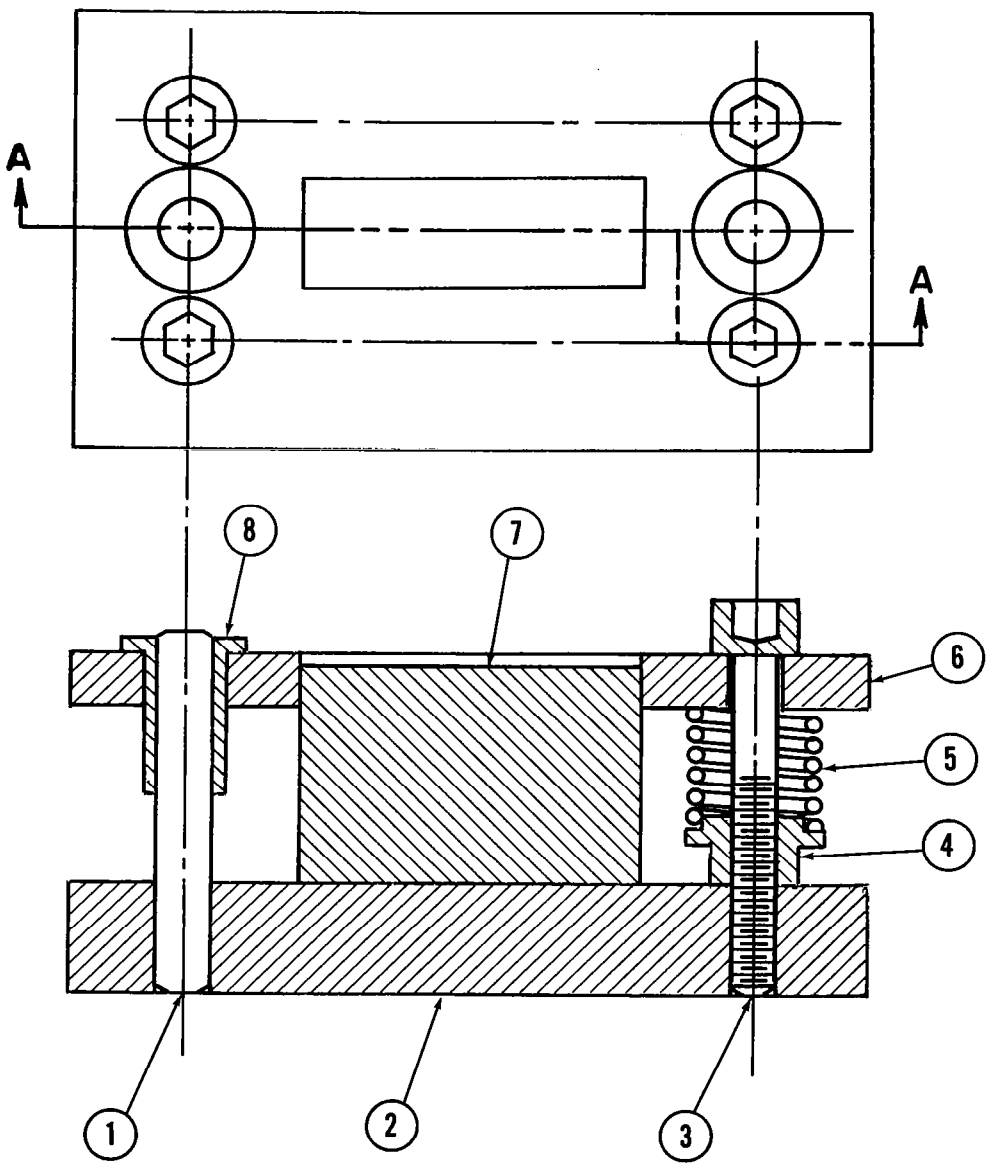

SECTION AA

Legend

1. Guide Pin
2. Base
3. Bolt
4. Locknut
5. Spring
6. Plate
7. Die
8. Bushing

Figure 2. Die Mold for Porous Powder Electrode Manufacture

Table 1

MAGNESIUM STRIP FORMS

Form and Thickness	Alloy	Supplier	g/in.^{2}	Amp-Min/in.^{2}
10 mil sheet	Primary Mg	Dow Chem. Co.	0.280	36.9
10 mil expanded (closed)	Primary Mg	Exmet Corp.	0.210	27.7
10 mil sheet	AZ31B	Dow Chem. Co.	0.287	37.8
10 mil expanded (closed)	AZ31B	Exmet Corp.	0.262	34.5
10 mil expanded (open)	AZ31B	Peerless Rolled Leaf	0.253	33.4
6 mil sheet	AZ31B	Peerless Rolled Leaf	0.133	17.5
est. 6 mil expanded (closed)	AZ31B	Peerless Rolled Leaf	0.151	19.9
6 mil expanded (closed)	AZ31B	Exmet Corp.	0.115	15.2
4 mil sheet	Primary Mg	H. Cross Co.	0.114	15.1
4 mil machine-punched	Primary Mg	Triangle Tool and Die	0.105	13.9
2 mil sheet	Primary Mg	MRC-Chemically milled	0.052	6.9

contained 1.5 to 2.0 g/in.^{2} with 30% to 40% void volume. The powders were pressed on 3.5-mil and 5.5 mil dynel fabric at 2 to 4 tons/in.^{2}. For the more detailed work on the magnesium anode, 2- to 10-mil continuous, expanded and perforated sheet were used.

For initial configuration and anode selection testing, either the open or sandwich cell described schematically in Figure 3 was used. At the high current drains considered, electrolyte IR losses may be significant, so interelectrode distances are important. The interelectrode distance "d" in these tests was 100 mils.

The ultimate cell used for both anode and cathode studies is shown in detail in Figure 4. The interelectrode distance is controlled by separator thickness, and the plastic anode retainer is porous or slotted to allow unhindered venting of parasitically produced hydrogen.

3. Results

a. Electrode Configuration and Anode Material Selection

The continuous foil, pressed powder, and flame-sprayed anodes all showed substantial IR losses due to hydrogen blockage. The open cell was used to screen the foil forms for over twenty electrolytes of various strengths. Selected results (Figure 5) indicate the losses encountered, particularly at high current drain. Magnesium, being more electronegative than aluminum, is affected more severely. Furthermore, with magnesium, the unusual "negative difference effect" (ref 2) occurs where parasitic hydrogen evolution actually increases as anodic current increases. In the relatively small interelectrode volume of the test cells, the gas produced blocks large areas of the electrode, resulting in extremely high electrolytic resistance in the blocked region and increased current density in the remaining accessible region.

This gas polarization is compounded in the closed sandwich cell where the hydrogen produced is virtually trapped. The shaded area in Figure 6 shows the poor results obtained with foil, pressed powder, and flame sprayed anodes in this test configuration. A significant improvement occurred when an expanded or perforated anode was used as indicated by curve 2 in Figure 6. Even in the closed sandwich cell, an appreciable amount of gas is vented through the back of the anode.

As illustrated in Figure 6, the discharge characteristics of the pressed powder anodes improve somewhat by going from the closed to open sandwich test configuration. The flame sprayed anodes discharged poorly, if at all, regardless of test configuration; hence, no detailed data are reported for them.

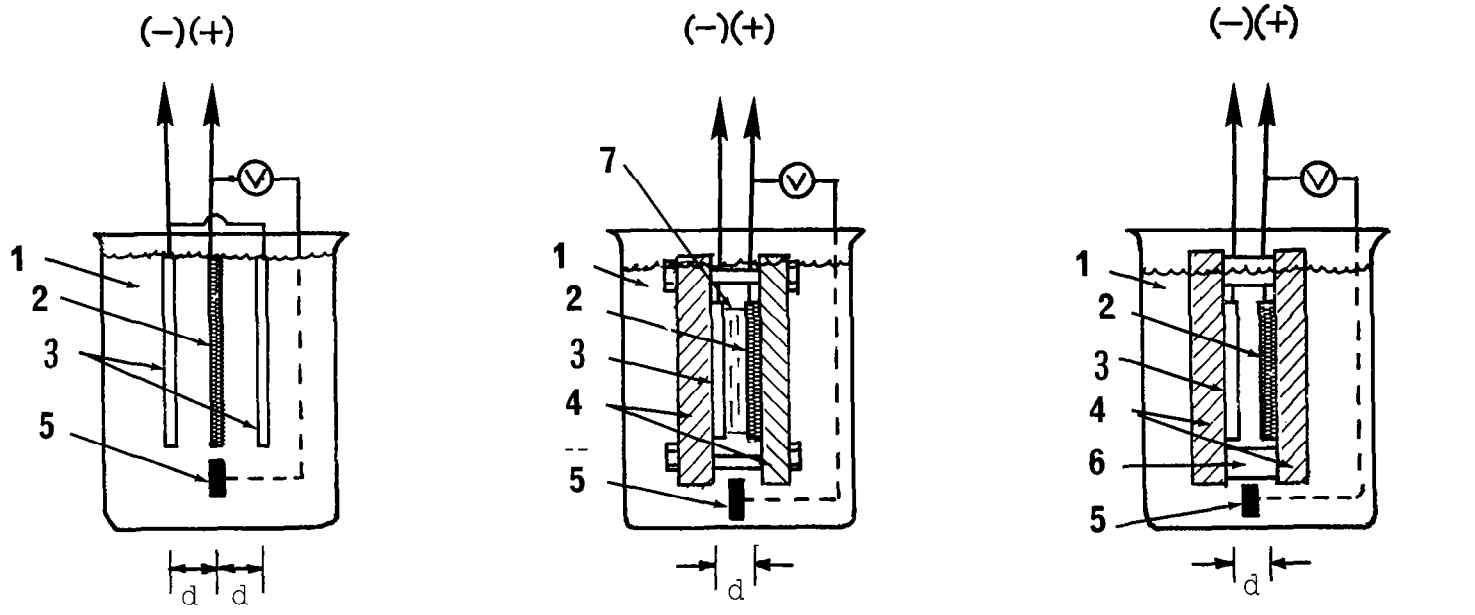

1. Electrolyte
2. Test Electrode
3. Counter Electrode
4. Lucite Retainers (2)
5. Reference Electrode
6. Spacer
7. Compressed Separator

Figure 3. Schematic Representation of Test Methods

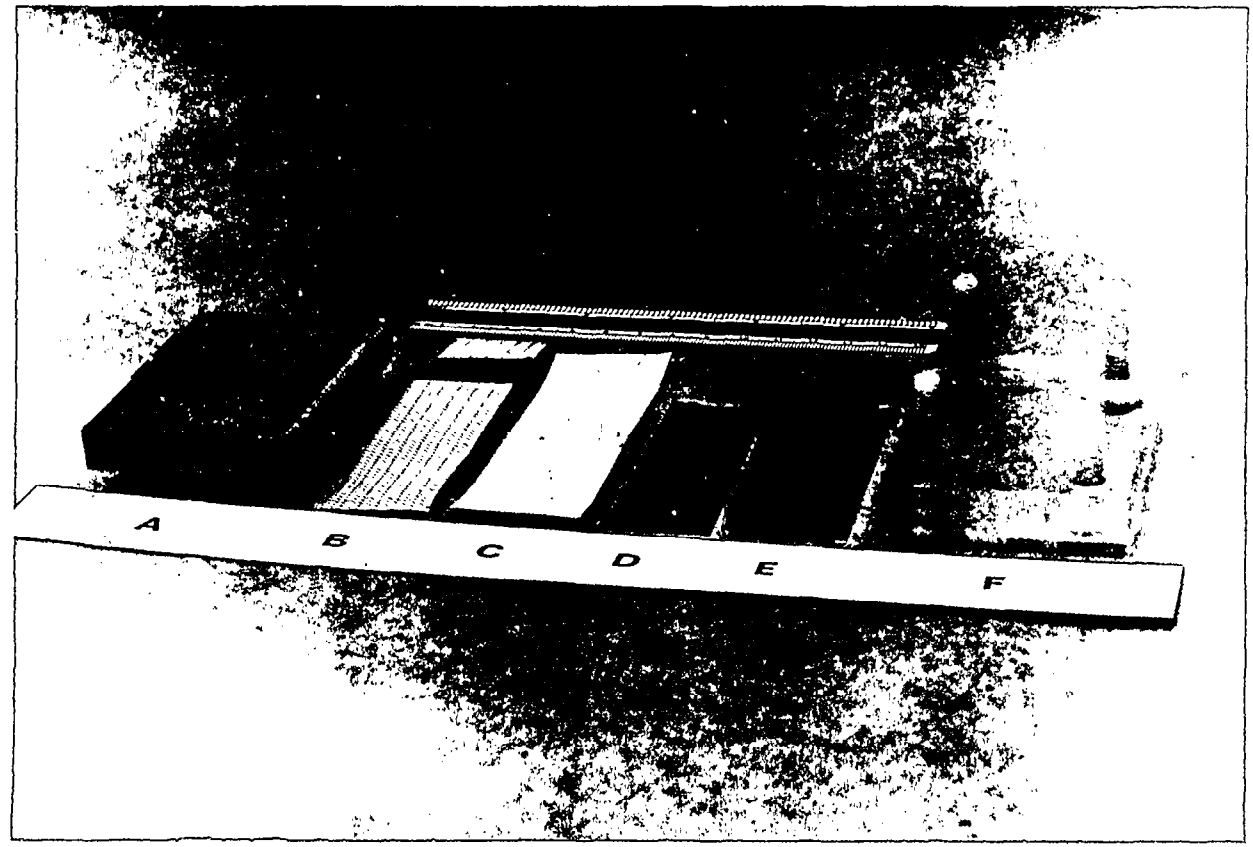

A. Porous Lucite anode retainer
B. Anode (expanded Mg shown)
C. Separator
D. Cathode
E. Cathode current collector (Pt foil shown)
F. Solid Lucite cathode retainer

Figure 4. Improved Sandwich Cell for Electrode Testing (Disassembled)

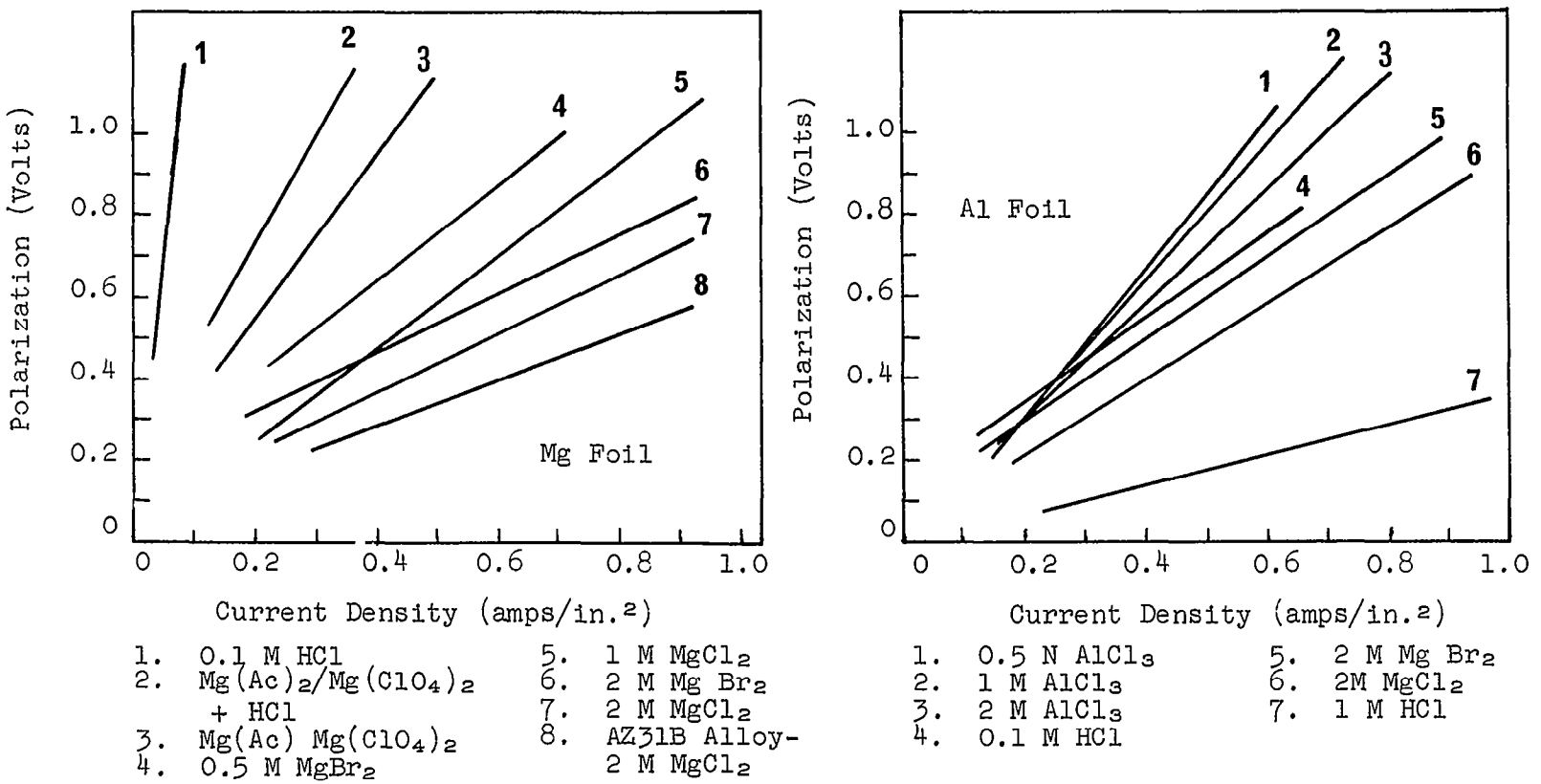

1. 0.1 M HCl
2. $Mg(Ac)_2/Mg(ClO_4)_2$ + HCl
3. $Mg(Ac)$ $Mg(ClO_4)_2$
4. 0.5 M $MgBr_2$
5. 1 M $MgCl_2$
6. 2 M $Mg\ Br_2$
7. 2 M $MgCl_2$
8. AZ31B Alloy-2 M $MgCl_2$

1. 0.5 N $AlCl_3$
2. 1 M $AlCl_3$
3. 2 M $AlCl_3$
4. 0.1 M HCl
5. 2 M $Mg\ Br_2$
6. 2M $MgCl_2$
7. 1 M HCl

Figure 5. Anodic Polarization of Magnesium and Aluminum Foil (Initial Screening Data)

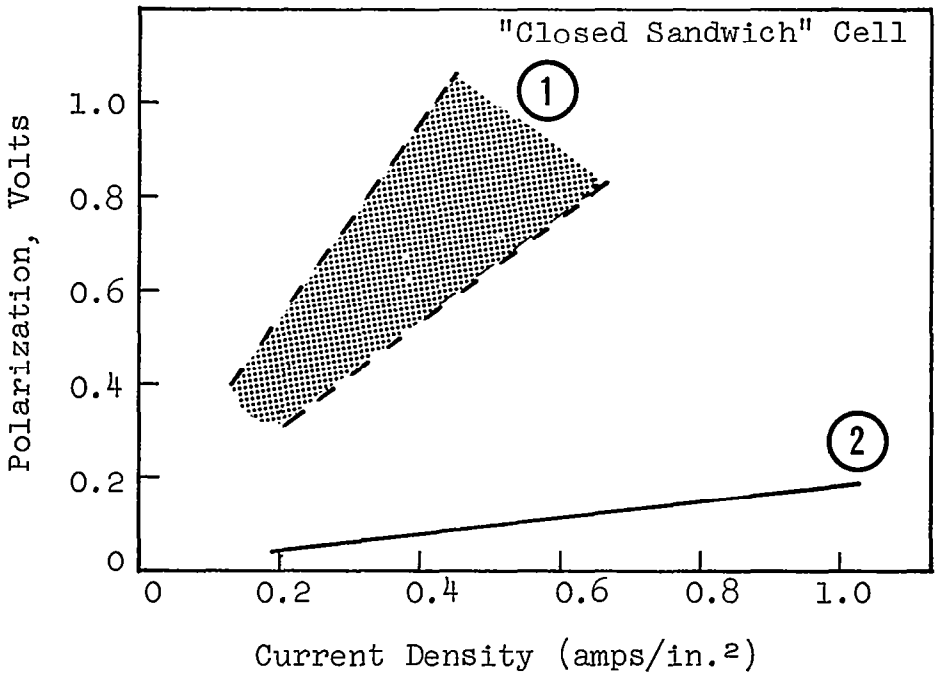

1. Most Results for Foil, Powder, Flame Spraying
2. Expanded Magnesium in 2M $MgCl_2$

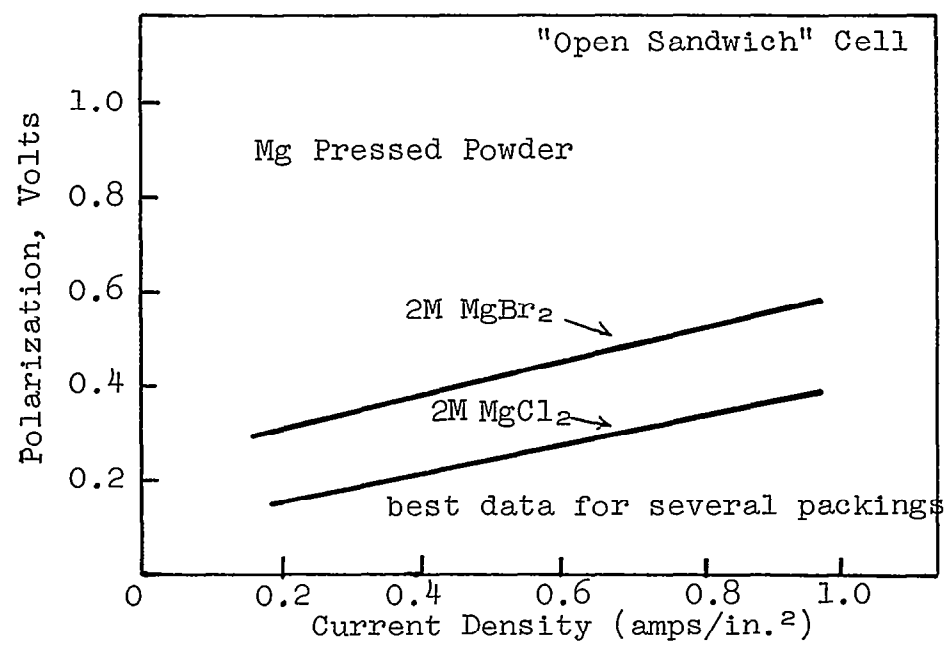

Figure 6. Comparison of "Closed Sandwich" Cell and "Open Sandwich" Cell Test Results.

While gassing cannot be eliminated, polarization due to gassing can be eliminated in the foil configuration by providing for easy hydrogen venting. This is accomplished by using expanded or perforated foil. The pressed powder anodes have increased surface area in an equivalent volume. The resultant increased gassing apparently clogs the pores rapidly, nullifying the increased surface area feature. The sprayed metal is so intimately attached to, and imbedded in, the tape backing that gas evolved becomes trapped, making efficient discharge impossible.

The discharge characteristics of magnesium and aluminum are similar. The more severe gassing of magnesium can be offset by using an open anode structure. Aluminum has a slight coulombic capacity advantage (2.98 amp-hr/g compared with 2.20 amp-hr/g for magnesium). However, magnesium is 0.8 volt more electronegative than aluminum [approximately -1.6 v to -1.8 v (SCE) compared with -0.8v (SCE) open circuit]. Because of higher single cell voltage and potentially higher power output, magnesium in expanded or perforated form was chosen as the prime anode material.

b. Magnesium Anode Characterization

Quantitative information describing polarization and corrosion of pure magnesium and several magnesium-aluminum-zinc alloys in various electrolytes was obtained.

Polarization studies were carried out in 2M $AlCl_3$, 2M $MgCl_2$, 2M $MgBr_2$ and 2M $Mg(ClO_4)_2$. A 3 x 1 in. magnesium foil, 5 mils thick, was placed 1/8 in. from a platinum foil electrode in the open cell. The plastic cell was submerged in a beaker of electrolyte. The spacing between electrodes was sufficient to eliminate gas polarization effects. The results of these studies are illustrated in Figure 7.

Both primary magnesium and its AZ61B and AZ31B alloys exhibited little polarization at current densities up to 1000 ma/in.^{2} As expected, half-cell voltages varied with the nature of electrolyte. Primary magnesium operated at about -1.8 to -1.9 v vs SCE in the most acidic electrolyte, aluminum chloride. Successive 0.1 volt drops occurred with magnesium chloride, magnesium bromide, and magnesium perchlorate electrolyte. The alloys operated at approximately 0.15 v poorer than pure magnesium in each electrolyte.

These results show that gassing was the major cause of polarization in the earlier screening studies. Providing for free escape of the hydrogen essentially eliminates gas polarization. Similar results, reported in Section III-B, were obtained using expanded or perforated magnesium in an actual tape configuration where the anode and cathode are separated only by a 3-5-mil separator tape.

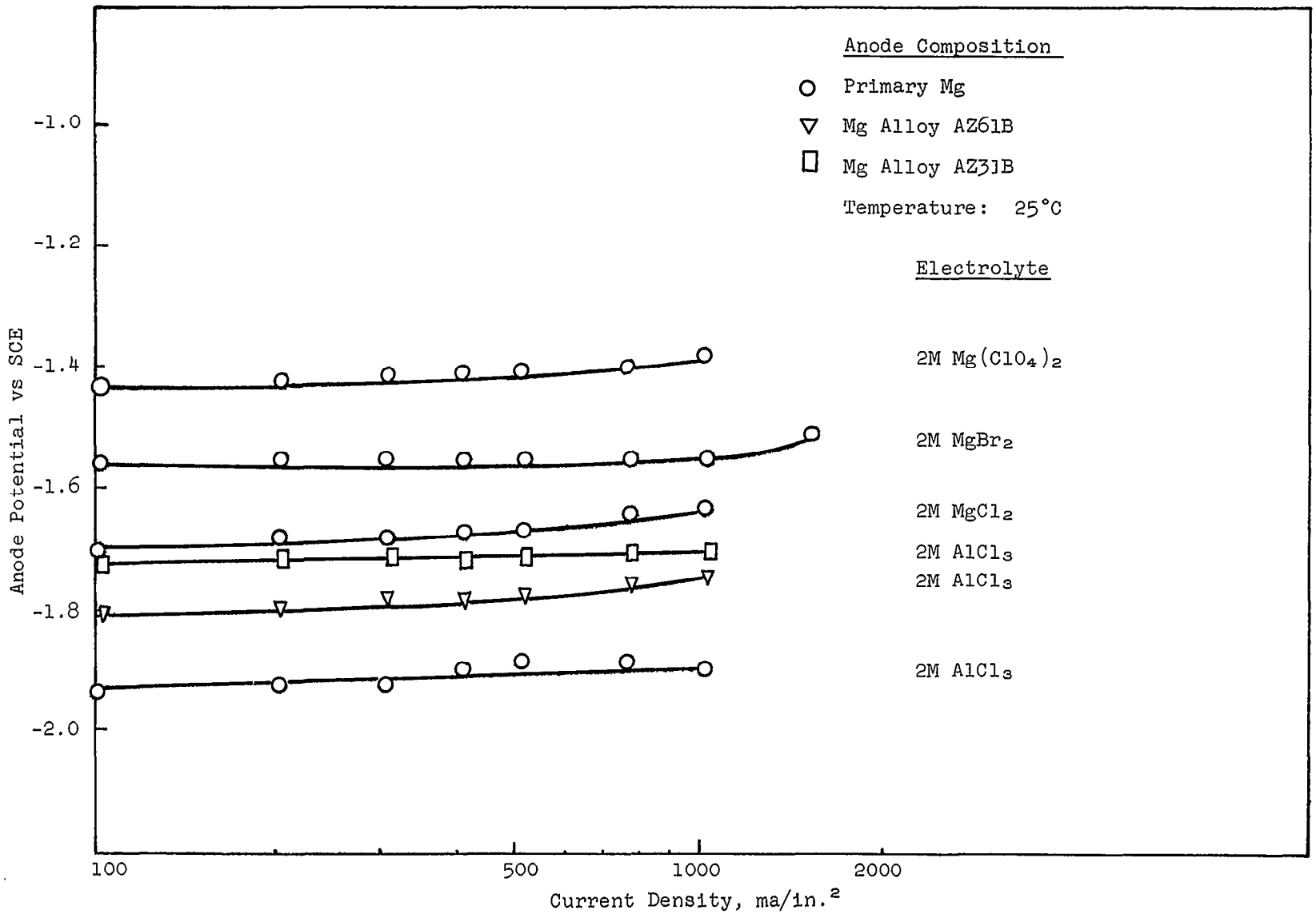

Figure 7. Pure and Alloyed Magnesium Anode Polarization Characteristics in Various Electrolytes

The desirability of being able to use a strong acid electrolyte is illustrated here. In 2M $AlCl_3$ (pH $\approx$ 1), magnesium discharges at about -1.9 volts versus SCE. In corresponding magnesium perchlorate or magnesium bromide (pH $\approx$ 6), the anode potential is approximately -1.5 versus SCE.

The chemical stability of magnesium in these electrolytes, particularly under high current load, is important. Table 2 lists corrosion data in aluminum chloride, magnesium chloride, and magnesium perchlorate under load. Weight loss measurements with time were recorded for a 2 x 1 in. area of magnesium. Table 3 shows relative chemical corrosion occurring under open-circuit conditions. Under no-load conditions neither pure magnesium nor alloyed magnesium showed significant short-term weight loss in 2M $MgCl_2$, 2M $MgBr_2$, or 2M $Mg(ClO_4)_2$. Corrosion increased in 2M $AlCl_3$ and was more severe for primary magnesium than for AZ31B and AZ61B alloys.

As expected, temperature severely affected primary magnesium corrosion in 2M $AlCl_3$ as illustrated in Table 4.

Under electrical load, however, the alloys corrode faster than a corresponding sample of pure magnesium.

Per cent weight losses for 5-mil foil are reported for both load and no load conditions. This is the approximate thickness of the ultimate tape anode. In actual operation the discharge time of any section of anode will be close to ten minutes. The maximum weight loss due to chemical corrosion for a 5 mil magnesium anode operating in 2M $AlCl_3$ at 500 ma/in.^{2} is about 40%. However, the actual discharge conditions in a tape configuration are much less severe than in the corrosion test described here. In the corrosion test, excess electrolyte is used and the pH does not change significantly. Under actual tape discharge conditions a minimum of electrolyte is used and the pH increases as acid is consumed by cathode discharge reactions. Qualitative observation of single cell and dynamic discharge of complete tape couples has shown that chemical corrosion and accompanying gas evolution was far less than predicted on the basis of the above data.

Another significant observation was the relatively slow corrosion of magnesium in concentrated aluminum chloride electrolyte. Corrosion was far less than in free hydrochloric acid solutions of identical pH. Attempts to discharge a m-dinitrobenzene/magnesium AZ31B alloy couple in 1M HCl acid and even 1M $FeCl_3$ or 1M $ZnCl_2$ resulted in complete deterioration of the anode in less than ten minutes.

Both zinc and ferric ion can be displaced from solution by magnesium, resulting in increased corrosion. Magnesium does not displace aluminum in aqueous solution. Furthermore, we speculate that aluminum chloride in solution keeps the free hydronium ion

Table 2

MAGNESIUM CORROSION UNDER VARYING CURRENT LOADS

Anode Material	Thickness (mil)	Electrolyte	Current Density, ma/in.^{2}	Weight Lost from 2 x 1 in. Area, mg (wt. %)		
				1 minute	5 minutes	10 minutes
Primary Mg	5	2M $AlCl_3$	250	5.8(2.0)	30.6(10.7)	65.5(22.8)
Primary Mg	5	2M $AlCl_3$	500	11.4(4.0	64.2(22.5)	123.4(43.3)
Primary Mg	5	2M $Mg(ClO_4)_2$	250	5.5(1.9)	26.6(9.4)	51.4(18.1)
Primary Mg	5	2M $Mg(ClO_4)_2$	500	8.6(3.0)	46.3(16.3)	93.0(31.5)
Primary Mg	5	2M $MgCl_2$	250	1.3(0.5)	16.8(5.9)	33.1(11.6)
Primary Mg	5	2M $MgCl_2$	500	1.6(0.6)	21.4(7.5)	48.8(16.5)
AZ31B Alloy	4-5	2M $AlCl_3$	250	8.1(2.8)	38.1(13.4)	78.5(27.6)
AZ31B Alloy	4-5	2M $AlCl_3$	500	15.7(5.5)	64.5(22.7)	124.8(43.4
AZ31B Alloy	4-5	2M $Mg(ClO_4)_2$	250	3.4(1.2)	13.2(4.6)	27.2(9.6)
AZ31B Alloy	4-5	2M $Mg(ClO_4)_2$	500	6.1(2.1)	27.9(9.8)	63.7(22.4)
AZ31B Alloy	25	2M $MgCl_2$	250	3.0	17.6	36.5
AZ31B Alloy	25	2M $MgCl_2$	500	6.3	38.3	83.0
AZ61B Alloy	10	2M $AlCl_3$	250	11.0	48.6	95. 2
AZ61B Alloy	10	2M $AlCl_3$	500	19.5	84.8	145.0
AZ61B Alloy	10	2M $Mg(ClO_4)_2$	250	0.8	10.5	27.5
AZ61B Alloy	10	2M $Mg(ClO_4)_2$	500	2.4	23.4	45.3
AZ61B Alloy	10	2M $MgCl_2$	250	2.2	14.3	36.4
AZ61B Alloy	10	2M $MgCl_2$	500	4.4	32.3	77.6

Table 3

MAGNESIUM CHEMICAL CORROSION

Open-Circuit Conditions
Temperature: 25°C

Anode Material	Electrolyte	Weight Loss, % for 5 mil Foil		
		1 minute	10 minutes	30 minutes
Primary Mg	2M $AlCl_3$	7	34	*
	2M $MgCl_2$	<1		3
	2M $MgBr_2$	<1		1
	2M $Mg(ClO_4)_2$	<1		1
AZ61B Alloy	2M $AlCl_3$	2	20	*
	2M $MgCl_2$	<1		2
	2M $MgBr_2$	<1		2
	2M $Mg(ClO_4)_2$	<1		<1
AZ31B Alloy	2M $AlCl_3$	3	25	*
	2M $MgCl_2$	<1		2
	2M $MgBr_2$	<1		<1
	2M $Mg(ClO_4)_2$	<1		<1

Table 4

EFFECT OF TEMPERATURE ON CHEMICAL CORROSION OF PRIMARY MAGNESIUM IN 2M $AlCl_3$

Open-Circuit Conditions

Temperature, °C	Weight Loss by 2 x 1 in. Area of 5 Mil Foil In 5 minutes, %
25	11
50	62
75	100*

* Complete solution

concentration at a tolerable level. One mole of aluminum chloride can form three moles of acid on hydrolysis

$$AlCl_3 + 3H_2O \longrightarrow Al(OH)_3 + 3HCl \qquad (1)$$

In solution, although three moles of acid are potentially available for reaction, there are not three moles of free acid existing at any one time. This is because of the stepwise hydrolysis of aluminum chloride.

$$HCl + H_2O \rightleftharpoons H_3O^+ + Cl^- \qquad pk_{A'} = \sim -7 \qquad (2)$$

$$Al(H_2O)_x^{+3} + H_2O \rightleftharpoons H_3O^+ + Al(H_2O)_{x-1}OH^{+2} \quad pk_{A'} = 4.9 \qquad (3)$$

Three molar hydrochloric acid solution is a stronger acid than one molar aluminum chloride.

As joint anode-cathode testing progressed, it was found that an aluminum chloride-hydrochloric acid mixed electrolyte was less corrosive than a free hydrochloric acid electrolyte of the same concentration. Magnesium corrosion in a 2M $AlCl_3 \cdot$1M HCl electrolyte was far less severe than that in 1M HCl. This indicates the possibility of some kind of association between aluminum chloride and hydrochloric acid similar to that encountered in organic solvents (S).

$$S + HCl + AlCl_3 \rightleftharpoons SH^+AlCl_4^- \qquad (4)$$

$$H_2O + HCl + AlCl_3 \rightleftharpoons H_3O^+AlCl_4^- \qquad (5)$$

The overall effect may be a decrease in hydrogen ion mobility. Discharge data for couples in mixed acid electrolyte are reported below and in the appendix (Tables A-1, A-2).

B. HIGH ENERGY CATHODE DEVELOPMENT

1. Background

Our previous work (ref.3) with organic nitro compound and positive halogen compound depolarizers in dry cell bobbin configurations served as a basis for choosing candidate cathode materials. When the feasibility of using strong acid electrolytes was demonstrated, high energy inorganic cathodes, potassium periodate, for example, which require strongly acid electrolytes were added. Theoretical coulombic capacities and half-cell potentials are listed in Table 5. The organic nitro compounds have the highest theoretical coulombic capacities. However, the positive chlorine compounds and potassium periodate

Table 5

COULOMBIC CAPACITIES OF DEPOLARIZERS

Compound	Theoretical Coulombic Efficiency (amp-min/g)	Experimental Open-Circuit Potential versus NHE
2,4,5-Trinitrotoluene	128	+0.25
Picric acid	125	+0.58
1-Carboxymethyl-3,3,5,5-tetra-nitropiperidine	120	+0.7
Ortho- and Meta-Dinitrobenzene	115	+0.4
2,5-Dinitrothiophene	111	+0.5
2,4-Dinitrothiophene	111	+0.5
3,6-Dinitrophthalic acid	76	+0.47
2,4,6-Trichlorotriazinetrione	42	+1.2
Hexachloromelamine	58	+1.2
Potassium periodate	49*	+1.3

* Based on reduction to iodine.

exhibit substantially higher half cell voltages, which make the resulting theoretical energy outputs comparable.

Estimates of couple energy densities are based on watt-hours per pound of total reactants. With periodate and organic nitro compounds, acid is consumed. Water is consumed during discharge of the positive chlorine compounds. Theoretical energy densities and reactions upon which they are based are listed in Table 6. During the course of the program, a more realistic estimate of attainable energy densities could be made using the actual measured operating cell voltages. The calculations in Table 6 are based on the highest operating voltages obtained to date.

Initially we assigned a coulombic capacity of 55 amp-min/g for potassium periodate in case some reduction to iodide occurred. Investigation has shown no significant reduction beyond iodine, so all previous efficiency data have been adjusted to the 49 amp-min/g basis.

The dry tape cathode configuration studies were made mainly with the organic nitro compounds since these were the best known of the candidates. Once the basic physical and mechanical parameters for satisfactory tape operation were determined, emphasis was shifted to the development and incorporation of more energetic cathodes. This is reflected in the progression from dinitrobenzene to picric acid to potassium periodate as the prime cathode. A complete characterization of picric acid and potassium periodate was carried out to meet the overall program objective of a practical working high energy couple on tape within the contract period. The active halogen compounds that are significantly more energetic are less well characterized and require further development to reach a stage of operation comparable to the periodate electrode. They are the prime candidates for the next generation tape cathode material.

A complete compilation of formulations and static discharge tests of potassium periodate cathodes is given in Table A-1 of the Appendix. A similar compilation for organic nitro compound cathodes is given in Table A-2 of the Appendix. The data given in the following sections are selected from Tables A-1 and A-2.

2. Method

Single cell or static discharge experiments were made using the improved sandwich cell shown in Figure 4. A 3 x 1 in. electrode was used and discharged against an expanded or perforated magnesium anode. Electrolyte was supplied by prewetting the separator tape or immersing the entire cell. As the program progressed, the latter technique was abandoned; using a prewet separator more closely approximated ultimate tape operation. A platinum foil or graphite sheet was used as the cathode current collector.

Table 6

ENERGY DENSITY ESTIMATE OF CANDIDATE COUPLES

Calculated Energy Density, watt-hr/lb. Reactants

Couple	At Standard Reversible Conditions	At Measured Cell Voltage, E
Magnesium-Potassium Periodate - Acid Electrolyte		
$2KH_5IO_6 + 7Mg + 14HCl = I_2 + 7MgCl_2 + 12H_2O$	575	310 (2.1 v. at 500 ma/in.^{2})
Magnesium-Picric Acid - Acid Electrolyte		
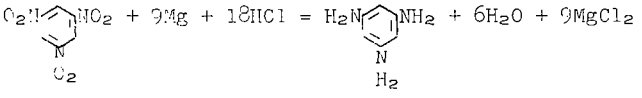	580	254 (1.1 v. at 500 ma/in.^{2})
Magnesium-m-Dinitrobenzene - Acid Electrolyte		
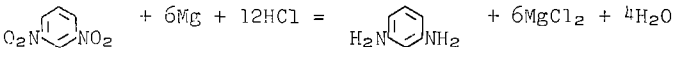	525	230 (1.1 v. at 500 ma/in.^{2})
Magnesium-Trichlorotriazinetrione - Neutral Electrolyte		
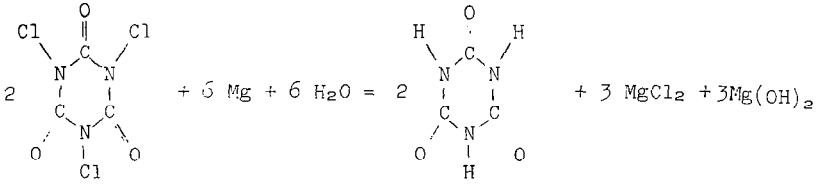	782	406 (2.0 v. at 100 ma/in.^{2})
Magnesium-Hexachloromelamine - Neutral Electrolyte		
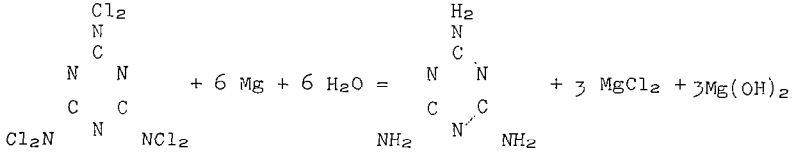	960	500 (2.0 v. at 100 ma/in.^{2})

The methods of tape preparation and description of materials are reported in the following section dealing with electrode configuration.

3. Results

a. Electrode Configuration

(1) Coating Technique

The most satisfactory cathode coated tapes are made by casting from an aqueous or organic slurry. For static cell work, aqueous slurries were usually used and the coating thickness was controlled by a Gardner Blade. Nylon, polypropylene, and acrylonitrile-vinyl chloride copolymer (dynel) were used as tape backing. The coated tapes were air dried at ambient temperatures. Some dry-pressed powder tapes were made, but this technique was abandoned early because of poor adhesion and flexibility.

Most cathode mixtures consisted of a 1:1 volume ratio of depolarizer and Shawinigan acetylene black (50% compressed) with approximately 5% binder and 5% fibrous reinforcing material. The dry materials were Waring blended or mixed with a mortar and pestle. The organic nitro compounds were normally mixed by hand, although these mixes showed no sensitivity to the standard Bureau of Mines impact test. An aqueous solution of binder was added to the dry components and the slurry was mixed until homogeneous.

(2) Conductor Properties

Shawinigan acetylene black (50% compressed) was found to be the most suitable conductor material. Table 7 shows the effect of various carbon substrates with o-dinitrobenzene. The major factor favoring acetylene black appears to be its incompressible nature, which results in an open pore electrode structure. For organic nitro compound or potassium periodate cathodes, at least 65 to 75% voids are required to achieve reasonable efficiencies. Substitution of graphitic carbons or mechanical compression resulted in higher packing densities, which led to poorer operation. Initial results with trichlorotriazinetrione indicate that substantially higher packing densities can be tolerated. The active chlorine compounds are much more soluble than either the nitro compounds or potassium periodate and, therefore, can act as leachable pore builders during discharge.

Potassium periodate, picric acid, and dinitrobenzene exhibit best discharge characteristics with approximately a 1:1 volume ratio of acetylene black conductor. Cathode efficiency data at various depolarizer/conductor ratios are shown in Tables 8, 9 and 10. Because of the higher density of potassium periodate, substantially less weight of carbon black is required compared with that needed for the nitro compounds.

Table 7

COMPARISON OF EFFECTIVENESS OF VARIOUS CARBONS AS SUBSTRATES FOR DINITROBENZENE

Cell: Mg/2M $AlCl_3$ or 2M $Mg(ClO_4)_2$/o-DNB and Carbon Substrate

Carbon	Carbon: o-DNB Vol. Ratio	Cathode Efficiency to 0.8 v		
		2 $Mg(ClO_4)_2$ 100 ma/in.^{2}	2M $Mg(ClO_4)_2$	2M $AlCl_3$
Shawinigan, 50% compressed	1:1	21-49		62 (at 200 ma/in.^{2}) 35 (at 300 ma/in.^{2})
Shawinigan, 50% compressed	1:2	15,22	7 (300 ma/in.^{2})	22, 24 (at 500 ma/in.^{2})
Nuchar-CN	1:2		6 (200 ma/in.^{2})	17 (at 300 ma/in.^{2})
Pure Carbon FC-13	1:1	Does not hold		9 (at 100 ma/in.^{2})
Columbian Conductex-SC	1:1	12		15 (at 500 ma/in.^{2})
Asbury Graphite A625	1:1	1		5 (at 100 ma/in.^{2})

Table 8

EFFECT OF o-DINITROBENZENE--CARBON RATIO ON CATHODIC REDUCTION EFFICIENCY

Cell:	Mg/2M $Mg(ClO_4)_2$/o-DNB
Current Density:	100 ma/in.^{2}
Cathode Type:	Basic (No Fiber)
Carbon:	Shawinigan Black, 50% compressed

Carbon: o-DNB Volume Ratio	Coulombic Efficiency (%) to -0.88v cutoff vs S.C.E.
0.2:1	8-9
0.4:1	15-22
1:1	40-50

Table 9

EFFECT OF PICRIC ACID--CARBON RATIO ON
CATHODIC REDUCTION EFFICIENCY

Cell: Mg/2.8M (sat'd) $AlCl_3$/Picric Acid
Cathode Loading: 100 $\pm$ 10 mg Picric Acid/in.^{2}
Cathode Type : Dynel Fiber, 1/4 in. (5%)
PVP Binder (5%)
Carbon: Shawinigan Acetylene Black, 50% compressed

Acetylene Black/ Picric Acid Volume Ratio	Coulombic Efficiency (%) To-0.88 volt Cutoff vs SCE	
	500 ma/in.^{2}	250 ma/in.^{2}
1:1	54	60
0.9:1	52	53
0.8:1	49	47
0.7:1	43	46
0.6:1	39	40
0.5:1	34	37

Table 10

EFFECT OF POTASSIUM PERIODATE--CARBON RATIO ON CATHODIC REDUCTION EFFICIENCY

Cell:	Mg/2.8M (sat'd)$AlCl_3$/Potassium Periodate
Cathode Type:	Dynel Fiber, 1/4 in. (5%)
	PVP Binder (5%)
Carbon:	Shawinigan Acetylene Black, 50% compressed

Carbon: KIO_4 Volume Ratio	Coulombic Efficiency (%) to -0.15 volt Cutoff vs SCE
1.7:1	65-70
1.3:1	60-70
1:1	60-70
0.5:1	40-45

(3) Binders

A number of water-soluble and non-water-soluble binders were screened. Suitable binding action is achieved with 2.0% to 5.0% polymer. At this concentration range neither type of binder appeared to interfere with the discharge characteristics of the cell (Table 11). Dynamic test results have shown that of all the binders studied water-soluble polyvinylpyrrolidone (PVP) and non-water-soluble polyvinylformal (PVF) impart the best mechanical properties to the cathode coat.

(4) Fibrous Fillers

Initial cathode coated tapes prepared for dynamic testing comprised 90-95% cathode material (1:1 volume ratio depolarizer: carbon black) and 5-10% PVP binder. The cathode coat cracked on drying and sloughed off the tape when wet out. The incorporation of short (1/8 to 1/4 in.) dynel or carbon fibers (approximately 5%) resulted in smooth, coherent coatings with good wet strength. No sloughing occurred during dynamic tests. An improvement in efficiency as well as reproducibility was noted upon addition of fibrous fillers. Results of experiments specifically designed to examine the effect of fibrous fillers on picric acid discharge are listed in Table 12.

The improved efficiency appears to be mainly due to mechanical improvements in the cathode. An improvement in electrolyte wet out is noted. There are also indications that the addition of carbon or graphite fibers may improve conduction through the cathode coat. This is discussed in more detail in the next section. Carbon fibers incorporated in the cathode mix result in a coating that is smoother and more coherent than the corresponding cathode coatings containing dynel fiber. For this reason, carbon fibers are currently used in all tape formulations.

b. Cathode Development

(1) Potassium Periodate

Potassium meta-periodate tape cathodes can be discharged at 60-80% coulombic efficiencies at 500 ma/in.^{2} versus magnesium in aluminum chloride or aluminum chloride-hydrochloric acid mixed electrolytes. Average operating cell potentials range from 1.9 to 2.1 v in single cell experiments. Cell cut-off voltage for efficiency calculations is 1.5 v.

Typical discharge curves are illustrated in Figure 8 for experiments in saturated aluminum chloride electrolyte. The operating potential is fairly flat until the end of the discharge where it drops sharply. The initial dip in potential is caused at least partially by slow wet out and reduced ion mobility due to the viscous saturated aluminum chloride electrolyte. The

Table 11

EFFECT OF BINDERS ON STATIC CELL OUTPUT

Test Cathode System: 50/50 vol ratio depolarizer acetylene black
Electrolyte: 2M $AlCl_3$
Base Tape: 3mil dynel
Current Density: 100 ma/in.^{2}

Depolarizer Type	mg/in.^{2}	Binder (5%)	Coulombic Efficiency to 0.8 volt, %
o-DNB	80	none (pressed powder)	50-55
o-DNB	74	polyvinylpyrrolidone, PVP NP-K30	50-60
o-DNB	70	polyvinylalcohol, Gelvatol 20-60	50-58
o-DNB	62	methylvinylether-maleic anhydride copolymer, Gantrez AN-139	35-50
o-DNB	80	hydroxymethyl cellulose, Methocel HG	30-50
Picric Acid	83	none (pressed powder)	55-60
Picric Acid	79	polyvinylpyrrolidone	50-60
Picric Acid	68	polyacrylamide, Cyanamer P-26	45-50
Picric Acid	95	polyvinylformal, PVF 15-95E	50-60

Table 12

EFFECT OF CATHODE FIBER CONTENT ON CATHODIC REDUCTION EFFICIENCIES OF PICRIC ACID

Cathode: Shawinigan Black:Picric Acid (1:1)

Anode: Magnesium

Electrolyte: 2M $AlCl_3$

Current Density: 500 ma/in.^{2}

Cathode Mixture Type	Cathode Coulombic Efficiency*, to 0.8v, %
No fiber	20-35
Dynel fiber	38-42
Graphite fiber	41-46

* At equivalent tape loadings

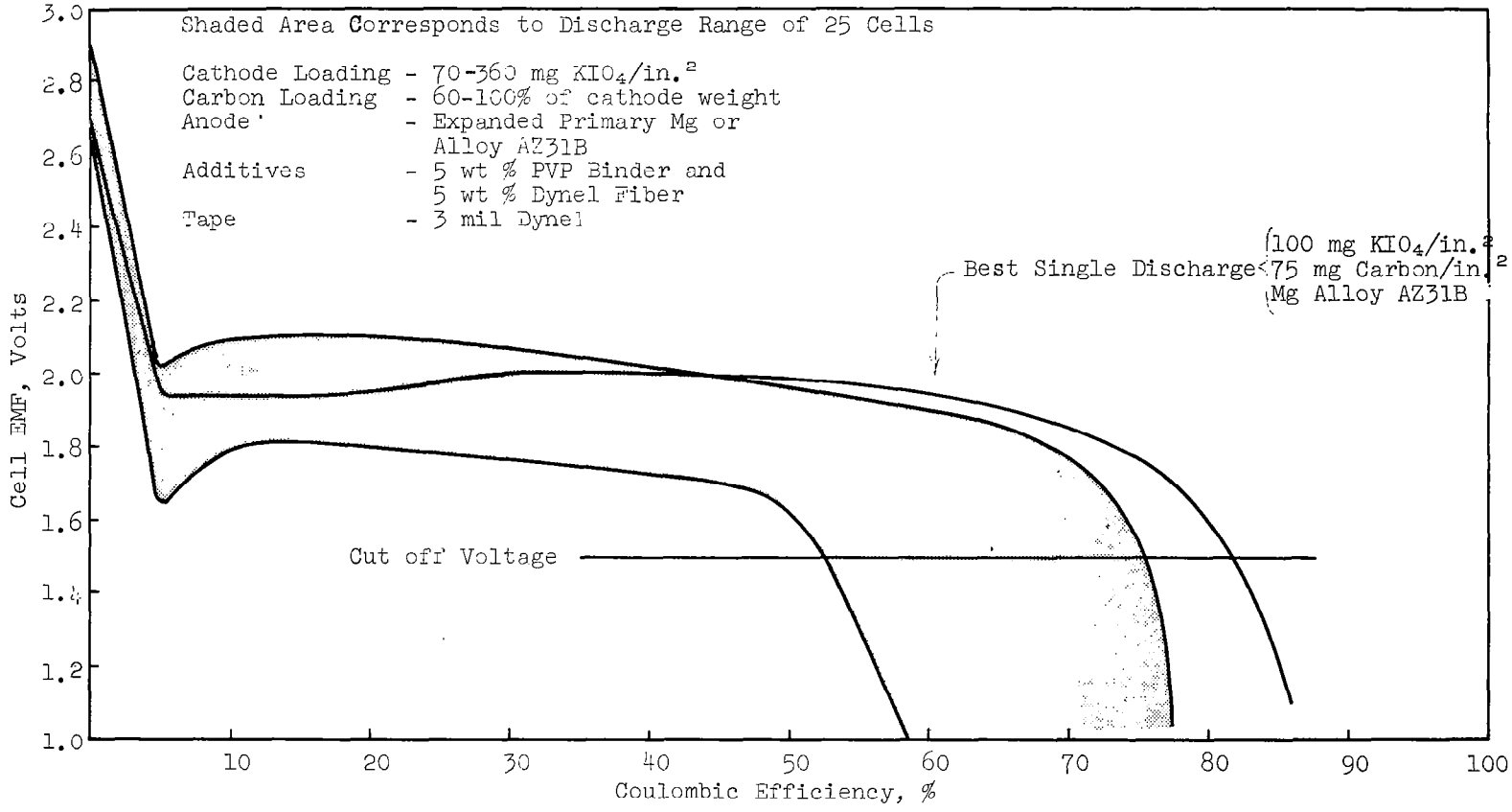

Figure 8. Discharge Characteristics of Potassium Periodate Cathode in Saturated $AlCl_3$ at 500 ma/in.^{2}

addition of free hydrochloric acid to form a mixed electrolyte with aluminum chloride eliminates this dip. A typical mixed electrolyte discharge curve is shown in Figure 9. A summary of all periodate tape cathode discharge experiments is contained in the Appendix. The best power density output obtained with a single cell potassium periodate cathode ranged from 80 to 90 watt-hr/lb total electrode weight plus electrolyte (see Table 10). Accurate minimum electrolyte requirement data were not taken during these static tests. The energy density figures are based on results of electrolyte requirement data reported in Section III-B.

No effort was made to minimize separator or anode weight in these tests. Electrolyte required is by far the largest weight contributor. The energy density is 236 watt-hr/lb total reactants. Addition of inert ingredients including conductor, tape, binder, etc., reduces the energy density to 122 watt-hr/lb. The reduction from 122 watt-hr/lb to 85 watt-hr/lb is due mainly to electrolyte required to wet out the electrode and electrolyte lost to anode corrosion. Cathodes such as periodate salts and organic nitro compounds that consume acid during discharge will be burdened with a high electrolyte weight penalty. Despite high coulombic efficiencies, it is estimated that a maximum of approximately 115 watt-hr/lb can be obtained with potassium periodate.

Potassium iodate (KIO_3) and sodium periodate ($NaIO_4$) were examined briefly. Both efficiencies and voltages were substantially lower than those of potassium periodate- magnesium cells. Since they offered no advantage over the potassium periodate electrode, their study was not pursued.

(2) Picric Acid

(a) Effect of Picric Acid Loading on Performance

Unlike potassium periodate cathodes, the performance of organic nitro compound cathodes becomes poorer at high loadings, apparently due to interference by reaction products. Table 14 lists the coulombic capacities and potentials of picric acid cathodes as a function of loading. Cells were immersed in a stationary pool of electrolyte contained in a beaker. The highest coulombic efficiencies (47-58%) were obtained with cathode loadings ranging from 20 to 100 mg picric acid/in.^{2} At higher loadings efficiencies became progressively lower. At the same time, operating potentials appear to improve with loading.

The effect on the complete cell is illustrated in Figure 10. The effect of circulating fresh electrolyte through the cell is shown by the data in Table 15. For this test series, the static cell holder was placed on its side and the electrolyte allowed to drain through continuously. The highly colored reaction products were continually removed from the electrode area.

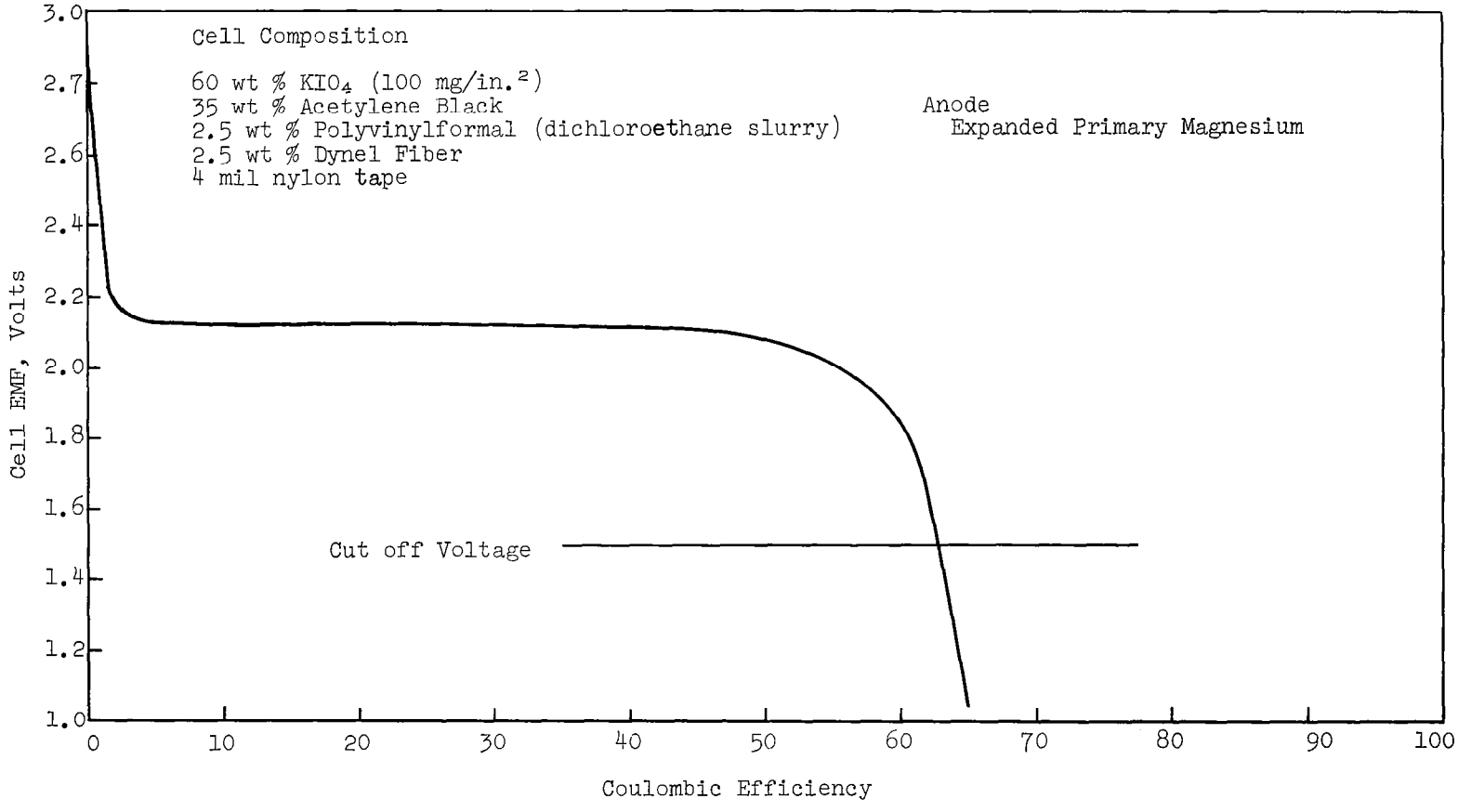

Figure 9. Discharge Characteristics of Potassium Periodate Cathode In 2M $AlCl_3$·0.5M HCL Electrolyte at 500 ma/in.^{2}

Table 13

SINGLE CELL POWER DENSITY OF MAGNESIUM-POTASSIUM PERIODATE SYSTEM

Total cathode electrode weight -	0.66g (includes separator, conductor, binder, filler)
Total anode weight	0.31g
Total electrolyte weight	1.50g
Total weight	2.47g
Cell area	3 $in.^2$
Theoretical Capacity	0.274 amp-hr
Efficiency	83% (1.5 amp current)
Cell emf	2.0 v
Energy output	2.0 x .274 x 0.83 = 0.46 watt-hr
Energy density	$\frac{0.46 \times 454}{2.47}$ = 85 watt-hr/lb

Table 14

EFFECT OF PICRIC ACID LOADING ON COULOMBIC EFFICIENCY

(Static Cell Test)

Cathode Composition:

Picric Acid (PA)	45%
Acetylene Black	45%
Dynel fiber, 1/8 in.	5%
PVP Binder	5%

Anode: Expanded Mg AZ31B alloy
Electrolyte: Saturated (2.8M) $AlCl_3$
Temperature: 25°C
Cathode cutoff potential: -0.88 v vs SCE

Cathode Loading, mg PA/in.^{2}	Average Theoretical Capacity, amp-min/in.^{2}	Coulombic Efficiency, %	Cathode Potential, volts vs SCE	
			OCP*	Average Operating Voltage
30 ± 10	3.5	54 - 58	0.5	-0.65
50 ± 10	6.3	54 - 55	0.4	-0.60
70 ± 10	8.7	48 - 60	0.4	-0.50
90 ± 10	11.3	47 - 58	0.4	-0.48
120 ± 10	14.7	37 - 45	0.4	-0.35
150 ± 10	18.8	25 - 33	0.4	-0.40
200 ± 10	25	20 - 25	0.4	-0.35

* Open-Circuit Potential

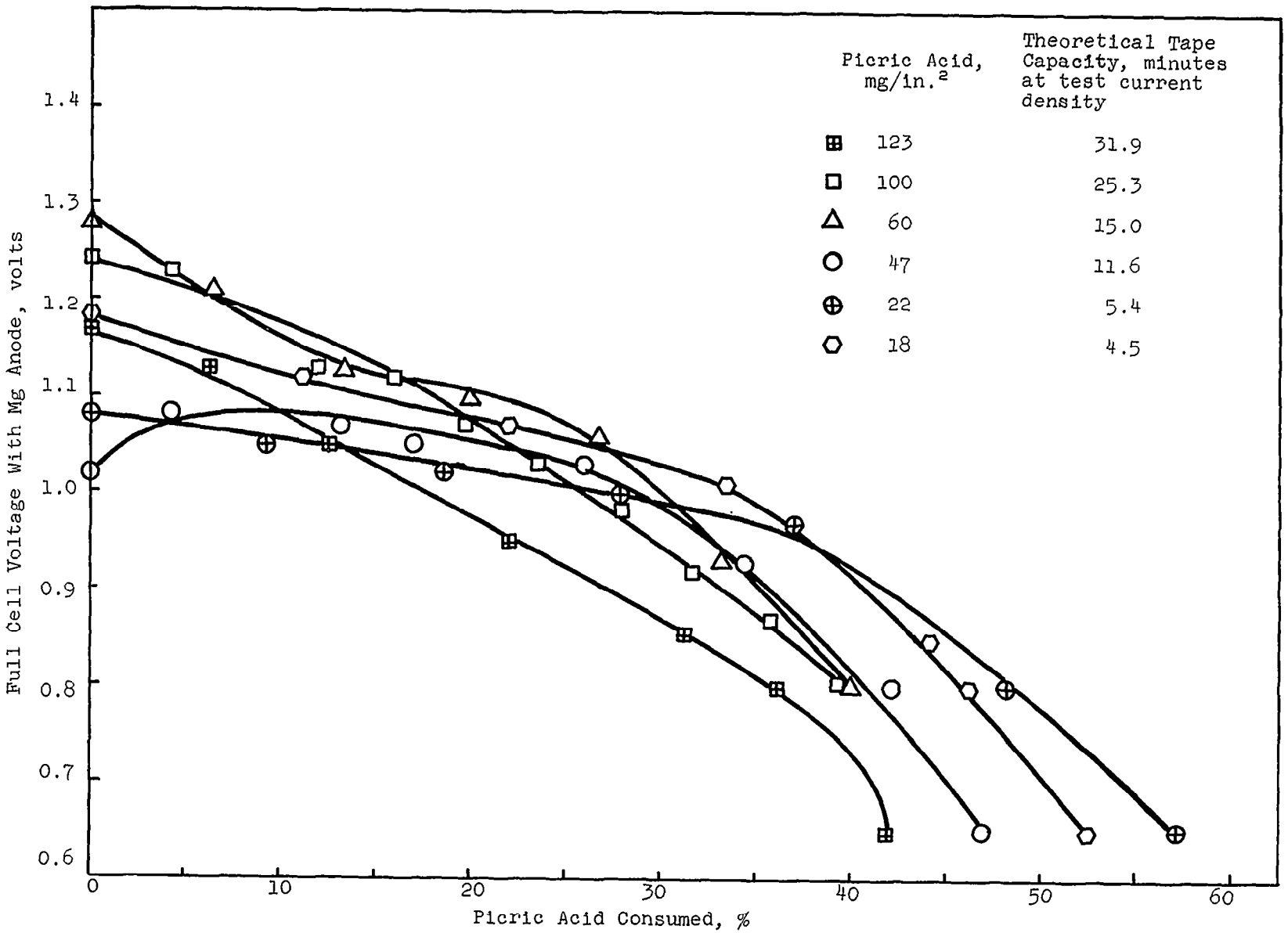

Figure 10. Effect of Picric Acid Loading on Static Discharge of Picric Acid in 2M $AlCl_3$ at 500 ma/in.^{2}

Table 15

EFFECT OF PRODUCT REMOVAL ON PICRIC ACID CATHODE OPERATION

Cathode Composition:

Picric Acid (PA)	45%
Acetylene Black	45%
Dynel fiber, 1/8 in.	5%
PVP Binder	5%

Anode: Expanded MgAZ31B alloy
Electrolyte: Saturated (2.8M) $AlCl_3$
Temperature: 25°C
Cathode cutoff potential: -0.88v vs SCE

Cathode Loading, mg PA/in.^{2}	Coulombic Efficiency, % Stationary Electrolyte	Coulombic Efficiency, % Circulating Electrolyte
200 ± 10	20 - 25	50 - 60
150 ± 10	25 - 33	51 - 53
100 ± 10	47 - 58	49 - 58

Interference of reaction products appears to be negligible for picric acid-Mg cells of 10-minute discharge capacity or less at 500 ma/in.^{2} current density. Concentration polarization due to reaction products does appear where discharge times are longer than 10 minutes at this current density.

The better operating potential with increased cathode loading is presumably due to the higher effective surface area of the cathode, which in effect lowers the real current density.

A number of picric acid cathodes were discharged at current densities of 250 and 750 ma/in.^{2} in addition to the 500 ma/in.^{2} reported above. The results are tabulated in Table 16 and illustrated in Figures 11, 12, and 13. Efficiencies did not improve under lower current drain (250 ma/in.^{2}) except for very low loadings. The long discharge times associated with low current densities led to reaction product polarization and anode corrosion problems for the moderate and high loading cathode tapes.

The reduction of a nitro group is a complicated reaction involving several steps.

$$\geq NO_2 \longrightarrow \geq NO \longrightarrow NHOH \longrightarrow NH_2 \qquad (6)$$

In neutral or basic solution, the intermediate products can react to form azo- or azoxy- compounds which either do not reduce readily or reduce at a lower potential

$$\geq NO + \geq NHOH \longrightarrow \geq N = \overset{\downarrow}{N}\leq + H_2O \qquad (7)$$
$$O$$

The presence of acid hinders these coupling reactions by tying up the intermediate products as acid salts until they can be reduced. Electrolyte screening reported earlier for anode performance and below for dinitrobenzene discharge performance indicated aqueous aluminum chloride to be the most suitable acid electrolyte.

(b) Effect of Aluminum Chloride Electrolyte Concentration on Picric Acid Energy Output

Table 17 shows the results of a study of the effect of changing aluminum chloride concentration on the coulombic efficiency and operating potential of the picric acid cathode vs magnesium. From the discharge reaction,

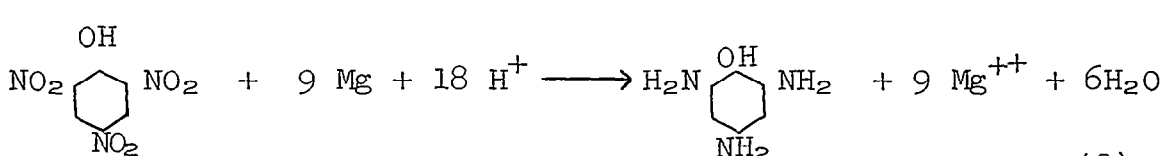

(8)

Table 16

COULOMBIC EFFICIENCIES OF PICRIC ACID CATHODES
AT SEVERAL CURRENT DENSITIES

Cathode Composition
- Picric Acid (PA) 45%
- Acetylene Black 45%
- Dynel fiber, 1/8 in. 5%
- PVP Binder 5%

Anode: Expanded Mg AZ31B alloy
Electrolyte: Saturated (2.8M) $AlCl_3$
Temperature: 25°C
Cathode cutoff potential: -0.88v vs SCE

Cathode Loading, mg PA/in.^{2}	Coulombic Efficiency, % (Average Operating Potential vs SCE) 250 ma/in.^{2}	500 ma/in.^{2}	750 ma/in.^{2}
200 ± 10	44-45 (-0.45)	50-60 (-0.35)	47-48 (-0.40)
150 ± 10	50-53 (-0.50)	51-53 (-0.40)	48-50 (-0.65)
100 ± 10	58-61 (-0.50)	49-58 (-0.48)	30-50 (-0.60)
30 ± 10	*	48-60 (-0.50)	25-28 (-0.72)
40 ± 10	66-68 (-0.55)	54-55 (-0.60)	0

* No data

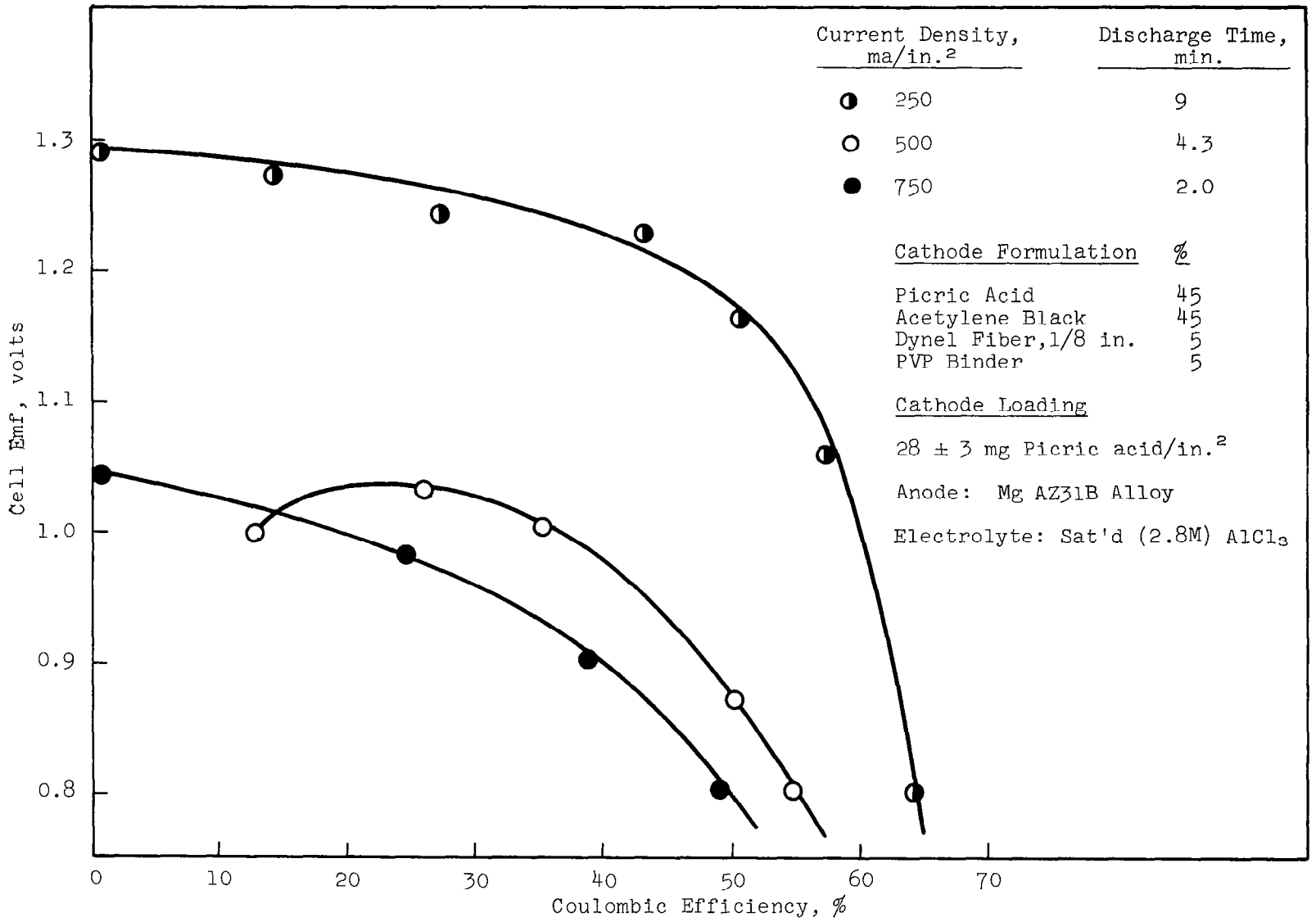

Figure 11. Effect of Current Density on Picric Acid Discharge Characteristics at Low Cathode Loadings

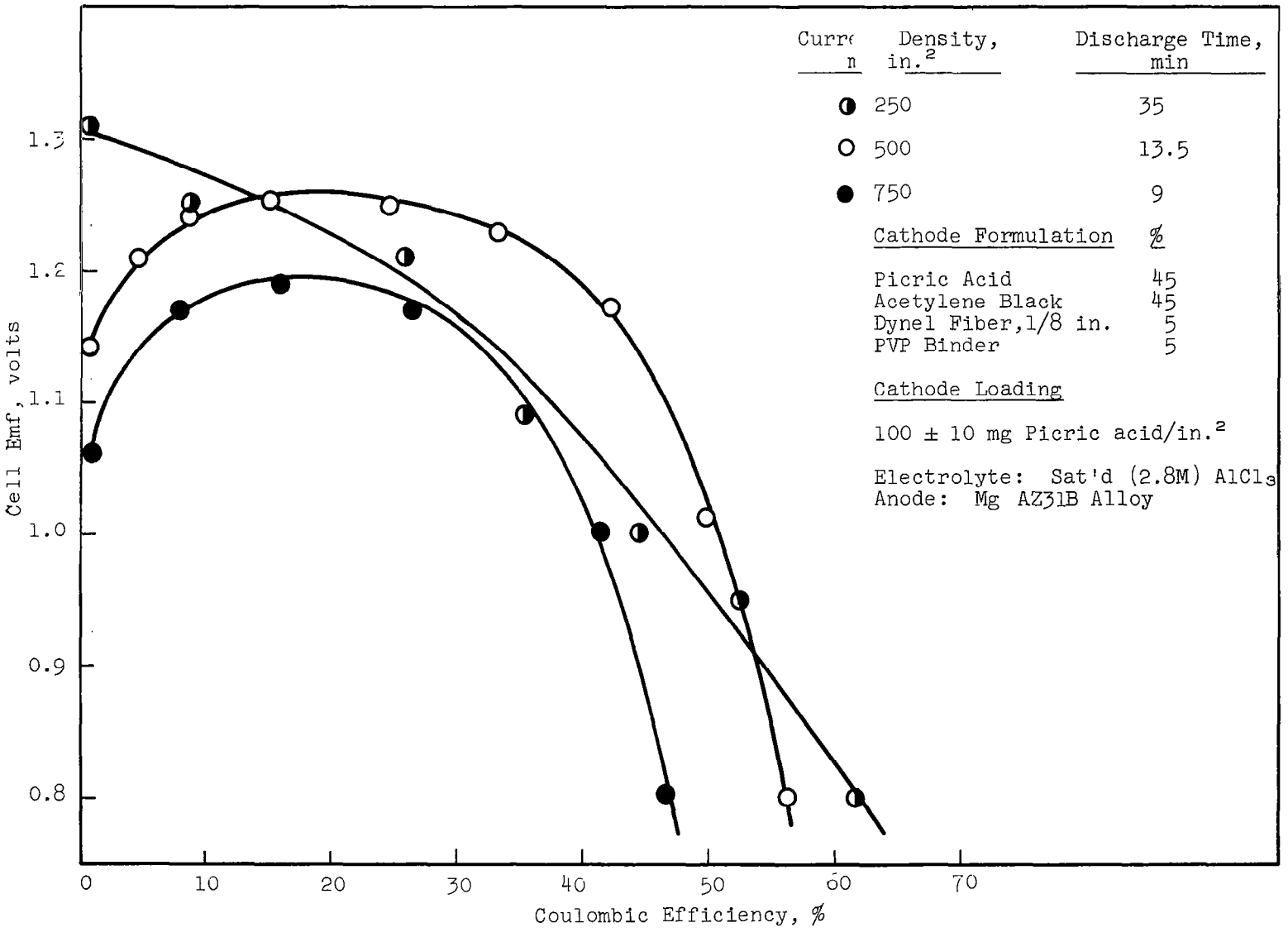

Figure 12. Effect of Current Density on Picric Acid Discharge Characteristics at Moderate Cathode Loadings

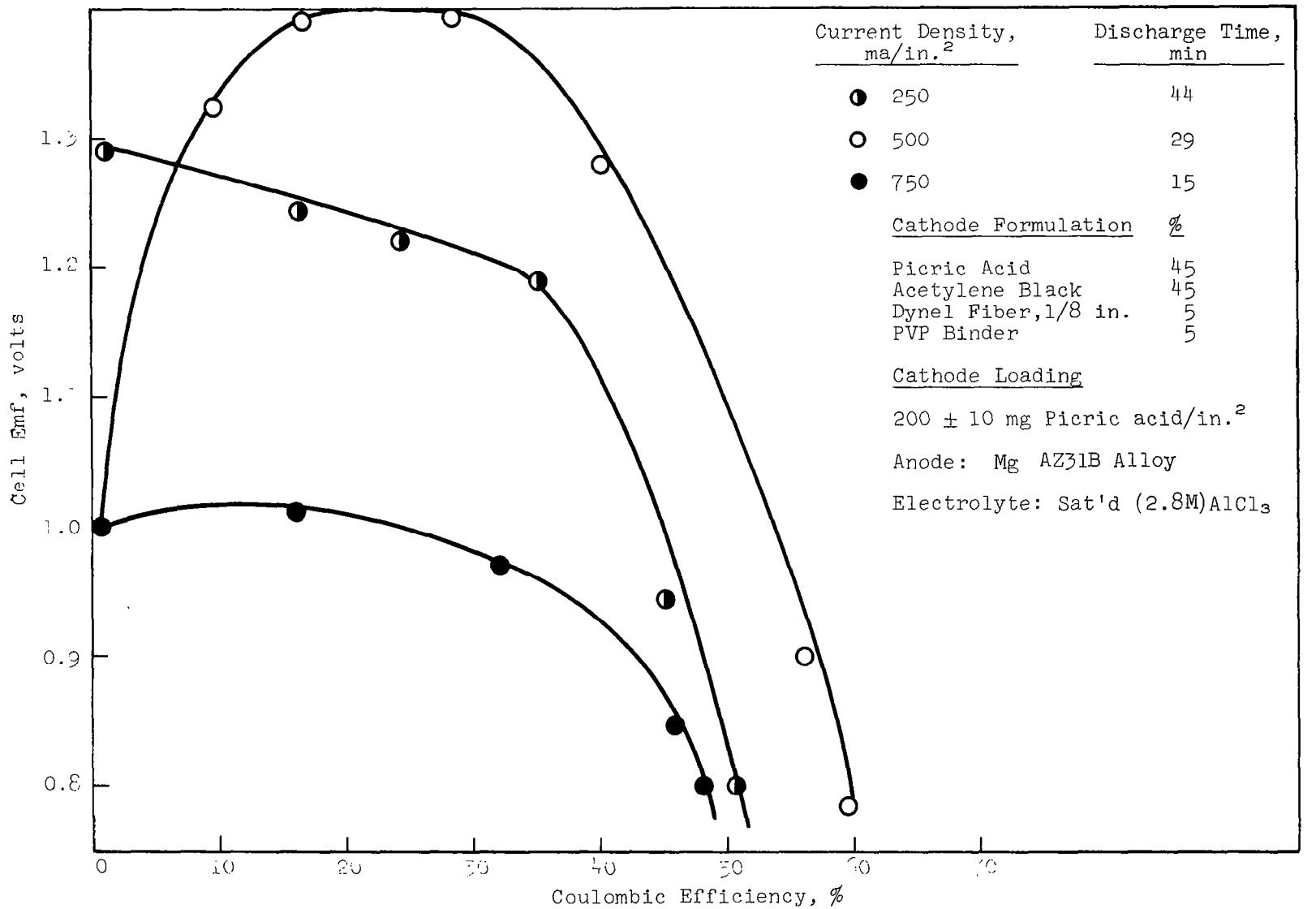

Figure 13. Effect of Current Density on Picric Acid Discharge Characteristics at High Cathode Loadings

Table 17

EFFECT OF ALUMINUM CHLORIDE ELECTROLYTE CONCENTRATION ON PICRIC ACID CATHODE PERFORMANCE

(Static Cell Test)

Cathode Composition:	Picric Acid	45%
	Acetylene Black	45%
	Dynel fiber, 1/4 in.	5%
	PVP Binder	5%
Anode:	Expanded Mg AZ31B alloy	
Cathode Loading:	90 ± 10 mg picric acid/in.^{2}	
Temperature:	25°C	
Cathode cutoff potential:	-0.88 v vs SCE	

$AlCl_3$ Concentration, Molarity	Coulombic Efficiency, %	Cathode Potential, volts vs SCE	
		OCP*	Average Operating Voltage
1	15 - 25	0.42	-0.65
2	35 - 50	0.34	-0.53
2.8 (saturated)	50 - 58	0.45	-0.45

* Open-Circuit Potential

it is apparent that picric acid requires a high concentration of hydrogen ion to operate properly. This is reflected in the poor efficiencies in a limited amount of 1M $AlCl_3$. All discharges reported in Table 17 were carried out with equal, limited volumes of electrolyte. The average operating potential increased approximately 0.1 volt with each increase in concentration. These changes correspond closely with the measured pH changes among the electrolytes and can be ascribed to a simple pH effect.

Full-cell data are illustrated in Figure 14. As in the case of potassium periodate, the initial potential dip followed by a rise to the normal operating potential appears to be correlated with aluminum chloride concentration. Highly concentrated electrolyte is fairly viscous. This could account in part for low ion mobility, at least initially before appreciable amounts of magnesium ions are formed or temperature increase lowers viscosity. It could also explain slow cathode wet out action. Addition of free hydrochloric acid or small amounts of magnesium perchlorate appeared to reduce internal resistance. Under optimum conditions, th picric acid cathode may be discharged vs magnesium at 500 ma/in.^{2} wi a cell emf close to 1.2 v and efficiencies near 60%.

(c) Effect of the Composition of Magnesium Anode on Picric Acid Discharge

Extensive studies have shown that picric acid cathodes discharge at higher coulombic efficiencies with magnesium-aluminum-zinc alloys than with primary magnesium. This occurred despite the fact that, initially at least, cell voltages were at least 0.1 volt higher with primary magnesium. Table 18 shows some typical results using primary magnesium, AZ31B alloy, and AZ61B alloy. Coulombic efficiencies of picric acid were higher with both alloys. Half-cell data indicate that all magnesium anodes operated normally. The cathode half-cell performance was poorer against primary magnesium.

Figure 15 shows a difference in the shape of the discharge curves of picric acid run against pure and alloyed magnesium. Against pure magnesium the full- and cathode half-cell potentials fell off steadi Against the alloys, a plateau occurred and was maintained until near the end of the run. Attempts to isolate the cause of this phenomenor have been unsuccessful so far. An interaction between picric acid and zinc ion produced by alloy corrosion and dissolution is suggested but this is strictly conjecture at this point.

(d) Fibrous Carbon and Graphite as Cathode Conductors

Several screening experiments were performed incorporating 1/4-in. carbon and graphite fibers in the cathode mix to improve conductivity. The "as received" fiber bundles were fluffed with a Waring Blender prior to use. Polarization studies shown in Figure 16 indicate that a picric acid cathode containing 10% carbon

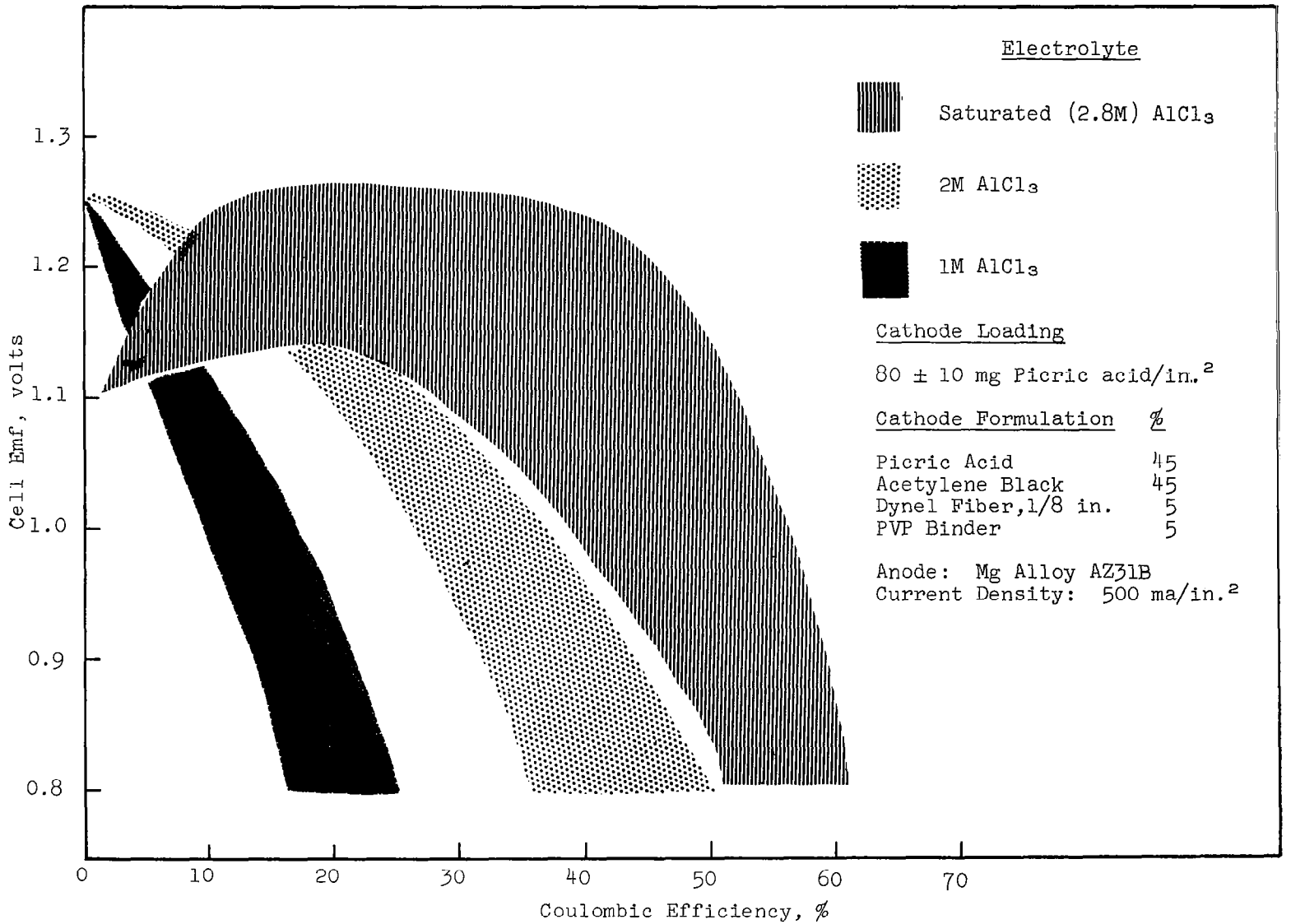

Figure 14. Effect of Aluminum Chloride Concentration on Picric Acid Discharge Characteristics

Table 18

EFFECT OF PURE AND ALLOYED MAGNESIUM ON PICRIC ACID CATHODE EFFICIENCY

(Static Cell Test)

Cathode Composition:	Picric Acid 45% Acetylene Black 45% Carbon Fiber 5% PVP Binder 5%
Cathode Loading:	90 $\pm$ 10 mg picric acid/in.^{2}
Electrolyte:	2M $AlCl_3$
Cutoff Potential:	0.8 v full cell -0.88 v vs SCE for alloys -1.05 v vs SCE for pure Mg

Anode	Cathode Coulombic Efficiency, %
Primary Mg	28 - 38
AZ61B Alloy	42 - 43
AZ31B Alloy	40 - 48

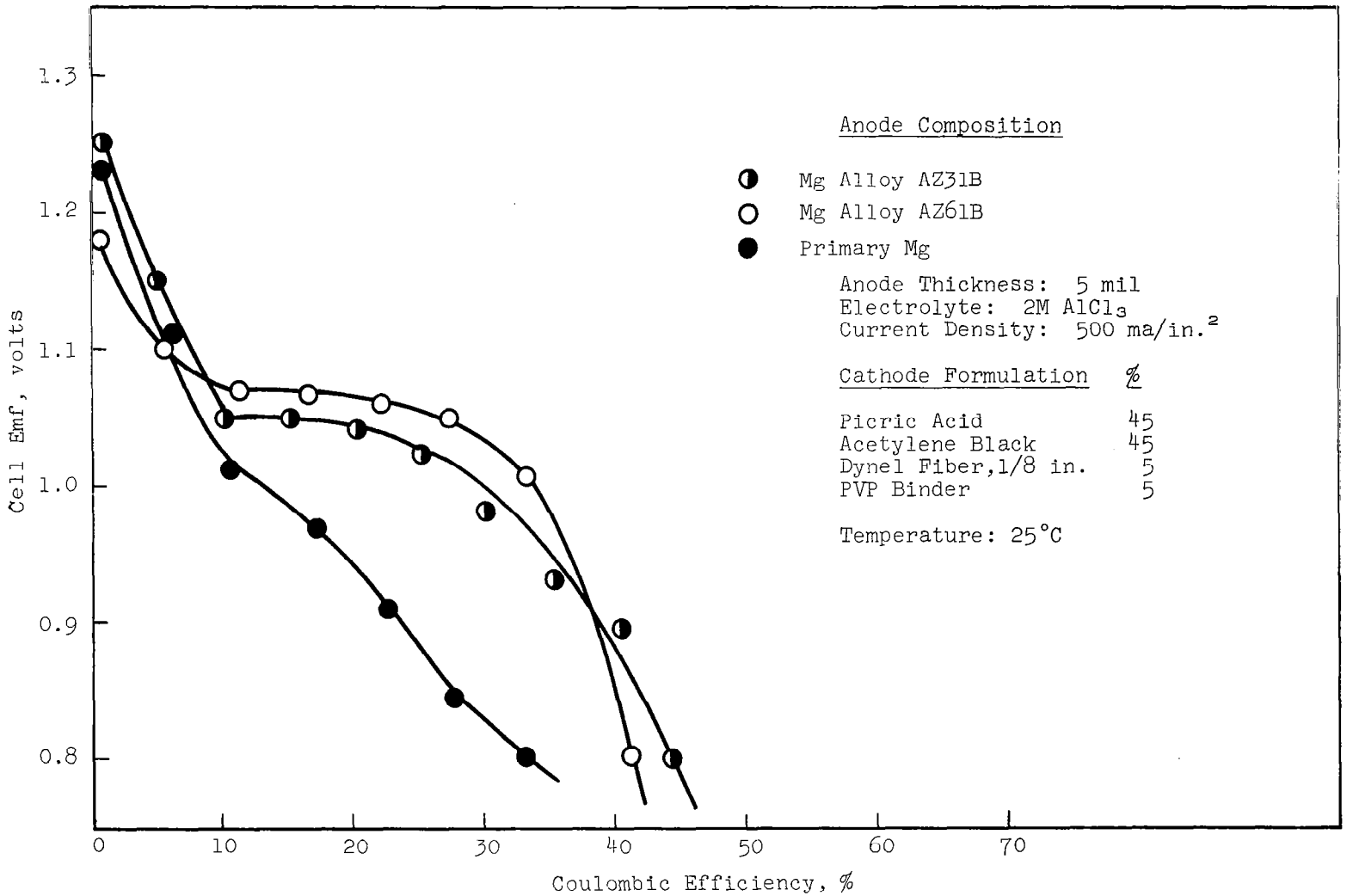

Figure 15. Discharge Characteristics of Picric Acid Cathode Against Pure and Alloyed Magnesium Anode

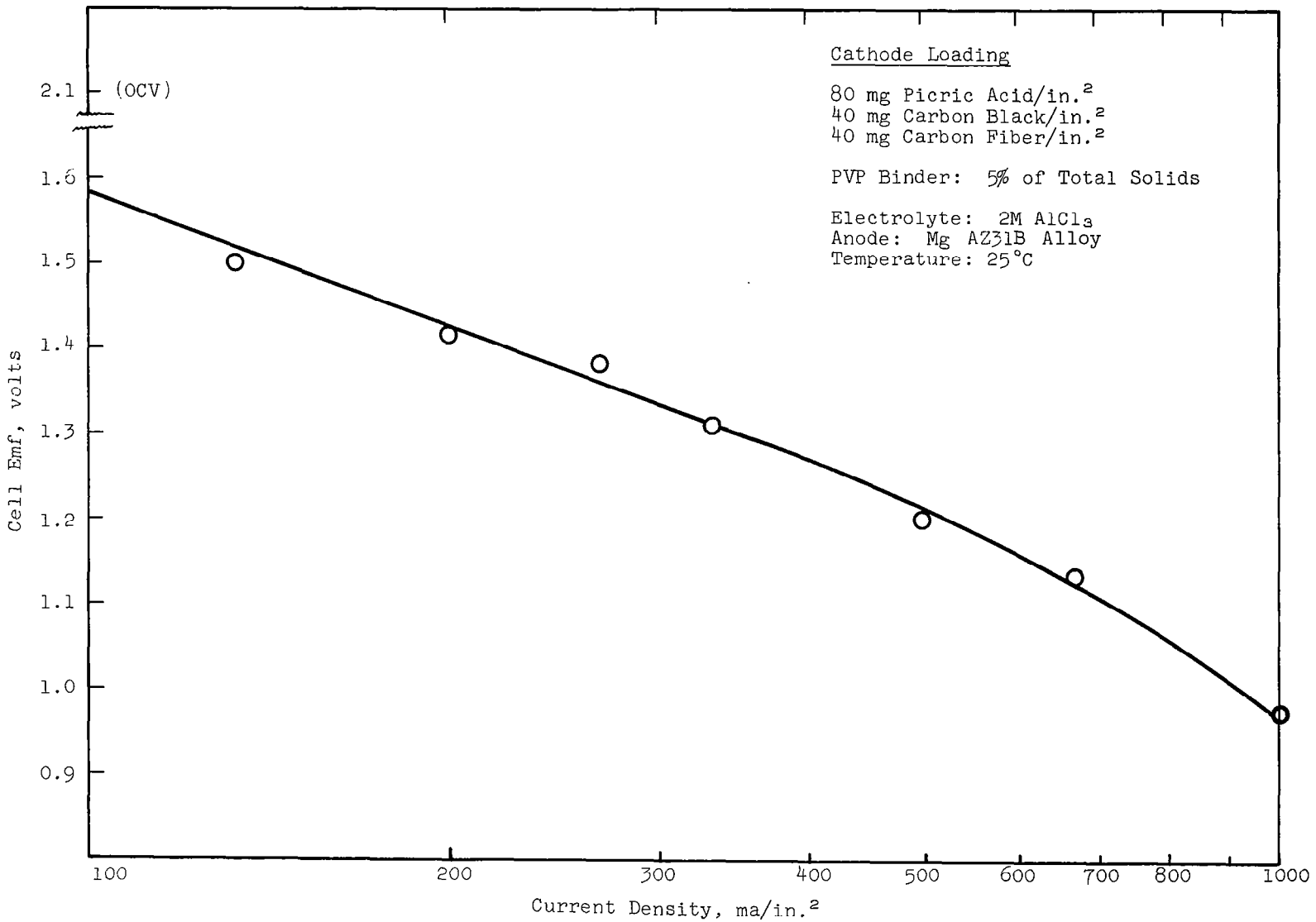

Figure 16. Polarization of Picric Acid Cathode Containing Carbon Fiber

fiber can maintain better than 1 volt vs magnesium at current drains up to 1000 ma/in.^{2} in 2M $AlCl_3$. Coulombic efficiencies of 18-20% were obtained from two discharge experiments at 1000 ma/in.^{2} using expanded magnesium AZ31B alloy as the anode in 2M $AlCl_3$.

(3) Dinitrobenzene and Other Nitro Compounds

(a) Electrolyte Screening

The data reported here for dinitrobenzene and certain other organic nitro compounds represent early work devoted primarily to initial tape configuration studies and electrolyte screening.

A tabulation of o-dinitrobenzene cathode efficiencies when discharged in various electrolytes is given in Table 19.

The best single neutral electrolyte found was 2M $Mg(ClO_4)_2$, and the best overall electrolyte was 2M $AlCl_3$. These electrolytes were therefore used in subsequent tests where other variables affecting discharge characteristics of the nitro compounds were studied.

The electrolyte studies were conducted with the basic (no fiber) type tape cathodes. Where only slight variations in cathode performance were observed, the order of effectiveness of the electrolytes is not defined clearly. However, the considerable advantage of 2M $AlCl_3$ over other electrolytes tested is evident. Its superiority as an electrolyte has also been confirmed in tests with picric acid on the improved (fiber type) tapes.

Two combinations of mixed electrolytes were tested with picric acid. A mixture of magnesium perchlorate with aluminum chloride was used to improve the ease of wetting of the electrodes. (Electrodes were wet more readily in 2M $Mg(ClO_4)_2$ than in 2M $AlCl_3$.) The mixed electrolyte, 1.6M $AlCl_3$ and 0.4M $Mg(ClO_4)_2$ improved the reduction efficiency of o-DNB on tapes with high loadings as shown in Table 20. These tapes have extremely high loadings of depolarizer, and the effectiveness of wetting the electrode is most critical.

A mixture of 2M $AlCl_3$ and 1M Li_2CrO_4 was tested as an electrolyte (Li_2CrO_4 is an inhibitor for magnesium attack). However, the chromate was reduced at more positive potentials than the nitro compounds, o-DNB and picric acid. In addition, either the chromate or its reduction products inhibited discharge of the nitro compounds even after the chromate adsorbed on the electrode was consumed, as shown by Table 21.

Organic acids were incorporated directly into the cathode coating to supply acid at the reaction site without causing corrosion of the magnesium anode. Initial attempts to improve discharge in neutral electrolytes of o-DNB by incorporation of oxalic acid in

Table 19

EFFECT OF ELECTROLYTE ON CATHODIC DISCHARGE EFFICIENCY AT 100 ma/in.^{2}

Cell: Mg/Electrolyte/o-DNB

Electrolyte	Carbon:Depolarizer Ratio	Reduction Efficiency to 0.8 v
Acid Salts		
2M $AlCl_3$*	50:50	62 (at 200 ma/in.^{2})
2M $Th(NO_3)_4$	50:50	29
Neutral Salts		
2M $Mg(ClO_4)_2$	50:50	20-49
2M $Mg(ClO_4)_2$	33:67	15,22
8M NH_4SCN	50:50	29
4M NH_4SCN	33:67	13,20
2M NH_4SCN	33:67	13,18
3M $Mg(ClO_4)_2$	50:50	19,15
1M $MgBr_2$	50:50	17-25
.5M NH_4ClO_4	50:50	18
1M $MgBr_2$ saturated with $Mg(OH)_2$	50:50	9,12

* $FeCl_3$, $ZnCl_2$ and $AlCl_3$ + NH_4Cl mixture proved too corrosive to the magnesium anode for use.

Table 20

EFFECT OF ELECTROLYTE ON CATHODIC DISCHARGE EFFICIENCY AT 200 ma/cm^2

Cell: Mg/Electrolyte/o-DNB

Electrolyte	o-DNB g/in.^{2}	Reduction Efficiency to 0.8 v, %
2M $Mg(ClO_4)_2$	0.125	26.4
1.6M $AlCl_3$; 0.4M $Mg(ClO_4)_2$	0.128 0.129	49.9 49.5
2M $AlCl_3$	0.111	33.0

Table 21

CELL DISCHARGES IN 2M $AlCl_3$ + 1M Li_2CrO_4

Cathode Material	Current Density ma/in.^{2}	Efficiency of Reduction Based on Cathode Material only, %	Amp-min to 0.8 v vs Mg
None	100	-	2.5
Picric Acid	500	20*	2.5
Picric Acid	100	54	3.2
o-Dinitrobenzene	500	20	2.5

* Normal efficiency in 2M $AlCl_3$ is 40%

the tape were not successful. However, incorporation of solid acid (equal weights succinic acid with picric acid) in the new type fiber electrode gave increases in both discharge potential and reduction efficiency in 2M $AlCl_3$ as shown in Figure 17 for low current densities. At 500 ma/in.^{2}, (Figure 18) improvement in reduction efficiency was obtained in 2M $AlCl_3$. It is possible that an acid with higher water solubility might be more effective at higher current drains. This technique was not emphasized primarily because of weight penalty incurred compared with supplying acid directly in the electrolyte.

2,4,5-Trinitrotoluene (TNT) would not maintain 0.8 v vs magnesium at 500 ma/in.^{2} in 2M $AlCl_3$ and was reduced at the lowest potentials of all the depolarizers in 2M $Mg(ClO_4)_2$ at 100 ma/in.^{2} as shown in Figure 19. The energy output of TNT may be improved by using a smaller particle size.

1-Carboxymethyl-3,3,5,5-tetranitropiperidine was almost completely inactive in the acid electrolyte, 2M $AlCl_3$. Its discharge in 2M $Mg(ClO_4)_2$ was flat, but both reduction efficiency and discharge potential were low, as shown in Figure 20.

2,5-Dinitrothiophene was discharged at higher potentials than the 2,4- isomer (see Figures 19 and 20) as would be expected from its structure (the nitro group in the 5- position is made more reactive to reduction by the electron withdrawing effect of the nitro group in the 2- position). Both isomers had flat discharges in 2M $Mg(ClO_4)_2$ at 100 ma/in.^{2}, but efficiencies were low. The 2,5-isomer did not maintain 0.8 v vs magnesium in 2M $AlCl_3$ at 500 ma/in.^{2} (See Figure 21).

2,5-Dinitrothiophene was checked on fiber-type electrode configurations. Efficiencies of reduction were the same on both type electrodes in 2M $Mg(ClO_4)_2$ at 100 ma/in.^{2} (13%) and in 2M $AlCl_3$ at 100 ma/in.^{2} (38%), indicating that the depolarizer activity and not the limits of the electrode configurations were measured on both type electrodes.

3,6-Dinitrophthalic acid has the advantage of having two equivalents of acid in its molecule. It is also very soluble in water. It had a high potential in the early part of the discharge at 100 ma/in.^{2} in 2M $Mg(ClO_4)_2$ (Figure 20) but did not maintain higher current drains well. Its theoretical capacity is low compared with that of picric acid and it appears to offer no advantage to compensate for this.

(b) Particle Size of Depolarizer

The coulombic efficiency of the m-DNB/Mg couple in 2M $MgCl_2$ increased from 8 to 25% as the particle size of the m-DNB was reduced from 200 to 48 μ, respectively.

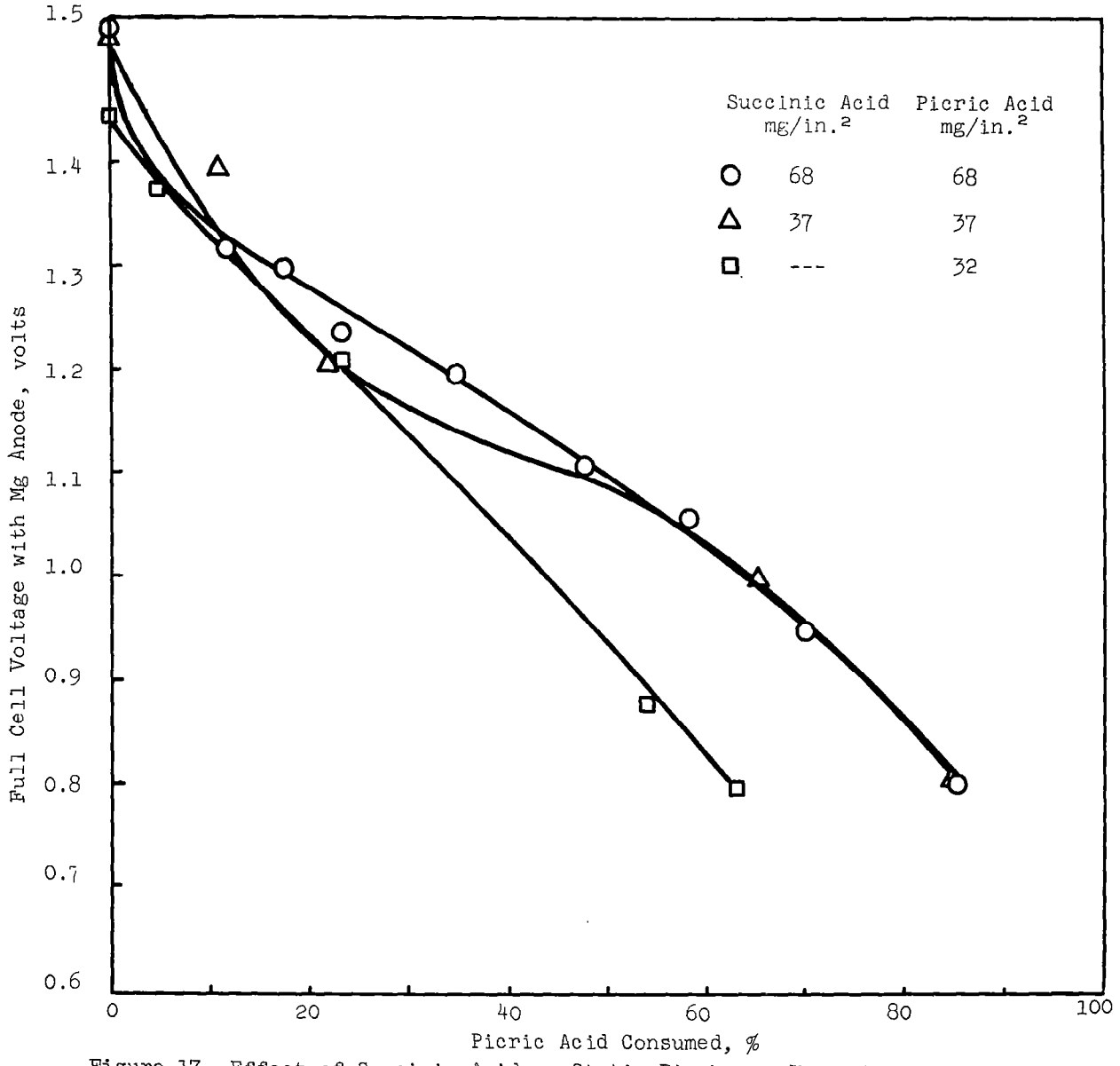

Figure 17. Effect of Succinic Acid on Static Discharge Characteristics of Picric Acid in 2M $AlCl_3$ at 100 ma/in.²

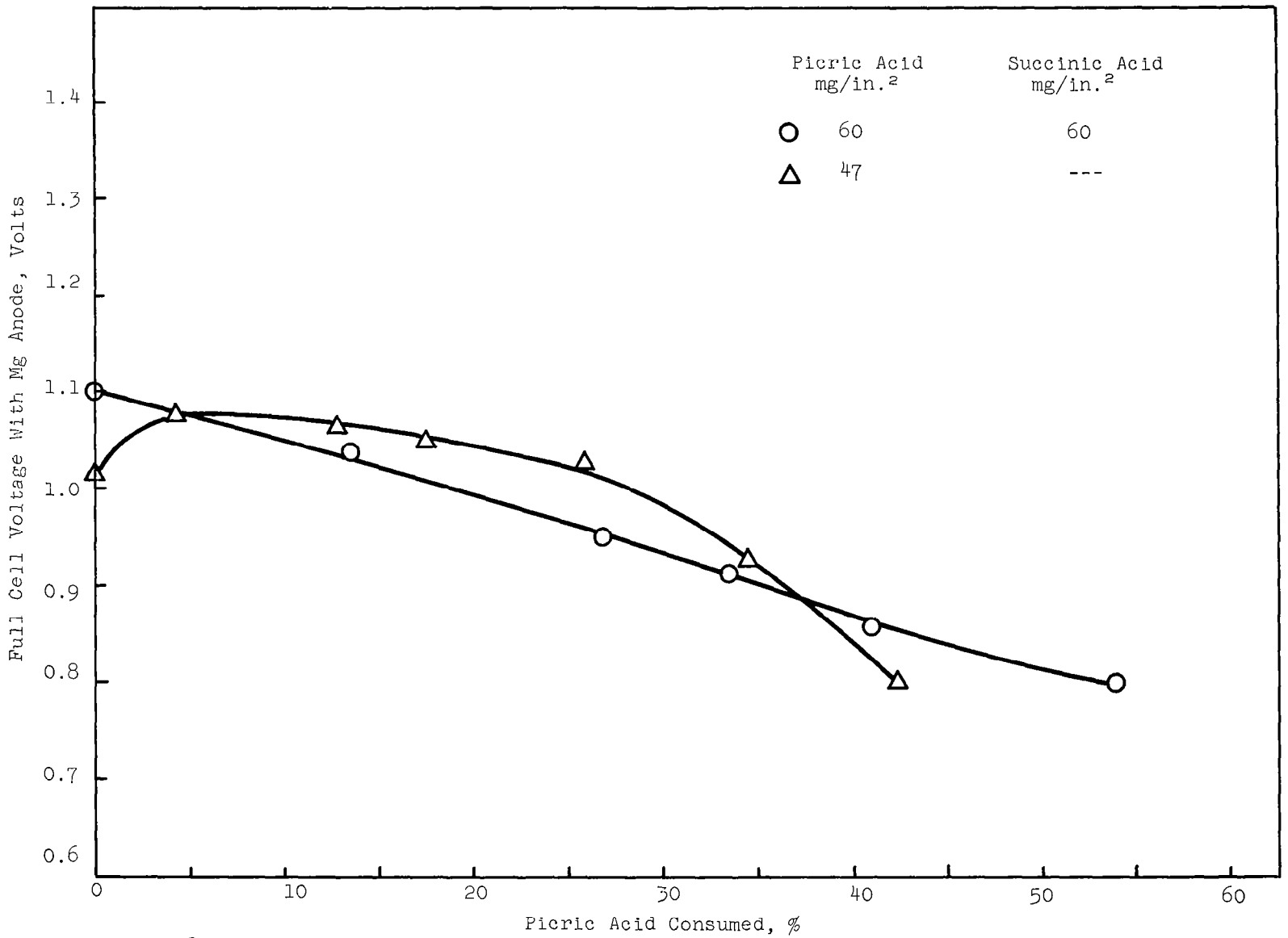

Figure 18. Effect of Succinic Acid Content on Static Discharge Characteristics of Picric Acid in 2M $AlCl_3$ at 500 ma/in.²

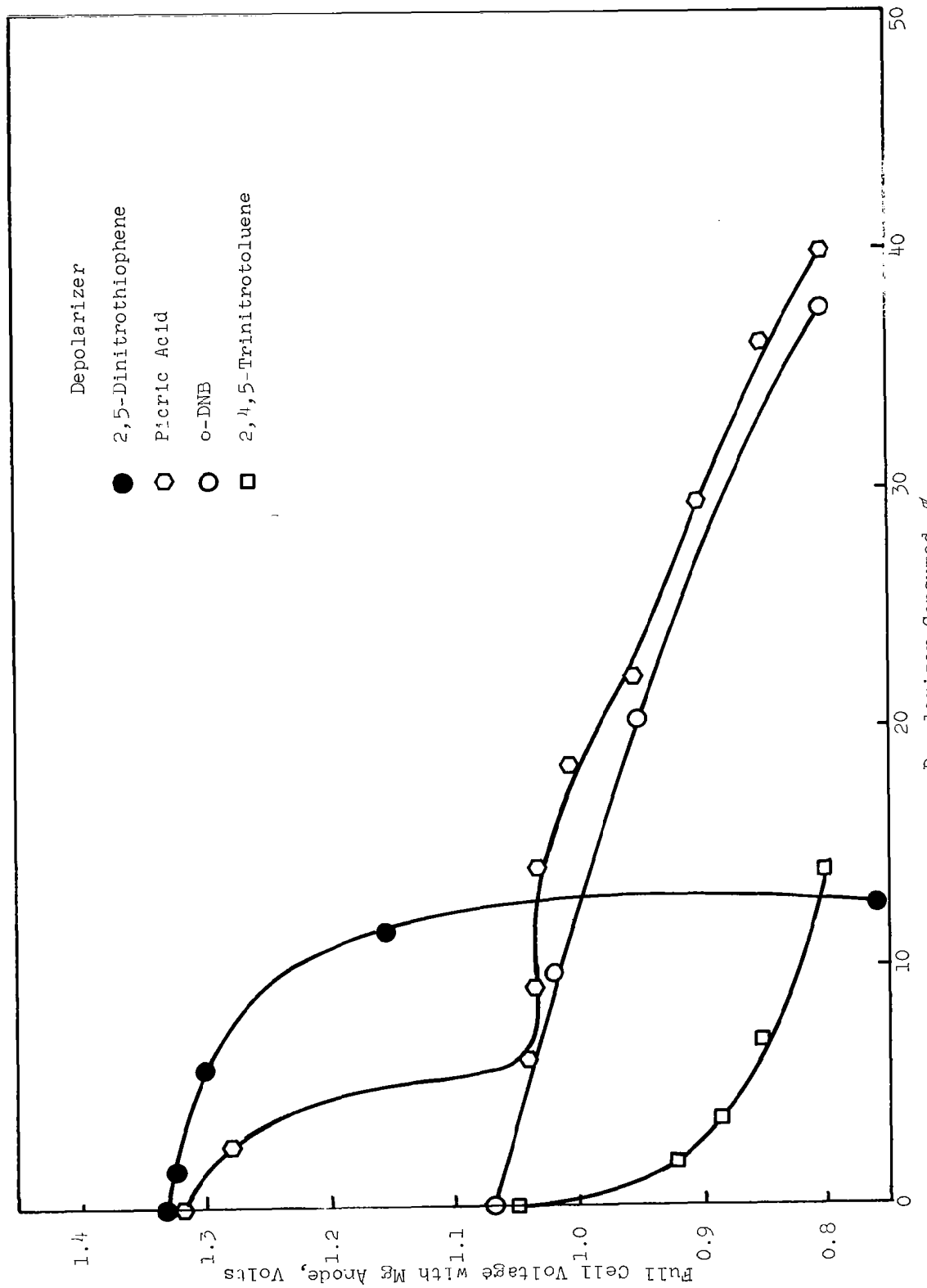

Figure 19. Static Discharges of Various Depolarizers in 2M $Mg(ClO_4)_2$ at 100 ma/in.^{2}

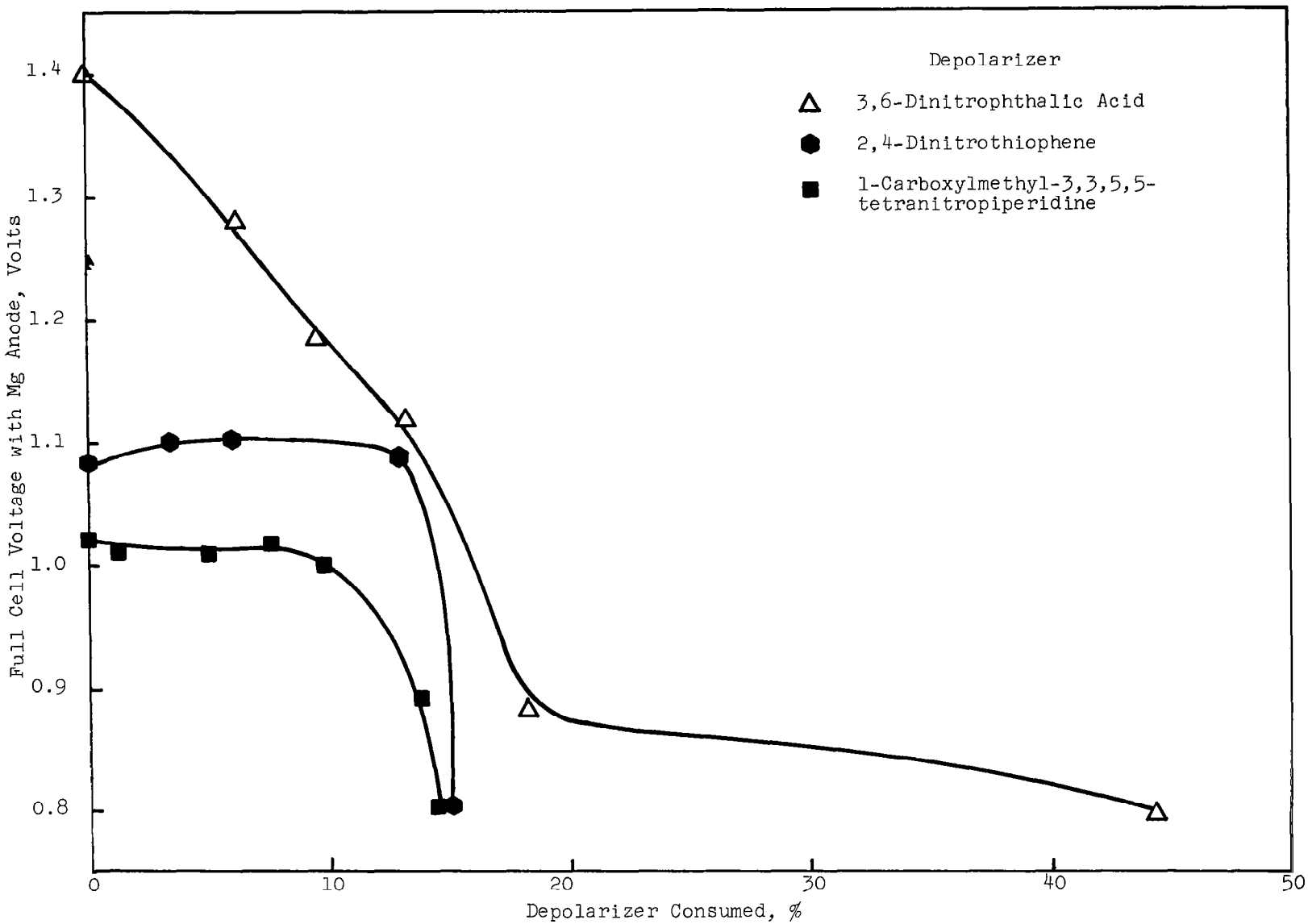

Figure 20. Static Discharge of Various Depolarizers in 2M $Mg(ClO_4)_2$ at 100 ma/in.^{2}

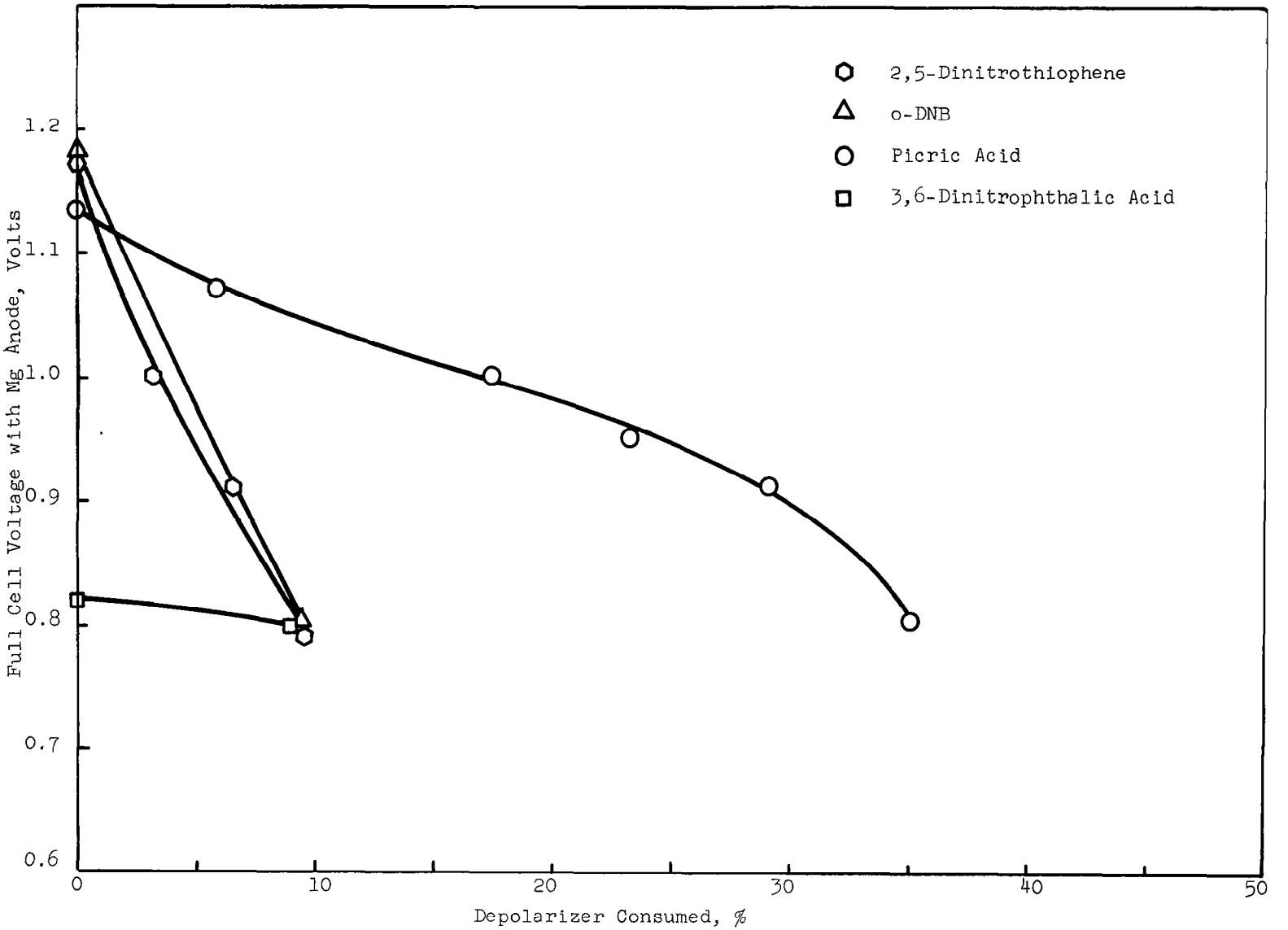

Figure 21. Static Discharges of Various Depolarizers in 2M $AlCl_3$ at 500 ma/in.^{2}

Reduction of particle size of o-DNB to 48 μ, however, did not increase reduction efficiency. Particle sizes of other depolarizers (except TNT) were similar to that of o-DNB. The particle size of TNT was slightly larger. Since TNT has very low solubility in water, its cathodic discharge may be improved by particle size reduction. The relatively high solubility of potassium periodate and picric acid eliminates particle size as a major discharge parameter.

(c) Catalysts

Palladium appeared to catalyze the discharge of o-DNB in 2M $AlCl_3$. The best test result gave an increase of 0.2 v in the discharge potential of o-DNB at 200 ma/in.^{2} (Figure 22) for a 1.2% loading of palladium* Catalysis was evident in a duplicate tape at low current densities but was ineffective at 500 ma/in.^{2}. This same cathode composition exhibited no catalytic effect in 2M $Mg(ClO_4)_2$. Another catalyst formulation, 2.5% palladium prepared by chemically reducing palladium on Shawinigan black by hydrazine, exhibited only a minor catalytic effect with o-DNB in 2M $AlCl_3$ (Figure 22). Similarly, small increases in discharge potential were obtained with picric acid as depolarizer. Palladium has been reported as a catalyst for m-DNB in sulfuric acid electrolyte (ref. 4).

(4) Trichlorotriazinetrione and Hexachloromelamine

The active halogen compounds trichlorotriazinetrione (also known as trichloroisocyanuric acid) and hexachloromelamine both have theoretical energy densities over 750- watt-hr/lb cell when coupled with magnesium. Little work has been done with these materials in improved electrode configurations, but preliminary experiments with both pressed powder and slurry cast tape electrodes in a variety of electrolytes have shown that they can be discharged successfully at practical current drains. Some representative data are contained in Table 22.

The operating voltages for both trichlorotriazinetrione (Figure 23) and hexachloromelamine are close to 2.0 volts. The hexachloromelamine data represents the best single run. Wet out difficulties were encountered due to the nature of the coating. Use of latest electrode manufacture technique should result in improved operation.

In addition to their significantly higher energy capacity compared with electrodes described above, these active chlorine compounds offer several other advantages. Since neutral electrolytes can

* 5% palladium on carbon, Englehard Industries, Inc., Newark, New Jersey

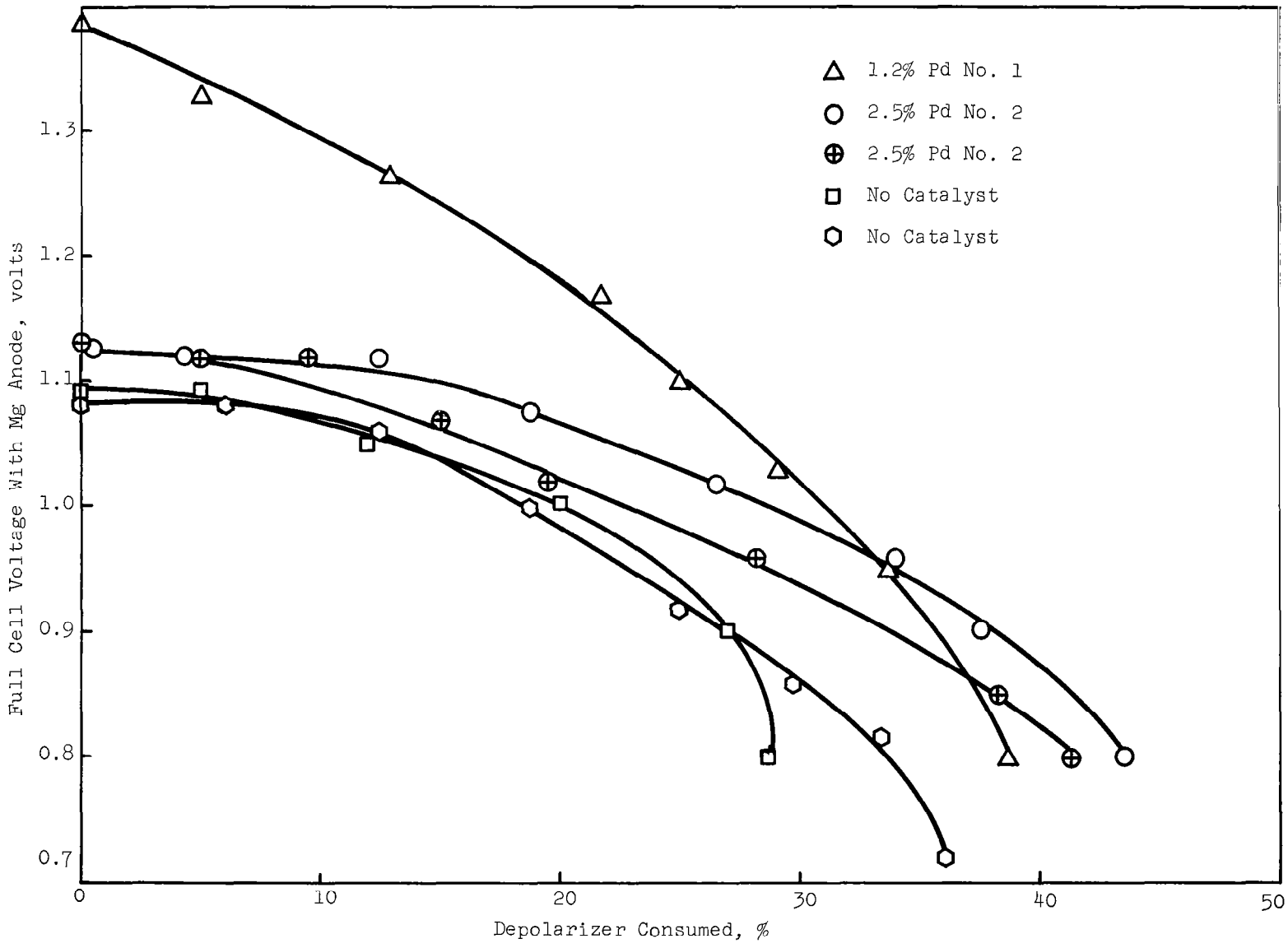

Figure 22. Effect of Catalysts on Static Discharge of o-Dinitrobenzene at Carbon Cathode in 2M $AlCl_3$ at 200 ma/in.^{2}

Table 22

DISCHARGE CHARACTERISTICS OF ACTIVE CHLORINE CATHODES

ANODE--Mg AZ31B ALLOY

Cathode	Conductor	Cathode:Conductor Volume Ratio	Electrolyte	Electrode Type	Current Density ma/in.^{2}	Cathode Efficiency to 1.5 v %
2,4,6-Trichlorotriazinetrione	Graphite A-625	1:1	4M LiBr	pressed powder	100	60
2,4,6-Trichlorotriazinetrione	Graphite A-625	1:1	2M NaCl	pressed powder	100	55
2,4,6-Trichlorotriazinetrione	Graphite A-625 and Acetylene Black Mix.	1:1	2M $Mg(ClO_4)_2$	pressed powder	100	50
2,4,6-Trichlorotriazinetrione	Graphite A-625	1:1	2M $AlCl_3$	pressed powder	100	50
2,4,6-Trichlorotriazinetrione	Acetylene Black	1:1	2M $Mg(ClO_4)_2$	water slurry	100	49
2,4,6-Trichlorotriazinetrione	Acetylene Black	1:1	2M $Mg(ClO_4)_2$	hexane slurry	100	50
Hexachloromelamine	Acetylene Black	1:1	2M $Mg(ClO_4)_2$	water slurry	100	30

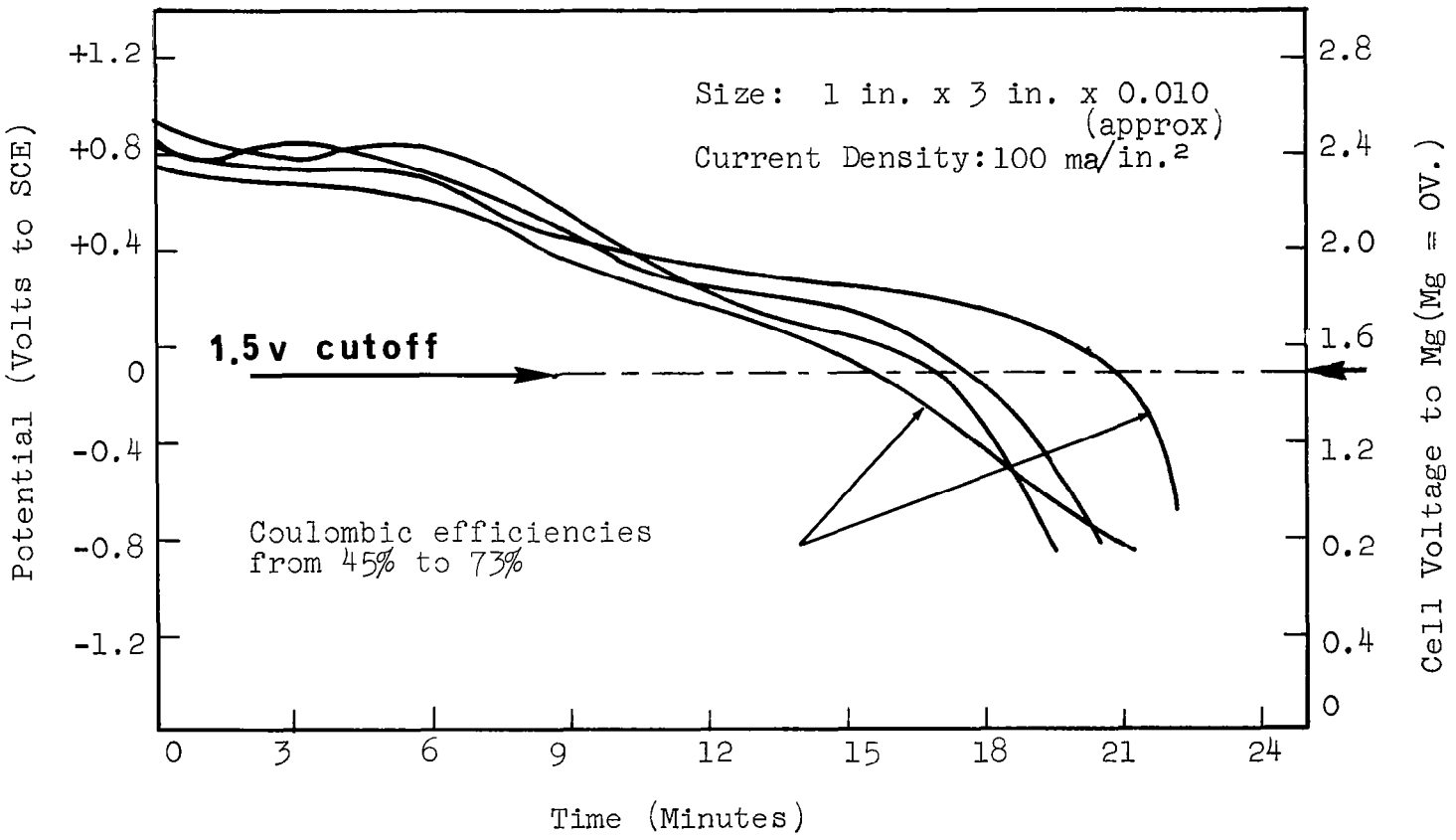

Figure 23. Typical Discharge Curves of 2, 4, 6,-Trichlorotriazine-trione Cathode

be used, anode corrosion can be reduced, and the severe weight penalty incurred by acid electrolyte can be reduced. Graphitec conductors and higher packing densities (up to 60% compared with 20-30% for other cathodes studied) may be employed which will result in thinner and mechanically more stable tapes.

At the present time, these materials offer the most promise for achieving in an aqueous system an ltimate goal of 200 watt-hr/lb delivered in a final package.

4. Conclusions

High energy couples can be discharged efficiently at high current drains in the dry tape electrode configurations. Efficiencies of 80% at 500 ma/in.^{2} are obtained with potassium periodate and picric acid when discharged versus magnesium in an acid electrolyte. The potassium periodate-magnesium cell operates at 1.9-2.1 volts while the picric acid-magnesium cell operates at 1.0-1.2 volts. Both periodate and organic nitro compound cathodes require large amounts of acid for satisfactory discharge. Electrolyte requirements for the periodate system comprise about 60% of total cell weight. The electrolyte weight burden makes ultimate power densities substantially higher than 100 watt-hr/lb unlikely for these systems.

Magnesium, in a tape configuration, can be discharged efficiently with no gassing polarization in acid aqueous electrolytes comprised of aluminum chloride or mixed aluminum chloride-hydrochloric acid.

Tape electrode configuration and operation capability appears to be applicable to high energy couples in general. Incorporation of more active components can now proceed with a minimum of electrode design work required. In preliminary studies, the active chlorine compounds, hexachloromelamine and trichlorotriazinetrione, were discharged versus magnesium in neutral electrolyte at 100 ma/in.^{2} with a 2.0 volt cell emf using a standard cathode tape configuration.

C. INCAPSULATION

1. Background

The operation of the tape battery requires the supply of a sufficient quantity of electrolyte to the discharge area for efficient discharge. The electrolyte must be storable and compatible with stop-start operation.

Three methods of meeting these requirements have been examined: (1) a bottle-pump system; (2) macroincapsulation; and (3) microincapsulation. With the latter two methods, the metering of electrolyte is inherent in the design; the first requires some means of metering. Microincapsulation (capsule size under 1000 μ) also offers the possibility of incorporating the electrolyte within the tape itself.

In considering the method for electrolyte supply, the amount and fraction of tape weight due to electrolyte must also be considered. As discussed elsewhere in this report, the electrolyte weight is a large portion of the total tape weight. Therefore, the method of supply must provide a high payload of electrolyte, both initially and after extended storage. In micro- or macroincapsulation, the capsule wall thickness must be minimized to provide a high payload. The smaller the capsule size, the thinner the wall must be to maintain the same payload. Consequently, the wall material must be more impermeable to meet storage requirements. The bottle-type supply eliminates this problem. It is effectively a giant macrocapsule and provides high payloads irrespective of the wall thickness.

The present contract effort was concentrated on macroincapsulation of aqueous electrolytes. Some work on microincapsulation was subcontracted to the Southwest Research Institute. This work indicated that microincapsulation of aqueous electrolyte would fulfill requirements only under special conditions. Microincapsulation may be useful for nonaqueous electrolytes or, in certain cases, for cathode or anode materials. A bottle-type system was not investigated other than to estimate the weight involved for purposes of comparison.

2. Macroincapsulation

a. Design Considerations

An electrolyte feed rate of 200 mg/in.^{2} of tape was used as a basis for designing a macroincapsulation system. While this was considerably in excess of theoretical requirements for originally anticipated capacities of 1 amp-min/in.^{2}, excess electrolyte will always be required to wet the active components and separator. A supply method such as that in Figure 24 was considered for using a single string of packets to supply two tapes. This

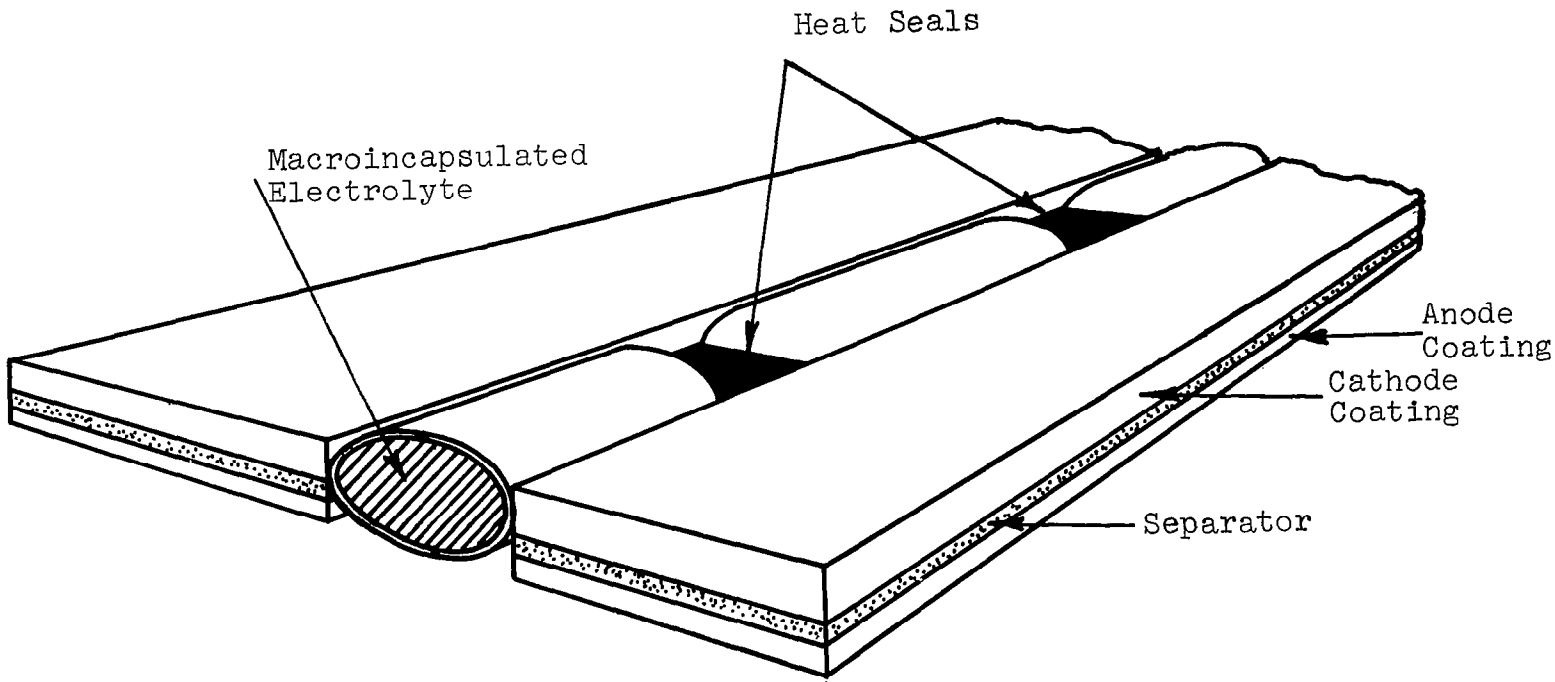

Figure 24. A Proposed Configuration for Tape-Electrolyte Incapsulation

arrangement offers the advantages that (1) the container material is not on the tape surface and will not interfere with the discharge, and (2)puncture of the capsule followed by passage through rollers will efficiently distribute electrolyte to the two tapes with little loss. The packet width would be varied to supply the desired quantity of electrolyte. A summary of preliminary payload calculations for this type of incapsulation is given in Table 23. The cylindrical cross-section shows not only a higher initial payload than the elliptical cross-sections but also lower loss on storage because of the lower surface-to-volume ratio.

Further work discussed below led to selection of tubing for incapsulation since it provided higher payloads and greater reliability than packets formed from film sealed on all sides. To supply the quantity of electrolyte required, the tubing must be sized to the tape dimensions, loading, and number of tapes. To cover the anticipated range of electrolyte requirements and to allow rapid estimation of payloads for design purposes, the volumetric capacity and payload of various tubing sizes should be known. The volumetric capacity of a tube is easily calculated from its dimensions. To allow for the reduction of this capacity due to heat seals, payloads were determined experimentally on finished packets made from several sizes of tubing. Using these data, a "squash factor" was calculated for each size tube where the "squash factor", β, is the ratio of the experimentally determined volume to the calculated volume of the tube. As would be expected, β decreases as the tube size increases, as shown in Figure 25.

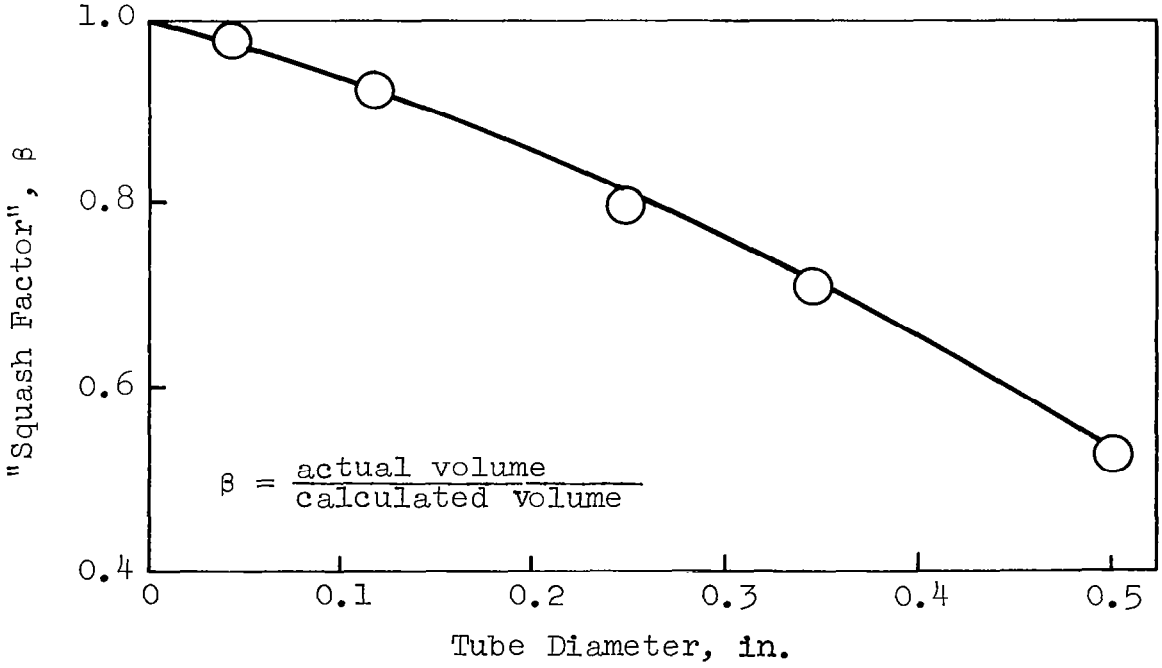

Figure 25. Reduction in Capacity of Kel-F 81 tubing Due to Heat Seals

Table 23

CALCULATED PAYLOAD AND SURFACE AREA-TO-VOLUME RATIO FOR CAPSULES OF ELLIPTICAL CROSS SECTION*

Axis of Ellipse, mils		Internal Volume	Initial Payload	Surface Area per Unit Volume	Payload** 3 Years
Major	Minor	cc	Wt-%	cm^{-1}	wt-%
300	10	0.20	82	40	60
150	10	0.10	80	31	65
150	20	0.15	83	28	68
130	130	0.20	90	13	80

* Capsule length - 1 in.; film density - 2.1 g/cc; film thickness - 1 mil; electrolyte density - 1 g/cc, includes allowance for heat seals

** Assuming 50% relative humidity difference at 25°C and film permeability of 0.002 g-mm/24 hr-sq m-cm Hg

The squash factor will also vary with wall thickness and type of material. The calculated payload and capacity for tubing covering the estimated range of electrolyte requirements is shown in Figure 26. Experimental payloads are shown for comparison.

The effects of wall thickness and film density parameters on payload are readily apparent in Figure 26. Initial payloads and tubing sizes for a specified electrolyte requirement can readily be obtained by reference to Figures 25 and 26. Further variation in liquid capacity can be achieved by changing the packet length. Other factors needed to complete the incapsulation specification are film permeabilities (i.e., loss rates) and electrolyte release efficiency. Experimental results on loss rates of electrolytes from capsules under various conditions are given in a later section. Work on electrolyte release indicates that at least 90% of the incapsulated electrolyte can be transferred to the tape.

b. Incapsulating Materials

Since electrolyte weight will be a major portion of the total weight of a completed system, it is necessary to obtain a high payload of electrolyte. This requires use of the thinnest, least dense containing materials consistent with permeability requirements. For the configuration illustrated in Figure 24, initial payloads greater than 80% are obtainable with film thicknesses of 1 to 2 mils (depending on film density) as the calculations summarized in Table 23 show. Payloads greater than 60% are obtained after three years if the film permeability is of the order of 0.002 g-mm/24 hr-sq m-cm Hg.

From these considerations and the general characteristics desired, thermoplastic films are the choice for capsule material. Thermoplastics also offer the advantage of relatively simple capsule fabrication by conventional sealing methods, the seals generally being at least as impermeable as the film. Permeability and density data of the more impermeable thermoplastic materials available as thin films are summarized in Table 24. It is apparent that a film thickness greater than 2 mils is needed with most thermoplastics to obtain the low electrolyte loss level with aqueous electrolytes.

c. Capsule Fabrication

Of the numerous methods for sealing or joining thin thermoplastic films, thermal impulse and ultrasonic sealing have the widest applicability to the materials of interest in this work. A thermal impulse sealer, Sentinel Model 12-12AS, was used to produce capsules of Aclar, Scotchpak 25A20 (a Mylar- aluminum laminate), etc., and polyethylene films with satisfactory results. Integral seals of good strength were obtained on all materials after the proper sealing conditions had been established. Both

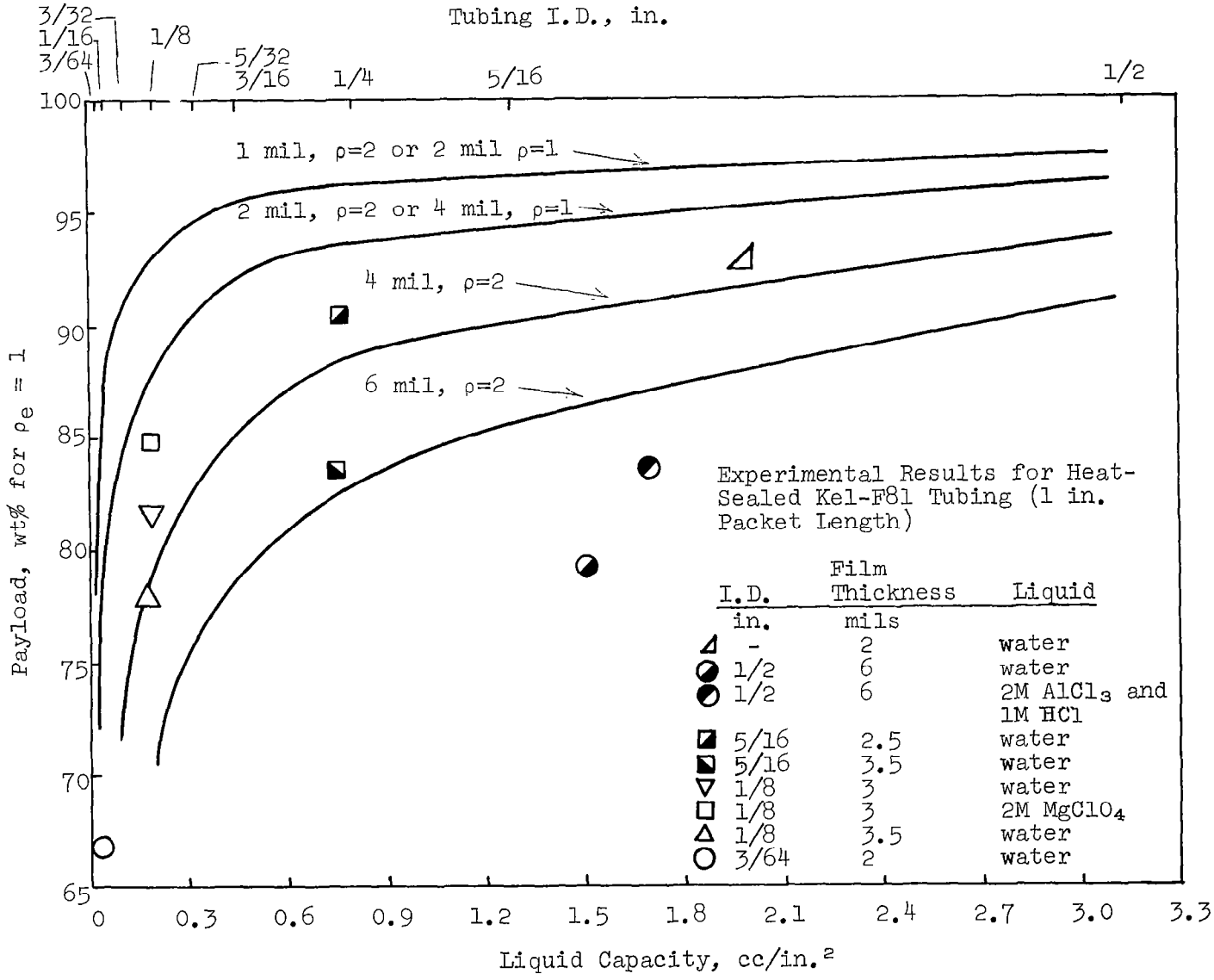

Figure 26. Calculated Film Thickness-Density-Payload Relationship for Tubing Without Heat Seals and Comparison with Actual Incapsulations

Table 24

PERMEABILITY TO GAS AND WATER VAPOR OF INCAPSULATION FILMS

Material	Thickness Mils	Approx. Density g/cc	Water vapor[1] Permeability g-mm/24 Hr. m^2-cm Hg at 25°C	Gas Permeability[1] cc(STP)-mil/100 $in.^2$-24 Hr-atm at 75°F	Polymer Type	Supplier
Teflon FEP Type A	2, 3	2.15	0.002		Copolymer TFE and HFP	E. I. DuPont Wilmington, Del.
Teflon TFE Type HB	2	2.1-2.2			Polytetrafluoroethylene	Dielectrix Corp. Farmingdale, L. I. New York
Aclar Type 33C	2	2.12	0.001-0.002[2]	CO_2 - 16	Polytrichloroethylene	Allied Chemical Morristown, N. J.
Aclar Type 33C	5			O_2 - 7		Carmer Industries Parsipinee, N. J.
Kel-F-81 (Tube)	2, 2.5, 3.5	2.1-2.2	0.015[3]		Polytrichloroethylene	Adam Spence Corp. Union, N. J.
Mylar-Aluminum-Mylar	1-0.5-1	1.1	0.003[4]			3-M Company St. Paul, Minn.
Polyethylene	1, 2	0.9-0.96	0.02-0.08	CO_2 - 1000 O_2 - 350		
Polypropylene		0.9	0.06			
Saran		1.2-1.7	0.01-0.03	CO_2 - 5 O_2 - 1	Vinylidene chloride Vinylchloride copolymer	
Mylar		1.4	0.05-0.1[5]	CO_2 - 25 O_2 - 8	Polyester	

[1] Data from ref.12 for water vapor transmission and ref. 5 for gas permeability

[2] Estimated from value of 0.015g/100 in^2 - 24 hr. for 2 mil film at 100°F and 90% relative humidity (RH), ref. 5.

[3] Estimated from data of Sivadjian and Ribeiro, ref. 14

[4] Estimated from value of 0.02g/100 in^2 - 24 hr. at 100°F, ref. 16

[5] Estimated from value of 110 g-mm/100$in.^2$-hr. at 103°F and 95% RH, ref. 12

tetrafluoroethylene-hexafluoropropylene copolymer (FEP) and tetrafluoroethylene (TFE) types of Teflon sheet have been sealed without undue problems. The TFE Teflon sheet* was supplied with one surface treated to make it heat bondable.

To form incapsulations from film material, the film was first sealed down two sides and at one end to make a tube of the desired length. The tube was then filled with the required liquid and heat sealed at intervals from the closed end to form a string of packets. When tubing was used as the starting material, the tube was sealed at one end and filled, and seals were made at intervals, normally one inch apart.

A narrow heat seal is desirable to minimize reduction of capsule payload due to seals. The upper head of the heat sealing unit was redesigned to reduce the clamping width from one in. to 3/16-in. The seal width was also reduced by using 1/16-in. wide heating ribbon rather than the 1/8-in. ribbon originally supplied. Occasional failure of the thinner heating ribbon has been minimized by lowering the tension on the ribbon proportionately. A partial cross section of the modified sealing head is shown in Figure 27 with the heads in the open position.

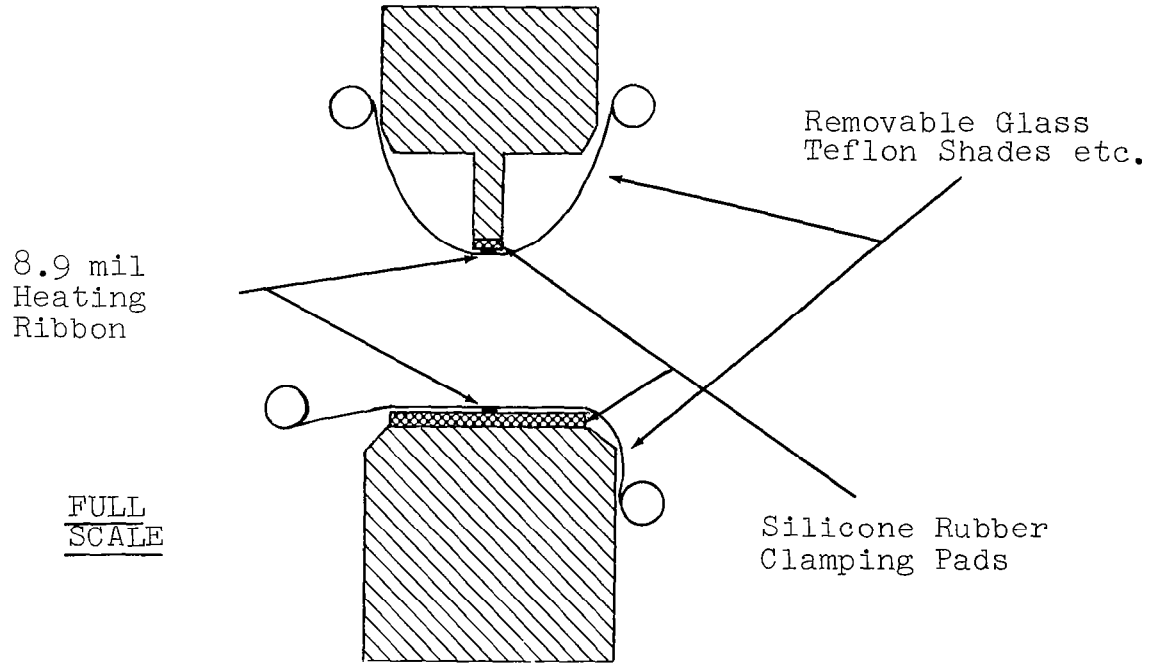

Figure 27 . Cross Section of Modified Heat Sealer Head

* Dilectrix Corp., Farmingdale, L.I., N.Y.

The heat sealer* provides control of a wide range of sealing variables, allowing almost any thermoplastic film to be heat sealed. Jaw clamping pressure, clamping time, heat impulse time, and heater voltage can all be varied independently to determine the conditions required for a particular type of film.

Final incapsulation manufacture from the selected Kel-F 81 tubing was readily accomplished in the lengths required with our present equipment. Finished incapsulations were rapidly tested by short-term (2-3 days) measurement of weight loss in vacuum at 39°C. A defective incapsulation can be detected by this test. Some of the finished incapsulations are shown in Figure 28.

d. Capsule Electrolyte Loss

The transmission of a vapor or gas through a polymer film takes place primarily by a diffusion controlled mechanism, wherein the gas dissolved in one surface of the film, passes through by an activated diffusion process, and evaporates from the opposite surface. Under steady-state conditions, and assuming that the diffusion coefficient, D, is not concentration dependent, the rate of permeation through the film per unit area, q, can be expressed by

$$q = \frac{D(c_1-c_2)}{t} \qquad (1)$$

where this film thickness, and c_1 and c_2 are the concentrations at the high and low pressure surfaces, respectively. Applying Henry's law,

$$q = \frac{DS(p_1-p_2)}{t} \qquad (2)$$

where S is the solubility of the vapor in cc/cc of polymer at a pressure of 1 cm Hg with the volume corrected to S.T.P., and p is the vapor pressure. The permeability c nstant, P, may be defined as cc of gas at S.T.P. permeating per second through a film of 1 cm^2 area and 1 mm thickness under a pressure difference of 1 cm Hg and may be expressed as

$$P = DS = \frac{tq}{p_1-p_2} \qquad (3)$$

For gases, P should be independent of thickness and pressure, while for vapors it may increase with pressure.

The temperature dependence of P may be expressed as an Arrhenius relationship:

$$P = P_o \exp(-E_p/RT) \qquad (4)$$

---

* Sentinel Model 12-12AS, Packaging Industries, Montclair, N.J.

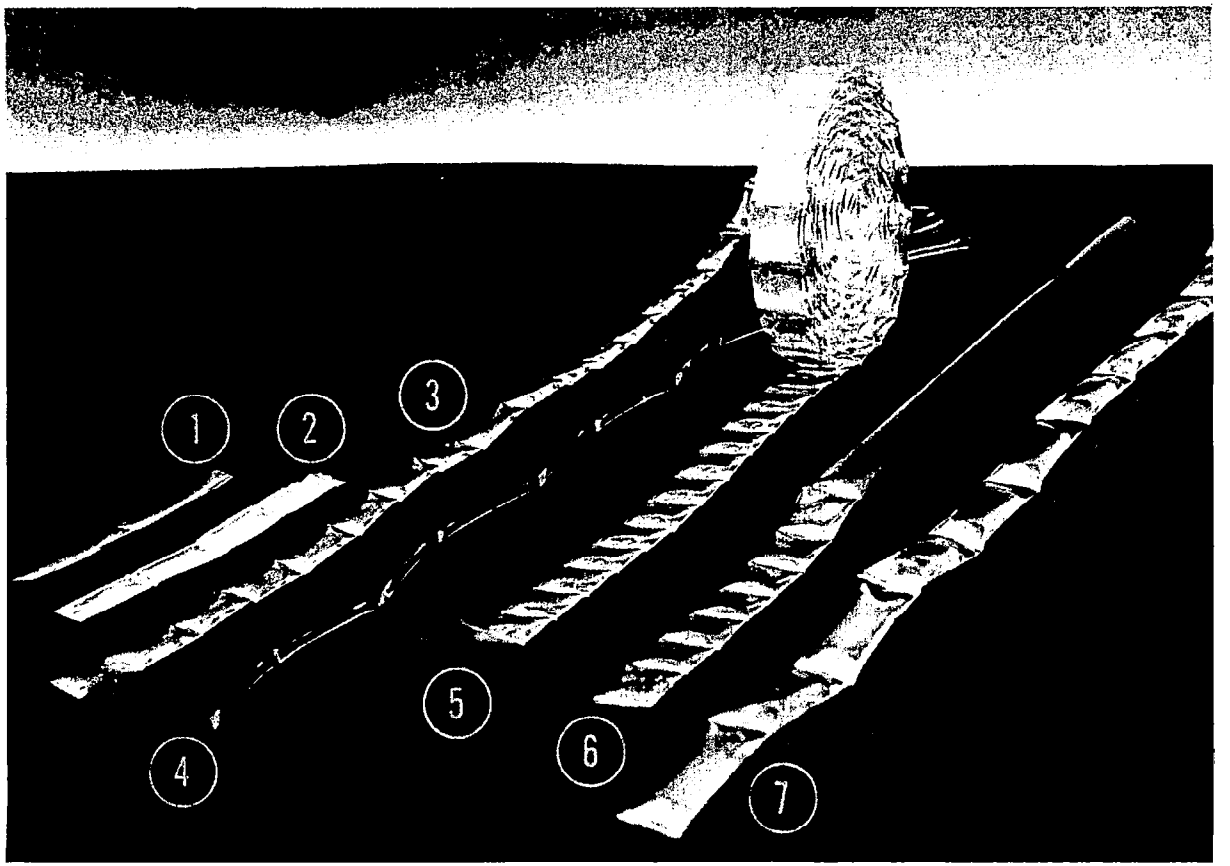

1. Al-Mylar, 2.5-mil wall
2. FEP Teflon, 2-mil wall
3. Kel-F 81, 5/16-in. x 3-mil wall
4. Kel-F 81, 1/8 in. x 2.5-mil wall
5.and6. Kel-F 81, 1/2 in. x 6-mil wall
7. same, 2 in. packet length

Figure 28. Incapsulated Electrolyte Configurations Formed by Heat Sealing

where E_p is the activation energy associated with the overall permeation process, and P_o is a constant. Since both the diffusion coefficient and the solubility depend on temperature, equation (4) will usually only approximate the temperature dependence of P. For pinhole-free films showing very low solubility for a vapor, the above relations should be quantitative and independent of whether a liquid or its vapor contact the film. The results should also be independent of the level of the relative humidity difference.

(1) Method

Various methods (refs. 5 through 10) have been employed to measure the permeability of thin films. A diffusion cell method, employed by Barrer (ref. 5), depends on measurement of the pressure rise with time in a previously evacuated chamber that is sealed by the test sample. A modification of the Patra method (ref. 7) involves weighing a dish, filled with desiccant, enclosed by the film and stored in a cabinet of constant temperature and humidity. A hydrophotographic method, depending on the sensitivity of a double silver and mercury salt to moisture, has been developed recently by Sivadjian (ref. 11). It should be noted that considerable variations in measured permeabilities have been found for different samples of the same material and for different measurement methods.

For our purposes, it was felt that tests on the completed incapsulations would be desirable since the results would then include any effects of heat seals, handling, etc. The gravimetric method used involves storing of capsules under the desired conditions and weighing them at intervals of time depending on the loss rate expected. The permeabilities of the films used are so low that the time during which the capsules were removed from controlled conditions for weighing is negligible compared to the total storage time and should not have affected the test results.

Three test conditions were used in the evaluation of incapsulations-ambient storage (approximately 25°C and 50% R.H.), and storage under vacuum at 25°C and 39°C (0% R.H.). Capsules of various dimensions were sealed as described in Section II.C.2.C. Water, 2M $Mg(ClO_4)_2$, 2M $AlCl_3$, and 30% KOH have been incapsulated in the films selected for tests. Physical data on the types of capsules tested are given in Table A-3 (Appendix).

Composition analyses were also made for incapsulations of aqueous potassium hydroxide to determine the relative effects of moisture loss and carbon dioxide up take through the capsule wall. In these tests, the composition of electrolyte was determined by standard titration methods using capsules stored for various lengths of time.

(2) Test Results

(a) Water Incapsulations

Initial tests of finished packets were made with water in a number of candidate films at ambient conditions. Test data on these capsules formed by thermal impulse sealing are summarized in Table 25 and Figure 29. While the 1-mil polyethylene capsule shows a large weight loss, the film density is low and, consequently, the payload is high. However, extrapolation of the data obtained indicates that after 100 days, the polyethylene capsule payload would be below that of the Al-Mylar capsule and below that of the Aclar film in 150 days. Use of a thicker polyethylene film would lower the initial payload but improve the slope of the payload versus time curve. It is necessary that the payload be essentially constant so that the quantity of electrolyte supplied will show no variation with time.

For comparison of weight loss data on films, all capsules should have the same specific surface area, i.e., the same area per unit volume of liquid incapsulated. This is illustrated by the results shown in Figure 30 for Aclar capsules with different specific surface areas. Obviously, the higher the specific surface area, the greater the percentage weight loss shown. A better comparison of film materials is obtained when packet dimensions vary by using the weight loss per unit area as shown in Figure 31. Here, the same incapsulations indicated in the previous illustration show about the same weight loss per unit area. Comparison of weight loss data for packets made from various films is shown in Figures 32, 33, 34 and 35.

The data are shown as weight loss per unit area of capsules, the area being estimated from the physical dimensions of the incapsulation. The fluorohalocarbon materials (Figure 32) show the lowest vapor transmission, with consistent results being obtained except for incapsulation number 4. The jump shown here after 14 days is believed to be due to a loss of a small portion of the film in handling since the continuation of the tests shows the same loss rate as obtained in the initial portion of the test. The Al-Mylar incapsulations show a much wider range of vapor transmission rates (Figure 35), the lowest of these rates being comparable with those obtained on the fluorohalocarbons. The wide variation is believed due to the heat seals since the higher loss rates were usually from capsules with proportionately greater heat seal length. The vapor transmission rates of FEP and TFE types of Teflon (Figure 33) are consistently higher than those of the fluorohalocarbon materials tested. With the exception of capsule E20, which showed a rapid increase in transmission after 25 days, the results are consistent. The increase noted with E20 is believed due to a failure of a small portion of the seal. The polyethylene incapsulations showed high loss rates (Figure 34) as expected, and would be unsuitable for most applications even though the film density is low.

Table 25

TEST DATA ON THERMAL-IMPULSE SEALED WATER MACROCAPSULES

Test Conditions: Ambient Temperature (25°C), atm. pressure
40 to 50% relative humidity

Material	No.	Film Thickness mils	Film Weight g	Liquid Loading cc/in.	Surface Area/Unit Weight $in.^2/g$	Initial Payload wt-%	Payload After Days	Payload After wt-%	Remarks
Al-Mylar 25A20	1	2.5	0.032	0.33	1.56	83.8	70	82.8	Single pack
Polyethylene	2	1	0.190	6.9	0.44	99.1	70	90.2	
Aclar	3	5	0.288	0.5	1.03	72.2	50	72.1	
Aclar	4	2	1.322	0.91	1.40	75.6	21	75.3	
FEP Teflon	5	2	0.419	0.088	5.7	43.3	-	-	Some air in capsules
Aclar	6	2	0.552	0.31	1.93	69.5	-	-	
KEL-F81 Tubing	7	3.5	0.335	0.17	6.5	78.2	11	78.0	Projected payload 3 years, 60 wt-%
Al-Mylar 25A20	8	2.5	0.223	0.21	4.8	81.9			

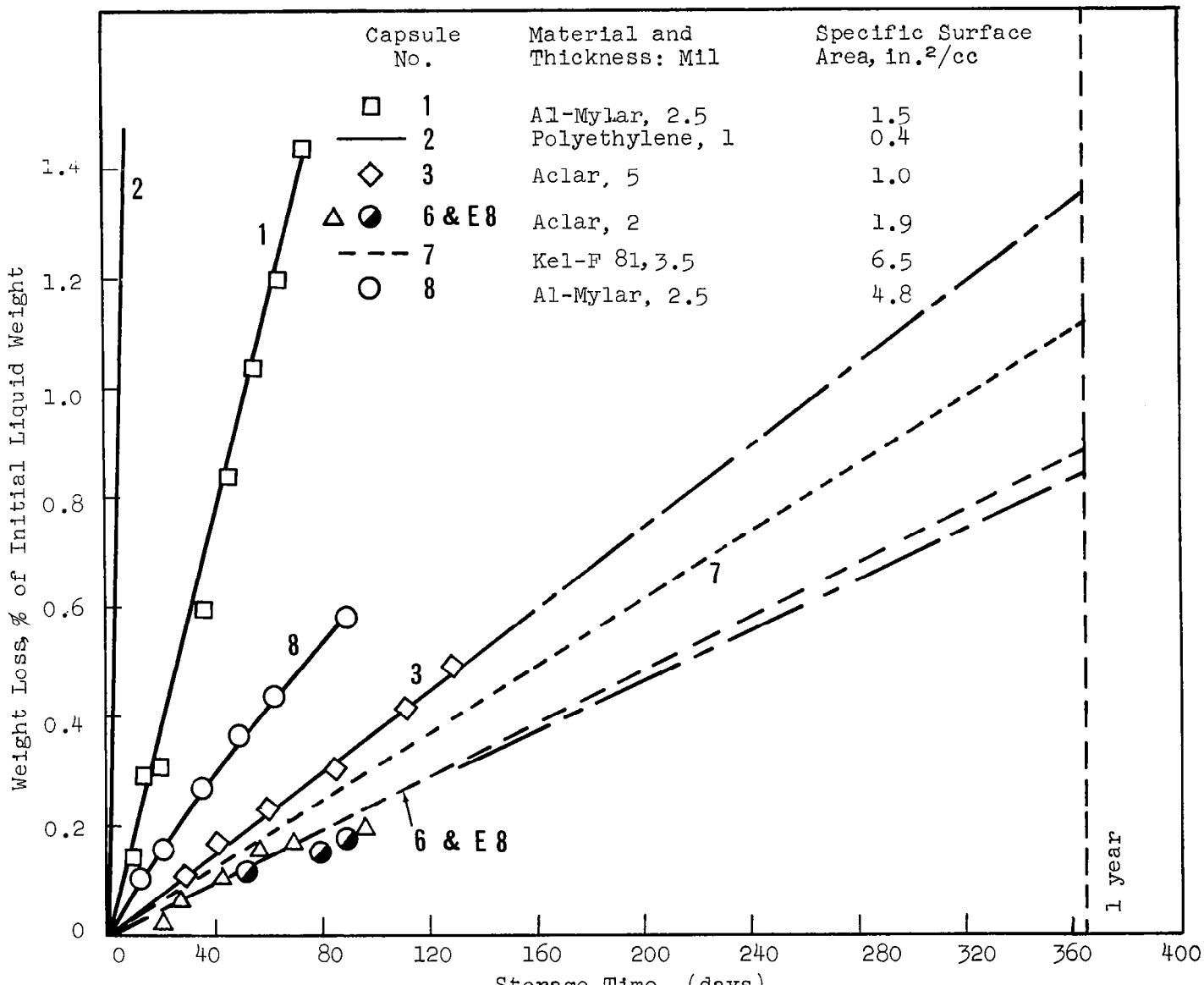

Figure 29. Weight Loss of Water from Various Shape Capsules at Ambient Conditions

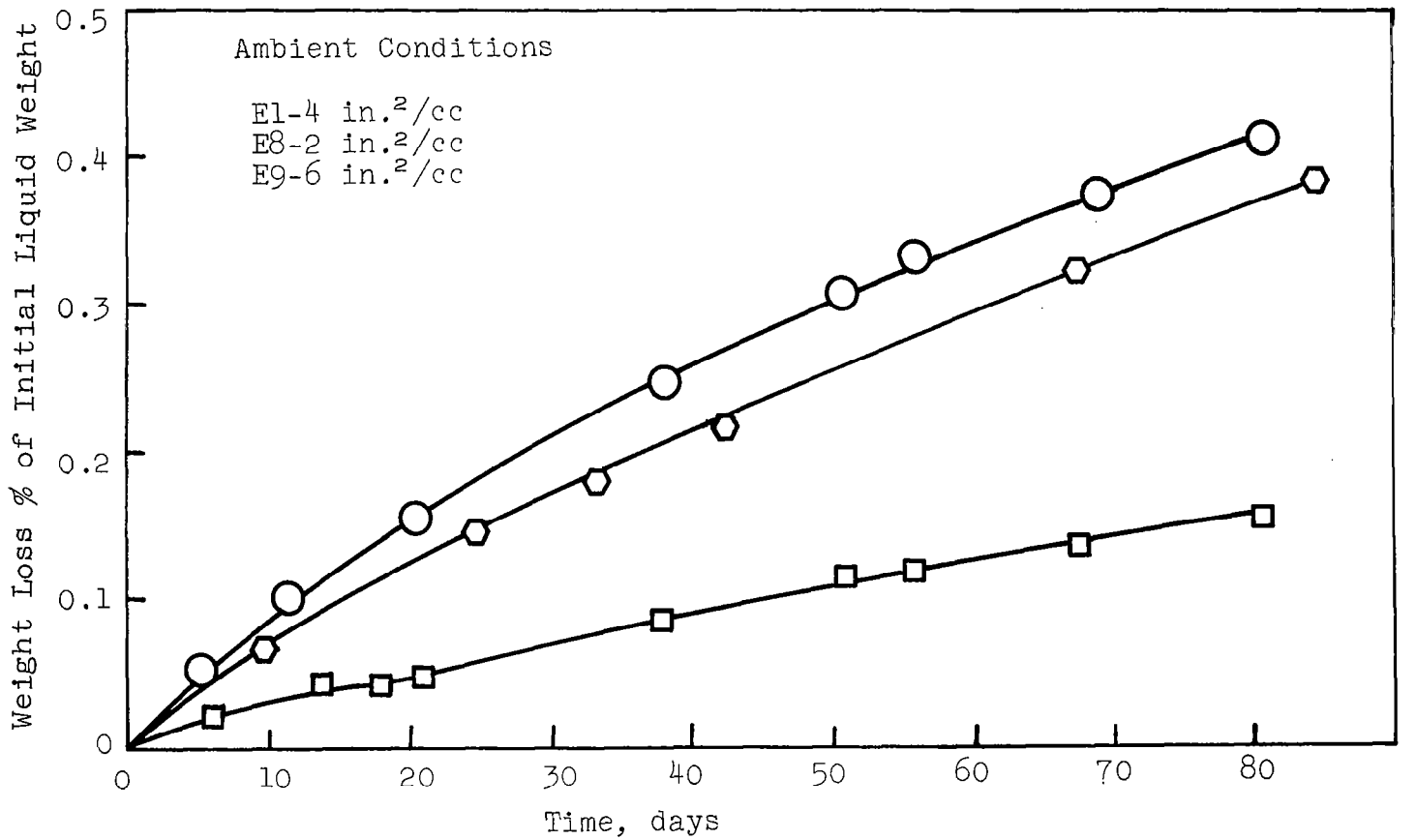

Figure 30. Comparison of Water Incapsulations in Aclar with Different Specific Surface Areas

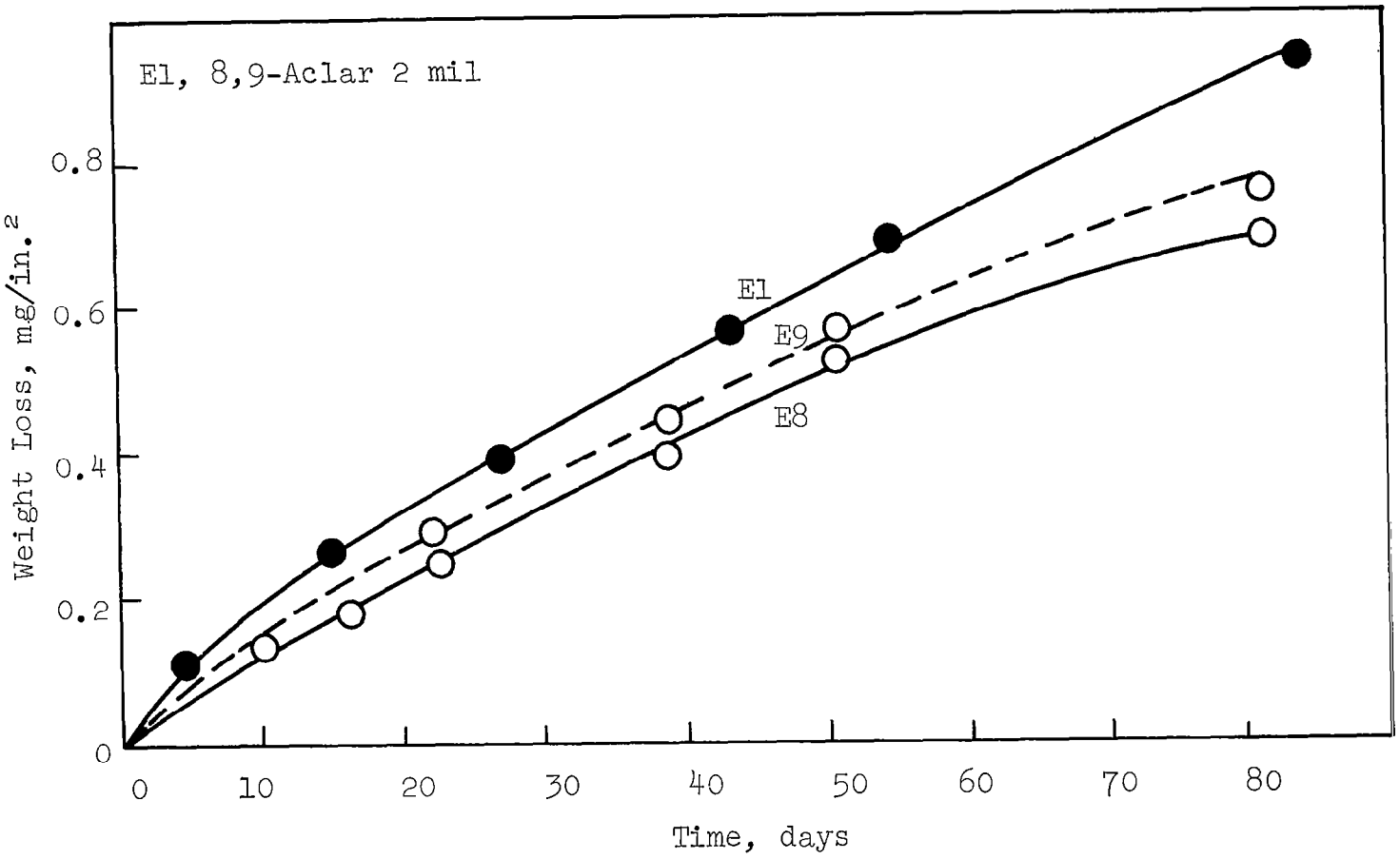

Figure 31. Weight Loss Data for Water in Aclar at Ambient Conditions

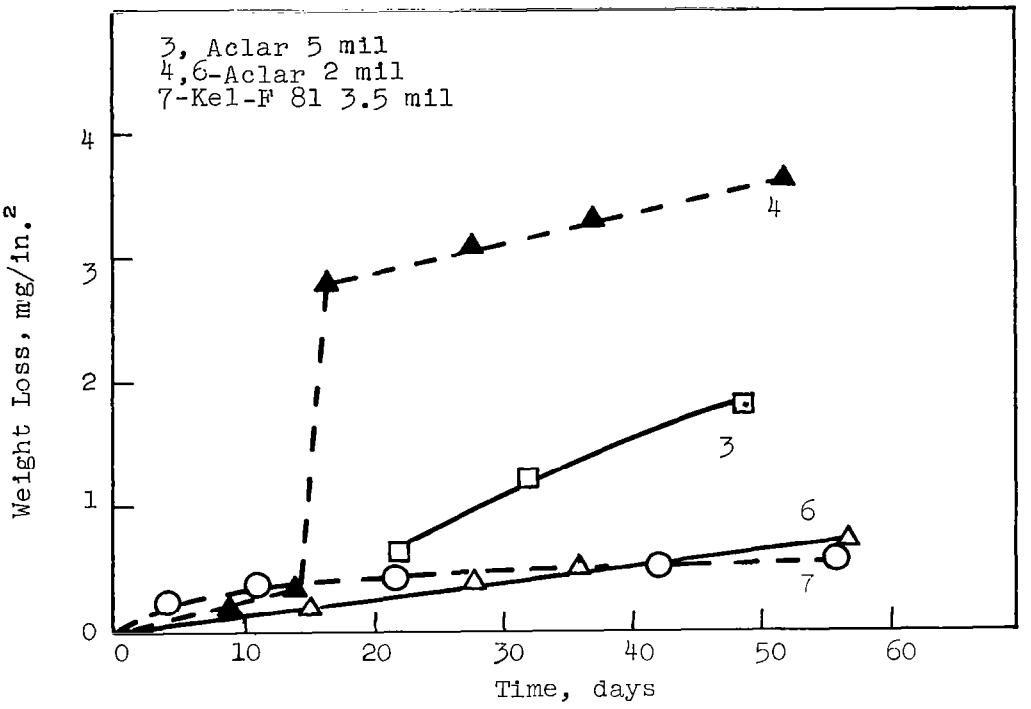

Figure 32. Weight Loss Data for Water Incapsulation in Fluorohalocarbon Films at Ambient Conditions

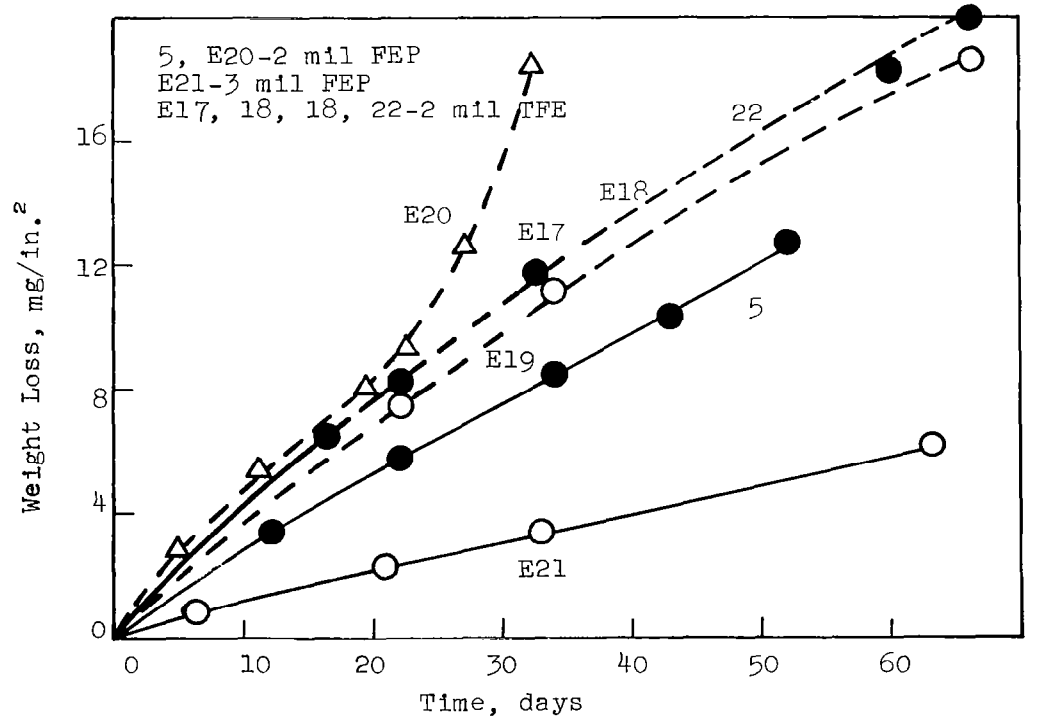

Figure 33. Weight Loss Data for Water Incapsulations in Teflon at Ambient Conditions

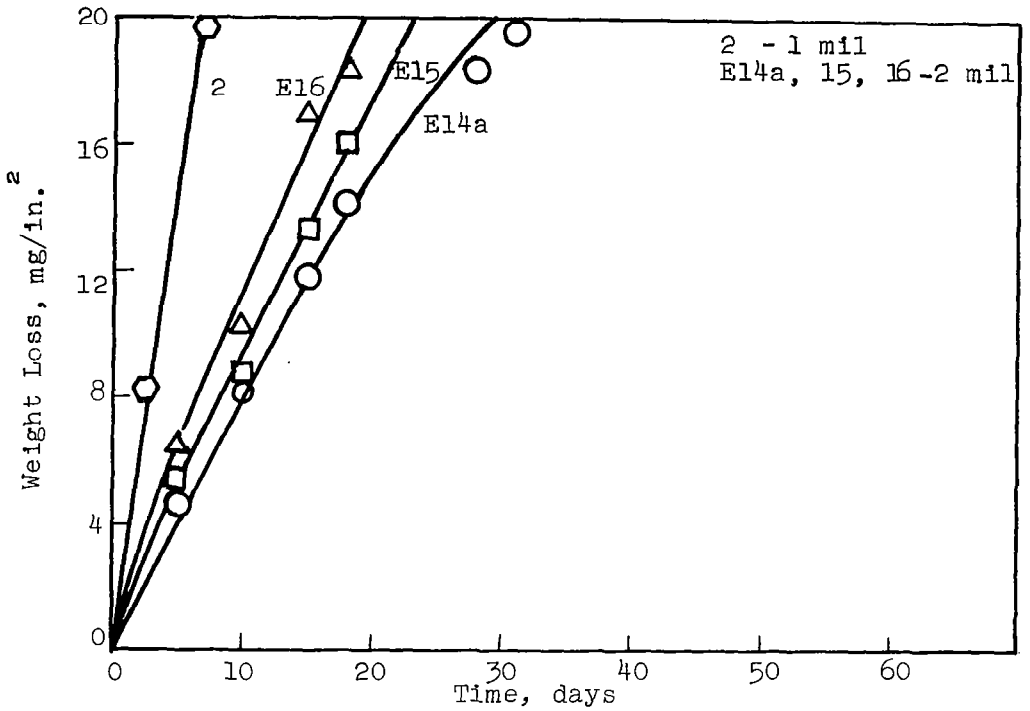

Figure 34. Weight Loss Data for Water Incapsulations in Polyethylene at Ambient Conditions

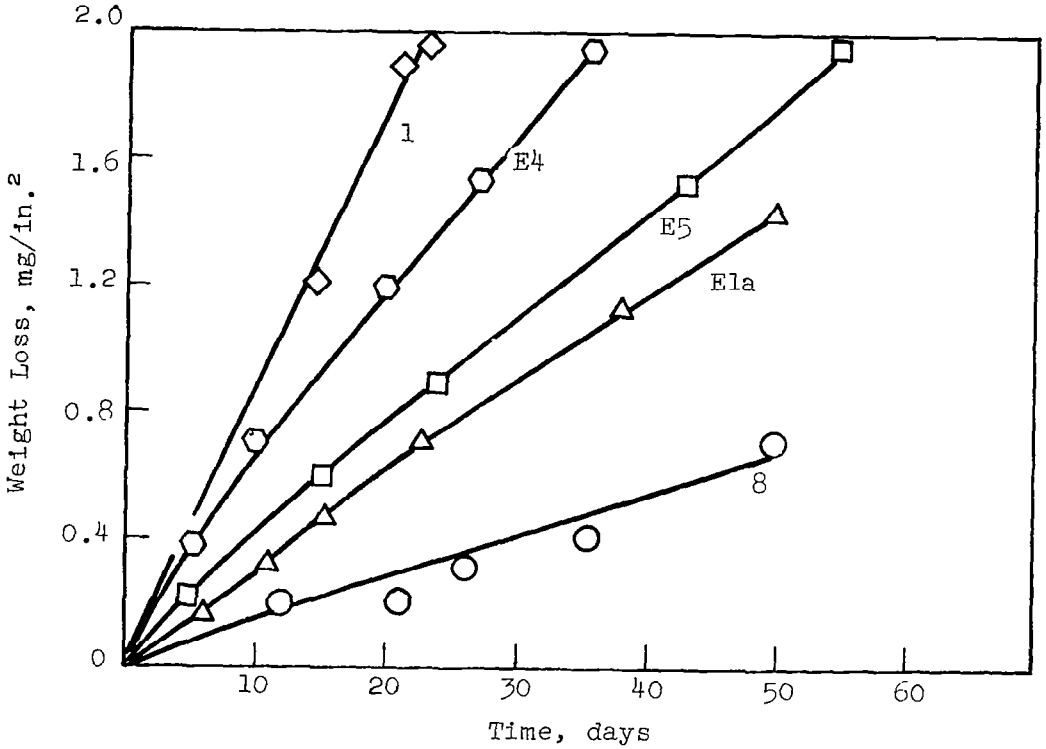

Figure 35. Weight Loss Data for Water Incapsulations in Al Mylar at Ambient Conditions

Permeability constants calculated from the vapor transmission rates are compared with values obtained from the literature in Table 26. Considerable disparity is evident in several cases, depending on the source of the values. Good agreement is evident for the fluorohalocarbon films except for reference 6 whose values are a factor of ten greater than ours. Both the Kel-F and Aclar films show very low permeability to moisture.

A comparison of materials from a per cent weight loss standpoint is shown in Figure 36 for incapsulations having approximately the same surface area per unit weight of liquid. The superiority of the Aclar film is evident.

(b) Electrolyte Incapsulations and Temperature Effects

Work discussed in the previous sections indicated that incapsulations with the desired payloads and loss rates could be attained best by heat-sealing packets from Kel-F 81 tubing. Limitations on minimum wall thickness in custom extrusion of this material currently range from 2.5 mil for 1/8-in. I.D. to 5.5 mils for 1/2-in. I.D. A 2.5 mil wall tube in 1/2-in. I.D. could also be obtained by forming a tube from film using ultrasonic sealing. However, the increase in payload with larger tube sizes tends to make the increase in wall thickness acceptable.

Weight losses were determined for incapsulations of water, 2M $Mg(ClO_4)_2$, 2M $AlCl_3$, and 30% KOH in Kel-F 81 tubing. These solutions can be contained satisfactorily in the heat-sealed packets. Weight loss data at ambient conditions with and without vacuum, and with vacuum at 39°C, are shown in Figures 37 through 40. All incapsulations were in Kel-F 81 tubing of equal lengths and are therefore directly comparable. Physical data on these incapsulations are given in Table 27.

A reduction in loss rate due to the presence of electrolyte is evident when the loss rates are compared with those for pure water. The decrease in loss rate is of the order expected as a result of the lowering of the vapor pressure of water by the salts; the greater the molar concentration of salt, the lower the loss rate should be. It is evident that 30% KOH (about 5 molar) reduced the loss rate significantly more than 2M $AlCl_3$ or 2M $Mg(ClO_4)_2$. The 2M $AlCl_3$ was more effective in reducing the loss rate than 2M $Mg(ClO_4)_2$ because the former hydrolyzes to produce acid, which in effect increased the molar concentration of solute present.

These effects on loss rate show up more clearly in Table 28, in which the permeability constants calculated from the experimental results are listed. Under ambient conditions, the loss rate was so low that experimental errors masked the effect of the solute. Also, under these conditions, the permeation of carbon dioxide into the capsule affected the loss rate measured for potassium hydroxide as discussed below. Under vacuum conditions the results fall into the order expected.

Table 26

COMPARISON OF PERMEABILITY CONSTANTS ESTIMATED FROM THIS WORK AND AVAILABLE LITERATURE

Material	Sample Thickness Mils	Test Conditions	Reported Value	Permeability Constant Estimated at 250°C g-mm/24 hr-m²-cm Hg	Literature Reference
Polytrifluoro-chloroethylene		25°C	0.015-0.180 $\frac{\text{g-mm}}{\text{24 hr-m}^2\text{-cm Hg}}$	0.015-0.180 0.00	12 13
KEL-F 81	6.1	25°C Liquid	0.0015 $\frac{\text{g-mm}}{\text{m}^2\text{-hr}}$	0.015	14
KEL-F 81		Vapor	0.0015 $\frac{\text{g-mm}}{\text{m}^2\text{-hr}}$	0.015	14
KEL-F 300		25°C	2.9×10^{-10} $\frac{\text{cc-mm}}{\text{cm}^2\text{-sec-cm Hg}}$	0.0002	15
KEL-F 300 P25		25°C	2×10^{-9} $\frac{\text{cc-mm}}{\text{cm}^2\text{-sec-cm Hg}}$	0.002	15
Aclar 33C Aclar 33C	1 2	{100°F, 90% RH}	0.025 g/100 in²-24 hr 0.015 g/100 in²-24 hr	0.0022 (100°F) 0.0027 (100°F)	5
Aclar 33C Aclar	2 5	{25°C ≈50% RH}		0.001-0.002 0.0075	this work
KEL-F 81	3.5	{25°C ≈50% RH}		0.00024-0.0018 0.0006 (vac.25°C)	this work
Teflon TFE		25°C		0.0	12
Teflon TFE (Type HB)	2	{25°C ≈50% RH}		0.025	this work
Teflon FEP		25°C		0.002	12
Teflon FEP		25°C	0.46 $\frac{\text{g-mil}}{\text{100 in}^2\text{-24 hr}}$	0.076	5
Teflon FEP	1.77	25°C Liquid	0.0013 $\frac{\text{g-mm}}{\text{m}^2\text{-hr}}$	0.013	14
		Vapor	0.0007 $\frac{\text{g-mm}}{\text{m}^2\text{-hr}}$	0.007	14
Teflon FEP (Type A) Teflon FEP (Type A)	2 3	{25°C ≈50% RH}		0.018-0.025 0.011	this work
Al-Mylar 25A20 Al-Mylar 25A20	2.5 2.5	100°F 25°C	0.02 g/100 in²-24 hr	0.0083 (100°F) 0.0014-0.005	16 this work
Polyethylene (Low density)	2 1	25°C {25°C ≈50% RH}		0.04 - 0.08 0.06 0.10	12 this work
Mylar		25°C		0.10	14
Saran		25°C		0.01-0.02	14

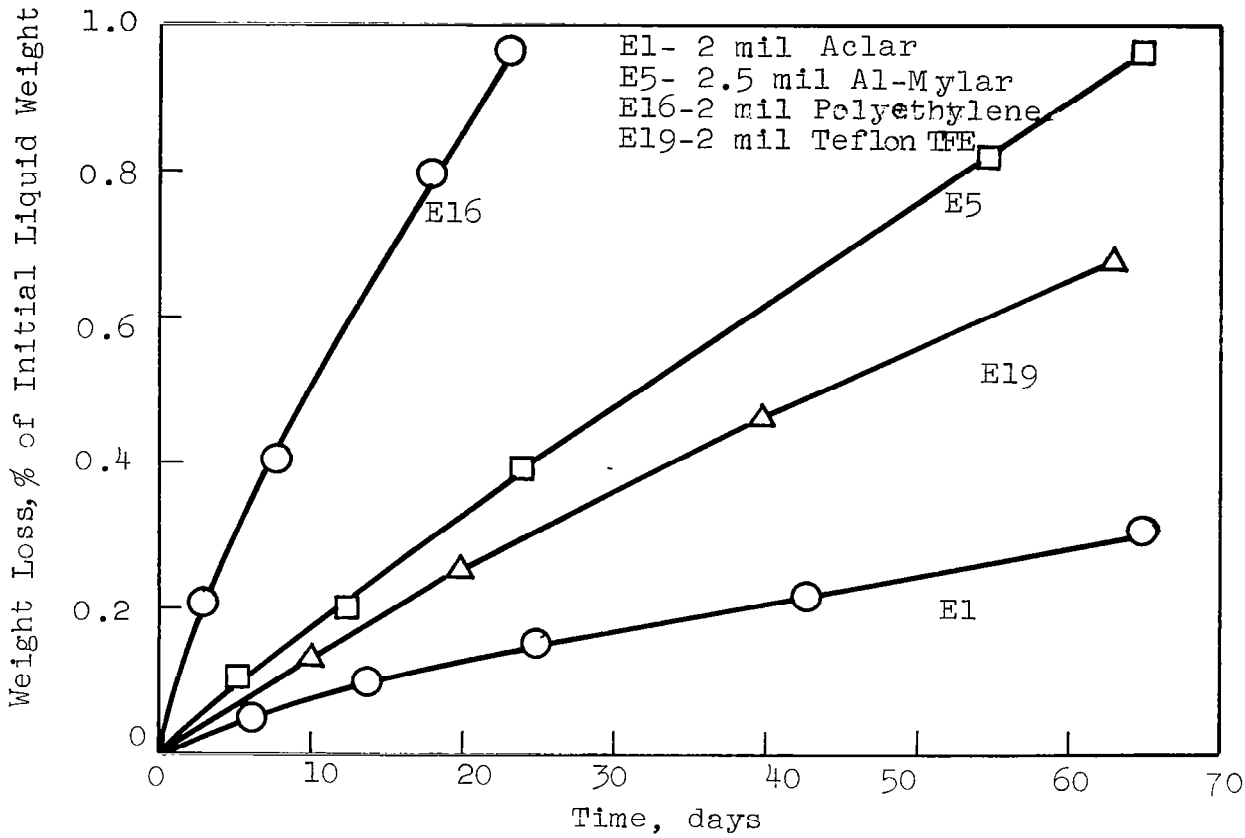

Figure 36. Comparison of Incapsulation of Water in Various Materials with a Specific Surface of 4 in.^{2}/cc Liquid

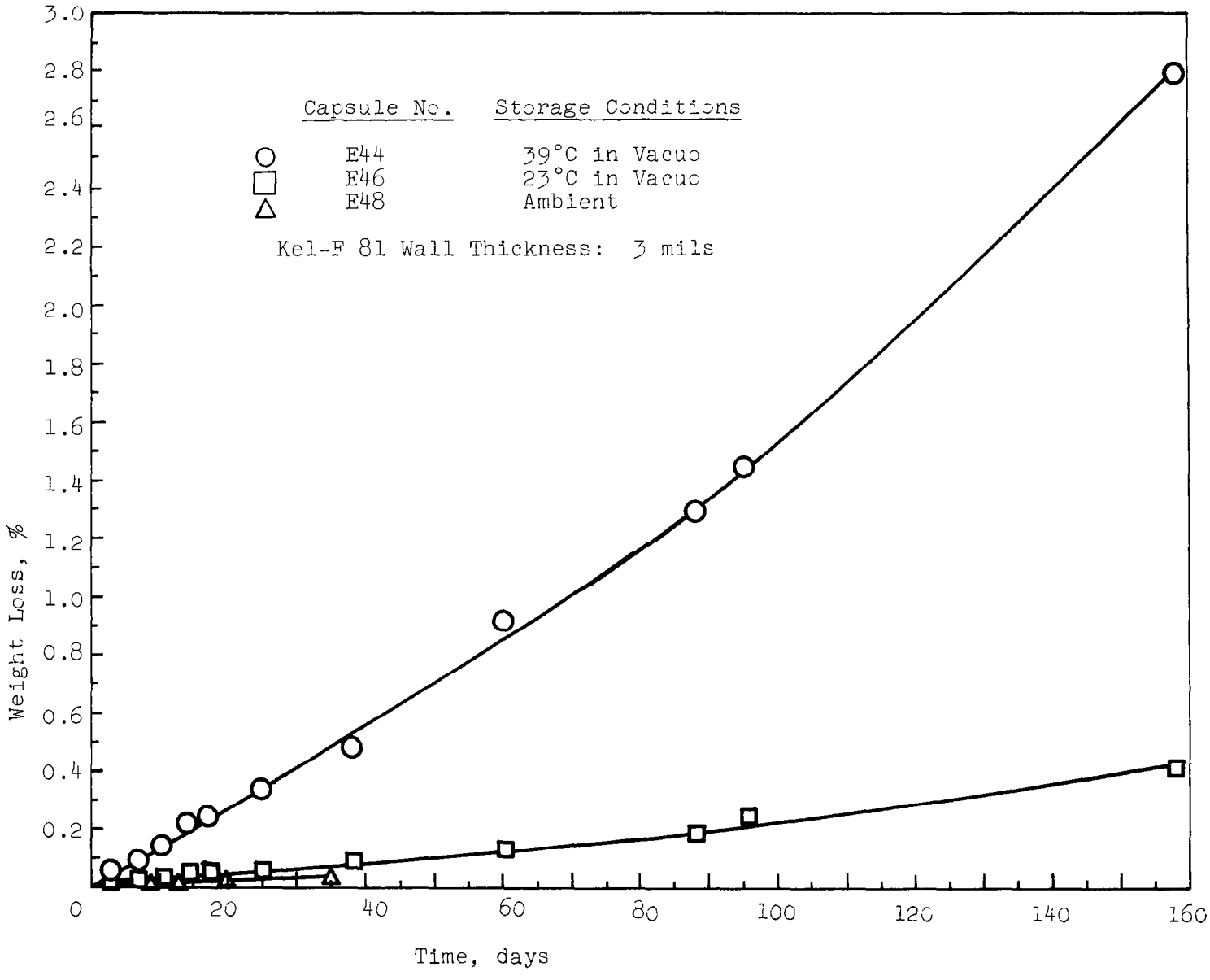

Figure 37. Weight Loss of Macroincapsulated Water in Kel-F 81 Tubing

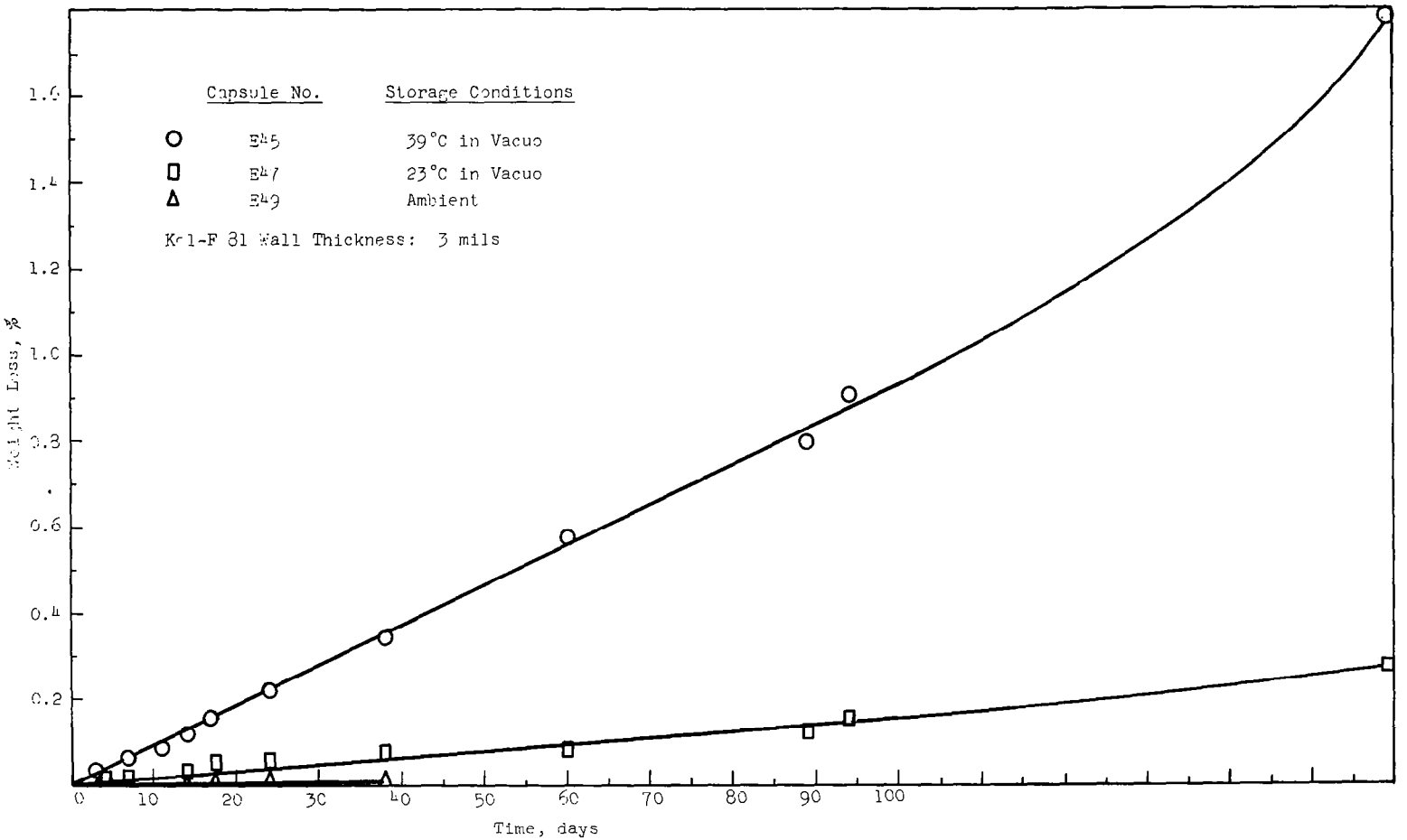

Figure 38. Weight Loss of Macroincapsulated 2M $Mg(ClO_4)_2$ in Kel-F 81 Tubing

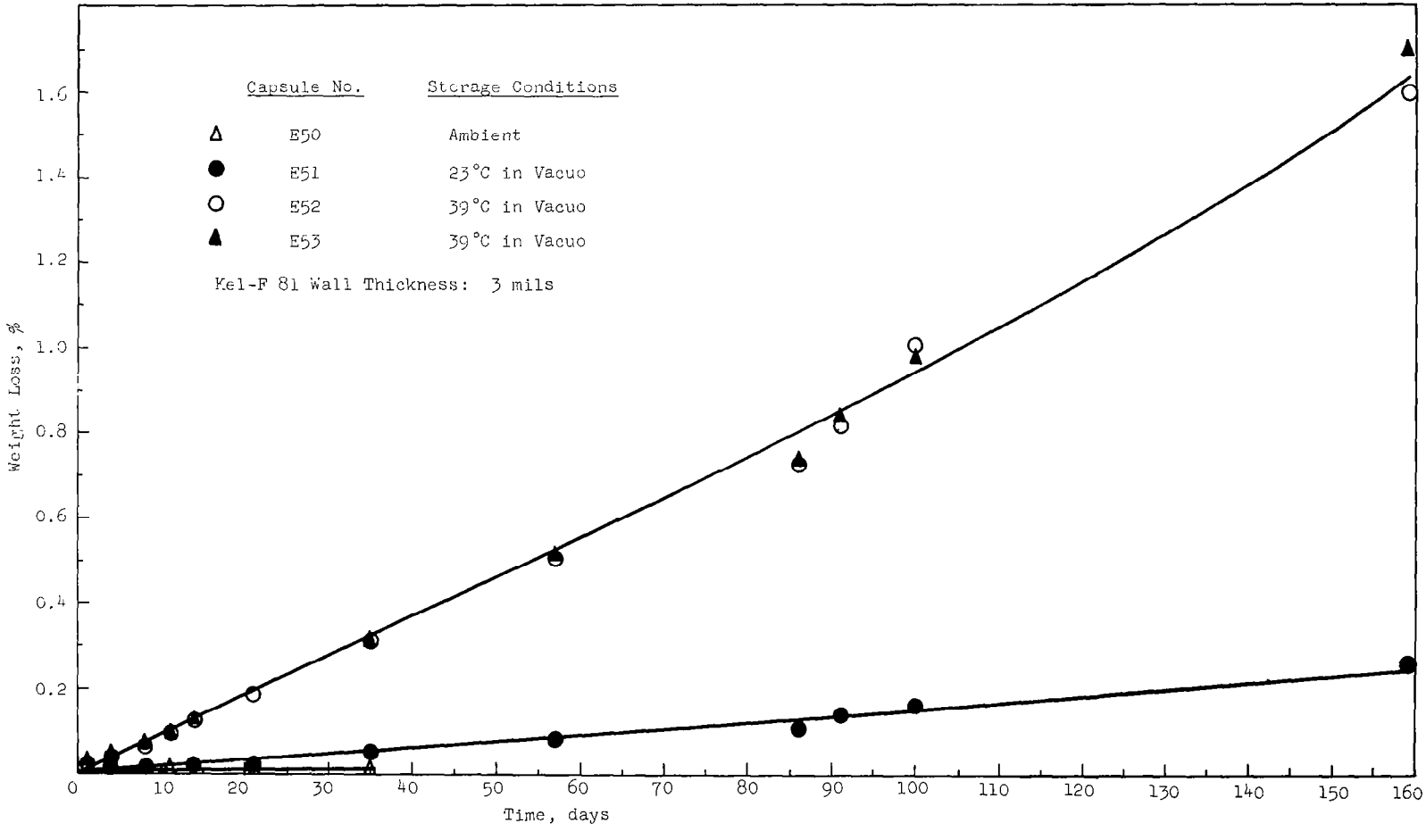

Figure 39. Weight Loss of Macroincapsulated 2M $AlCl_3$ in Kel-F 81 Tubing

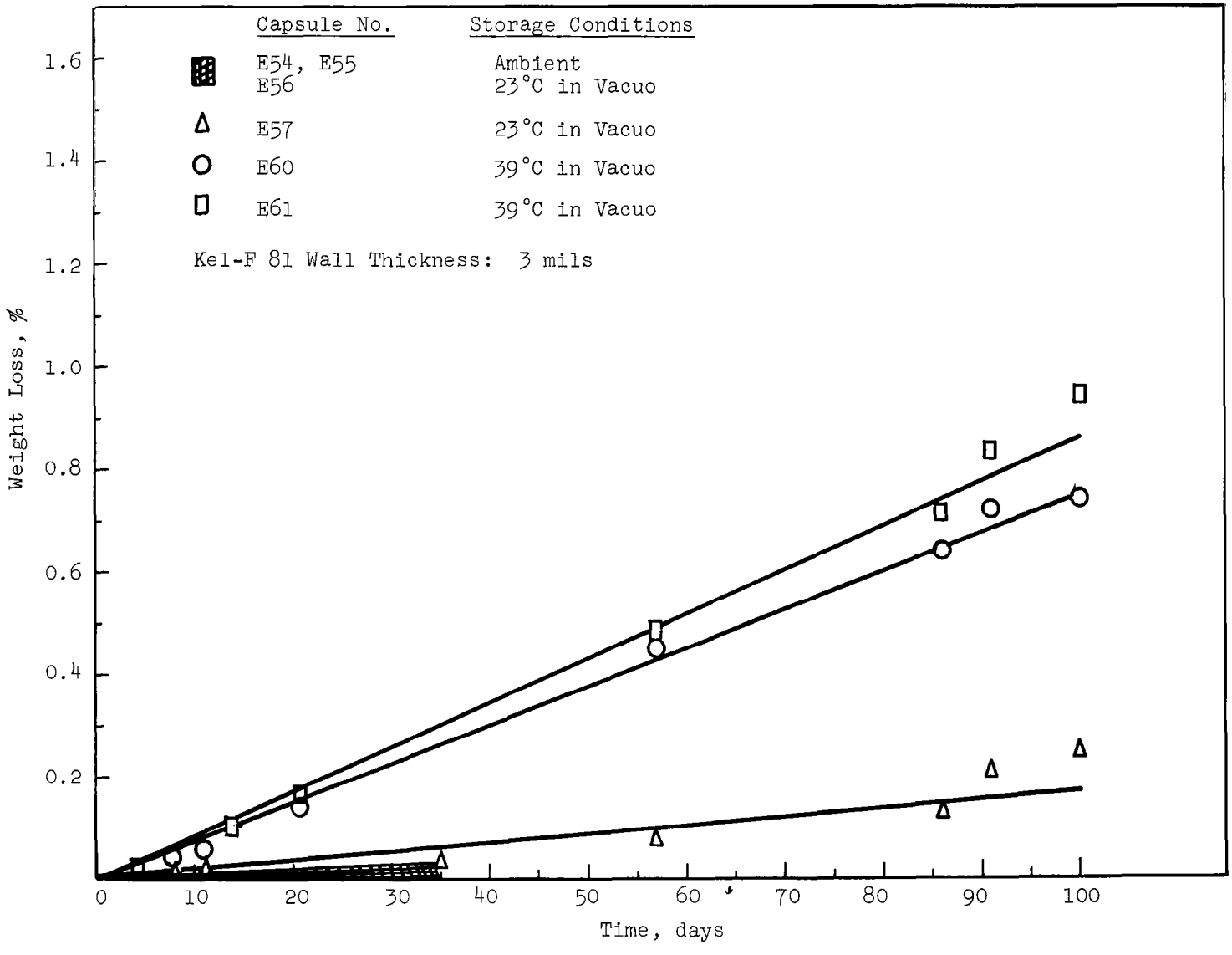

Figure 40. Weight Loss of Macroincapsulated 30% KOH in Kel-F 81 Tubing

Table 27

PHYSICAL DATA ON CAPSULES PREPARED FOR PERMEABILITY TESTS

Capsule I.D. 0.12 in., Length 6.0 in., Surface Area 2.36 in.^{2}, Film Thickness 3 mils

Capsule Number	Capsule Material	Liquid	Conditions‡	Film Weight, g	Total Weight, g	Liquid Weight, g	Initial Payload Weight, %
E44	Kel-F 81	Water	C	0.2733	1.4907	1.2174	81.7
E45	Kel-F 81	2M $Mg(ClO_4)_2$	C	0.2674	1.8456	1.5782	85.3
E46	Kel-F 81	Water	B	0.2703	1.5016	1.2313	82.1
E47	Kel-F 81	2M $Mg(ClO_4)_2$	B	0.2704	1.8893	1.6189	85.6
E48	Kel-F 81	Water	A	0.2833	1.6218	1.3385	82.6
E49	Kel-F 31	2M $Mg(ClO_4)_2$	A	0.2696	1.8540	1.5844	85.6
E50	Kel-F 81	2M $AlCl_3$	A	0.2798	1.8033	1.5235	84.6
E51	Kel-F 81	2M $AlCl_3$	B	0.2760	1.8123	1.5363	84.9
E52	Kel-F 81	2M $AlCl_3$	C	0.2788	1.8166	1.5378	84.5
E53	Kel-F 81	2M $AlCl_3$	C	0.2739	1.7376	1.4637	84.1
E54	Kel-F 81	30% KOH	A	0.2785	1.8743	1.5958	85.3
E55	Kel-F 81	30% KOH	A	0.2792	1.8506	1.5714	84.9
E56	Kel-F 81	30% KOH	B	0.2792	1.8760	1.5968	84.9
E57	Kel-F 81	30% KOH	B	0.2763	1.8892	1.6129	85.3
E58	Kel-F 81	30% KOH	C	0.2764	1.8361	1.5597	84.8
E59	Kel-F 81	30% KOH	C	0.2807	1.8330	1.5523	84.8
E60	Kel-F 81	30% KOH	C	0.2850	1.9113	1.6263	85.2
E61	Kel-F 81	30% KOH	C	0.2790	1.8954	1.6164	85.1

‡ A - Ambient
B - 25°C, Vacuum
C - 39°C, Vacuum

Table 28

PERMEABILITY OF KEL-F 81 INCAPSULATIONS OF ELECTROLYTES UNDER VARIOUS CONDITIONS

Incapsulations made by Heat Sealing Kel-F 81 Extruded Tubing, 3-mil wall thickness, 1/8 in. I.D.

Incapsulated Liquid	Permeability Constant, 10^{-4} g-mm/24 hr-m^2-cm Hg		
	at 25°C, 50% R.H.	at 25°C, vacuum	at 39°C, vacuum
Water	2.4	7.0	17.5
2M $Mg(ClO_4)_2$	2.4	6.5	14.1
2M $AlCl_3$	1.5	5.4	13.0
37% KOH	1.5	4.6	12.5

Table 29

BASIC STRENGTH OF POTASSIUM HYDROXIDE INCAPSULATIONS IN KEL-F 81 TUBING

Conditions	Basicity of Solution, meq/g		
	23 days	50 days	81 days
Ambient, 25°C	4.850	4.817	4.154
Vacuum, 25°C	4.857	4.837	4.706
Vaccum, 39°C	4.852	4.869	4.718

It should be noted that the permeability constants are nearly an order of magnitude lower than our previously reported values on this film. This is the result of longer test periods, which yielded more precise values. Also, the previous results were an average of values obtained on several thicknesses.

Still lower permeabilities have been reported for certain Kel-F type films as shown in Figure 41. Here the results of Myers, et al (ref. 15), are shown compared with our results on an Arrhenius type plot. While the test methods differ somewhat, the results are in fair agreement for the temperature dependence of the permeability with an activation energy of about 12 kcal/mole for the permeation process. With this information, loss rates can be estimated for other temperatures below the glass transition temperature for this material (about 70°C). At this temperature the curve shows an inflection and the permeability increases more rapidly with further increases in temperature. It should be noted that the increase in transmission rate with temperature is not completely accounted for by the greater vapor pressure of the liquid. The remaining increase is presumably due to the effect of temperature on the film itself. No effect of these electrolytes on the stiffness or clarity of the film was evident.

(c) Composition Analysis

Incapsulations of approximately 30% KOH were analyzed by acid titration after storage for various times under the conditions previously used. A significant drop in the concentration of base was evident in the capsules stored at ambient conditions (see Table 29. This was undoubtedly due to permeation of carbon dioxide into the capsule. The driving force was the partial pressure of carbon dioxide in air compared with its partial pressure in the capsule (essentially zero). A slight increase in basicity was observed initially during storage at 39°C under vacuum because of the more rapid loss of water than uptake of carbon dioxide. For long-term storage of potassium hydroxide at ambient conditions, a thicker capsule wall may be desirable.

e. Electrolyte Release Methods

The electrolyte must be released from the incapsulation and distributed to the dry tape prior to or during the movement of the tape through the collector area. The time required for adequate distribution and wet-out will vary with the nature of the tape and electrolyte. Tapes with good discharge characteristics have had wet-out times of less than one minute. In many cases electrolyte distribution is adequately achieved by the fibrous tape base material when the electrolyte is fed to the uncoated side of the cathode tape. Wet-out times have been reduced by addition of wetting agents to the electrolyte or tape coating mix.

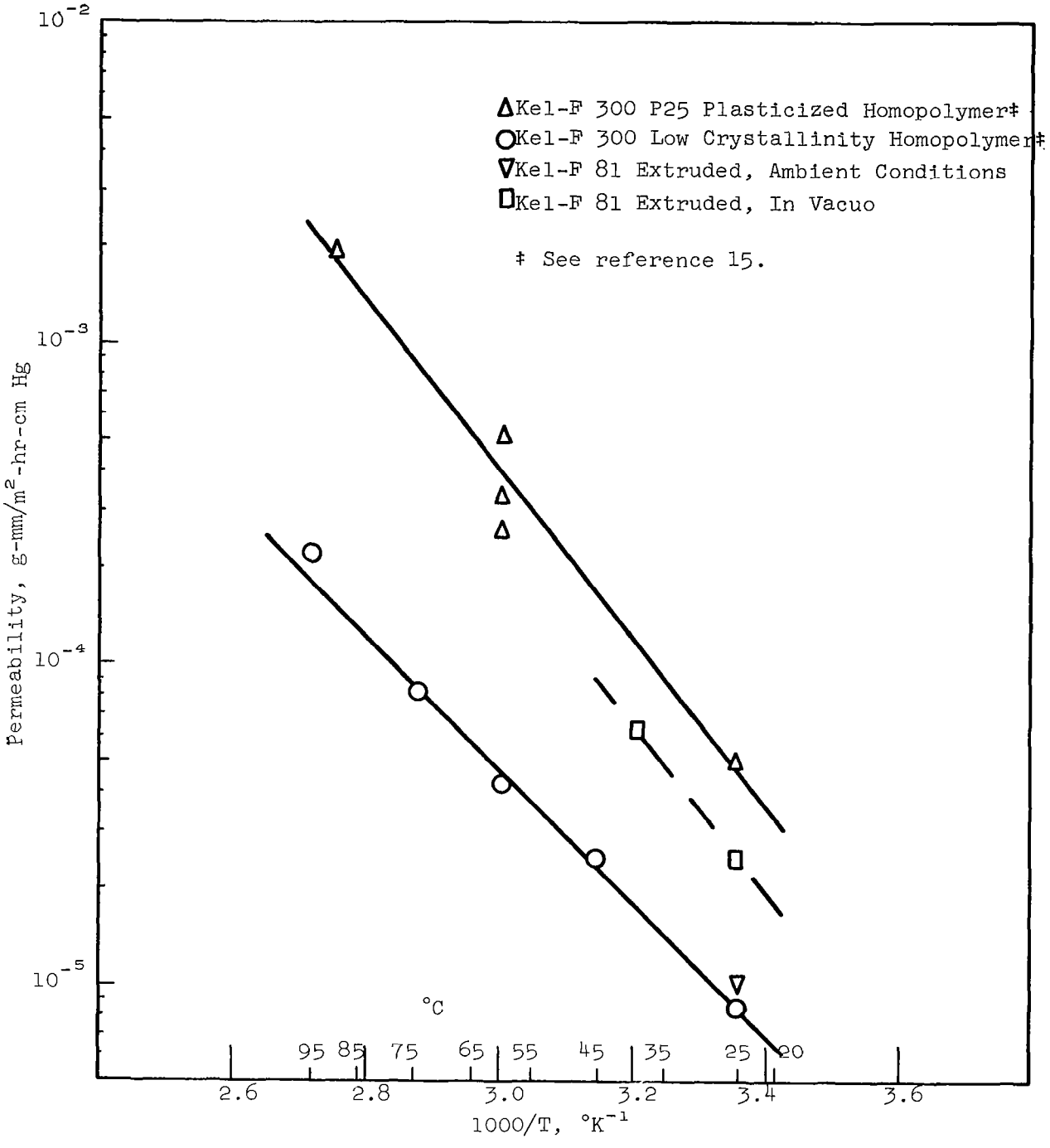

Figure 41. Effect of Temperature on Permeation of Water through Kel-F 81 Tubing

With these considerations in mind, release methods applicable to the incapsulation selection of Kel-F tubing have been investigated. A number of the methods incorporated in a collector head are illustrated in Figure 42. Earlier tests on one method, slitting by a stainless steel blade followed by squeeze-rolling, were carried out with a rather flat packet of 2-mil polyethylene film. The test results were encouraging, showing both a low pulling force required and over 90% transfer of the incapsulated liquid to a dummy tape.

With slight modification, the method was next tried on the custom-extruded Kel-F tubing 1/8-in. I.D. subsequently obtained. Two drawbacks were noted in the slitting of this size tubing, resulting both from the greater stiffness of the film and the rounder shape compared to that of the polyethylene incapsulation. First, a considerable increase in pulling force (rising from about 18 oz. to over 2 lb) was usually necessary when the blade encountered the heat seal. Second, the orientation of the slit packets at the rollers varied causing occasional increase in pulling force.

A second method of release appeared to present few difficulties and offers better reliability. This method employed sharp-toothed sprocket wheels of 3-mil thick stainless steel to puncture the capsules, a puncture being made about every 1/16 to 1/8 in. as the incapsulation is pulled over and against the wheel. The punctured capsules next move through a slot of controlled width to remove the electrolyte. This method has given a release efficiency of 95% but the slot width required for good efficiency resulted in excessive drag. Rollers were tried to reduce the drag but some electrolyte passed through the rollers lowering the efficiency. Simply pulling the punctured incapsulation around a roll provided good release and lowered the drag to about 10 oz.

The use of a single incapsulation for supplying four tapes with electrolyte in the tape conversion device was desirable to conserve weight. This required an increase in tubing size, which made the packets much flatter and thus made the slitting method feasible. The final incapsulation release device incorporating slitting is discussed in section IV.

An initial attempt to obtain electrolyte conservation by passing a dummy tape (several layers of nonwoven nylon) through pressure rolls was ineffective. At the low tape speeds used, the electrolyte wicks forward through the rolls to the drier area. Some feedback was obtained by pulling the tape through rapidly or exerting extreme pressure on the tape. The latter then requires high pulling force. Subsequently it was found that actual electrolyte consumption with the KIO_4-Mg system was large and left little opportunity for electrolyte conservation so this work was terminated.

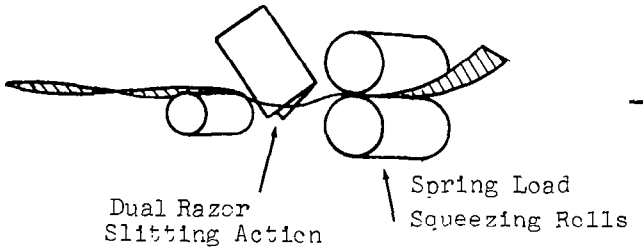

a. Slitting of Flat Capsules Followed by Squeeze Rolls

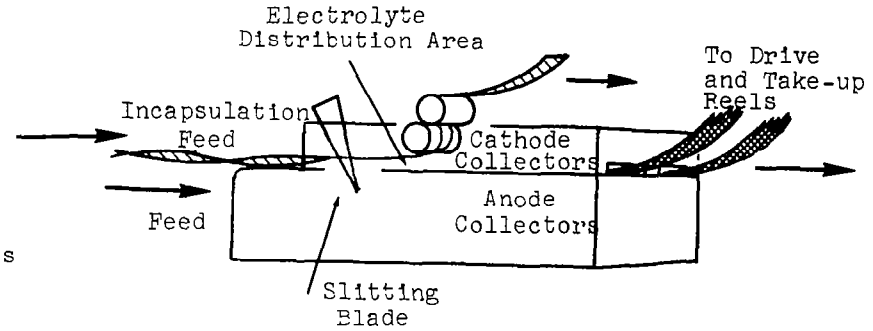

b. Slitting Method Incorporated into Tape Discharge Head for two Tape Operation

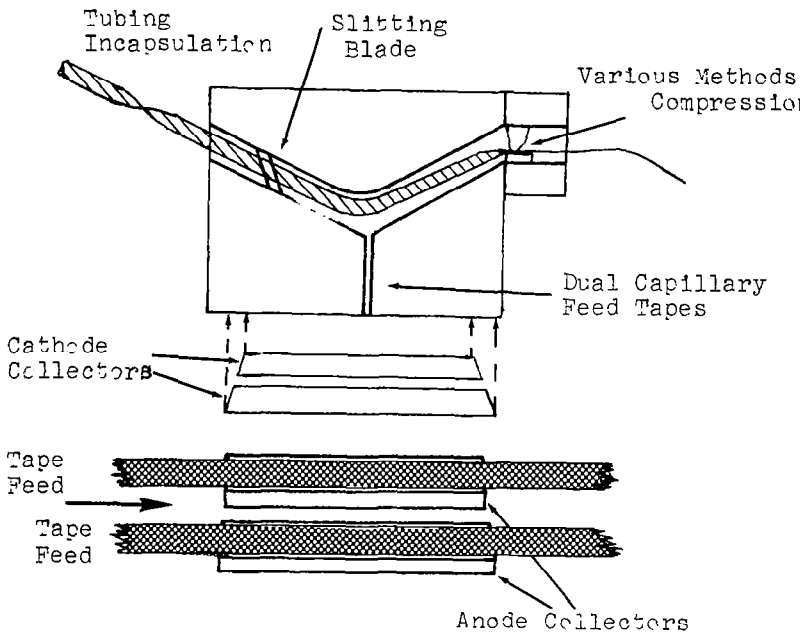

c. Tubing Incapsulation Slitting with Feed Through or Ahead of Discharge Area

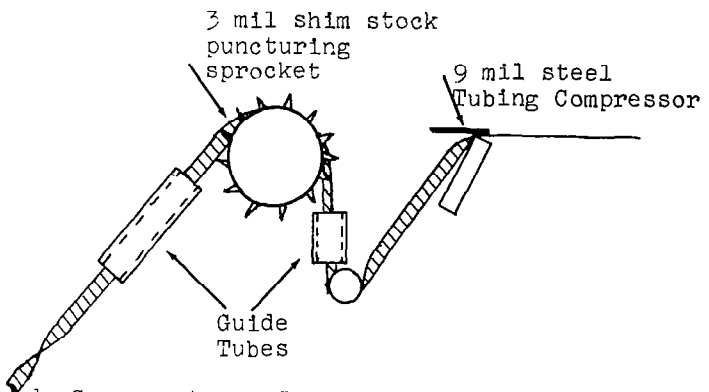

d. Components of Tubing Puncture Method for Electrolyte Release

Figure 42. Methods of Electrolyte Release

3. Microincapsulation

a. Background

Microincapsulation is one scheme for separating the dry anode and cathode materials from the electrolyte and, at the same time, to provide intimate contact of the electrodes with electrolyte on demand. Microcapsules of the liquid, approximately 500 μ in diameter, would be imbedded in the dry tape and the liquid released by applying pressure rollers immediately before the current collector.

The microincapsulation of electrolytes was undertaken by the Southwest Research Institute as a result of a subcontract with Monsanto Research Corporation. The complete final report of the Southwest Research Institute on this subject is reproduced in its entirety in the Appendix. We have prepared the following Summary and Recommendation sections to appraise the results of the microincapsulation program and to compare this scheme with other means of containing liquids during storage and releasing them for tape activation.

b. Summary of Microincapsulation Report

Both aqueous and nonaqueous electrolyte were incapsulated in microcapsules with diameters of from 500 to 1700 μ. The payload of these capsules ranged from 40 to 72%. The weight loss of microcapsules of aqueous solutions, taken from the slope of the loss-time curves after the initially very high loss rate, was from 0.4 to several per cent per day for aqueous electrolytes and from 0.1 to 1% per day for nonaqueous solutions.

4. Discussion

A comparison of methods of supplying electrolyte is shown in Figure 43. In this comparison, electrolyte loss due to water vapor permeation through the containing wall is not included. This will not significantly affect the values for macroincapsulation or the bottle and pump system since the loss rates in these cases are negligible. For microincapsulation, however, the very high loss rates obtained in the present work would require a steeper slope of the lines. This would present a further problem in matching the feed rate to that required. That is, if the tape is put into operation after very short storage time, excess electrolyte would be present. The low electrolyte payloads actually obtained in microincapsulation (less than 60%) and the high loss rates indicate that microincapsulation would only be advantageous in a special application.

A comparison of the bottle and pump system to the macroincapsulation and release system shows that the weights involved are not greatly different, with the former system offering a weight saving for tape times longer than about 50 hours. A volume reduction would also be obtained with the bottle and pump system.

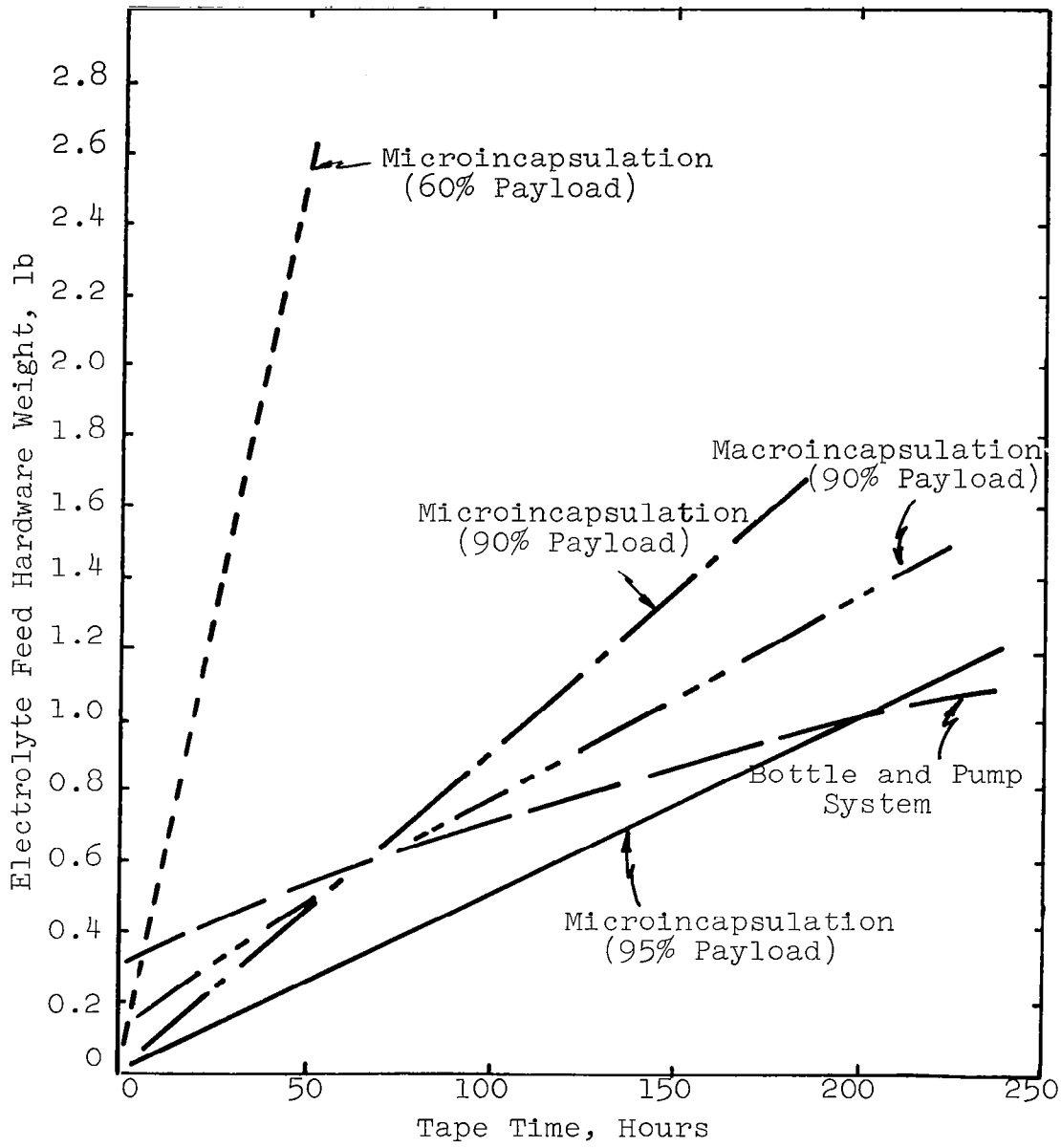

Figure 43. Comparison of Weight Required to Supply Electrolyte by Various Methods (Calculations based on weight ratios of electrolyte and incapsulations, assuming zero electrolyte loss through capsule wall.)

5. Conclusions

(1) The best macroincapsulating material is Kel-F 81 plastic film, preferably in tubing form. The permeability constant for Kel-F 81 tubing is of the order of 0.0002 to 0.001 g H_2O-mm/24 hr-m^2-cm Hg for various aqueous solutions. Electrolyte contained in macrocapsules of the size used in this work loses about 1% of its water per year.

(2) Other polytrifluorochloroethylenes and the Al-Mylar laminate have very low permeability coefficients.

(3) The very high loss rate of electrolytes from microincapsulations eliminates this electrolyte-containing scheme for use in dry tapes for all except unusual and special applications. Apparently, no means of microincapsulating aqueous liquids with good load but with suitably low loss rate is known.

D. HIGH ENERGY COUPLES IN NONAQUEOUS ELECTROLYTES

1. Background

The use of high energy couples that are not compatible with aqueous electrolytes in the tape configuration was explored. Metallic lithium with its very high coulombic capacity of 232 amp-min/g was of particular interest as an anode candidate. For comparison, the capacities of cadmium, zinc and magnesium are 29, 49, and 132 amp-min/g, respectively. In addition to its high coulombic capacity, lithium is also a very active metal with a high anodic potential (E^0 = 3.0v). Lithium reacts readily with water to evolve hydrogen and forms the oxide and nitride readily in the presence of moist air (ref. 17). Utilization of lithium as an anodic material, therefore, requires the use of a nonaqueous electrolyte and an inert atmosphere to prevent spontaneous oxidation or nitride formation.

The cell lithium-lithium perchlorate in butyrolactone-cupric chloride was reported by Meyers (ref. 18) to have an energy density of 106 watt-hr/lb at a current density of 13 ma/in^2. The low discharge rate was required because of the high resistance of the nonaqueous electrolyte. The common aqueous battery electrolytes have specific conductances in the range of 10^{-1} to 1 mho/cm, while the best nonaqueous electrolytes have specific conductances in the range of 10^{-3} to 10^{-2} mho/cm (see Figure 44). The use of active metal anodes in nonaqueous systems would be expected to produce high voltages and good energy densities at rather low current densities. Increasing current density may be possible if tapes can be designed to reduce IR voltage losses associated with high electrolyte resistances.

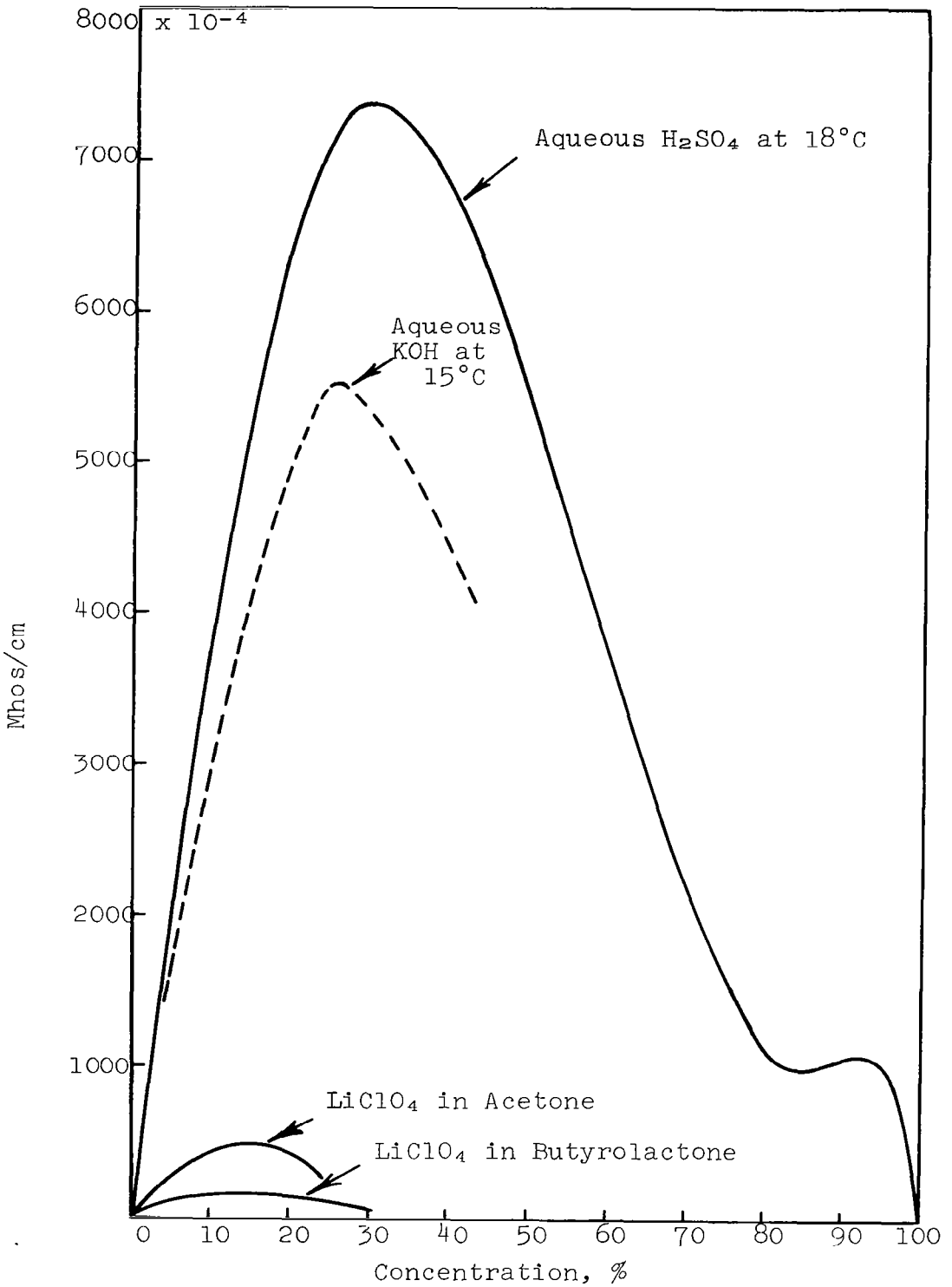

Figure 44. Specific Conductance of Aqueous and Nonaqueous Electrolytes

2. Experimental Method

All cells were assembled and discharged in an argon dry box. For anodes, commercial lithium ribbon, 1/16-in. thick, was degreased with ethylene trichloride and the tarnished surface removed by scraping with a knife. Cathodes were prepared by one of the methods described in the following paragraphs.

a. Type A Cell

Cathode Mix

	%
$CuCl_2$, analytical reagent	67
Shawinigan Black	20
Carbon Fibers, 1/4-in.	3
Polyvinylpyrrolidone (PVP) binder	10

The cupric chloride, carbon black, and carbon fibers were mixed in a Waring Blender. The PVP binder was dissolved in 13 times its weight of water, and the dry cathode mix was stirred into the solution. Cathode grids of 20 x 20 mesh Ni screen, 4 x 1/2 in., were coated with the thick cathode paste and dried overnight at room temperature and then in a vacuum oven at 200°C. The cathodes were transferred to the argon dry box, saturated with an electrolyte of 1M $LiClO_4$ in butyrolactone, and assembled into a two-electrode cell with the lithium anode. A 6-mil thick polypropylene separator saturated with the electrolyte solution was placed between the electrodes, and the assembly was clamped between polyethylene blocks. A piece of freshly scraped cadmium metal was clamped to a protruding section of the separator for use as a reference electrode.

b. Type B Cell

Cathode Mix

	%
$CuCl_2$, analytical reagent	72.3
Asbury A-625 Carbon	24.1
Paper Fiber, Whatman Ashless Filter Disks	3.6

The ingredients were dry-mixed in a Waring Blendor and then pressed onto wire screen grids with a hydraulic press. The cathodes were dried for 16 hours at 200°C in a vacuum.

A cell was assembled from one lithium anode, 8-mil thick glass filter sheet (Whatman), a 7-mil anion exchange membrane (Whatman AE-81), and one cupric chloride cathode. The separators and ion exchange membrane were saturated with 12% $LiClO_4$ in butyrolac-

tone. The cell assembly was clamped between horizontal blocks of polyethylene, and a cadmium reference electrode was inserted between the separators, which protruded one inch beyond the active plates.

Butyrolactone solvent was dried by storing over molecular sieves. Reagent-grade lithium perchlorate was dried in a vacuum at 200°C for 24 hours.

Constant current discharges were made at a current density of 13 ma/in.^{2} at 25°C. Cell voltages and cathode and anode potentials were continuously recorded until the cell voltages, initially 3.5 v, dropped to 2.5 v. Current-voltage relationships for freshly assembled cells were made by polarizing a cell at constant current for two minutes each at increasing current densities until voltage failure occurred.

3. Discharge of Lithium-Cupric Chloride Cell

A typical current-voltage relation for a freshly assembled lithium-cupric chloride cell is shown in Figure 45. The high open-circuit voltage of 3.6 v is characteristic of this system. The voltage remained above 3 volts at current densities lower than 19 ma/in.^{2} but fell rapidly at higher current densities. The working voltage at low current densities also decreased as the cell discharged.

A typical constant current discharge is shown in Figure 46. The cathode rather than the anode failed for most discharges. However, when the separators were replaced with new separators, freshly wet with electrolyte, another discharge, almost as long as the first discharge, could be obtained. After replacing the separators, the cathode and anode usually failed together. The originally bright lithium anode surface was tarnished with a black coating at the end of a discharge. The anodes gave a positive test for copper contamination. Apparently, cupric or cuprous chloride is somewhat soluble in the solvent and is reduced at the lithium surface after diffusing through the separators. Potential readings with and without IR voltage loss, shown in Figure 46, indicate that the cell resistance is constantly increasing from a value of about 7 ohm-in.^{2} at the start of a discharge to about 45 ohm-in.^{2} at the time of voltage failure.

Discharges of several cell types having different cathode loadings, formulation pressures, and grid types are given in Table 30. Although all cathode efficiencies are low, those with high formulation pressure are least active. Apparently, highly compacted cathodes, while desirable for electrode rigidity, are less active than more porous cathodes.

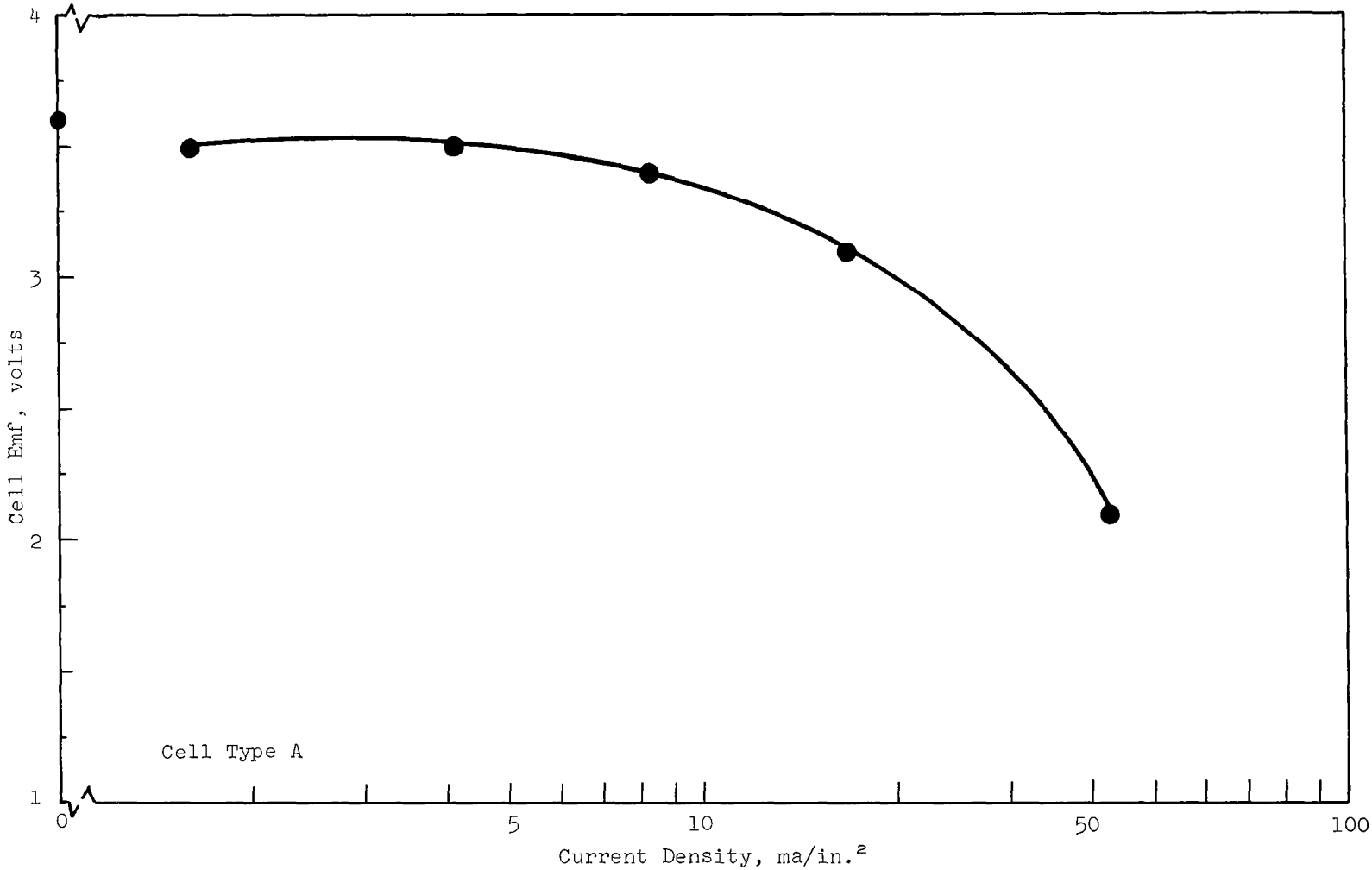

Figure 45. Discharge Characteristics of the $Li/LiClO_4$ in Butyrolactone/$CuCl_2$ Cell

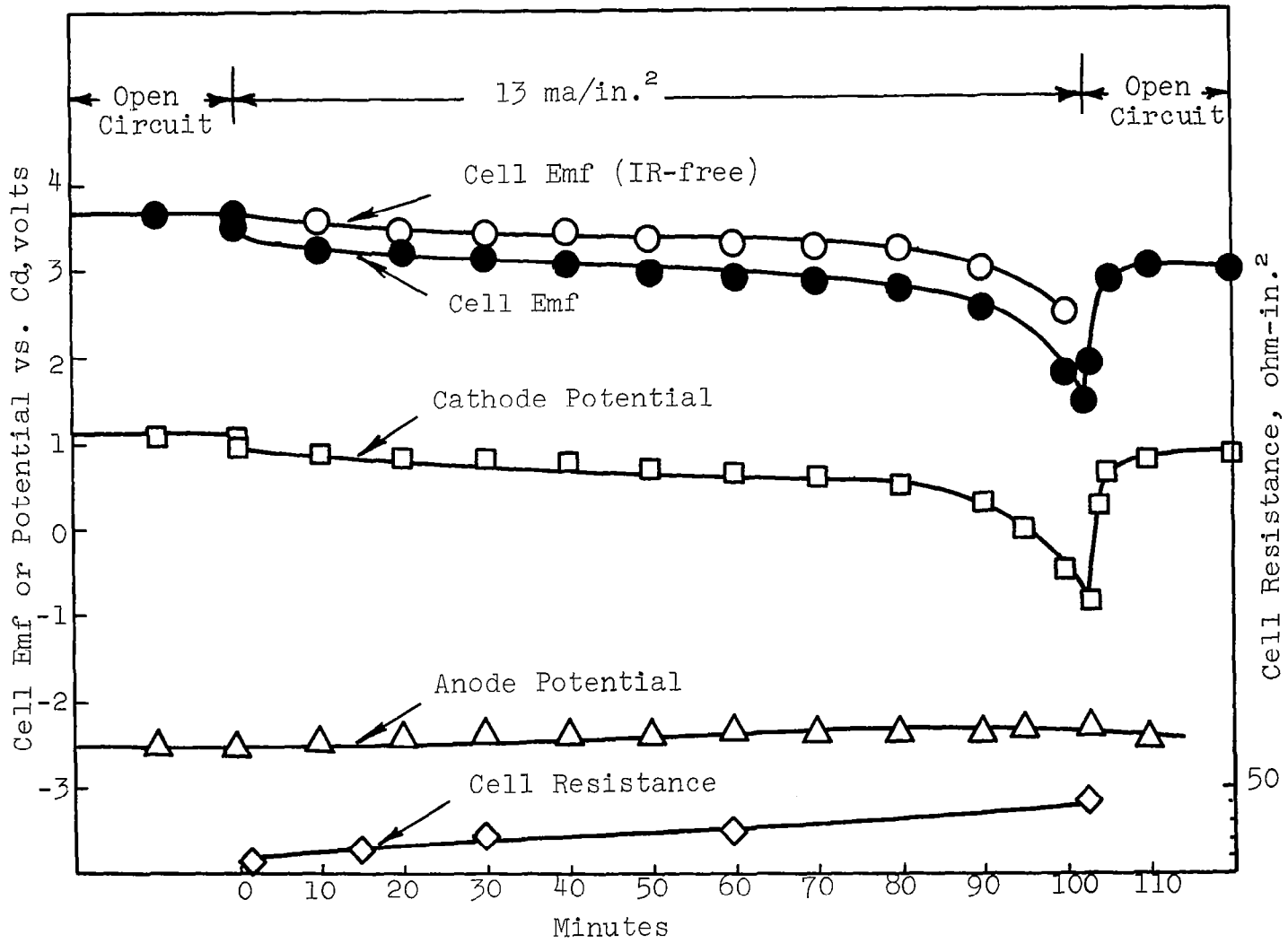

Anode: Lithium
Cathode: $CuCl_2$
Electrolyte: 12% $LiClO_4$ in Butyrolactone Temperature 25°C

Figure 46. Static Discharge Characteristics of the Li/$LiClO_4$ in Butyrolactone/$CuCl_2$ Cell

Table 30

CUPRIC CHLORIDE- LITHIUM CELL CAPACITY TESTS

Depolarizer - $CuCl_2$
Cathode Mix - B
Drying Time- 16 hrs at 200°C in vacuo
Temperature - 25°C

Separators
Whatman Anion Exchange Membrane AE-81, 7 mils thick
Whatman Glass Filter Sheet GF-1, 8 mils thick

Cathode Loading mg $CuCl_2$/in.^{2}	Cathode Grid	Formulation Pressure, psi	Minutes to 2.5 v at 13 ma/in.^{2}	Experimental Capacity amp-min/in.^{2}	Theoretical Capacity amp-min/in.^{2}	Cathode Efficiency, %
510	ss	10,000	115	1.50	12.3	12.2
520	ss	10,000	110	1.43	12.5	11.5
541	ss	10,000	110	1.43	13.0	11.0
560	Ni	10,000	74	0.96	13.4	7.2
570	Ni	4,000	105	1.37	13.7	10.0
620	Ni	8,000	95	1.23	14.9	8.3
630	Ni	5,000	103	1.34	15.1	8.9
670	Ni	9,000	145	1.88	16.1	11.7
720	Ni	24,000	8	0.10	17.3	0.6
740	Ni	16,000	50	0.65	17.8	3.7
780	Ni	25,000	330	0.39	18.7	2.1
860	Ni	18,000	82	1.07	20.6	5.2

The effect of electrode loading on cathode efficiency is shown by the data presented in Table 31, and plotted in Figure 47. Efficiencies were better for low cathode loadings than for high loadings. This relation again indicated that only the cathode surface was active, and cupric chloride beneath the electrode surface was not in the right physical state to be electrochemically active.

4. Discussion

Although the lithium-cupric chloride system had very good voltage characteristics on open circuit or at low current drains, the cell resistance of our configuration was much too high to allow a reasonable current density (100 ma/in.^{2}) to be drawn without severe IR loss. A practical maximum for cell resistance is of the order of one ohm in.^{2}, since with this resistivity a practical current density of 100 ma/in.^{2} would result in an IR drop of 0.1 v. Nonaqueous electrolytes have characteristically high specific resistances (Figure 47), so approaches to devising tape configurations using nonaqueous systems should include reducing the cell resistance by the use of closer spacing and lower resistance separators as well as searching for nonaqueous electrolytes with higher specific conductances.

5. Conclusions

The lithium-lithium perchlorate in butyrolactone-cupric chloride cell had characteristically high voltages at low current rates (13 ma/in.^{2}) and during the initial discharge period. Cathode efficiencies were low, and cell resistance increased during continuous discharge at 25°C.

Table 31

EFFECT OF CATHODE LOADING ON CATHODE COULOMBIC EFFICIENCY

Depolarizer $CuCl_2$
Cathode Mix B *
Formulation Pressure 10,000 lbs/in.^{2}
Drying Time - 16 hrs at 200°C in vacuo
Anode 1/16 in. Li
Temperature 25°C

Separators

Whatman Anion Exchange Membrane AE-81 7 mils thick
Whatman Glass Filter Sheet GF-1 8 mils thick

Cathode Loading mg $CuCl_2$/in.^{2}	Minutes to 2.5 v at 13 ma/in.^{2}	Experimental Capacity amp-min/in.^{2}	Theoretical Capacity amp-min/in.^{2}	Cathodic Efficiency, %
240	75	0.98	5.7	17.2
346	95	1.24	8.3	15.0
437	55	0.72	10.5	6.9
541	63	0.82	13.0	6.3
614	110	1.43	14.8	9.6
660	120	1.56	15.8	9.9
860**	65	0.85	20.6	4.2
860**	65†	1.70	20.6	8.3
860**	30‡	2.09	20.6	10.2
860**	30†	2.48	20.6	12.2
880	105	1.36	21.1	6.4
985	125	1.62	23.6	6.9

* Ball milled 24 hours
† Fresh separators and electrolyte supplied before second discharge
‡ Additional electrolyte only supplied
** Same cell redischarged

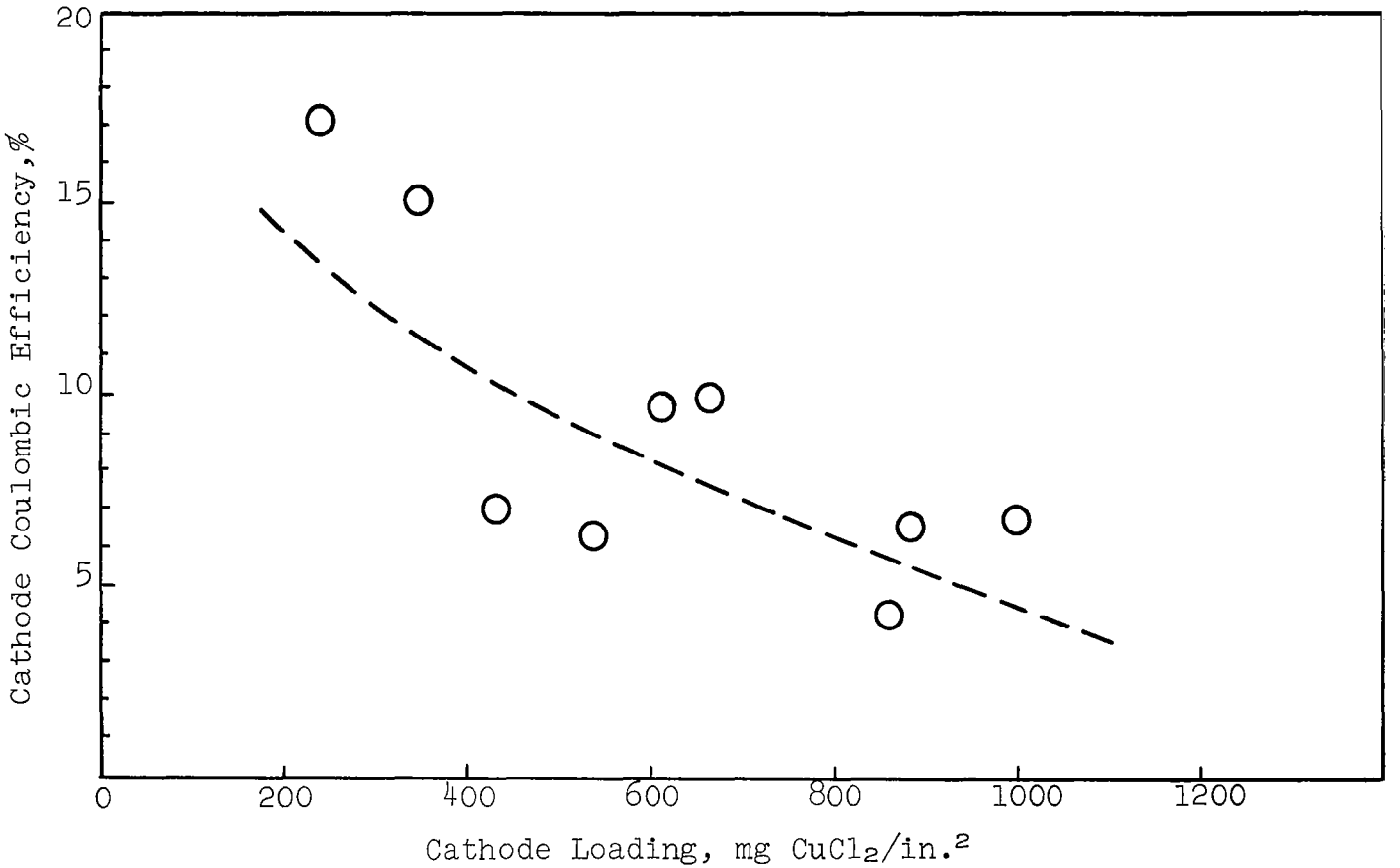

Figure 47. Effect of Loading on Discharge Efficiency of $CuCl_2$ Cathode

PHASE 2. DRY TAPE DESIGN

A. TAPE MANUFACTURING METHODS

1. Background

The ability to buy commercially, or to produce "in house", complete tape strips of reasonable lengths was recognized as a necessary adjunct to the testing program. Early in the work, the natural division of effort into cathode-tape composites and anode strips was made. This acknowledged the probability that the cathode materials would most likely be deposited on the tape substrate (separator) and later mated to the anode. The problems encountered in each area were widely different. Availability was of primary concern when thin sheet stock of magnesium anode was needed; commercially available rolled stock was not manufactured thinner than 10 mils. For cathodes, elimination of cracking upon drying, continuous extrusion of uniform quantities of slurry, and maintenance of uniform loading and thickness tolerances were among the problems to solve.

2. Anodes

a. Materials and Configuration

For reasons stated earlier in this report, magnesium metal was selected as the anode material. However, magnesium reacts with the acid electrolytes needed for efficient cathode performance, evolving hydrogen. Difficulties arose not from the coulombic losses this represented but rather from the polarization and increased I^2R heating suffered under excess gassing conditions. Accordingly, the provision of gas escape mechanisms was a necessary consideration in all anode configurations. With the pressed powder and other high surface area forms ruled out, attention was focused on "block" anodes and various types of thin strips.

b. Block Anodes

This concept concentrates the magnesium in a single location for each cell and exposes one face of the block to the cathode for reaction. Consistent with the gas evolution requirements, several designs were incorporated, ranging from solid to slotted to machined blocks with drilled holes (see Figure 48). With proper precautions, magnesium was readily machined, and no difficulty was encountered in obtaining the desired shapes. Initial tests were conducted with a slotted block in which both the bands and grooves were approximately 1/8 in. wide. Excess electrolyte, however, tended to collect in the grooved sections.

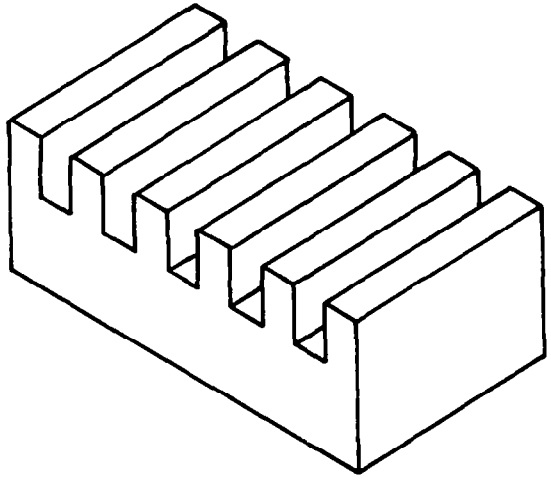

Slotted Block

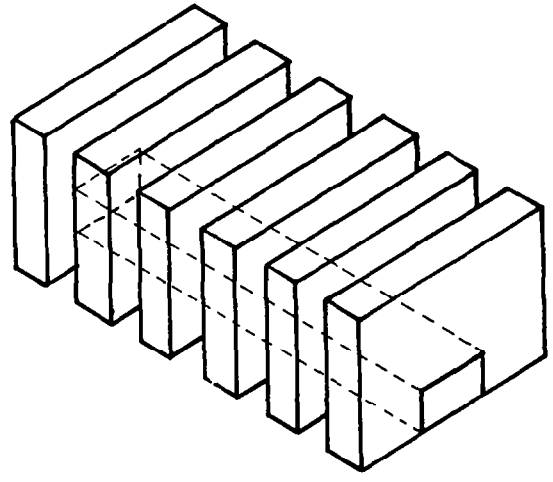

Slotted Block With Open Base

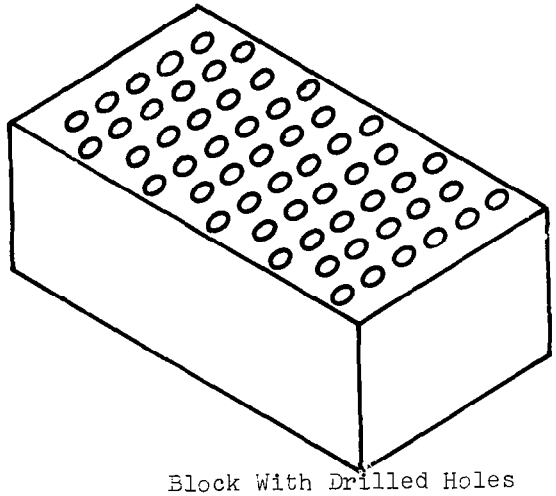

Block With Drilled Holes

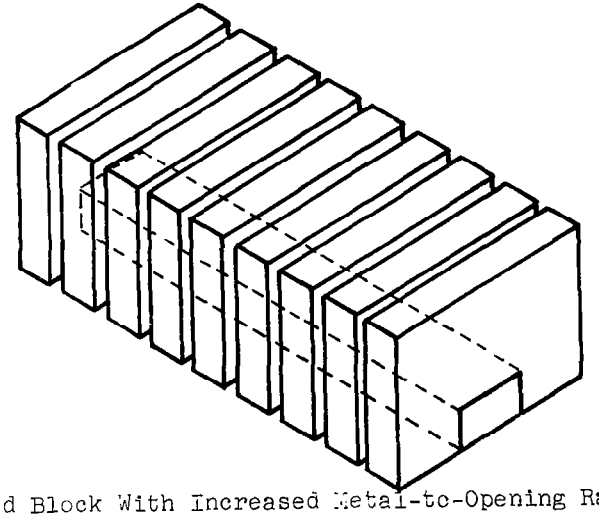

Slotted Block With Increased Metal-to-Opening Ratio

Figure 48. Solid Block Magnesium Anode Designs

Accordingly, the unit was modified to eliminate the base of the grooves, leaving the area between the bands unfilled and removing pockets in which liquid could collect. Nevertheless, maximum tape performance could not be obtained with either design. The difficulty lay in the uneven forces pressing against the tape surface by an anode that was partly solid, and partly open space. Because of correspondingly uneven cathode collector contact, cathode current density was not uniform and outputs suffered.

Considerable improvement was obtained by the substitution of an anode with small holes drilled perpendicular to the exposed face and with the ratio of solid area to open area markedly increased. Similar performance was also noted with a slotted collector in which the void spaces were considerably reduced.

The block anode concept, while desirable from several standpoints, has a number of disadvantages when considered for use with start-stop tape devices. Since local electrolyte excesses may accumulate, anode corrosion may be excessive. This could be particularly troublesome after each stop when additional unconsumed electrolyte is present. Some accumulation of dark reaction products was noticed, even under dynamic conditions, although the extent of detrimental effects was not determined over extended periods of time (i.e. tens of hours). Certainly, this accumulation will present some difficulties for each restart. Consequently, it was decided to stop further efforts with block anodes and shift emphasis to the provision of magnesium in strip form along with the cathode tape.

c. Expanded and Punched Strips

The desire to incorporate the magnesium anode with the cathode tape in strip form placed special emphasis on the acquisition of magnesium in thin, continuous coils. Initial efforts in this area uncovered no readily available stock thinner than 10 mils. This provides a theoretical capacity of approximately 37 amp-min/in.^{2}, far in excess of the 3 to 8 amp-min/in.^{2} output range that appeared reasonable for the cathode loadings. Even with an assumed oxidation efficiency of 65%, thinner material was obviously required. A reference summary of many of the materials obtained later in the program and the corresponding theoretical capacities is shown in Table 1 (page 6).

(1) Thin Sheet Material

At the start, the configuration of magnesium was undetermined, but the need for the basic thin gage material was pressing. Two possibilities were foreseen to reduce the thickness to an estimated 3-5 mils. Roll milling (hot or cold) appeared likely if vendors with this type of experience could be located, and chemical milling (etching) was a likely process if cost was not prohibitive for our moderate quantities. Following visits to

Dow Chemical Company, Midland, Michigan and Chemical Micromilling Co., Philadelphia, Pennyslvania, etching baths were set up in our laboratories. While accurate tolerances were not maintained, it was found that the process was sufficiently straight-forward for us to supply our own requirements until a more refined source was developed. With Chemical Micromilling Co., steps were taken to define the cost and time involved in establishing a small, pilot-size capability for producing continuous strips of magnesium in the 3-5 mil range. While capital cost was reasonable (less than $1000), set-up and prove-in time would run dangerously close to the end of the contract period and give us little benefit. In view of this, the commercial etching approach was abandoned while we awaited results of the concurrent roll milling program discussed below. In the interim, preparations were made for doing the work in-house if required. The process steps used are shown in Appendix A-4.

A great number of roll milling firms, particularly those specializing in thin foil materials, were contacted to obtain thin gage magnesium. Most contacts were fruitless. Some extended lengths of 6-mil stock were obtained from Peerless Rolled Leaf Co., Union City, N. J., but this was the remaining shelf stock of earlier experimental work. The process (understood to be cold rolling of 16 mil) was later dropped due to economics and low demand. The Hi Cross Co., Wehauken, N. J., using a hot rolling process, agreed to roll some 4-mil samples from 10-mil stock supplied by us. These were evaluated and found to be satisfactory, and arrangements were made to obtain continuous lengths. This procedure proved satisfactory for our present needs. The 10-mil coils are purchased from Dow Chemical Co., slit to proper width, and re-rolled by Hi Cross Co.

(2) Anode Configuration

With the base stock available, the proper design features for gas release could be incorporated. Early anode work had shown an open mesh expanded form to operate best, but this was later determined to be true only for excess electrolyte conditions such as are encountered in beaker cell static testing. In translating to the limited electrolyte dynamic testing, a relatively flat, closed mesh was used. This design presented maximum surface for contact to the wetted separator and provided a uniform current density distribution with the positive electrode while still maintaining a slight three dimensional effect. The consumption of the magnesium during discharge, however, weakened the expanded metal joints and caused frequent rupturing of the strip. In addition, contact for current collection was more difficult.

Design emphasis shifted to perforated strips where continuity was more assured and anode contact was simplified. Using chemically milled samples and manual perforating techniques, a variety of designs were evaluated. The final arrangement is shown

in Figure 49. A local tool and die shop manufactured the punches and die mountings for use with standard kick presses to produce the continuous lengths. The photograph in Figure 50 shows the punched strip along with one of the earlier flat expanded forms.

Performance of the anode under dynamic testing conditions has been very satisfactory. Both the limited electrolyte quantities and the pressure effect of close contact with separators appear to have reduced the gassing problem from the rapid evolution noted early in the contract period.

3. Cathode Tapes

a. Background

This portion of the electrode processing work was concerned with the production of cathode tape composites of sufficient length to meet the requirements of the dynamic testing and demonstration programs. Aside from the obvious demands of uniformity, flexibility, and physical strength, the process had to be adaptable to a variety of depolarizer materials and cathode formulations. Since the coating materials were not similar to any known commercial coatings, a specific process had to be developed. At the same time, it was expected that good use could be made of the experience and methods employed by painting, laminating, and similar industries.

b. Knife Casting

With this method, a small quantity of slurry, is drawn over a stationary tape by a moving adjustable blade (Gardner Knife). It was used for all early cathode testing and was conveniently done on a small scale basis. Analysis for scale-up, however, pinpointed several detrimental features. The reservoir of slurry behind the knife edge is pulled over the entire length of tape and an impregnation rather than a surface coating tends to result. Consequently, thicker base tapes are usually required to give adequate electrode separation. Unless subsequent treatments are applied, cracking upon drying is troublesome, particularly when organic solvents are used to prepare the slurry. Temperature variations to speed up or slow down the drying had little effect. While thickness control was generally adequate, the metering control of slurry output was sensitive to lumps, density variations, and other inconsistencies in the slurry itself. Accordingly, more sophisticated methods were sought.

c. Power Spraying

The DeVilbiss spray gun used for this work has two separate feed systems. The first employs adjustable air pressure over the slurry material to be sprayed, forcing it through the exit nozzles at a controlled rate.

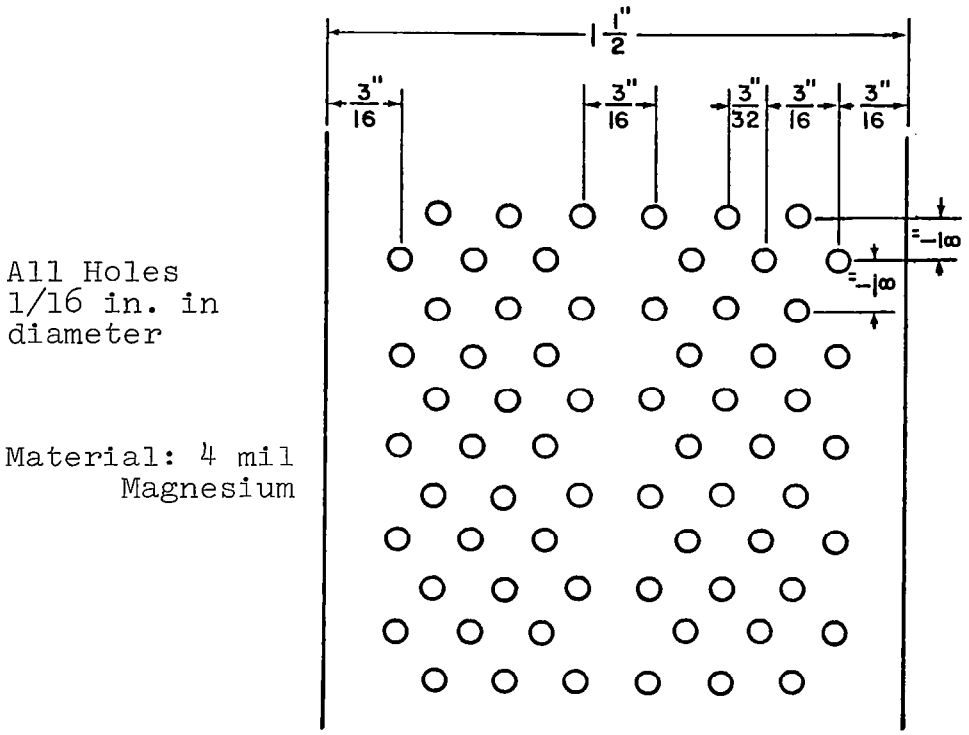

Figure 49. Punched Magnesium Strip Design

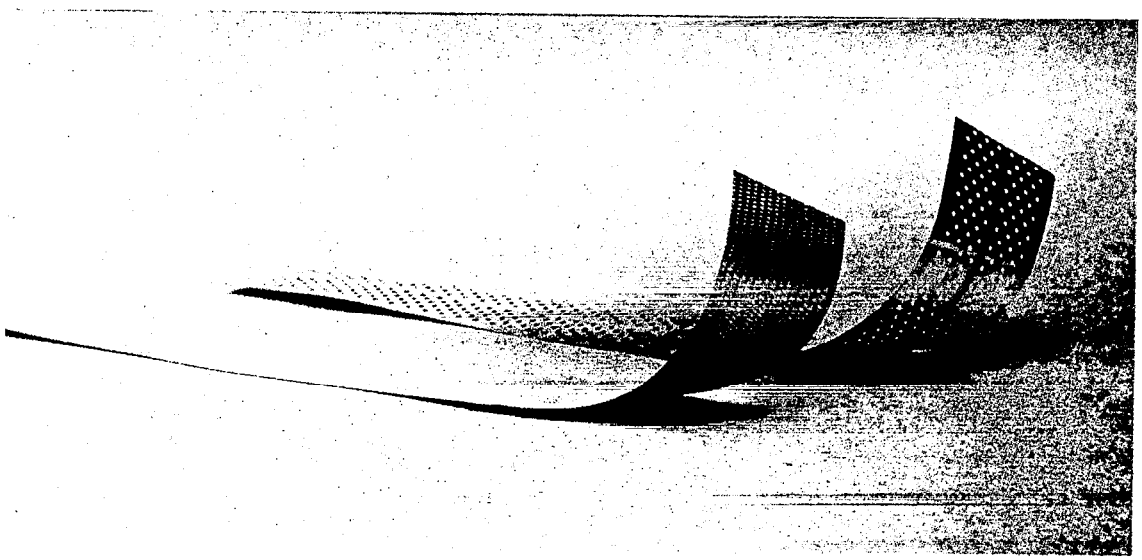

Figure 50. Comparison of Punched and "Flat Expanded" 4-mil Magnesium

The second system, equally controllable, supplies only the air stream (or air for atomization) on which the particles from the solution reservoir are carried to the work. To permit effective use of the equipment, a rotating drum approximately 15 in. in diameter was attached by pulley and drive belt to an adjustable-speed motor. Base tape material was attached to the circumference of the drum, allowing production of cathode tapes approximately 1 foot wide by 4 feet long. These were later slit to desired width.

Water and organic slurries were used. The water-based type, however, was eliminated immediately because of severe soaking and impregnation. The organic slurries, however, produced good quality tapes from the outset. The naturally rapid evaporation of these solvents plus their breakdown into a fine mist by the atomization air resulted in almost instant drying. Thus, the solvents served excellently as a carrier medium to the gun exit nozzle but the net effect from the point was virtually a spraying of solid matter. Barely sufficient moisture remained to promote adhesion to the tape material and the tapes were totally dry within 1-3 seconds. These same factors permitted layer to be sprayed upon layer as the drum rotates, since over 95% of the evaporation takes place before the tape is coated. A secondary benefit is realized in that the added material is a true surface coating making possible the use of thinner base materials.

Tapes prepared by the spray method were more fragile than many of those cast with a Gardner knife, particularly those cast with dynel fibers. Nevertheless, flexibility was excellent and they did meet maximum standards of durability to allow winding on a reel, unwinding, discharge, and rewinding without visible material loss. Care was required when slitting to proper width. Surfaces were quite smooth, which promoted good collector contact. A major problem area was an occasional uneven slurry flow that caused thickness variations ($\pm$ 0.1 to $\pm$ 0.2 mils). Some corrosion of the spray gun passageways was evident despite the use of stainless steel parts for all vital areas. To correct both of these difficulties and to permit use of the gun with all of the cathode materials likely to be investigated, Teflon parts were substituted for all slurry-carrying passageways. This change eliminated the intermittant action of the gun and reduced clogging difficulties. Also, to prevent clogging, dynel or carbon fibers were eliminated from all spray formulas.

As the evaluation of the spray gun technique progressed, increasingly heavier cathode loadings were being demanded by the other aspects of the dry tape program. To meet these requirements, a thorough analysis of the capabilities and limitations of the process was conducted. As the loadings increased, the coating became somewhat loose and fluffy. This was reflected in the low density of the sprayed coat, which dropped as low as 11% solids packing. While this in itself is not detrimental (even desirable),

it is characterized by poor adherance to the tape and flaking problems. A secondary operation was added to compress the sprayed tape between a set of steel rollers and, although improvements were noted, rippling sometimes resulted and physical quality was still minimal. This, coupled with the requirement for multiple passes over the tape surface, combined to diminish the value of the power spraying technique. A summary of the characteristics of sprayed tapes is shown in Table 32 where all the processes are compared. The numerical ranges listed do not necessarily reflect absolute limitations of the process; in some cases, attempts were not made to achieve a wider range.

d. Extrusion and Compression

Previous studies in the area of cathode cracking with drying brought to light the advantages of working the cast materials while still wet, to bring the moisture to the surface in the manner of cement troweling. Cracking was greatly reduced or even eliminated.

This principle had been adapted in a one-step process in the 1 x 3 in. compression molding die used for earlier cathode testing. Electrode ingredients were mixed with a minimum quantity of water or other solvent to form a semi-dry paste. A known volume of the paste was then dispensed into the die cavity. Upon compression, excess solvent was forced out through the die clearances resulting in a molded tape-cathode, almost completely dry, whose surface was uniformly smooth. Since the coatings were also quite rigid, the method was considered unsatisfactory for tape usage except possibly for a magazine dispenser where the tape is loaded in a zig-zag fashion.

The same principle was applied in the two-step metering and compression process. Using this approach, the cathode paste was first metered onto the tape in uniform quantities, and then the tape was passed between a set of steel rollers to squeeze out the liquid. The resulting tape was, as above, almost completely dry and had a smooth surface. Since the process is inherently continuous, and since preliminary experiments showed it to be entirely feasible, full scale pilot equipment was designed and constructed. A photograph of the equipment layout is shown in Figure 51.

The two-step approach has been given considerable testing and has had several modifications. In summary, the compression rolls appeared to perform adequately as designed, but the metering step possessed some problems. Bridging of mix particles and fibers at the exit ports was troublesome as was tearing of the tape due to excess pressure by the edge guides and center runner (the process was designed for a double tape system). Several die designs were tried, the general progression of which is represented schematically in Figure 52. The major improvements were

Table 32

SUMMARY OF PHYSICAL DATA FOR CATHODE TAPE PROCESSING METHODS

	Knife Cast	Power Spraying		Compression	
		As Made	Rerolled	Range	Final Design
Coating Thickness, mils	8-40	5-33	9-22	12-28	18
Tape loading, mg/in^2	85-250	80-150	80-150	120-396	200
Theoretical capacity, amp-min/in.^{2} (various formulas)	4.5-14.4	3.0-9.0	3.0-9.0	3.5-15.5	6.7
Solids packing,%	18-23	11-18	17-20	21-38	23

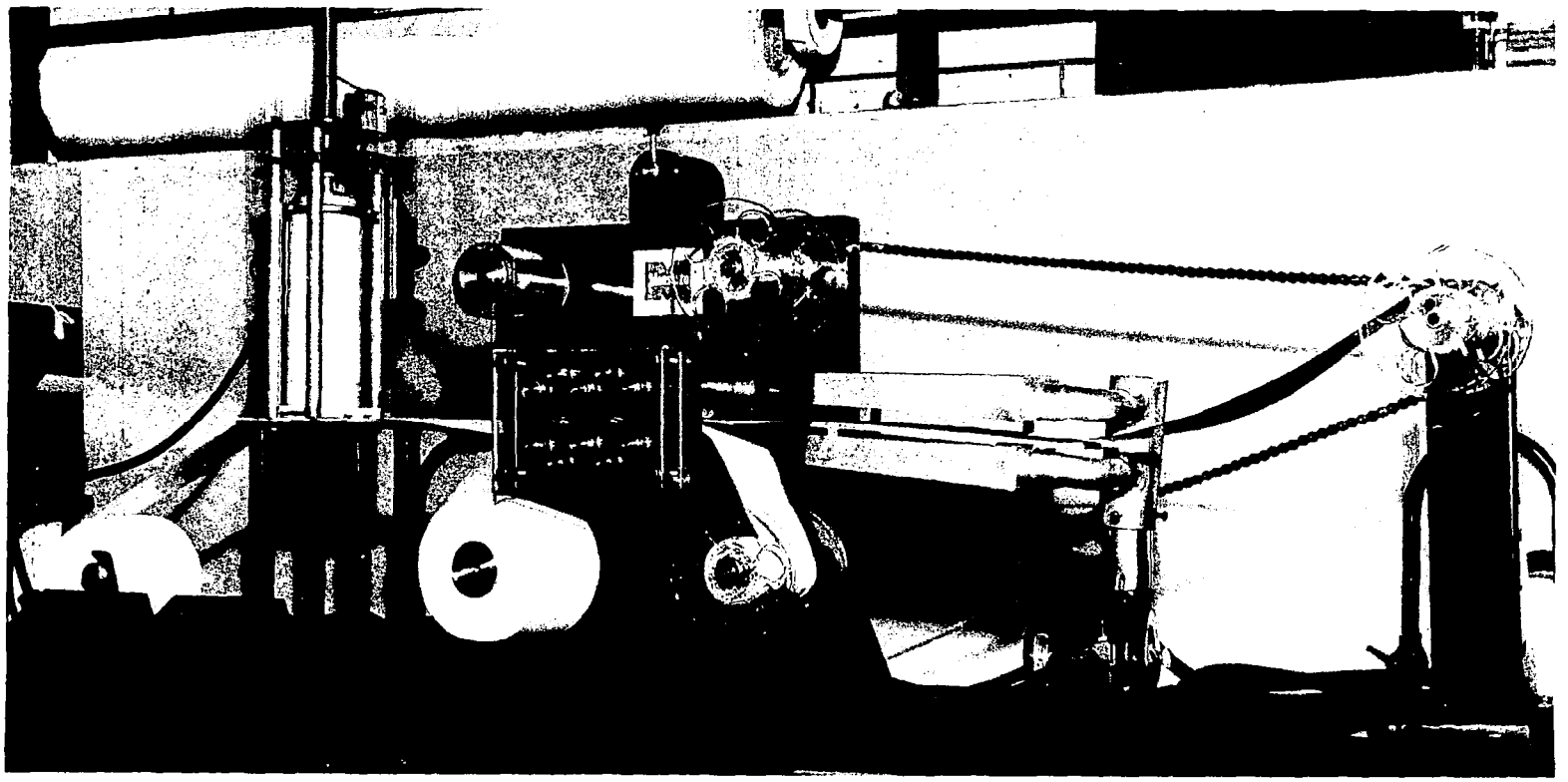

Figure 51. Cathode Tape Manufacturing Equipment

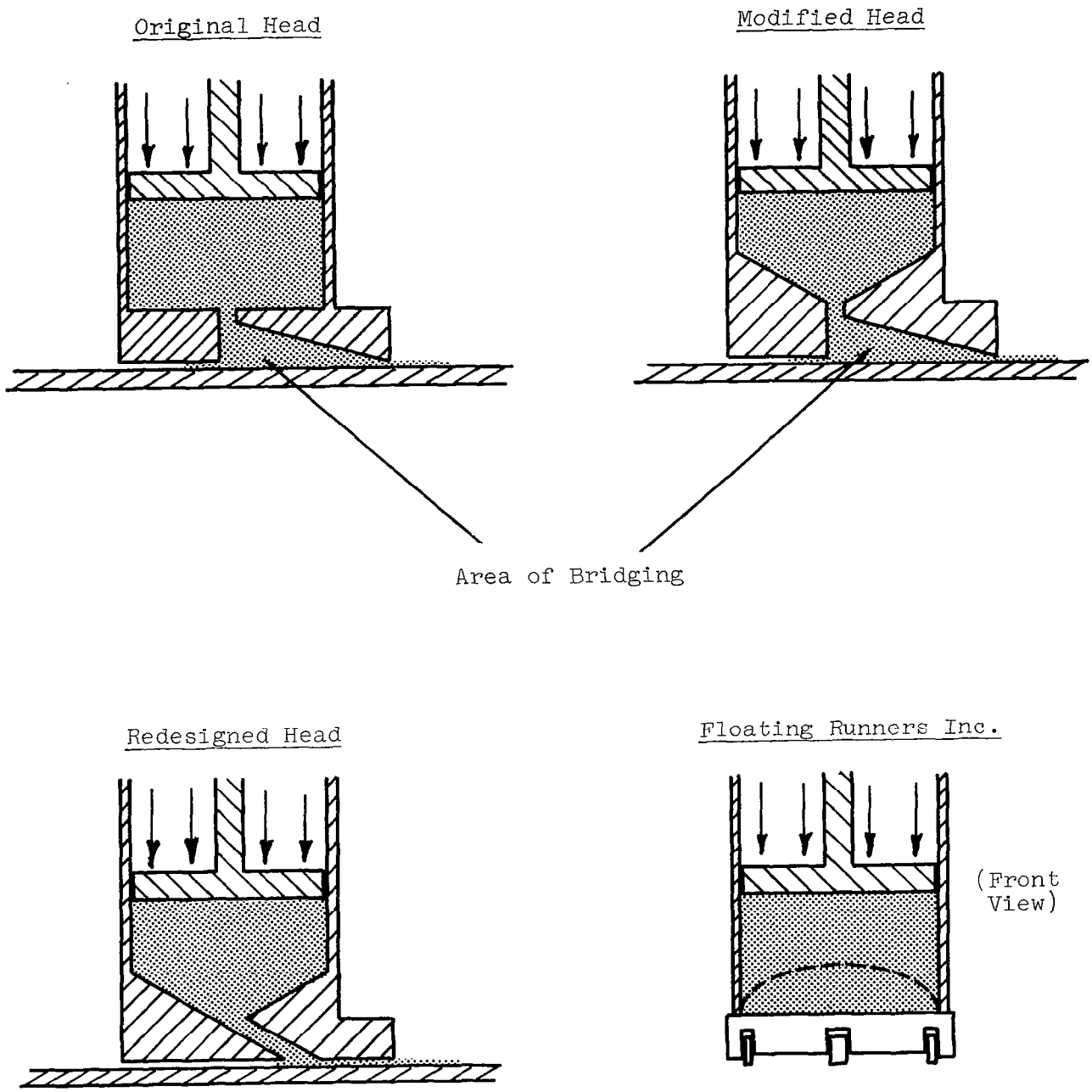

Figure 52. Schematic of Slurry Extrusion Dies

the elimination of the 90-degree turn within the head, the elimination of the lead out angle (lead out compression zone), and the incorporation of floating runners for edge and center definition. A photograph of the final die is shown in Figure 53. The latter, made of stainless steel for greater rigidity, performed satisfactorily from the start.

The electrical performance of machine-made tapes was initially below par (compared to comparable knife-cast tapes). Several factors were responsible. Solids packing tended to be considerably higher at first; reducing the density by adding fugitives or opening the compression roller gap did little to improve performance. The best results were obtained by adjusting the carbon black content which, due to its incompressible nature, produced an open pore structure and, apparently, a higher surface area with the same void volume. The binder content was also a factor since higher quantities of binder produced higher solids packings. This was in opposition to our efforts to promote good adhesion to the tape surface.

The problem was resolved by pre-dissolving the binder in the slurry solvent prior to mixing, thereby assuring excellent dispersion and obtaining maximum utilization of the amount present. An additional benefit lay in the fact that during the slurry extrusion, the base tape became wetted with solvent that contained the binder. This helped strengthen the binding link between the coating and the tape.

A general tabulation of many of the process trials is presented along with the mix formulas in Appendix Tables A-5 and A-6. The listing reflects our attempts to resolve the interrelating factors of electrical performance, physical stability, cathode loadings, binder content, and collector sticking. An interesting note on the latter problem is the incorporation of a grooved pattern into the coating surface during cathode-tape manufacture. This is accomplished by inserting a nylon netting between the top blotting paper and the slurry coating prior to roller compression and removing it following the compression rolls. The pattern provides a multitude of interconnected channels that serve to distribute electrolyte more evenly, particularly on the collector contact surface (which should be kept moist to prevent sticking). Some benefit arises, also, in flexibility and stability due to the grooving. The cathode pattern can be seen in Figure 54.

4. Composite Tapes

A large effort was not expended on techniques for mating the anode and cathode sections since only a minimum level was required to satisfy our program requirements. Some comparisons were conducted, however, on the suitability of various adhesives and on the type of joint required. Satisfactory composite tapes were made using a PVP-chloroform solution (about the consistency

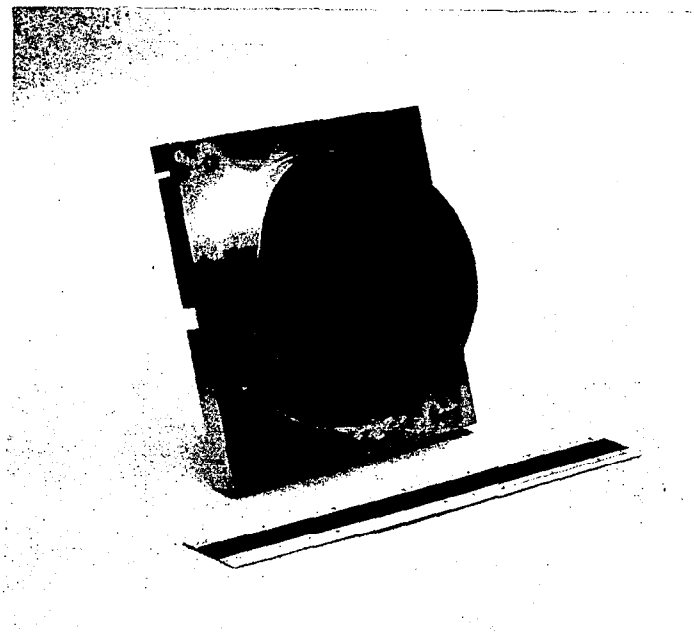

Topside showing slurry
lead-in section

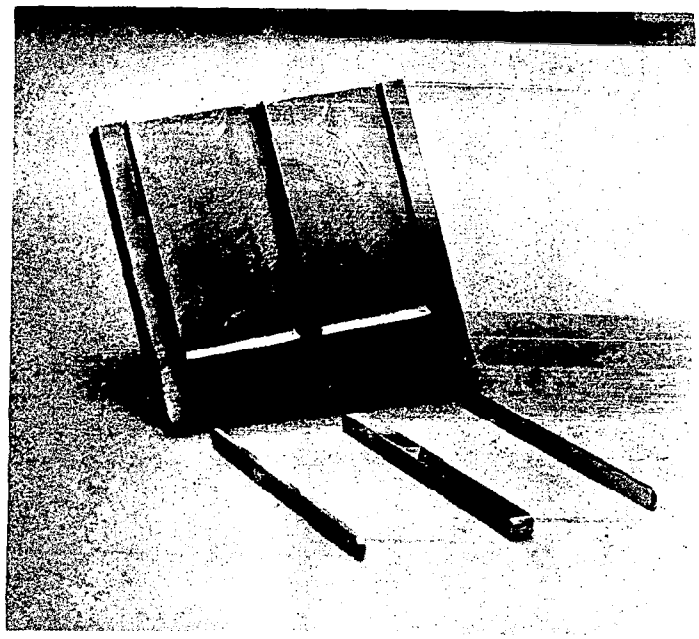

Underside with floating
runners removed

Figure 53. Final Extrusion Die

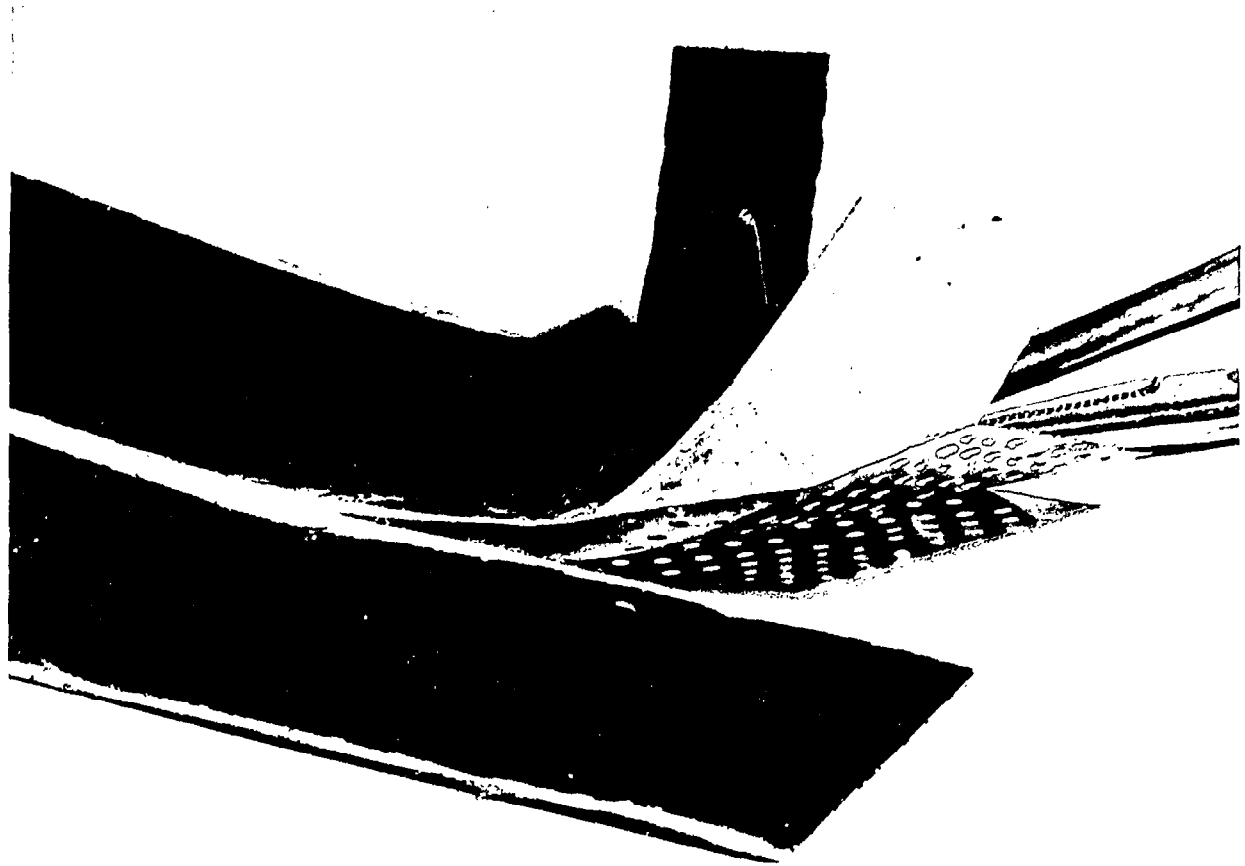

Figure 54. Composite Tape Assembly

of motor oil) and placing 1/8 in. dots of the glue approximately 3/4 in. apart on the solid portions of the magnesium strip. They were wound with the cathode to the outside since there was sufficient stretch in the coating to allow for the larger diameter. The complete tape is shown in Figure 54.

5. Conclusions

With the background in tape fabrication obtained during the contract period, we have the capability to manufacture cathode tapes from a wide variety of depolarizer materials and slurries. The two-step process is satisfactory from a tape quality standpoint and is adaptable to scale-up to pilot line or production operations. The product is uniform and electrochemically active although only minimal in adherance and ruggedness. It is felt that improvement in the latter areas can be accomplished without major change in the essential process steps.

Adequate sources of supply for thin magnesium coil were developed. Further treatment in the form of punching, expanding, etc. can be done without undue problems. With the $AlCl_3$-HCl mixed electrolyte, a perforated magnesium pattern performs satisfactorily with respect to corrosion and gas escape. With our present experience, obtaining and handling other uncommon metallic anode configurations can be approached with confidence.

Mating of anode strips and cathode tapes into a composite structure was performed on a minimum basis only. No outstanding problems are foreseen in this area although some sophistication seems desireable.

B. JOINT ANODE-CATHODE (DYNAMIC) TESTING

1. Background

The dynamic testing phase of the dry tape program is concerned with the engineering aspects of discharging moving tapes. The objectives of this portion of the work were: (1) to develop a system capable of discharging tapes continuously with the close control of variables necessary to achieve steady-state conditions; and (2) subsequently to characterize tapes quantitatively using this system. The tapes used in the early portions of this work were based on a variety of cathode materials with magnesium anode and were made by the techniques described earlier. Stationary block, flame-sprayed, and milled magnesium strip anodes were tested. Initial tests were qualitative and were concerned with tape integrity and other physical performance factors. These tests, discussed briefly in the following sections, led to various modifications in the tape formulation and makeup methods and in the dynamic test equipment itself. In later work, with long lengths of uniform tapes available, various discharge parameters were explored and their effects on discharge efficiency determined.

This work was done with potassium periodate cathodes and provided data for the design of a demonstration unit.

2. Equipment

The dynamic tape test device is shown in Figure 55. The discharge head (1) is discussed in detail below with reference to Figure 56. The tape shown is a double tape (2) pulled through the discharge head by the take up reel (3), which is driven by the motor (4) through two speed reducers. Most tests were conducted on single tapes, in which case only the front collector head was used. The large diameter reel was used to limit speed variation due to diameter changes as the tape was wrapped on the reel. Test times of over one hour required less than two wraps on the reel. Tape speed was set by the motor speed control and determined by reading the voltmeter, (6) which was connected to a tachometer generator on the motor shaft. This system provided close control and reproducibility of tape speeds from 0.05 to 0.50 in./min. Speed was maintained constant within 3% of the desired value for test durations of over an hour.

Electrolyte was fed to the tape through the discharge head from syringes (7), the rate being controlled by varying the available hydrostatic head. The feed rate was determined from the syringe readings taken at fixed time intervals. Tapes with good wetting characteristics were found to take up electrolyte over a wide range of head, the flow evidently being controlled primarily by the wicking properties of the cathode and separator materials. Tapes with poor wetting characteristics would not absorb sufficient electrolyte to wet the separator and magnesium surface well. In these cases, additional electrolyte was added through the punched magnesium from another syringe.

The tape was discharged through two parallel connected, 15-ohm variable resistors (8), one being used for coarse adjustment to the desired current, the other for fine control. The discharge circuit is shown in Figure 57. Depending on the discharge rate, the current was read on a 1.5-amp or 3-amp meter along with cell and reference voltages (9). Both cathode- and anode-to-reference voltages were measured using a silver-silver chloride reference (10). The reference electrode was made from fine silver strip that was anodized in 1M HCl at 25 ma/cm^2 for 10 to 15 minutes. The strip was wrapped in a dynel separator that contacted the anode and cathode surfaces downstream from the discharge head.

The discharge head in its final form as used with the potassium periodate cathode is shown in Figure 56. The graphite cathode collector (1) is made from graphite block*, 3 x 1.5 x 1/4 in. thick.

---

* U. S. Graphite 443

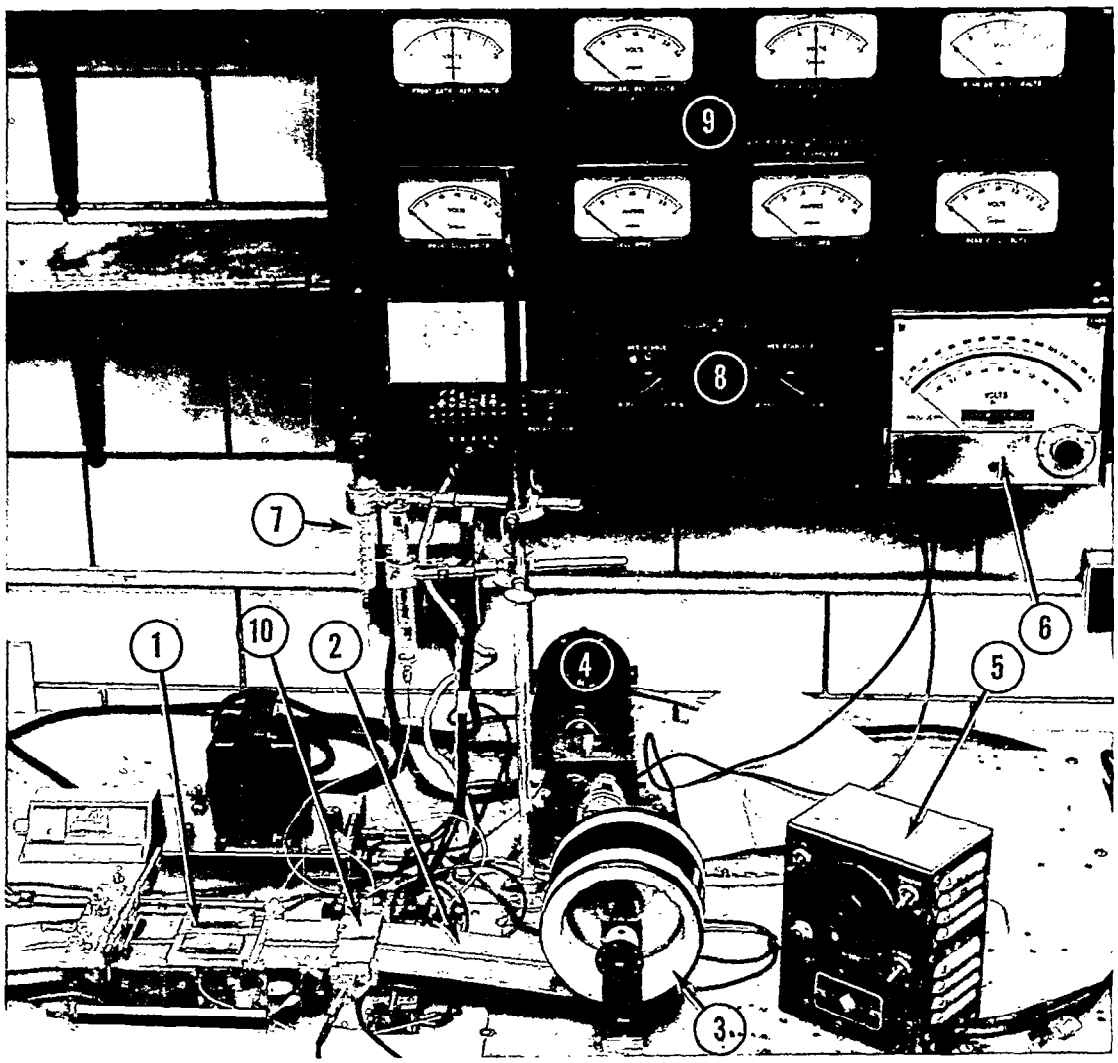

1. Discharge head
2. Double tape extrusion--KIO_4-Mg tape
3. Take-up reel
4. Drive motor and drive train
5. Speed control
6. Tape speed meter
7. Electrolyte feed syringes
8. Load resistors
9. Output meters
10. Ag-AgCl reference electrodes

Figure 55. Dynamic Tape Test Apparatus

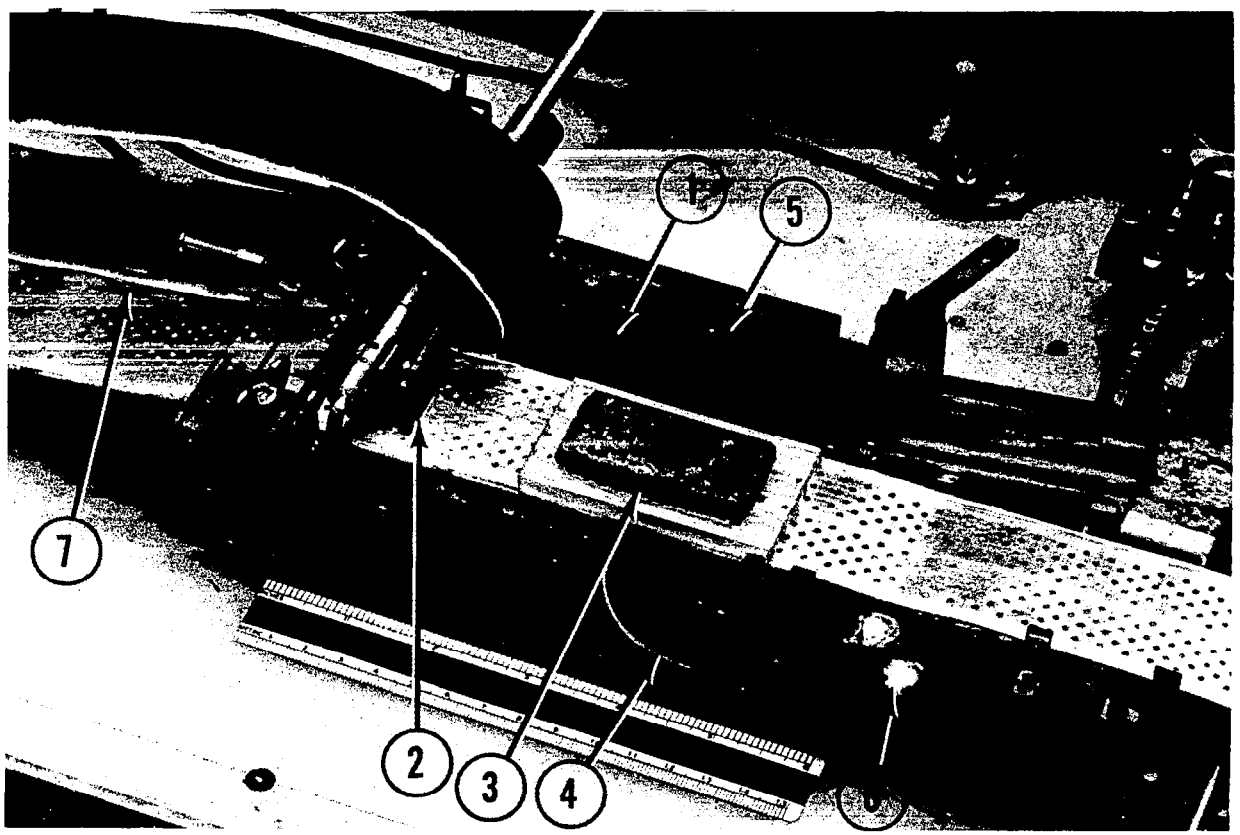

LEGEND

1. Graphite cathode current collector
2. Spring-loaded anode current pick-up
3. Slotted Plexiglas anode pressure plate with weight
4. Electrolyte feed tube
5. Electrolyte dispensing ports
6. Light and mirror for viewing discharged cathode coating
7. Double tape extrusion--KIO_4 cathode-Mg anode

Figure 56. Detail of Discharge Head in Figure 55

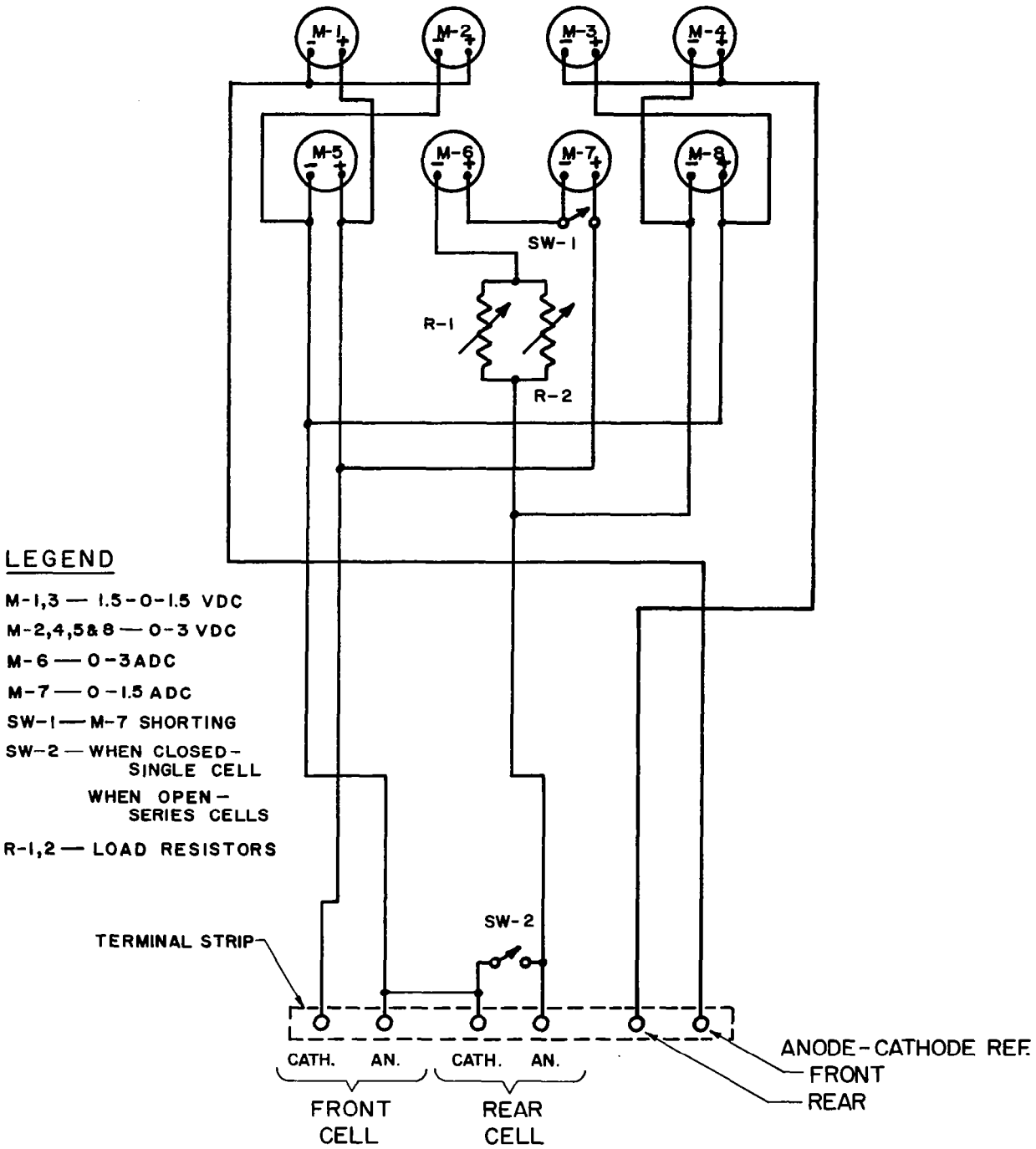

Figure 57. Dry Tape Discharge Circuit

The leading edge was chamfered for the first half inch and taped over to provide a smooth entrance for the cathode coating. The active cathode collector area was 3.75 in. with this discharge head. Anode current pickup was accomplished by a sharp-toothed copper-beryllium tab (2) with adjustable spring loading pressing it on the magnesium upstream of the wetted discharge area. Contact pressure at the discharge area was maintained by lead weights placed on a slotted (for gas release) plexiglas plate (3).

Electrolyte was fed from the syringe through Teflon tubing (4) to a manifold in the graphite cathode collector and then through the dispensing parts and slots (5) to the cathode surface. The slots were found beneficial in providing uniform electrolyte distribution. A mirror and light arrangement (6) was also provided for convenient viewing of the discharged cathode surface.

Earlier test work was also done with 1 in. wide tapes on another discharge head. On this head, both platinum and graphite were tried as cathode collector materials, the graphite collector being somewhat less prone to sticking to the cathode coating. Slotted cathode collectors of several designs were also tried in this setup. The slotted collector designs varied from a single narrow slot across the collector to wide (1/8-in.) multiple slots. Electrolyte was fed both through the cathode collector and directly to the separator material. Feed through the cathode collector generally reduced the sticking problem, but certain tapes required additional electrolyte to the separator as mentioned previously. In one case, the slots were filled with Silastic insulating material, to provide intermittent nondischarge areas for redistribution of electrolyte for the elimination of sticking. This method did not substantially alleviate sticking with tapes that were prone to adhere to the collector surface. It was found that feed of a large excess of electrolyte at the cathode collector surface would effectively eliminate sticking. This reduced output, however, by "floating" the cathode surface off of the collector thus reducing the area of electronic contact. The best method found for eliminating sticking was to reduce the packing density of the cathode coating thereby allowing a greater quantity of electrolyte to be taken up in the coating. When the packing density was reduced sufficiently to provide take-up of electrolyte in accord with the discharge requirements as discussed below, sticking was generally alleviated.

In one case, a static discharge of a cell using a tape cathode and magnesium anode was run with mercury as the cathode collector to eliminate sticking possibilities. The discharge on mercury compared favorably with discharges on platinum and graphite collectors. However, indications of oxidized mercury were noted on the discharged cathode surface when the cell was opened up. It was felt that any loss of mercury would not be tolerable from a weight standpoint and this approach was not pursued further.

3. Dynamic Test Results

Dynamic tests were made on trichlorotriazinetrione, picric acid, and potassium periodate cathode tapes with magnesium anodes. Early test work was conducted on trichlorotriazinetrione and picric acid cathodes. The later, more complete test results with potassium periodate as tabulated in Appendix Table A-7 reflect improvements in the test equipment as well as the tape itself. Representative data from the early tests are given in Table 33. The use of a block anode of primary magnesium was demonstrated in early tests with trichlorotriazinetrione cathode tapes. While continuous magnesium foil anodes were used in all later testing, the block magnesium anode appears feasible for use with neutral or acid electrolytes and may offer advantages in these cases.

The following test procedure was generally employed with potassium periodate. With the dry tape in position, the tape speed was set and electrolyte feed started. When complete wetout of the tape in the discharge head was accomplished, the open-circuit voltage was read and the circuit was then completed, the current being adjusted to the desired value by varying the load resistance. Under open-circuit conditions, chlorine evolution occurred, evidenced by the odor of chlorine gas. This was undoubtedly due to the oxidation of chloride ion present in the electrolyte by the periodate at the high open-circuit potentials developed. The rate of this oxidation was not rapid, however, since short times on wet stand did not appreciably affect static discharge efficiencies.

Upon initiation of discharge, the cell potential decreased from the high open-circuit value of about 2.9 v to about 2.3 v and continued to fall as steady-state conditions were approached. The load resistance was adjusted as necessary to maintain constant current and cell voltage. Other pertinent data were recorded at short time intervals, usually every 4 minutes. At the tape speed used most frequently, 0.25 in./min., 10 minutes were required for complete change of tape over the 2.5 in. collector length. Within this time, the cell voltage fell to an essentially constant value unless the discharge rate was greater than the tape could support, in which case the discharge rate was reduced. The run was continued for a sufficient time to effect discharge of a minimum of two collector lengths of tape before any change in conditions was made.

Sample discharge curves are shown in Figures 58 and 59 for several tapes. Small voltage deviations from a steady value during a run were caused by variations in wet-out or tape characteristics, but a continued decrease in voltage was caused by inability of the tape to support a particular drain rate or, as was often the case, the adhering of a portion of the cathode to the cathode collector. In some of the tabulated runs, steady-state conditions could not be attained for this reason. When a

Table 33

EARLY DYNAMIC TEST RESULTS WITH PICRIC ACID, TRICHLOROTRIAZINETRIONE AND POTASSIUM PERIODATE CATHODE DEPOLARIZERS

Tape No.	Depolarizer % weight	Depolarizer mg/in.^{2}	Anode Material	Anode Thickness mils	Electrolyte	OCV, volts	Cell Voltage, volts	Current Density, ma/in.^{2}	Tape Speed, in./min	Cathode Coulombic Efficiency, %
Picric Acid Depolarizer‡										
TW-4	47.5	95	AZ31B	3	Sat'd $AlCl_3$	2.05	1.0	150	0.15	-
TW-4	47.5	95	AZ31B	3	Sat'd $AlCl_3$+0.25M HCl	-	0.8	350	0.15	39
52764-DO-2	-	-	AZ61B	8	Sat'd $AlCl_3$	1.63	0.9	250	0.17	-
52765-1-A-1	47.5	82	Mg	3	2M $AlCl_3$+0.25M HCl	2.05	1.0	500	0.15	-
52766-2-A	47.5	82	Mg	3	Sat'd $AlCl_3$	2.15	1.0	255	0.15	32
52765-2-A	47.5	82	Mg	3	2M $AlCl_3$+0.25M HCl	2.2	1.0	300	0.15	39
52765-1-B	47.5	82	AZ61B	4	2M $AlCl_3$+0.25M HCl	1.9	1.0	400	0.25	31
52765-2-C	47.5	82	Exp.AZ31B	10	Sat'd $AlCl_3$	2.05	1.0	225	-	-
52765-2-C	47.5	82	Exp.AZ31B	10	2M $AlCl_3$+0.25M HCl	-	1.0	300	-	-
52768-1-B	47.5	80	Exp.AZ31B	8	Sat'd $AlCl_3$	1.9	0.9	200	0.15	30
52768-1-B	47.5	80	AZ31B	8	2M $AlCl_3$+0.25M HCl	2.0	1.0	230	0.10	46
52768-1-B	47.5	80	AZ31B	8	2M $AlCl_3$+0.25M HCl	-	0.85	325	0.15	30
52771-5	47.5	64	Mg	3	2M $AlCl_3$+0.25M HCl	1.8	1.0	290	0.15	45
Trichlorotriazinetrione‡‡										
S-6-A	45	25	Mg	Block	2M $Mg(ClO_4)_2$	-	2.0	60	0.55	16
S-6-B	45	25	Mg		2M $Mg(ClO_4)_2$	-	1.5	80	0.66	28
Potassium Periodate Depolarizer‡‡‡										
52776-2-2	45	145	AZ31B	4	Sat'd $AlCl_3$	2.4	1.5	410-470	0.15	58-68
52776-1-2	60	190	AZ31B	4	2M $AlCl_3$+0.5M HCl	-	1.5	210	-	-
52776-2-3	45	117	AZ31B	4	Sat'd $AlCl_3$	2.58	1.5	220	0.15	40
52776-2-3	45	117	AZ31B	4	2M $Mg(ClO_4)_2$ *	-	-	-	-	-
52776-2-3	45	117	AZ31B	4	Sat'd NaCl	1.70	1.7	280	0.15	-

Typical Cathode Casting Mix Compositions, Wt %:

‡
Picric Acid	47.5
Shawinigan Black	38.0
Carbon Fiber	9.0
Polyvinylpyrrolidone	5.5

‡‡
Trichlorotriazinetrione	45
Shawinigan Black	45
Opalon-506	7
Santicizer-160® Plasticizer	3

‡‡‡
Potassium Periodate	45
Shawinigan Black	45
Dynel Fibers	5
PVP	5

* Cathode swells and flows

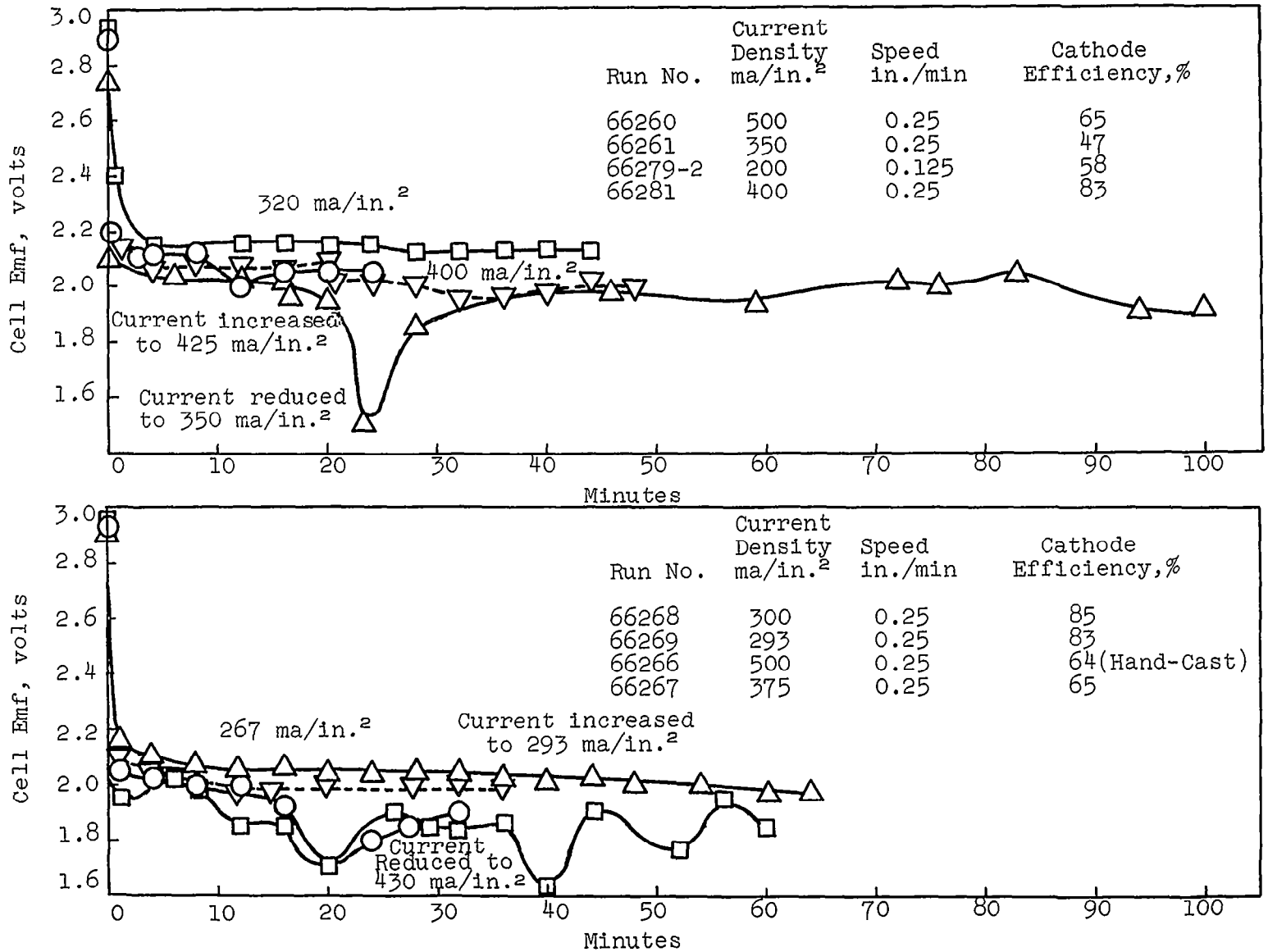

Figure 58. Representative Dynamic Test Results for Potassium Periodate-Magnesium Couple in 2M $AlCl_3$-1M HCl Electrolyte

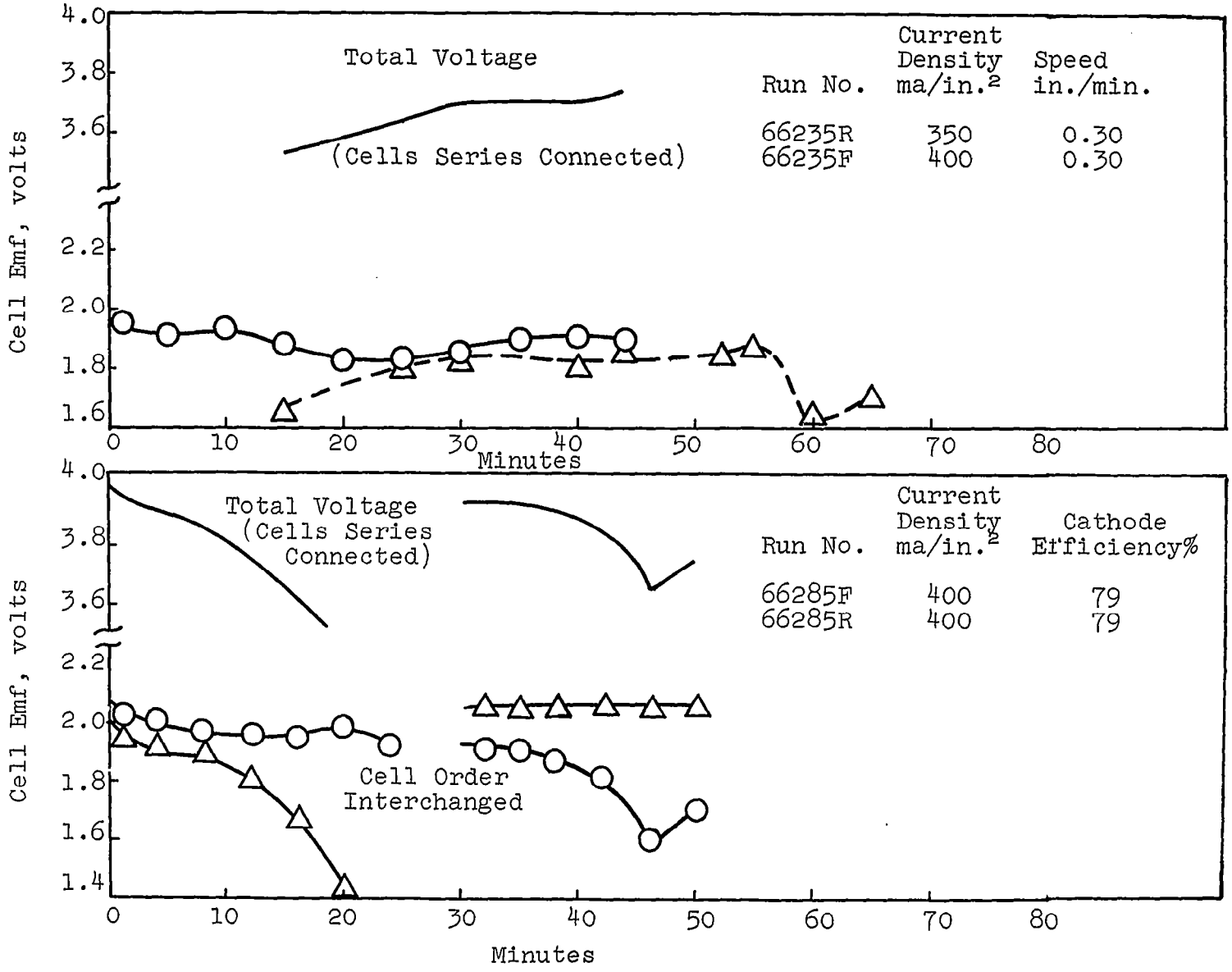

Figure 59. Dynamic Test Results for Series-Connected Double Tapes Using Potassium Periodate-Magnesium Couple

run was terminated because of cathode sticking, an "S" follows the run time as given in Appendix Table A-7.

When double tapes were discharged, the procedure was identical to that above except that sw-2 in Figure 57 was opened to connect the cells in series, and the appropriate individual cell and reference voltages were recorded. The double tapes were extruded on a single separator and this separator provided an electrolyte path between the two cells. This path apparently affects the cell voltage as indicated in Figure 59. When the cell order was interchanged, the poorer cell improved while the better cell showed a drop in voltage. This effect was reduced by wet-proofing the portion of the separator between the two tapes but conclusive results on this effect have not been obtained.

a. Anode

The preferred anode material was primary magnesium. Magnesium AZ31B and AZ61B alloys offered no stability advantages with the electrolyte as used under the dynamic test conditions and resulted in lower cell voltages. The machine punched magnesium strip, 4 mils thick, operated with lower polarization than the strip without holes and provided more uniform contact than the perforated and expanded magnesium. The expanded magnesium was prone to break at the areas of reduced cross-section. For very low tape speed, less than 0.15 in./min or high delivered cathode capacity, greater than about 8 amp-min/in.^{2}, a greater thickness of magnesium would be required. This was evident when operation at 0.1 in./min or a 2.5-in. long collector was attempted. With the acid electrolyte used, the 25-minute residence time beneath the collector head was sufficient to cause disconnuity of portions of the magnesium from the upstream anode current collector. When residence time was shortened by decreasing the collector length, low speeds could be used without anode disconnecting. Anode coulombic efficiency was not maximized, but satisfactory operation was achieved with anode coulombic efficiencies of better than 50% in acid electrolytes.

Separate voltage probes showed that 20 to 30 mv was lost at the anode current pickup with a current of 1.5 amp when primary magnesium was used. Other methods of anode contact, such as rolling knife pickup, were less satisfactory. The surface condition of the magnesium also affected the contact voltage drop; dirty or highly oxidized surfaces gave losses as high as 150 mv. The magnesium AZ31B alloy showed lower contact losses than the primary magnesium, probably due to a thinner or less perfect surface oxide layer.

b. Cathode

(1) Current Collector

Selection of a suitable cathode collector material depends on the type of cathode depolarizer used. The only materials found suitable for discharge of potassium periodate were platinum and high conductivity, dense graphite (USG443). The graphite was preferred since its inherent flaking action reduced sticking. Lead wires to the collectors were coated with epoxy or Silastic resin to avoid possible contact with electrolyte and the resulting depression of cell voltage. A relatively smooth collector surface was found desirable for providing a low resistance contact with the cathode coating and keeping pulling force low. A chamfered, leading edge on the collector reduced scraping of the cathode coating. Rendering the lead-in chamber nonconducting by covering with tape provided time for the electrolyte wet-out to occur before discharge. While the current-density profile on the collector was not measured, results of static constant voltage discharges indicated that the current density was high over the leading one-third of the collector with the maximum current density occuring at about one-third of the way through the collector.

Several constant voltage static discharge curves are shown in Figure 60. The abscissa, time, corresponds approximately to the distance through the collector and the ordinate, current, to local current density in a dynamic test. The cathode coulombic efficiencies in these tests approximated those obtained in dynamic tests of these tapes. It is evident that the major portion of the capacity (the area under the curve) is delivered in the early portion of the discharge corresponding to the forward portion of the collector in dynamic tests.

During the course of dynamic testing, considerable heat evolution was evident in the collector area. It was thought that this might be a major factor in the cathode sticking problem if temperatures high enough to melt the binder were attained. Accordingly, a thermocouple was placed in a cathode slot during one discharge test. Temperatures up to 50°C were measured. In another test, a traverse of the temperature was made with a thermocouple on the anode side. Temperatures ranged from 40°C at the inlet and outlet to a maximum of 63°C about one third of the way into the collector. It was tentatively concluded that the major position of the heat generated was a result of chemical action of the electrolyte on the magnesium since the measured IR losses were far too low to account for the temperatures measured, even if no heat losses to the surroundings were allowed. The heating was not a major contributor to the sticking problem since the binders used do not soften appreciably until temperatures near 94°C are reached.

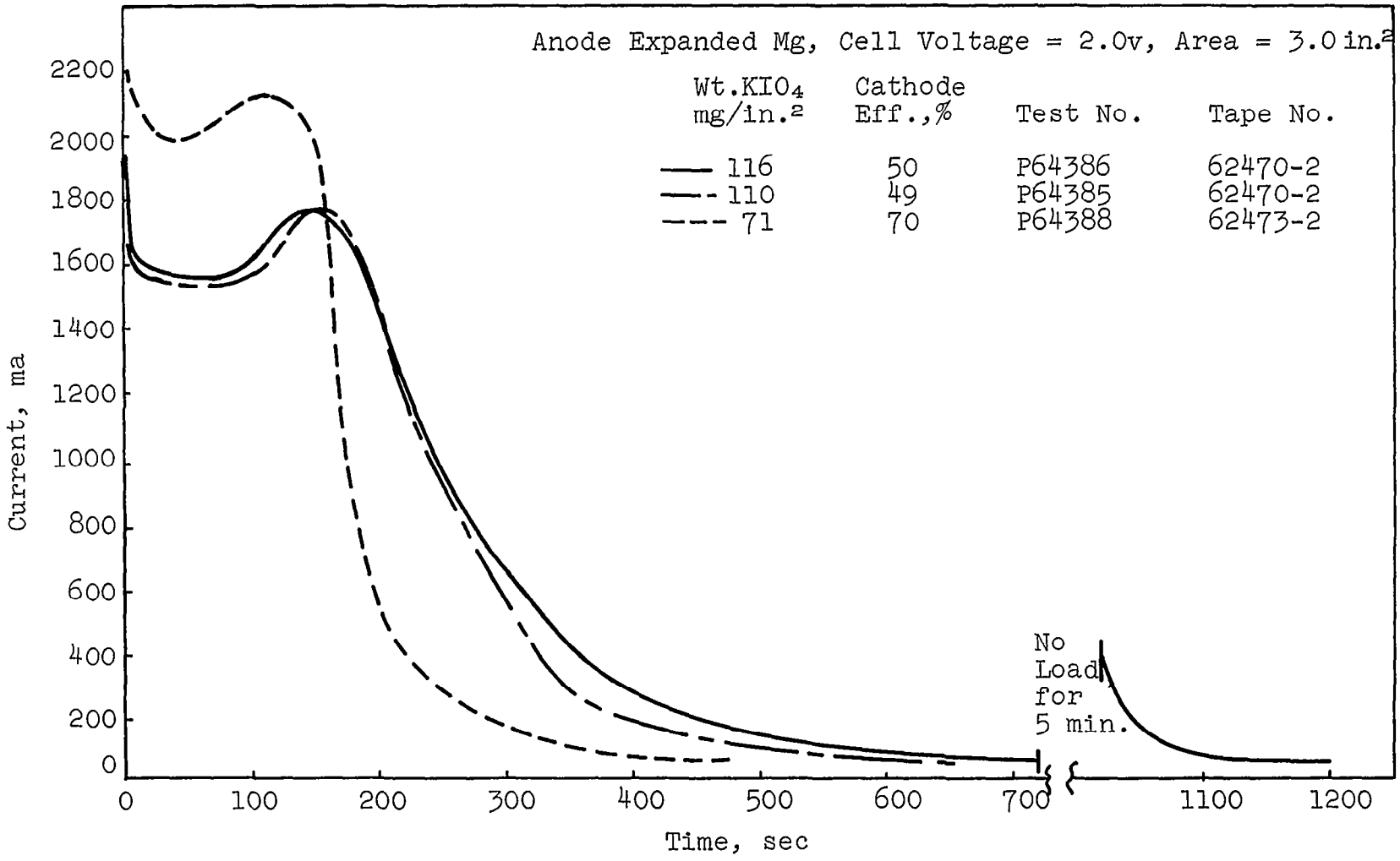

Figure 60. Constant Voltage (2.0v) Static Discharge of Potassium Periodate-Primary Magnesium Couple in 2M $AlCl_3$-0.5M HCl Electrolyte

Some pressure must be applied to the current collector to insure good collector-to-cathode contact. In laboratory tests, pressure was applied by putting small lead weights on top of the upper current collector. The amount of weight required for good contact depended a great deal on the physical nature of the cathode coat surface. A smooth cathode coat required less current collector pressure for good contact than a rough cathode coat. The machine-extruded cathode coatings were much smoother and more uniform than those produced by hand casting. Compared with the hand-cast cathodes, machine-extruded cathode tape required only half the collector weight to insure good contact. In addition to surface property differences, the hand-cast cathode coats were much less dense than the machine-extruded coatings. Increased weight undoubtedly improved particle-to-particle contact as well as current collector contact.

(2) Electrolyte

A mixed electrolyte, 2M $AlCl_3$ - 1M HCl was found to be most suitable for dynamic discharge of the potassium periodate-magnesium tapes. The hydrochloric acid imparts good conductivity and wetting properties to the electrolyte while the aluminum chloride reduces the rate of attack on the magnesium and provides additional acid (by hydrolysis) for consumption in the cathode discharge reactions. The periodate discharge reaction requires 7 gram equivalents of acid per gram-mole of potassium periodate. The weight requirements of electrolyte to provide this acid are shown in Figure 61. The 2M $AlCl_3$ - 1M HCl electrolyte is effectively about 6.8N in acid, and about 0.54 g of this electrolyte is needed to wet out the separator as indicated by the dotted line in Figure 61 for the 4-mil nylon separator used in most tests. As indicated by the results of static discharge tests with limited electrolyte, the cathode efficiencies at the high voltages and current densities desired in this work appear to be electrolyte limited.

The results shown (shaded area) for dynamic discharge of potassium periodate tapes do not reach the electrolyte limiting level probably because larger quantities of electrolyte were fed to avoid sticking problems. As a result of the acid consumption by the discharge reaction, the pH of the electrolyte eventually increases sufficiently to cause considerable hydrolysis of aluminum chloride. The resulting aluminum hydroxide gel ties up the remaining water. The formation of this voluminous gel in the electrode is not desirable and probably contributes to the sticking problem. The feeding of excess electrolyte retards the pH change and attendant gel formation. Separate titration studies showed that aluminum chloride provided about 2.8 equivalents of acid per mole before reaching a pH of 4.5 but gel formation began at pH as low as 1.5.

On way to reduce the electrolyte weight required is to use a more concentrated acid electrolyte. This was, in fact, the

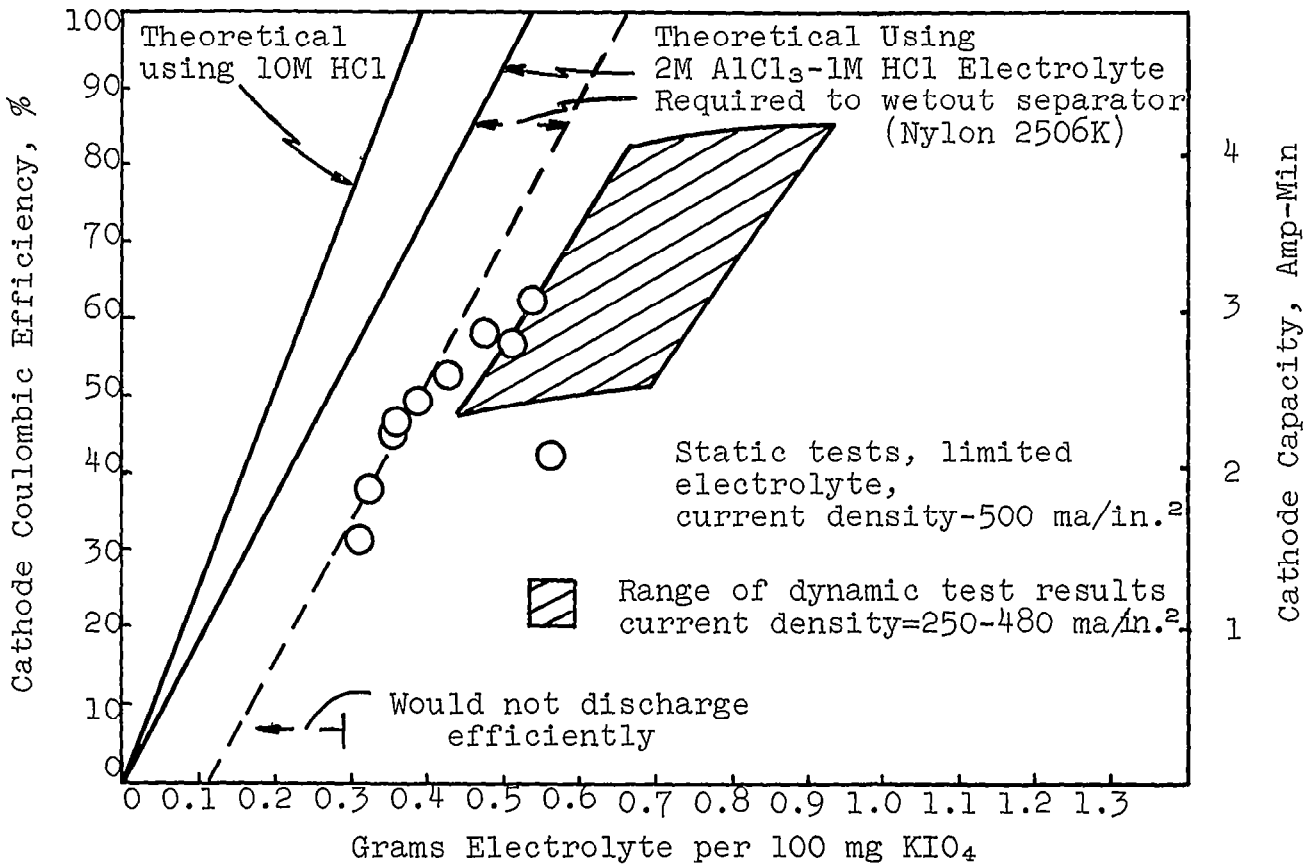

Figure 61. Electrolyte Usage Compared with Theoretical Acid Requirements for Potassium Periodate Depolarizer

direction taken in arriving at the 2M $AlCl_3$ - 1M HCl mixed electrolyte; that is, saturated aluminum chloride was first used and, subsequently, better performance was obtained as increasing concentrations of hydrochloric acid were used. However, use of hydrochloric acid concentrations over one molar resulted in excessive corrosion and gassing of the magnesium and deterioration of the nylon separator. It may be possible to overcome this and also to limit distribution of aluminum ion throughout the electrode by incorporating a dry aluminum chloride layer in the separator adjacent to the anode. Use of a straight hydrochloric acid electrolyte (say 10N) for wet out may then be possible since the aluminum chloride should provide a protective action at the anode. The more concentrated hydrochloric acid should also provide higher discharge voltage and cathode efficiency in addition to reducing the required electrolyte weight (see Figure 61). Electrolyte weight can also be reduced somewhat by reducing the separator thickness or changing the type of separator. The effects of these changes on the energy-densities obtained are discussed below.

c. Energy Densities

The energy densities calculated from dynamic test data ranged from 50 to 70 watt-hr/lb for the improved potassium periodate tapes. This figure includes electrolyte fed over and above that indicated as necessary for the discharge (Figure 61) and the actual weights of separator and magnesium used. Using the minimum electrolyte (2M $AlCl_3$ - 1M HCl) weight as indicated in Figure 61, a 2-mil rather than 4-mil nylon separator, and the minimum weight of magnesium successfully used in testing (about 50% coulombic anode efficiency) energy densities were raised to about 85 watt-hr/lb. It should be noted that electrolyte weight still accounted for about 60% of the total weight in this system. If a further reduction in electrolyte weight can be achieved (by use of 10N HCl, for example), energy densities over 100 watt-hr/lb can be attained with the magnesium potassium periodate couple. Even with this reduction, the electrolyte weight is still the largest contributor to the weight of the system. Table 34 indicates the weight distribution that would be realized from the use of 10N HCl as an electrolyte. Experimental weights were assigned to all components other than electrolyte for the compilation weight percentages.

Table 34

COMPONENT WEIGHTS OF DRY TAPE DEVICE
USING 10N HCl AS ELECTROLYTE

Cathode Coating	19.1	
Separator	2.2	
Anode	8.7	
Electrolyte (10N HCl)	43.6	
Incapsulating Material	4.4	
Hardware	22.0	
	100.0	(10.9 lbs)

These percentages apply approximately to a four tape unit with capacity for 75 ft of tape.

PHASE 3. CONVERSION DEVICE DEVELOPMENT

A. BACKGROUND

The dry tape device must first contain the dry tape components on spools and then, on demand, move the tapes through an electrolyte release mechanism and through the current collectors, and finally roll the spent tape on an empty spool. The minimum weight consideration is important to achieving a high watt-hr/lb output for the entire device (battery components plus mechanical hardware). The pertinent design considerations were: (1) minimum weight, (2) auxiliary "start" system, (3) parasitic operation, (4) tape speed control (for regulating power output), and (5) reliability. An auxiliary energy system required to start the device following a period of inactivity when no parasitic power is available for driving the tape reel.

Parasitic operation of the driving motor is required for continually moving the tape with a small fraction of the power generated by the dry tape battery.

Variable speed control of the tape permits matching tape electrical output to the external load for efficient tape discharge at either high or low current loads.

B. TAPE DRIVE MECHANISM

1. Tape Transport Device

Several of the more important design concepts of the tape device are similar to those of a commercial tape recorder. Two methods for the tape transport were analyzed: (1) fixed speed capstan drive, and (2) variable speed take-up-reel drive. Both systems are used in commercial recorders. Careful analysis of both designs, against the background of minimum weight and reliability requirements, indicated that a capstan drive design should be used for moving the dry tape.

2. Start Systems

Three methods of "start" systems were: (1) a primary battery (silver oxide) package with no recharging capability, (2) a secondary battery package (nickel-cadmium) with provisions for recharging, and (3) an all mechanical system with energy storage in a spiral power spring. Tests of these three devices showed that the mechanical system was the most reliable but also the heaviest.

3. Speed Control

Two methods for tape speed control were: (1) a manually operated rheostat control in series connection with a dc motor armature, and (2) an electronic control system that would automatically regulate tape linear speed to maintain a constant discharge voltage. The electronic control was not available for the transport device at the final assembly period. The "back-up" manual control was substituted and can be seen in the left-hand leg of Figure 62. The manual control can be adjusted so that the tape linear speed varies from 0.1 to 0.2 in./min.

4. Motors

Measurements during breadboard tests indicated that 150 oz/in. of motor torque was required to move the tape. Of the several light weight, low power input, commercial motors, a small dc permanent magnet gearmotor* had the best torque for least power consumption (see Figure 62). This motor had adequate torque and speed in the low voltage range (2 to 4 v dc) to be of interest for dry tape application. Comparative data on the best motor candidates are given in Table 35.

C. MATERIAL INVESTIGATION

1. Structural Metals and Plastics

Early breadboard tests indicated that to move the tape reliably would require a rigid chassis structure to maintain the original alignments. Rigidity is a calculable function of geometric shape and Young's modulus of elasticity.

To a large degree the shape of the chassis was determined by the anode-cathode tape and electrolyte tape configurations. Analysis of the specific stiffness index of some of the more available structural metals and plastics indicated that magnesium alloy had an excellent specific stiffness characteristic surpassed only by that of natural mica. (See Table 36). The specific stiffness index permits a quick comparison of the stiffness per unit specific weight of the various construction materials under analysis. From the several materials listed in Table 36, magnesium AZ31B-H24 alloy was selected on the basis of ready availability and workability.

A further comparison of materials of construction on a basis of specific tensile strength (Table 37) provided a further criterion for the selection of structural materials.

---

* Globe Industries, Inc., Model 43A836

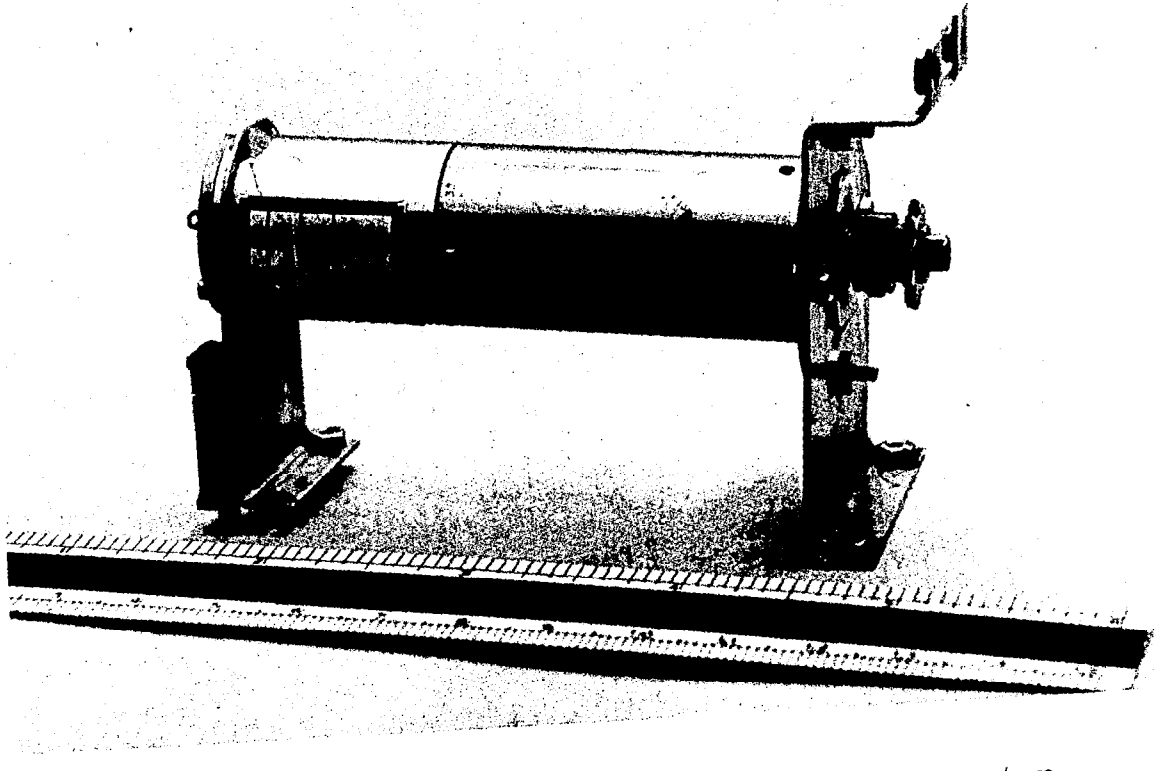

Figure 62. Low-Voltage, Permanent Magnet Gearmotor

Table 35

TAPE DRIVE MOTORS

Characteristics	Sigma Instruments Inc.	Cramer Div. of Giannini Controls Corp. Type No. 220	Glob Industries, Inc. Type 43A836	Hankscraft Co. (Prototype)	Haydon Div. of General Time, No.MD83-000K
Type	Synchronous Stepping Motor	d-c Permanent Magnet Gear Motor	d-c P/M Gear Motor	d-c P/M Gear Motor	d-c P/M Gear Motor
d-c Volts	4	4	4	4	4
Current Input, ma	500	35	52	12	13
Power Input, MW	2000	140	208	48	52
RPM	1/10	1/12	1/19	1/4	1/10
Torque-oz.in.	40	38	97	38	38
Max. Torque Allowance	300	40	300	40	40
Weight-Grams	280	130	168	90	180
% Parasitic Power From 8 Watt System	25	1.75	2.6	0.6	0.65

TABLE 36

SPECIFIC STIFFNESS INDEX OF MATERIALS

Material	Specific Stiffness,* $\frac{lb/in.^2}{lb/in.^3}$
Natural Mica	210×10^6
Magnesium AZ31B-H24 Alloy	160×10^6
Delrin	115×10^6
Steel	105×10^6
Aluminum	100×10^6
Phenolic Resin	40×10^6

* Specific stiffness = $\frac{F/A}{e/L} \times \frac{1}{W}$

where

F = Tensile force within elastic limit (lbs)

L = Original length of specimen (in.)

A = Cross sectional area ($in.^2$)

e = Elongation within elastic limit (in.)

W = Specific weight of specimen ($lb/in.^3$)

TABLE 37

SPECIFIC TENSILE STRENGTH OF MATERIALS

Material	Specific Tensile Strength,* $\frac{lb/in.^2}{lb/in.^3}$
Polyester-glass laminate	61×10^4
Steel	60×10^4
Aluminum	59×10^4
Magnesium AZ31B-H24 alloy	50×10^4
Phenolic Resin	48×10^4
Delrin	20×10^4

* Specific Tensile Strength = $\frac{F}{A} \times \frac{1}{W}$

where

F = Ultimate force at time of rupture (lb)

W = Specific weight of specimen ($lb/in.^3$)

A = Cross sectional area ($in.^2$)

2. Corrosive Effect of Electrolytes on Materials

The qualitative corrosive effects of electrolyte on candidate materials of construction are listed in Table 38.

3. Protective Films

Magnesium alloy without film protection is subject to rapid corrosive attack when exposed to the electrolyte solution, 2M $AlCl_3$, 0.25M HCl.

Suppliers of magnesium metal* recommended one of the following surface treatments: (1) application of a clear vinyl film to the alloy surface; (2) application of a film of white titanium dioxide (primer paint†); (3) for maximum corrosion protection, anodizing with Dow No. 17 process to a thickness of 1 mil and then application of a titanium dioxide primer; or (4) electroless nickel plating. Step (3) was used to anodize magnesium parts during fabrication. Several of the magnesium components whose function did not permit the use of thick films were electroless nickel plated.

D. TRANSPORT DEVICE DESIGN

A complete, weight-optimized transport device is shown in Figure 63. The total weight of this device as shown is 2.4 lb. A breakdown of the major sub-assemblies of the device is given in Table 39.

1. Chassis

Two transport devices were assembled. The first used cast-in-place polyurethane foam as a means for imparting additional rigidity to the chassis, which was fabricated from 16-mil thick magnesium alloy AZ31B-H24 alloy. The second chassis was fabricated without foam but using epoxy adhesive** between all lap joints and for filleting where required. This method resulted in a weight saving of 2 oz with no significant sacrifice of rigidity.

Figure 64 shows top and bottom views of the chassis showing the preferred foam-less construction. This construction resulted as a consequence of the transport design. With all components and sub-assemblies mounted beneath the chassis deck, very little volume was available for the use of sandwich construction. Therefore, the adhesive-rivetting technique was employed and with good results.

* Dow Metal Products Co.
† Sherwin Williams Co.
** Minnesota Mining and Metallurgy Co., Epoxy Adhesive EC-2216

TABLE 38

ELECTROLYTE CORROSION ACTION ON MATERIALS OF CONSTRUCTION

Materials	24-Hour Immersion in Electrolyte 2M $AlCl_3$ + 0.2M HCl
Phenolic, NEMA X	no effect
Delrin	no effect
Monel	slight gassing
Magnesium, AZ31B-H24	dissolved
Viton-A Elastomer	no effect
Stainless type 304	blackened slightly
Aluminum	dissolved
Teflon film	no effect
No. 17 anodized magnesium alloy	slight attack
No. 17 anodized magnesium with zinc chromate primer (film)	no attack
No. 17 anodized magnesium with titanium dioxide primer (film)	no attack
Electroless plated magnesium alloy	no attack

Table 39

WEIGHTS OF TRANSPORT SUB-ASSEMBLIES

Item	Figure Number	Weight, oz.
Chassis	64	8.8
Current Collector	65, 66, 67	8.4
Motor with Mounts	62	7.0
Tape Reels (2)	63, 71	4.2
Electrolyte Reel	70	3.4
Capstan Drive	69	3.0
Hardware	-	2.7
Electrolyte Pump	68	1.0

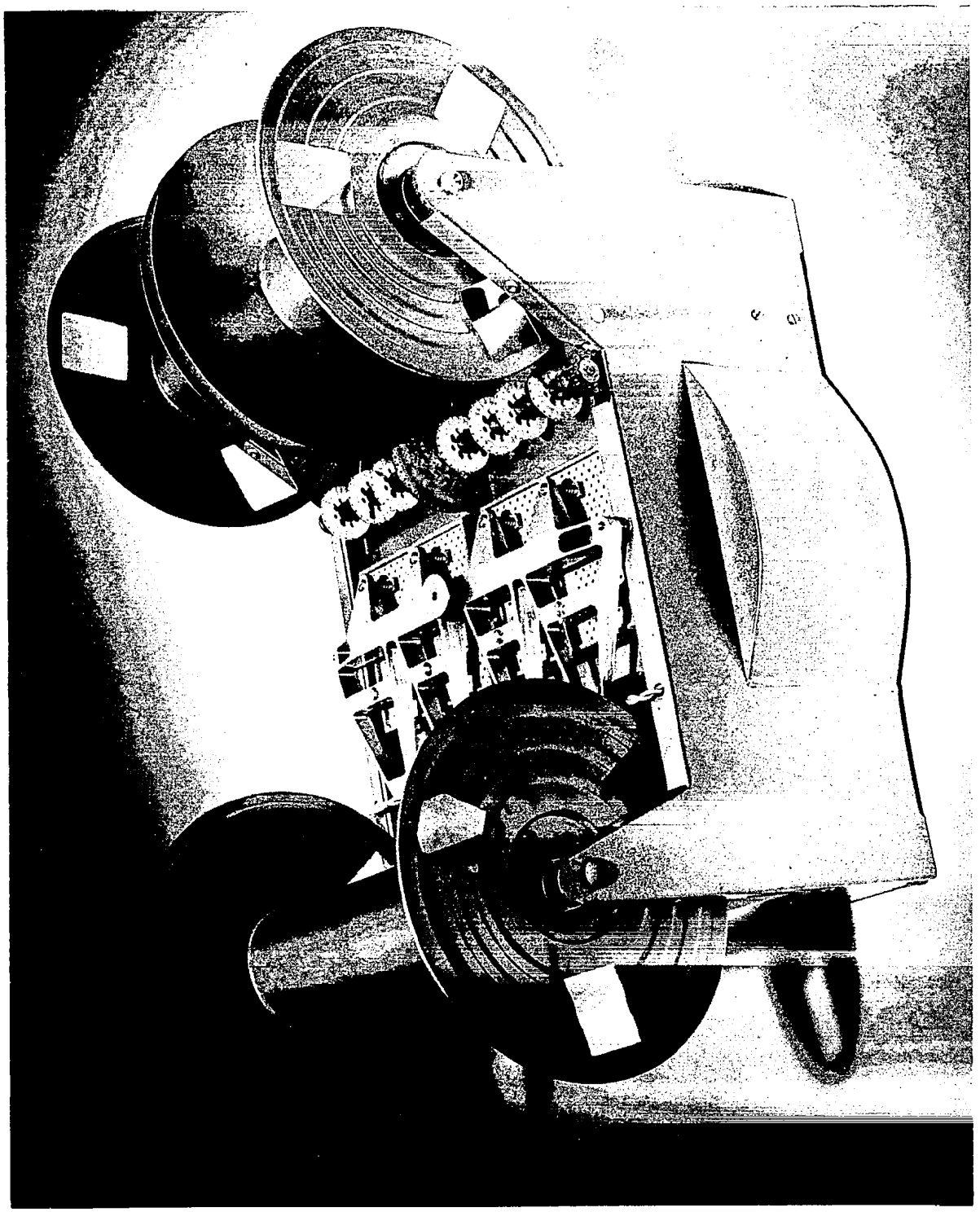

Figure 63. Complete Tape Transport Device

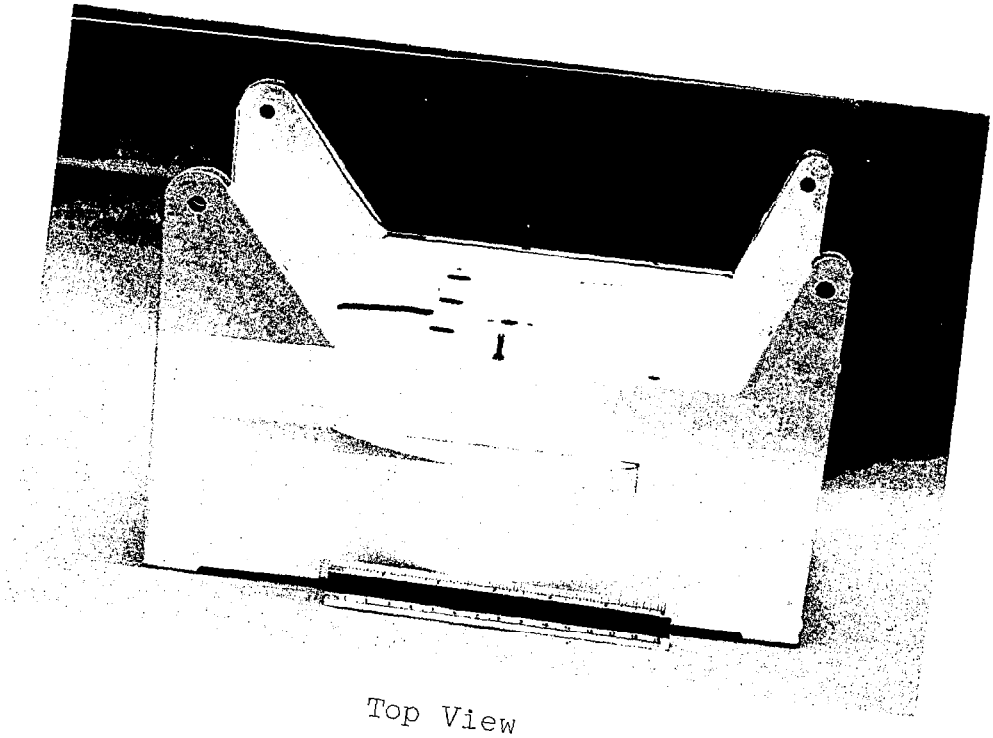

Top View

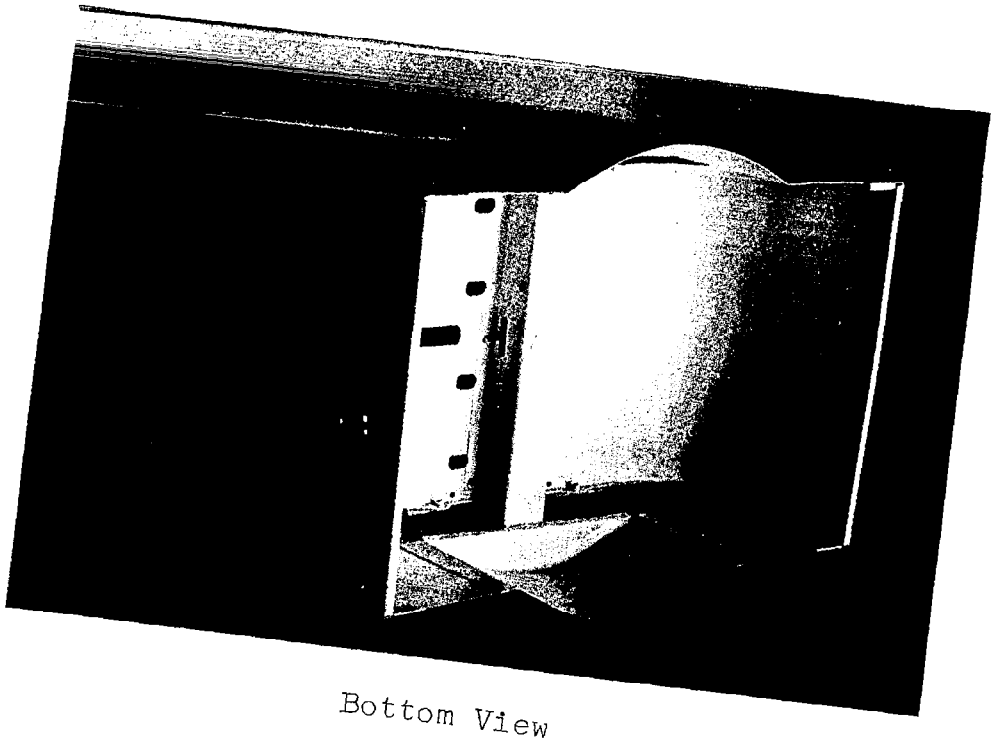

Bottom View

Figure 64. Tape Transport Chassis

2. Current Collector Assembly

The complete anode-cathode current collector assembly is shown in Figure 65. Additional details of the anode collector are shown in Figure 66, which shows the four saw-toothed contacts (for contact with magnesium tape), four electrical leads, and four perforated phenolic plastic pressure pads for squeezing the anode, separator, and cathode against the cathode collector. The cathode collector, Figure 67, is made of graphite*.

3. Electrolyte Pump Assembly

The electrolyte pump, shown in Figure 68, is a positive displacement pump for supplying electrolyte to the cathode current collector (Figure 67). The incapsulated packets of electrolyte are drawn into the sealed chamber of the pump body by the spines of a capstan wheel. There the packets are slit, electrolyte is released, and the film is flattened and discharged.

The electrolyte is continuously discharged from the ends of the four Teflon tubes because of the displacement action of the progressively advancing packets. These displace the free liquid from the pump body, and the free liquid is forced into and out of the tubes as the sealed packets advance. The other ends of the tubes are fastened to the carbon cathode blocks shown in Figure 67. The electrolyte is distributed to the surface of the cathode tape either by appropriate grooves cut in the carbon or by its inherent porosity, depending on the grade of carbon-graphite selected. The entire tape system is wet out in the region between the current collectors and an electrochemical reaction produces current between the current collectors and an external load. The electrolyte pump is fabricated from monel metal and Viton-A elastomer for corrosion protection.

4. Capstan Drive Assembly

The capstan drive assembly is shown in Figure 69. Two each of the smaller one-inch diameter wheels pull the tape through the current collectors. Small spines project 1/32 in. beyond the one inch diameter, thus assuring a positive drive independent of friction.

The large center wheel of the capstan is two inches in diameter and pulls the flattened film of the electrolyte packet chain. The larger diameter is required to pull the electrolyte packets through at twice the linear rate of the electrode components.

---

* United States Graphite Company, No. 443 electrical brush grade carbon-graphite

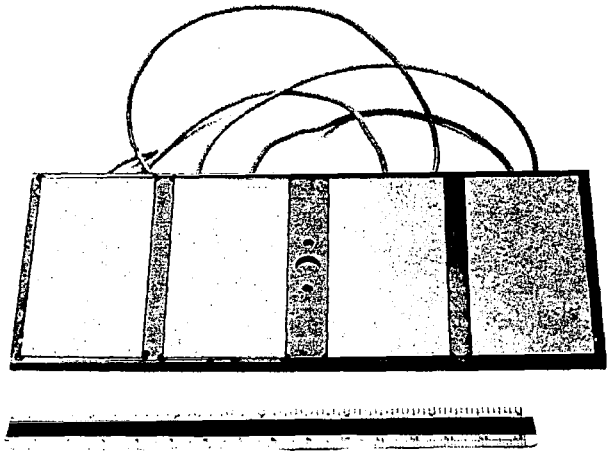

Figure 65. Complete Anode-Cathode Current Collector Assembly

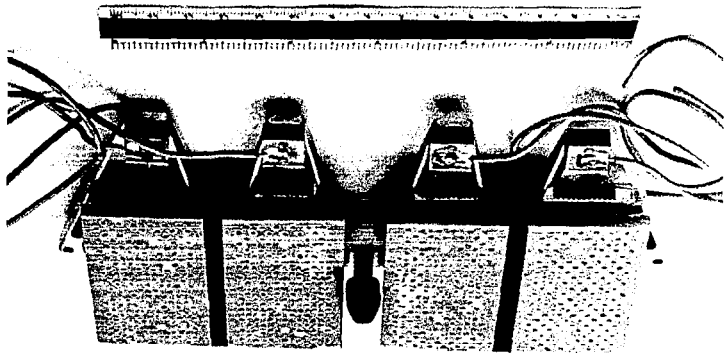

Figure 66. Anode Current Collector

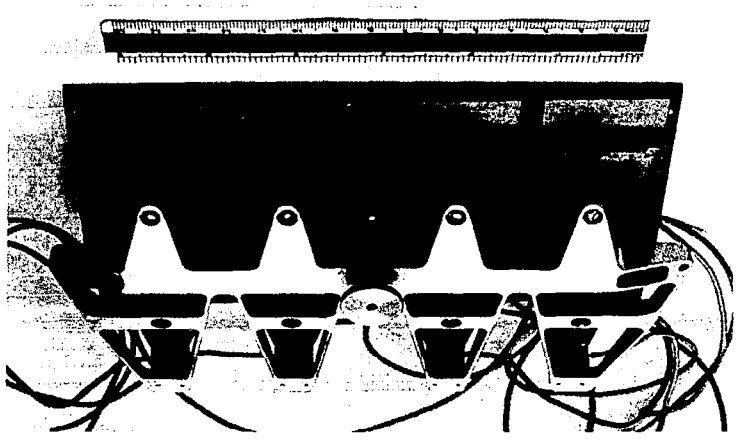

Figure 67. Cathode Current Collector

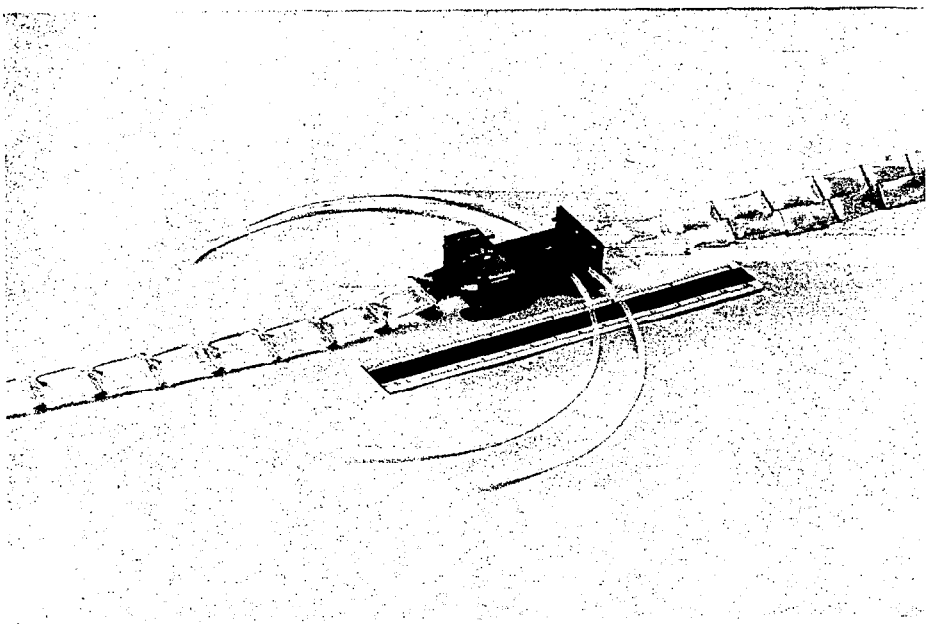

Figure 68. Electrolyte Pump

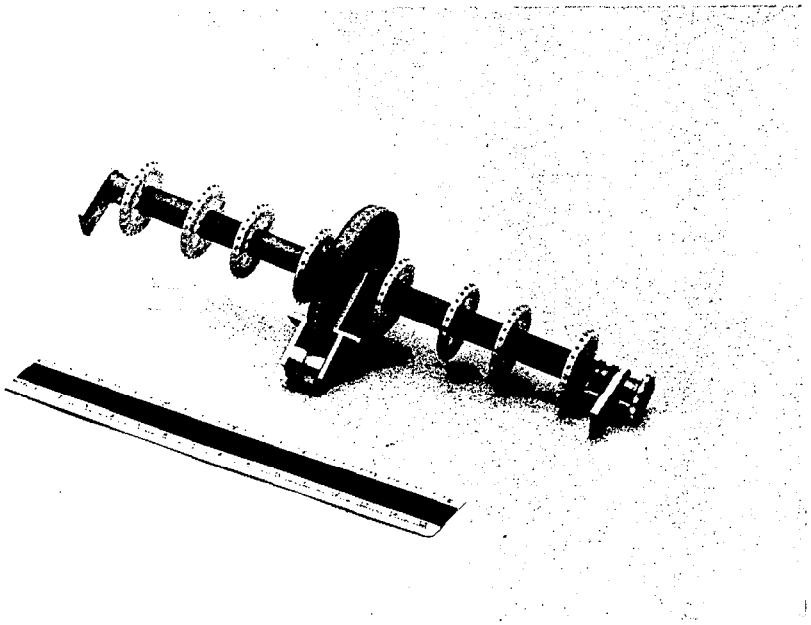

Figure 69. Capstan Drive Assembly

The capstan is, in turn, driven by a sprocket and roller chain system, which concludes at the mounted sprocket of the motor shaft (see Figure 62).

5. Motor

The low voltage dc permanent magnet gearmotor is shown in Figure 62. This motor will operate in the range of 2 to 4 v and develop 150 oz/in. of torque. The motor draws 0.3 watt at 4 volts dc.

6. Electrolyte Storage Reel

The electrolyte storage reel is shown in Figure 70. The reel was fabricated from magnesium AZ31B-H24 alloy and epoxy adhesive. The reel is mounted underneath the transport chassis inside the "side bubble" feature seen in Figure 64. Thus, the electrolyte system is normally not seen and is completely protected. This design approach permitted efficient utilization of the envelope volume.

7. Take-Up Reel

The spent tapes and electrolyte film are wound up and stored on the reel shown in Figure 71. This reel is positively driven by a sprocket and roller chain and always keeps the tape under tension. The reel does not add significantly to the pull of the tape, although it is driven by the same roller chain as the capstan drive. The take-up reel shaft system contains a miniature slip clutch that is preset to a friction value that will always maintain tension on the tape without influencing the linear tape speed, which is controlled by the capstan drive only.

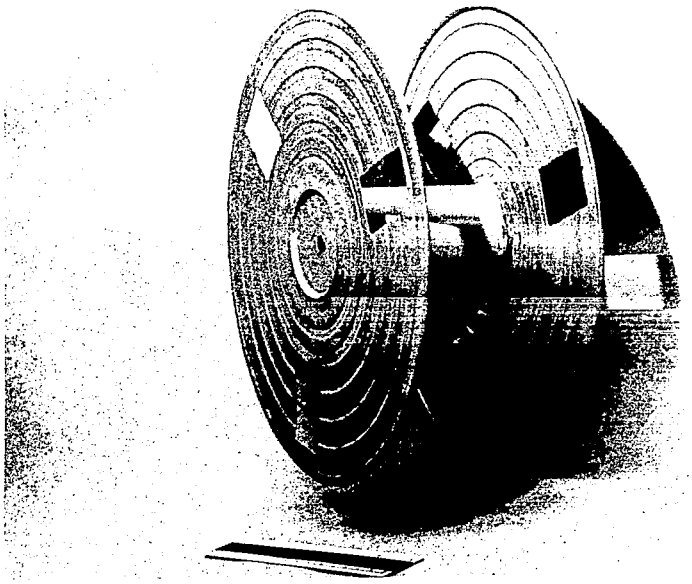

Figure 70. Electrolyte Storage Reel

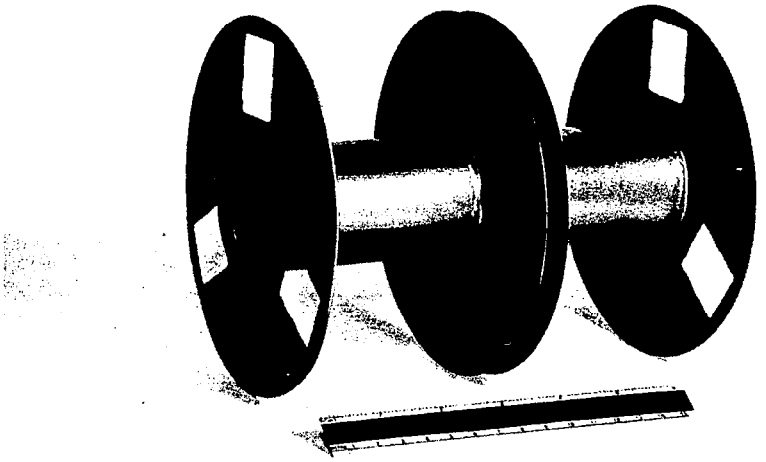

Figure 71. Take-up Reel

REFERENCES

1. B. A. Gruber, et. al., "Feasibility Proof of Dry Tape", Contract NAS3-2777, Final Report, 31 March 1964, MRC Report No. MRB5001F.

2. J. L. Robinson and P. F. King, J. Electrochem. Soc., 108, 36-41(1961).

3. B. A. Gruber, et. al., "Research on Organic Depolarizers", Contract No. DA 36-039-SC-87336.

4. G. Cohn and A. P. Handel, Engelhard Industries, Inc., Technical Bulletin 2, 54 (1961).

5. Allied Chemical Tech. Bulletin, Aclar Fluorohalocarbon Film, ADT 1263, p. 16, General Chem. Div., Bridgeport, Conn.

6. R. M. Barrer and G. Skirrow, J. Polymer Sci., 3, 549 (1948).

7. H. J. Lelie, Modern Packaging, 37, 145 (1964).

8. F. S. Symington and R. F. Burroughs, Fibre Containers, 28, 107 (1943).

9. Tappi, T448m-49.

10. ASTM E96-53G.

11. J. Sivadjian and F. Corral, J. Applied Polymer Sci., 6, 561 (1962).

12. "Modern Plastics Encyclopedia Issue 1964", 41, No. 1A, September 1963, Films Chart.

13. "Modern Plastics Encyclopedia" Issue 1964, Vol. 41, No. 1A, September 1962.

14. J. Sivadjian and J. RiRibeiro, Applied Polymer Sci., 8, 1403 (1964).

15. A. W. Myers, V. Tammela, V. Stannett, and M. Szwarc, Modern Plastics, 139 (1960).

16. Commercial Development Report "Preservation and Protective Packaging in Scotchpak Films", 3M Company, Commercial Development Laboratory, St. Paul, Minnesota.

17. M. S. Chandrasekharaiah and J. L. Margrave, J. Electrochem. Soc., 108, 1008-1012 (1961).

18. W. F. Meyers, "Development of High Energy Density Primary Batteries 200 Watt Hours per Pound Total Weight Minimum" Final Report, Contract NAS3-2775, Report No. NASA CR-54083.

APPENDIX A

EXPERIMENTAL DATA

Table I-1

FORMULATIONS AND STATIC CELL DISCHARGE CHARACTERISTICS OF MAGNESIUM-POTASSIUM PERIODATE TAPE CELLS

Test No.	Depolarizer wt-%	Conductor wt-%	Filler wt-%	Binder wt-%	Tape	Depolarizer Loading ma/in.^{2}	Anode	Electrolyte	Current Density ma/in.^{2}	Efficiency % to 1.5 volts	Operating Emf volts	Comments
4331-9	KIO_4(45%)	SAB(45%)	1/8"dynel(5%)	PVP(5%)	dynel	279.3	exp.AZ31B	Sat'd $AlCl_3$	500	[illegible]	1.70	
4331-10	" "	" "	" "	" "	"	261.2	"	"	"	[illegible]	1.73	
4331-11	" "	" "	" "	" "	"	351.2	"	"	"	57	1.70	
4331-12	" "	" "	" "	" "	"	376.3	"	"	"	76	1.65	
4331-1	KIO_3(45%)	" "	" "	" "	"	130.2	"	"	"		1.70	
4331-2	" "	" "	" "	" "	"	150.7	"	"	"	20	1.90	
4331-[illegible]	" "	" "	" "	" "	"	228.1	"	"	"	[illegible]	1.60	
4332-13	KIO_4(45%)	" "	" "	" "	"	109.3	"	"	"	64	1.65	KIO_4 ground to -200 +300 mesh
4332-14	" "	" "	" "	" "	"	102.0	"	"	"	61	1.78	" " " " " "
4340-1	" (54%)	" "	1/4"carbon(2.75)	" (2.75)	"	110.9	"	"	"	55	1.70	
4340-2	" "	" "	" "	" "	"	114.6	"	"	"	54	1.75	
4340-3	" (59%)	" (32%)	" (3%)	" (3)	"	111.3	"	"	"	55	1.70	
4340-4	" "	" "	" "	" "	"	114.1	"	"	"	51	1.80	
4342-1	" (54%)	" (40.5%)	1/8"dynel(2.75)	" (2.75)	"	104.1	"	"	"	63	1.95	
4342-2	" "	" "	" "	" "	"	92.0	"	"	"	72	1.85	
4342-4	" (59%)	" (35%)	" (3%)	" (3)	"	100.5	"	"	"	68	1.90	
4342-[illegible]	" "	" "	" "	" "	"	98.8	"	"	"	62	2.00	
4342-[illegible]	" (54%)	" (40.5%)	" (2.75)	" (2.75)	"	98.3	primary Mg	"	"			Low voltage due to gassing- not sufficiently perforated
4342-[illegible]	" (59%)	" (32%)	" (3%)	" (3)	"	102.8	"	"	"	64	1.80	Perforated anode
4334-1	" (49%)	" (45%)	" (5%)	" (5)	"	182.0	AZ31B	"	"	65	1.80	Perforated anode ran poorly at start due to insufficient electrolyte
4341-1	" "	" "	" "	" "	"	76.4	Primary Mg	"	"			Potential did not rise above 1.2 -Different sections of same tape
4349-2	" "	" "	" "	" "	"	79.3	exp.AZ31B	"	"	> 8	1.85	
4349-1	$NaIO_4$ "	" "	" "	" "	"	68.0	"	"	"	<10		
4350-2	" "	" "	" "	" "	"	74.6	"	"	"	"		Voltage fell fast for all $NaIO_4$ cells
4350-3	" "	" "	" "	" "	"	80.6	"	"	"	"		
4349-1	KIO_4(60%)	" (30%)	" (3.5)	" (5.5)	"	196.1	"	"	"			Potential dropped below 1.5 immediately - poor wetting
4350-1	" (59%)	" (23%)	1/4"carbon(5)	" (3)	"	93.3	"	"	"	"		
4350-2	" "	" "	" "	" "	"	123.2	"	"	"	46		Sharp initial voltage dips followed by slow rise to max. emf. indicates poor wetting
4350-3	" "	" "	" "	" "	"	91.6	"	"	"	40		
4350-4	" "	" "	" "	" "	"	95.0	"	"	"	42		
4350-5	" "	" "	" "	" "	"	99.8	"	"	"	45		
4350-6	" "	" "	" "	" "	"	89.4	primary Mg	"	"	30		
4351-1	" (59%)	" (35%)	1/8"dynel(3)	" "	"	93.0	exp.AZ31B	"	"	16	1.5	
4352-2	" "	" "	" "	" "	"	78.8	"	"	"	39	1.6	
4352-4	" "	" "	" "	" "	"	100.6	"	"	"	53	1.6	0.5 psi wt. on cell
4352-5	" "	" "	" "	" "	"	112.3	"	"	"	60	1.75	" " " " "
4352-6	" "	" "	" "	" "	"	98.4	"	"	"	59	1.70	1 psi wt. on cell
4352-7	" "	" "	" "	" "	"	108.6	"	"	"	47	1.70	" " " " "
4352-8	" "	" "	" "	" "	"	117.5	"	"	"	34	1.80	1.5 psi wt. on cell
4352-9	" "	" "	" "	" "	"	105.4	"	"	"	50	1.60	" " " " "
4352-10	" "	" "	" "	" "	"	93.2	"	"	"	48	1.55	2 psi wt. on cell
4352-11	" "	" "	" "	" "	"	109.6	"	"	"	59	1.68	" " " " "
4352-12	" "	" "	" "	" "	"	92.9	"	"	"	44	1.50	No added weight
4277-3a	" (59%)	" (30%)	" (3)	" (2)	"	103.3	"	"	"			Did not run with 0.5 psi wt.
4277-3b	" "	" "	" "	" "	"	199.3	"	"	"	5	1.5	Graphite coated cathode

Table A-1 (Cont'd)

FORMULATIONS AND STATIC CELL DISCHARGE CHARACTERISTICS OF MAGNESIUM-POTASSIUM PERIODATE TAPE CELLS

Test No.	Depolarizer wt-%	Conductor wt-%	Fiber wt-%	Binder wt-%	Tape	Depolarizer Loading mg/in.²	Anode	Electrolyte	Current Density ma/in.²	Efficiency % to 1.5 volts	Operating Emf volts	Comments
64357-1	KIO_4 (60)	SAB (30)	1/8"dynel(5)	PVP(5)	dynel	94.2	exp.AZ31B	Sat'd $AlCl_3$	500			Ran at approx. 1.40 volts
64357-2	" "	" "	" "	" "	"	101.9	"	"	"	41	1.60	Graphite powder coated on cathode
64357-3	" "	" "	" "	" "	"	94.5	"	"	100	62	2.00	Graphite coated cathode
64357-4	" "	" "	" "	" "	"	88.9	"	"	250	30	1.60	Graphite coated cathode
64357-5	" "	" "	" "	" "	"	94.2	"	"	500			Ran below 1.5v-carbon current collector, silicone treated to fill pores
64357-6	" "	" "	" "	" "	"	86.0	"	"	100	38	1.85	Untreated carbon collector
64357-7	" "	" "	" "	" "	"	96.4	"	"	"	44	1.93	" " "
64357-8	" "	" "	" "	" "	"	93.2	"	"	250	43	1.70	" " "
64357-9	" "	" "	" "	" "	"	101.5	"	"	"	41	1.60	" " "
64360-1	" (54)	" (40.5)	" (2.75)	"(2.75)	"	92.3	"	"	500	52	1.60	Air dried tape
64360-3	" "	" "	" "	" "	"	93.8	"	"	"			Ran below 1.5 volts
64357-10	" (60)	" (30)	" (5)	" (5)	"	102.4	"	"	"	44	1.80	
64360-11	" (54)	" (40.5)	" (2.75)	"(2.75)	"	87.5	"	"	"	59	1.75	Ovendried tape
64360-2a	" "	" "	" "	" "	"	92.6	"	"	"			Ran at 1.30 volts, carbon collector
64360-2b	" "	" "	" "	" "	"	92.6	"	"	"			Ran at 1.20 volts carbon collector
64360-5	" "	" "	" "	" "	"	98.3	"	"	"	59	1.70	Pt collector
64360-6	" "	" "	" "	" "	"	98.3	exp. pri.Mg.	"	"	68	2.00	" "
64360-4	" "	" "	" "	" "	"	103.1	exp. AZ31B	"	170	63	2.00	
										68	2.10	IR free K.M. Bridge
52779-1b	" "	" "	" "	" "	"	85.4	exp. pri.Mg.	"	500	42	1.85	
52779-1c	" "	" "	" "	" "	"	88.2	"	$2MAlCl_3 \cdot 0.5MHCl$	"	52	1.85	No initial voltage dip
52779-1a	" (41)	" (30)	" (2)	" (2)	"	73.1	"	Sat'd $AlCl_3$	"	30	1.90	25% oxalicacid in cathode
52779-1a	" "	" "	" "	" "	"	93.9	"	$2MAlCl_3 \cdot 0.5MHCl$	"	40	1.95	" " " "
64360-7	" (54)	" (40.5)	" (2.75)	"(2.75)	"	101.5	"	"	"	49	2.05	
64360-8	" "	" "	" "	" "	"	110.3	"	"	"	57	2.00	Separator coated with agar-agar
64360-9	" "	" "	" "	" "	"	104.9	"	"	"	53	1.95	Cathode pressed at 2000 psi
64360-10	" "	" "	" "	" "	"	104.8	"	"	"	59	1.92	Not pressed
64366-1	" (59)	" (35)	1/4"carbon(3)	PVF(3)	"	133.5	"	Sat'd $AlCl_3$	"	47	1.84	
64366-2	" "	" "	" "	" "	"	113.1	"	"	"	54	1.85	
62457-U	" (68)	" "	" "	" "	"	136	"	$2MAlCl_3 \cdot 0.5MHCl$	"			Ran below 1.5 volts
62457-U	" "	" "	" "	" "	"	117	"	"	"	23	1.85	
62457-V	" "	" "	" "	" "	"	116.9	"	"	"	30	1.90	
62457-V	" "	" "	" "	" "	"	116.1	"	"	"	40	1.90	
62457-W	" "	" "	" "	" "	"	128.8	"	"	"	27	2.00	
62457-W	" "	" "	1/8"dynel	" "	"	125.2	"	"	"	29	1.98	
52779-2	" (54)	" "	" "	" "	"	47	"	"	"	43	1.92	
52779-2a	" "	" "	" (5)	PVP(5)	"	65.2	"	"	"	46	1.95	
64357-12	" (60)	" (30)	" "	" "	"	114.5	"	$2MAlCl_3 \cdot 0.5HBF_4$	"	30	1.90	Severe corrosion
64357-11	" "	" "	" "	" "	"	97.1	"	$1.5MAlCl_3 \cdot 1.5MHCL$	"	30	2.00	
64370-1	" "	" "	" "	" "	"	122.1	"	$2MAlCl_3 \cdot 1MHCl$	"	45	2.00	Flat plateau followed
64370-2	" "	" "	" "	" "	PVF "	163.6	"	$2MAlCl_3 \cdot 2MHCl$	"	47	2.00	by rapid drop
64370-3	" "	" "	" "	" "	" "	126.0	"	$2MAlCl_3 \cdot 1MHCl$	"	38	2.00	Voltage drops gradually
64370-4	" "	" "	" "	" "	PVP "	121.3	"	$2MAlCl_3 \cdot 2MHCl$	"	46	2.00	" " "
64371-1	" "	" "	" "	" "	PVF "	124.0	"	$1.5MAlCl_3 \cdot 1.5MHCl$	"	44	2.00	
64371-2	" "	" "	" "	" "	" "	124.3	"	"	"	37	2.00	$CHCl_3$ slurry
64371-3	" "	" "	" "	" "	PVP "	148.8	"	$2MAlCl_3 \cdot 3MHCl$	"	36	2.00	" "
64371-4	" "	" "	" "			127.1	"	"	"	45	2.00	

Table A-1 (Cont'd)

FORMULATIONS AND STATIC CELL DISCHARGE CHARACTERISTICS OF MAGNESIUM-POTASSIUM PERIODATE TAPE CELLS

Test No.		Depolarizer wt-%	Conductor wt-%	Fiber wt-%	Binder wt-%	Tape	Depolarizer Loading mg/in.^{2}	Anode	Electrolyte	Current Density ma/in.^{2}	Efficiency % to 1.5 volts	Operating Emf volts	Comments
64372-1		KIO_4(60)	SAB (35)	1/8"dynel(2.5)	PVP(2.5)	dynel	114.5	exp.pri.Mg.	Sat'd $AlCl_3$	500	52	1.85	
64372-2		" "	" "	"	" "	"	115.5	"	"	"	50	1.90	
64372-3		" "	" "	"	" "	"	111.5	"	$2MAlCl_3 \cdot 2MHCl$	"	46	2.00	Anode severely corroded
64372-4		" "	" "	"	" "	"	155.1	"	"	"	44	2.00	" " "
64374-1		" "	" "	"	PVF "	"	66.5	"	Sat'd $AlCl_3$	"	50	1.73	Ethylene
64374-2		" "	" "	"	" "	"	92.5	"	$2MAlCl_3 \cdot 0.5MHCl$	"	55	1.99	chloride
64374-3		" "	" "	"	" "	"	70.0	"	"	"	44	1.95	slurry
64375-1		" (60)	" (25.6)	1/8"carbon	(2.4)PVF(0.6)	nylon	110.1	"	"	"	52	1.90	Machine made tapes
64375-2		" "	" "	"	" "	"	111.1	"	"	"	54	1.90	" " "
64375-3		" "	" "	"	" "	"	112.0	"	"	"	43	1.95	" " "
64375-4		" "	" "	"	" "	"	104.7	"	"	"	39	1.93	" " "
52731-7	I	" (60)	" (36)	"	(2) PVP (2)	dynel	123.5	"	"	"	55	1.95	CMC adhesive on tape
52731-7	II	" "	" "	"	" "	"	135.0	"	"	"	53	2.04	Cell not bolted. Weighted 500gm/in^2
62470-3		" (55)	" (32)	"	(2.2)PVF(0.6)	nylon	98.6	"	"	"	50	2.05	Machine made tape
52731-7	III	" (60)	" (36)	"	(2) PVP (2)	dynel	97.0	"	"	"	53	1.95	CMC adhesive used
62470-1		" (55)	" (32)	"	(2.2)PVF(0.2)	nylon	113.6	"	"	"	45	2.08	PVP/VA adhesive on tape*
62470-2		" "	" "	"	" "	"	107.0	"	"	"	48	2.02	PVF " " " *
62470-5		" "	" "	"	" "	"	128	"	"	"	42	2.05	" " " " *
62470-6		" "	" "	"	" "	"	127	"	"	"	40	2.08	PVP/PVA " " " *
52731-5		" (60)	" (36)	"	(2) PVP (2)	dynel	206	"	"	"	64	2.10	
52731-8a		" "	" "	"	" "	"	107.5	"	"	"	54	2.00	
52731-8b		" "	" "	"	" "	"	165	"	"	"	56	2.00	
62473-1		" 67)	" (29.4)	"	(2.4)PVF(0.6)	nylon	77.8	"	"	"	61	2.04	*Machine made tapes
62473-2		" "	" "	"	" "	"	119	"	"	"	48	2.10	
62477-3		" "	" "	"	" "	"	157	"	"	"	47	2.05	" " "
62477-4		" "	" "	"	" "	"	162.5	"	"	"	50	2.08	" " "
62477-2		" "	" "	"	" "	"	160.8	"	"	"	54	2.05	" " "
62477-5		" "	" "	"	" "	"	160.1	"	"	"	50	2.10	" " "
62479-1		" (66.6)	" (36)	"	(2) " (1.4)	"	93.4	"	"	"	61	2.05	" " "
62470-2		" (62)	" (34)	"	" " (2)	"	109.5	"	"	"	48	2.05	" " "

Abbreviation.

SAB - Shawinigan Acetylene Black
PVP - polyvinylpyrrolidone
PVF - polyvinylformal
PVB - polyvinylbutyral

Table A-2

FORMULATIONS AND STATIC CELL CHARACTERISTICS OF ORGANIC NITRO COMPOUND CATHODES
(All cathodes discharged vs. expanded magnesium AZ31B unless otherwise noted)

Test No.	Depolarizer wt		Conductor (Note 1) wt.	Fiber Content of Coating, % (Note 2)	Binder Content of Coating, % (Note 3)	Fabric (Note 4)	Depolarizer mg/in.²	Electrolyte	Current Density ma/in.²	Cell Efficiency % to 0.8 v	Cell Efficiency % to 0.65 v	Comments
60661	Picric Acid	(41.3)	41.3	6	11.4 PVP	D	99.7	2M $AlCl_3$	500	39.5	45.3	
60661	" "	"	41.3	6	11.4 PVP	D	96.5	2M $AlCl_3$/ 1M Li_2CrO_4	500	20.7	27.0	
60662	" "	"	41.3	6	11.4 PVP	D	53.1	2M $AlCl_3$/ 1M Li_2CrO_4	100	54.3	-	
63102	Blank	(24)	0	6	11.4 PVP	D	-	2M $AlCl_3$/ 1M Li_2CrO_4	100	(25 min)	(65 min)	
63103	Picric Acid	(39.5)	39.5	6	15 PVP	D	90.0	2M $AlCl_3$	500	44.3	51.1	
63103	" "	"	39.5	6		D	78.5	2M $AlCl_3$	200	55.2	61.2	
63106	" "	"	39.5	6		D	94.6	2M $AlCl_3$/ 1M Li_2CrO_4	500	21.1	35.9	
63107	" "	(41.5)	41.5	-	17 PVP	N-2	73.1	2M $AlCl_3$	200	61.3	70.0	
63107	" "	"	41.5	-	17 PVP	N-2	58.0	2M $Mg(ClO_4)_2$	100	59.3	71.7	
63108	" "	(35.5)	35.5	-	29 PVP	N-2	66.8	2M $Mg(ClO_4)_2$	100	55.2	74.3	
63109	" "	(40.75)	40.75	7.5	11 PVP	D	118	2M $Mg(ClO_4)_2$	300	26.6	36.7	
63109	" "	"	40.75	7.5	11 PVP	D	96.1	2M $AlCl_3$	500	39.5	45.7	
60662	" "	(41.5)	41.5	6	11 PVP	D	38.2	2M $AlCl_3$	500	41.8	-	
60662	" "	"	41.5	6	11 PVP	D	112	2M $Mg(ClO_4)_2$	300	28.9	40.8	
60663	" "	"	41.5	6	11 PVP	D	45.7	2M $Mg(ClO_4)_2$	300	25.7	40.8	
60623	o-DNB	(44.5)	44.5	-	11 PVP	N	115	2M $Mg(ClO_4)_2$	100	12	-	Conductex SC (Columbian)
60624	" "	"	44.5	-	11 PVP	N	117	2M $AlCl_3$	100	14.9	18.5	Conductex SC (Columbian)
60624	" "	(45.4)	45.5	-	9 PVP	N	114	2M $AlCl_3$	100	9		FC-13 Carbon
60623	" "	"	45.5	-	9 PVP	N	84.7	2M $Mg(ClO_4)_2$	100	≈ 1	6.5	Asbury Graphite A625
60623	" "	"	45.5	-	9 PVP	N	81.1	2M $AlCl_3$	100	5.4	-	Asbury Graphite A625
60619	" "	(59.3)	29.7	-	11 PVP	N	109	2M $Mg(ClO_4)_2$	200	6.4	9.5	Nuchar CN
60619	" "	"	29.7	-	11 PVP	N	98.5	2M $AlCl_3$	300	17.2	18	Nuchar CN

NOTES: 1. Shawinigan acetylene black, 50% compression unless otherwise noted.

2. 1/4 in. 3-denier Dynel fibers unless otherwise noted.

3. PVP = Polyvinylpyrrolidone, G = Polyvinylacetate-polyvinyl alcohol.

4. D = Webril nonwoven DYNEL No. 1410, N = Pellon Nylon No. 2505B, N-2 = 60 mil Nylon 524.

Table A-2 (continued)

FORMULATIONS AND STATIC CELL CHARACTERISTICS OF ORGANIC NITRO COMPOUND CATHODES
(All cathodes discharged vs. expanded magnesium AZ31B unless otherwise noted)

Test No.	Depolarizer wt	Conductor (Note 1) wt.	Fiber Content of Coating, % (Note 2)	Binder Content of Coating, % (Note 3)	Fabric (Note 4)	Depolarizer mg/in.^{2}	Electrolyte	Current Density ma/in.^{2}	Cell Efficiency % to 0.8 v	Cell Efficiency % to 0.65 v	Comments
60619	o-DNB (59.3)	29.7	-	11 PVP	N	109	2M $Mg(ClO_4)_2$	300	9.6	19	A
60619	" " (44.5)	44.5	-	11 PVP	N	92.8	2M $Mg(ClO_4)_2$	300	5.6	14	A
60631	" " (80.1)	8.9	-	11 PVP	N	14.6	2M $Mg(ClO_4)_2$	100	41.7	53.5	A
60631	" " "	8.9	-	11 PVP	N	20	2M $Mg(ClO_4)_2$	100	34.8	-	A
60633	" " "	8.9	-	11 PVP	N	11.7	2M $Mg(ClO_4)_2$	50	40.8	44.7	A
60633	" " "	8.9	-	11 PVP	N	13.0	2M $AlCl_3$	100	40.2	-	A
60629	" " (44.5)	44.5	-	11 PVP	N	83.6	2M $AlCl_3$	500	26	31.2	A
60629	" " "	44.5	-	11 PVP	N	120	2M $AlCl_3$	500	21.8	-	A
60629	" " "	44.5	-	11 PVP	N	112	2M $Mg(ClO_4)_2$	200	≈10	-	A
60617	" " (74)	15	-	11 PVP	N	61.7	2M $Mg(ClO_4)_2$	100	8.5	19.7	
60617	" " "	15	-	11 PVP	N	47.0	2M $Mg(ClO_4)_2$	100	9.2	20.3	
60654C	Picric Acid (44.2)	44.2	-	11.7 PVP	D	112	2M $AlCl_3$	500	21.4	28.6	
60636-2	" " "	44.2	-	11.7 PVP	D	68.6	2M $AlCl_3$	500	35	-	
60646A	" " "	44.2	-	11.7 PVP	D	146	2M $Mg(ClO_4)_2$	500	13.7	21.9	
60646B	" " "	44.2	-	11.7 PVP	D	147	2M $AlCl_3$	500	19.0	24.7	
52292	" " "	44.2	-	11.7 PVP	D	59.5	2M $AlCl_3$	17	77.5	81.0	
52292	" " "	44.2	-	11.7 PVP	D	107	2M $AlCl_3$	200	35.9	41.8	
52297	" " "	44.2	-	11.7 PVP	D	106	2M $AlCl_3$	500	32	43.4	
52230	" " "	44.2	-	11.7 PVP	D	55.7	2M $AlCl_3$	200	28.8	33.1	
60665	" " (41.5)	41.5	6	11.1 PVP	D	21.6	2M $AlCl_3$	500	48.2	57.5	
40665	" " "	41.5	6	11.1 PVP	D	18.1	2M $AlCl_3$	500	46.2	55.2	
60665	" " "	41.5	6	11.1 PVP	D	46.7	2M $AlCl_3$	500	42.1	47.3	
60665	" " "	41.5	6	11.1 PVP	D	21.5	2M $Mg(ClO_4)_2$	300	29.1	44.7	
60666	" " "	41.5	6	11.1 PVP	D	141	2M $AlCl_3$	500	23.5	26.4	Sample pressed
60666	" " "	41.5	6	11.1 PVP	D	79.3	2M $AlCl_3$	100	34.3	40.6	
60667	" " "	41.5	6	11.1 PVP	D	76.6	2M $AlCl_3$	100	59.5		10% by wt Pd
60670	" " "	41.5	6	11.1 PVP	D	54.5	2M $AlCl_3$	500	27.2	33.8	B
60670	" " "	41.5	6	11.1 PVP	D	61.5	2M $AlCl_3$	500	24.6	29.8	B
60670	" " (58.9)	24	6	11.1 PVP	D	59.3	2M $AlCl_3$	500	28.4	33.7	
60670	" " "	24	6	11.1 PVP	D	95.1	2M $AlCl_3$	500	25.2	38.3	
63114	" " "	24	6	11.1 PVP	D	31.8	2M $AlCl_3$	100	62.9	65.7	
63115	" " "	24	6	11.1 PVP	D	25.3	2M $Mg(ClO_4)_2$	100	38.0	57.0	

COMMENTS: A. 1:1 FC-13:Shawinigan black

B. 100% Compressed acetylene black

C. Succinic acid:Picric acid is 1:1

D. o-DNB under 300 mesh

Table A-2 (continued)

FORMULATIONS AND STATIC CELL CHARACTERISTICS OF ORGANIC NITRO COMPOUND CATHODES
(All cathodes discharged vs. expanded magnesium AZ31B unless otherwise noted)

Test No.	Depolarizer wt.	Conductor (Note 1) wt.	Fiber Content of Coating, % (Note 2)	Binder Content of Coating, % (Note 3)	Fabric (Note 4)	Depolarizer mg/in.^{2}	Electrolyte	Current Density ma/in.^{2}	Cell Efficiency % to 0.8 v	Cell Efficiency % to 0.65 v	Comments
55480	o-DNB (45.1)	45.1	-	9.7 G	N	48.0	1M $MgBr_2$	100	21.6	47	
55480	" " (60.2)	30.1	-	9.7 G	N	25.2	1M $MgBr_2$	100	31.0	55	
55480	" " "	30.1	-	9.7 G	N	38.4	1M $MgBr_2$	100	24.9	52.2	
55482	" " (45.1)	45.1	-	9.7 G	N	50.5	1M $MgBr_2$ saturated with $Mg(OH)_2$	100	12	29	
55483	" " "	45.1	-	9.7 G	N	54.8		100	8.7	17.5	
60643	" " (44.2)	44.2	-	11.7 PVP	D	114	2M $AlCl_3$	500	17	21	1.2% Pd
60643	" " "	44.2	-	11.7 PVP	D	119	2M $AlCl_3$	500	15	-	
60644	" " "	44.2	-	11.7 PVP	D	95.8	2M $AlCl_3$	200	38	40.8	1.2% Pd
60644	" " "	44.2	-	11.7 PVP	D	104	2M $AlCl_3$	200	29	-	
60644	" " "	44.2	-	11.7 PVP	D	82.5	2M $Mg(ClO_4)_2$	200	10		1.2% Pd
60645	" " "	44.2	-	11.7 PVP	D	131	2M $Mg(ClO_4)_2$	200	9.3	17	
60651	" " "	44.2	-	11.7 PVP	D	105	2M $AlCl_3$	200	41.3	51.3	Pd
60651	" " "	44.2	-	11.7 PVP	D	113	2M $AlCl_3$	200	43.2	-	Pd
60652	" " "	44.2	-	11.7 PVP	D	174	2M $AlCl_3$	500	20.7	25.3	Pd
60653	" " "	44.2	-	11.7 PVP	D	171	2M $AlCl_3$	200	32.7	36.4	Pd
60640	Picric Acid (41.5)	41.5	-	17 PVP	D	57.3	2M $Mg(ClO_4)_2$	300	42	-	
60640	" " "	41.5	-	17 PVP	D	52.7	2M $Mg(ClO_4)_2$	300	≈25	-	
60641	" "(66)	17	-	17 PVP	D	57.8	2M $Mg(ClO_4)_2$	300	≈10	-	
60643	" " "	17	-	17 PVP	D	112	2M $Mg(ClO_4)_2$	100	23.6	27.2	
60643	" " "	17	-	17 PVP	D	105	2M $AlCl_3$	100	19	-	
52295	" "(44.2)	44.2	-	11.7 PVP	D	71.5	2M $AlCl_3$	100	43.6	48.1	
52298	" " "	44.2	-	11.7 PVP	D	116	2M $AlCl_3$	200	41.3	44.8	
60649	2,5-Dinitrothiophene	44.2	-	11.7 PVP	D	139	2M $AlCl_3$	500	9.7	22.7	
60649	" " "	44.2	-	11.7 PVP	D	64.2	2M $AlCl_3$	100	43.7	50.7	
60649	" " "	44.2	-	11.7 PVP	D	62.7	2M $Mg(ClO_4)_2$	100	13	13	
60650	" " "	44.2	-	11.7 PVP	D	146	2M $Mg(ClO_4)_2$	100	18.5	19.4	
63125	" "(40.9)	40.9	6.5	11.7 PVP	D	48.0	2M $AlCl_3$	100	37.5	39.4	
63125	" " "	40.9	6.5	11.7 PVP	D	59.0	2M $Mg(ClO_4)_2$	100	13	13	
63101	2,4,5-Trinitrotoluene	44.2	-	11.7 PVP	D	44.7	2M $AlCl_3$	200	0		
63101	" (44.2)	44.2	-	11.7 PVP	D	128	2M $AlCl_3$	500	0		
63102	" "	44.2	-	11.7 PVP	D	43.8	2M $Mg(ClO_4)_2$	100	14.2	-	
52298	2,4-Dinitrothiophene	44.2	-	11.7 PVP	D	55.1	2M $Mg(ClO_4)_2$	200	8	-	
52299	" "	44.2	-	11.7 PVP	D	56.0	2M $Mg(ClO_4)_2$	100	14.5	15.5	
52299	" "	44.2	-	11.7 PVP	D	123	2M $AlCl_3$	500	0		
52230	" "	44.2	-	11.7 PVP	D	116	2M $AlCl_3$	200	29.5	35.7	

Table A-2 (continued)

FORMULATIONS AND STATIC CELL CHARACTERISTICS OF ORGANIC NITRO COMPOUND CATHODES
(All cathodes discharged vs. expanded magnesium AZ31B unless otherwise noted)

Test No.	Depolarizer wt%	Conductor (Note 1) wt%	Fiber Content of Coating, % (Note 2)	Binder Content of Coating, % (Note 3)	Fabric (Note 4)	Depolarizer mg/in.^{2}	Electrolyte	Current Density ma/in.^{2}	Cell Efficiency % to 0.8 v	Cell Efficiency % to 0.65 v	Comments
63115	Picric Acid (58.4)	24	6	11.1 PVP	D	59.5	2M $Mg(ClO_4)_2$	300	32.4	40.4	
63116	" " (41.5)	41.5	6	11.1 PVP	D	31.5	2M $AlCl_3$	100	63.5	68.5	B
63116	" " (41.2)	41.2	6.6 Graphite	11.1 PVP	D	43.1	2M $AlCl_3$	500	46.4	55.7	
63117	" " (41.5)	41.5	6	11.1 PVP	D	36.6	2M $AlCl_3$	100	85.2	87.5	C
63117	" " (41.5)	41.5	6	11.1 PVP	D	111	2M $AlCl_3$	500	21.6	26.9	
63119	" " (41.2)	41.2	6.6 Graphite	11.1 PVP	D	62.8	2M $AlCl_3$	500	41.2	47.2	
63119	" " (41.5)	41.5	6	11.1 PVP	D	57.8	2M $AlCl_3$	100	59.3	63.6	
63120	" " "	41.5	6	11.1 PVP	D	85.4	2M $AlCl_3$	300	32.8	36.1	
63121	" " "	41.5	6	11.1 PVP	D	68.4	2M $AlCl_3$	100	85.3	87.6	C
63121	" " "	41.5	6	11.1 PVP	D	59.5	2M $AlCl_3$	500	50.4	63.8	C
63125	" " "	41.5	6	11.1 PVP	D	64.6	2M Mg $(ClO_4)_2$	100	49.4	61.7	
60661	" " "	41.5	6	11.1 PVP	D	58.1	2M Mg $(ClO_4)_2$	200	38.6	57.8	C
60617	o-DNB (74.1)	14.9	-	11 PVP	N	144	2M $AlCl_3$	400	12	-	
60617	" " (67)	22	-	11 PVP	N	35.4	2M $Mg(ClO_4)_2$	100	14.7	41.8	
60616	" " "	22	-	11 PVP	N	44.1	2M NH_4SCN	100	13.8	22.8	
60616	" " "	22	-	11 PVP	N	52.4	4M NH_4SCN	100	13.3	29.9	
60616	" " "	22	-	11 PVP	N	56.7	2M NH_4SCN	100	18.4	27.6	
60616	" " "	22	-	11 PVP	N	40.9	4M NH_4SCN	100	23.3	38.0	
60614	" " (43.5)	43.5	-	13 PVP	N	36.5	3M $Mg(ClO_4)_2$	100	19.0	35.6	
60614	" " "	43.5	-	13 PVP	N	35.0	8M NH_4SCN	100	29.7	49.5	
60627	" " (42.8)	42.8	-	16.5 PVP	N	43.8	1.5M NH_4ClO_4	100	17.8	31.7	
60603	" " (43.5)	43.5	-	13 PVP	N	37.0	2M $Mg(ClO_4)_2$	100	49	-	
60603	" " "	43.5	-	13 PVP	N	38.2	2M $Mg(ClO_4)_2$	100	37.6	91	
60603	" " "	43.5	-	13 PVP	N	34.8	2M $Mg(ClO_4)_2$	100	20.2	52.7	
60603	" " "	43.5	-	13 PVP	N	34.3	2M $Mg(ClO_4)_2$	200	12.5	27.5	
60604	" " "	43.5	-	13 PVP	N	42.7	2M $Mg(ClO_4)_2$	100	44.8	91.7	
60604	" " "	43.5	-	13 PVP	N	47.8	2M $Mg(ClO_4)_2$	200	21.9	40.2	
60604	" " "	43.5	-	13 PVP	N	50.8	2M $Mg(ClO_4)_2$	200	15.4	34.3	
60605	" " "	43.5	-	13 PVP	N	39.6	3M $Mg(ClO_4)_2$	100	15.3	28.5	
60605	" " "	43.5	-	13 PVP	N	61.7	3M $Mg(ClO_4)_2$	100	19.7	39.4	
60606	" " "	43.5	-	13 PVP	N	35.9	2M $Th(NO_3)_4$	100	29.1	38.8	
60607	" " "	43.5	-	13 PVP	N	25.2	2M $Th(NO_3)_4$	50	31	37.9	
60607	" " "	43.5	-	13 PVP	N	25.5	2M $AlCl_3$	50	51.2	56.2	
60611	" " "	43.5	-	13 PVP	N	42.0	2M $AlCl_3$	200	62.2	74.5	
60611	" " "	43.5	-	13 PVP	N	45.0	2M $AlCl_3$	300	35	52.5	
60612	" " "	43.5	-	13 PVP	N	38.2	2M $Mg(ClO_4)_2$	100	34		Oxalic acid in cathode
55477	" " (45.1)	45.1	-	9.7 G	N	39.2	1M $MgBr_2$	100	26.6	35.5	D
55477	" " "	45.1	-	9.7 G	N	22.2	1M $MgBr_2$	100	31.5	43	D

Table A-2 (continued)

FORMULATIONS AND STATIC CELL CHARACTERISTICS OF ORGANIC NITRO COMPOUND CATHODES
(All cathodes discharged vs. expanded magnesium AZ31B unless otherwise noted)

Test No.	Depolarizer	Conductor (Note 1) %	Fiber Content of Coating, % (Note 2)	Binder Content of Coating, % (Note 3)	Fabric (Note 4)	Depolarizer mg/in.²	Electrolyte	Current Density ma/in.²	Cell Efficiency % to 0.8 v	Cell Emf Volts	Comments
60633	3,5-Dinitro- (44.2) phthalic Acid	44.2	-	11.7 PVP	D	59.4	3M $Mg(ClO_4)_2$	100	42		
60633	" " "	44.2	-	11.7 PVP	D	71.6	2M $AlCl_3$	500	9		
60634	" " "	44.2	-	11.7 PVP	D	66.1	2M $Mg(ClO_4)_2$	100	17		
60634	" " "	44.2	-	11.7 PVP	D	34.8	2M $Mg(ClO_4)_2$	100	15		
60636	1-Carboxymethyl-" 3,3,5,5-tetra-" nitropiperidine	44.2	-	11.7 PVP	D	118	2M $AlCl_3$	100	14		
60681	" " "	44.2	-	11.7 PVP	D	71.3	2M $AlCl_3$	100	4		
60680	" " "	44.2	-	11.7 PVP	D	67.3	2M $Mg(ClO_4)_2$	100	14		
60691	o-DNB	44.2	-	11.7 PVP	N	28.3	2M $Mg(ClO_4)_2$	100	24.6		
60691	" "	44.2	-	11.7 PVP	N	21.0	2M $Mg(ClO_4)_2$	100	33.0		24°C
60691	" "	44.2	-	11.7 PVP	N	19.9	2M $Mg(ClO_4)_2$	100	32.3		24°C
60691	" "	44.2	-	11.7 PVP	N	18.4	2M $Mg(ClO_4)_2$	100	56.7		40°C
60693	" "	44.2	-	11.7 PVP	N	19.2	2M $Mg(ClO_4)_2$	100	36.2		42°C
60693	" "	44.2	-	11.7 PVP	N	23.5	2M $Mg(ClO_4)_2$	100	37.0		53°C
63134-21	Picric Acid (41.3)	41.3	1/4" Dynel (6.2)	11.2 PVP	D	189	2M $AlCl_3$	500	11	0.86	59°C
63134-22	" " "	41.3	" " "	" "	"	172	1.6M $AlCl_3$·0.4M $Mg(ClO_4)_2$	"	18	0.95	
63134-23	" " (37.2)	37.2	" " (5.6)	20.1 PVP	"	184	"	"	19	1.00	
63134-24	" " "	37.2	" " "	" "	"	190	2M $AlCl_3$	"		-	ran below 0.8 volts
63134-19	" " (41.3)	41.3	" " (6.2)	11.2 PVP	"	128	1.6M $AlCl_3$·0.4M $Mg(ClO_4)_2$	"	24	1.00	
63134-20	" " "	41.3	" " "	" "	"	132	1M $AlCl_3$·1M $Mg(ClO_4)_2$	"	20	1.05	
63134-25	" " (37.2)	37.2	" " (5.6)	20.1 PVP	"	124	"	"	16	0.95	
63134-26	" " "	37.2	" " "	" "	"	104	"	"	14	0.98	
60668-B	" " (41.3)	41.3	" " (6.2)	11.2 PVP	"	81.3	2M $AlCl_3$	200	45	1.20	20 mil extruded primary Mg anode
60668-A	" " "	41.3	" " "	" "	"	119	"	300	20	0.94	same as above
63118-4	" " "	41.3	" " "	" "	"	85.7	"	500	30	1.01	primary Mg-holes punched in anode
63146-3	" " "	41.3	" " "	" "	"	110	"	"	36	1.01	electrolyte saturated with Santomerse
63146-4	" " "	41.3	" " "	" "	"	102	"	"	40	1.10	same as above
63156-5	" " "	41.3	" " "	" "	"	104	"	"	39	0.90	3 mil primary Mg anode
63156-4	" " "	41.3	" " "	" "	"	118	"	250	37	1.06	same as above
52759-CF-1	" " (47.5)	23.7	1/4" Carbon (23.7)	5 PVP	"	78	"	500	36	1.18	
63163-1	" " (41.3)	41.3	1/4" Dynel (6.2)	11.2 PVP	"	62.3	"	"	38	0.97	5 mil AZ61-B-perforated

Table A-2 (continued)
FORMULATIONS AND STATIC CELL CHARACTERISTICS OF ORGANIC NITRO COMPOUND CATHODES
(All cathodes discharged vs. expanded magnesium AZ31B unless otherwise noted)

Test No.	Depolarizer wt%	Conductor (Note 1) wt%	Fiber Content of Coating, % (Note 2)	Binder Content of Coating, % (Note 3)	Fabric (Note 4)	Depolariger mg/in.^{2}	Electrolyte	Current Density ma/in.^{2}	Cell Efficiency % to 0.8 v	Cell Emf Volts	Comments
63163-4	Picric Acid (41.3)	41.3	1/4" Dynel (6.2)	11.2 PVP	D	63.7	2M $AlCl_3$	500	47	1.05	perforated AZ 61-B-double thickness
52761-3	" " (47.5)	23.7	1/4"Carbon(23.7)	5 PVP	"	60	"	"	31	1.00	high open circuit 2.45v
52761-2	" " "	23.7	Graphite (23.7)	" "	"	58	"	"	31	1.00	high open circuit 2.30v
63177-1	" " (45)	45	1/8" Dynel (5)	5 PVP	"	70.8	"	"	34	0.97	5mil primary Mg-perforated 2.35 OCV
63177-2	" " "	45	" " "	" "	"	82.4	"	250	38	1.11	same as above
63177-3	" " "	45	" " "	" "	"	72.6	"	500	41	1.05	AZ61-B Mg-perforated 2.17 OCV
63177-4	" " "	45	" " "	" "	"	76.3	"	"	42	1.01	same as above
63177-5	" " "	45	" " "	" "	"	72.3	"	"	48	0.95	AZ61-B Mg-double layer
63177-7	" " (47.5)	37.5	1/4" Carbon (10)	" "	"	70.6	"	"	43	0.98	AZ61-B Mg
63177-8	" " "	37.5	" " "	" "	"	78.1	2M $AlCl_3$·1M $MgCl_2$	"	28	1.00	primary Mg anode
63177-6	" " "	37.5	" " "	" "	"	73	2M $AlCl_3$	"	48	1.15	
63182-1	" " "	37.5	1/8" Dynel "	" "	"	76.7	"	"	44	1.20	
63182-2	" " "	37.5	" " "	" "	"	81.2	"	"	44	1.05	primary Mg anode-AZ31-B placed in solution
63182-3	" " "	37.5	" " "	" "	"	73.4	"	"	34	1.00	primary Mg anode
52763-2	" " "	37.5	" " "	" "	"	126	"	"	25	1.00	SAB pretreated with HNO_3
63193-1	" " (57)	30.4	1/8" Carbon(7.6)	" "	"	131	"	"	32	1.15	carbon black and fiber
63193-2	" " "	30.4	" " "	" "	"	134	"	"	30	1.18	vacuum treated at 150°C
63193-4	" " "	30.4	" " "	" "	"	128	"	750	23	1.12	for 1 hour
63193-5	" " "	30.4	" " "	" "	"	120	"	400	22	1.16	"
63192-1	" " (47.5)	42.8	" " (4.7)	" "	"	70.1	"	500	33	1.14	"
63192-2	" " "	42.8	" " "	" "	"	63.8	"	"	33	1.13	"
63196-5	" " (45)	45	" " (5)	" "	"	79.5	Sat'd $AlCl_3$	"	61	1.30	
63196-1	" " "	45	1/8" Dynel (5)	" "	"	86	2M $AlCl_3$	"	40	1.14	
63196-2	" " "	45	" " "	" "	"	81.2	Sat'd $AlCl_3$	"	56	1.27	
63196-6	" " "	45	1/4" Carbon(5)	" "	"	86.6	"	"	56	1.19	
63199-2	" " "	45	1/8" Dynel (5)	" "	"	78.7	"	"	60	1.16	
63199-3	" " "	45	" " "	" "	"	88.8	1M $AlCl_3$	"	26	1.16	HCl added to make pH 0.01
63199-4	" " "	45	" " "	" "	"	94.9	Sat'd $AlCl_3$	"	56	1.23	
63199-5	" " "	45	" " "	" "	"	87.2	2M $AlCl_3$·1/4M HCl	"	47	1.20	
63199-6	" " "	45	" " "	" "	"	112	0.1M $Mg(ClO_4)_2$ satd w $AlCl_3$	"	57	1.24	
63199-7	" " "	45	" " "	" "	"	99.7	0.1M $Mg(ClO_4)_2$·satd $AlCl_3$	"	58	1.15	
63199-8	" " "	45	" " "	" "	"	87	1M $AlCl_3$	"	15	1.01	
63199-9	" " "	45	" " "	" "	"	87.6	"	"	22	1.01	
64304-3	" " "	45	" " "	" "	"	31.7	Satd $AlCl_3$	"	54	0.95	
64304-4	" " "	45	" " "	" "	"	33.8	"	"	58	1.00	

Table A-2 (continued)
FORMULATIONS AND STATIC CELL CHARACTERISTICS OF ORGANIC NITRO COMPOUND CATHODES
(All cathodes discharged vs. expanded magnesium AZ31B unless otherwise noted)

Test No.	Depolarizer wt.	Conductor (Note 1) wt.	Fiber Content of Coating, % (Note 2)	Binder Content of Coating, % (Note 3)	Fabric (Note 4)	Depolarizer mg/in.^{2}	Electrolyte	Current Density ma/in.^{2}	Cell Efficiency % to 0.8 v	Cell Emf volts	Comments
64309-36	Picric Acid (45)	45	16" Dynel (5)	5 PVP	D	87.4	Sat'd $AlCl_3$	250	52	1.16	Separator wet only
64309-37	" " "	45	" " "	" "	"	84.3	"	500	49	1.10	" " "
64316-6	" " "	45	" " "	" "	"	118	"	250	58	1.10	" " "
64316-7	" " "	45	" " "	" "	"	115.5	"	"	61	1.15	" " "
64316-11	" " "	45	" " "	" "	"	163.5	"	500	51	1.15	" " "
64316-12	" " "	45	" " "	" "	"	160	"	"	53	1.13	" " "
64316-16	" " "	45	" " "	" "	"	145	"	750	50	1.02	" " "
64316-14	" " "	45	" " "	" "	"	159.2	"	"	48	1.01	" " "
64312-61	" " "	45	" " "	" "	"	210.4	"	250	45	1.10	" " "
64312-62	" " "	45	" " "	" "	"	244	"	"	44	1.10	" " "
64309-48	" " "	45	" " "	" "	"	90.8	"	"	50	1.10	Separator wet only-cell ran 53 minutes
64309-41	" " "	45	" " "	" "	"	91.3	2M $AlCl_3$+0.1M $ZnCl_2$	500		1.10	Separator wet only 28% to-0.88 vs SCE
64325-1	" " (47.5)	47.5	" " "	-	"	88.8	2M $AlCl_3$	500	44.8	1.24	perforated zinc anode cathode sprayed from Hexane slurry
64325-2	" " "	47.5	" " "	-	"	68.7	"	"	39	1.25	same as above
64323-1	" " 45	45	" " "	5 PVP	"	84.2	Sat'd $AlCl_3$	"	54	1.00	
64323-2	" " "	45	" " "	" "	"	82.6	"	"			Carbon cathode collector used-cell did not maintain 0.8v
64323-5	" " "	45	" " "	" "	"	84.7	"	300	40	1.00	carbon collector
64323-6	" " "	45	" " "	" "	"	73	"	"	54	1.04	carbon collector
64323-7	" " (47.7)	42.3	" " "	" "	"	102	"	500	50	0.97	
64323-8	" " "	42.3	" " "	" "	"	85.2	"	"	54	1.01	
64323-9	" " "	42.3	" " "	" "	"	84.7	"	250	52	1.17	
64323-10	" " "	42.3	" " "	" "	"	90.6	"	"	53	1.10	
64324-13	" " (50.4)	39.6	" " "	" "	"	89.5	"	500	48	1.05	
64324-14	" " "	39.6	" " "	" "	"	81	"	"	50	1.05	
64324-15	" " "	39.6	" " "	" "	"	77.7	"	250	46	1.13	
64324-16	" " "	39.6	" " "	" "	"	87.7	"	"	47	1.15	
64324-21	" " (54)	36	" " "	" "	"	91.2	"	500	43	1.05	
64324-22	" " "	36	" " "	" "	"	102.2	"	"	42	1.10	
64324-19	" " "	36	" " "	" "	"	85.8	"	250	46	1.21	
64324-20	" " "	36	" " "	" "	"	81.5	"	"	46	1.21	
64327-4	" " (56.7)	33.3	" " "	" "	"	103.5	"	500	39	1.10	
64327-6	" " "	33.3	" " "	" "	"	106.5	"	"	39	1.10	
64327-3	" " "	33.3	" " "	" "	"	100.1	"	250	39	1.20	
64327-5	" " "	33.3	" " "	" "	"	98.9	"	"	40	1.20	
64327-10	" " (58.5)	31.5	" " "	" "	"	121.5	"	500	34	1.00	
64327-8	" " "	31.5	" " "	" "	"	108.5	"	"	35	1.05	
64327-7	" " "	31.5	" " "	" "	"	105	"	250	37	1.16	
64327-11	" " "	31.5	" " "	" "	"	95.8	"	"	37	1.14	

Table A-2 (continued)
FORMULATIONS AND STATIC CELL CHARACTERISTICS OF ORGANIC NITRO COMPOUND CATHODES
(All cathodes discharged vs. expanded magnesium AZ31B unless otherwise noted)

Test No.	Depolarizer %	Conductor (Note 1) wt	Fiber Content of Coating, % (Note 2)	Binder Content of Coating, % (Note 3)	Fabric (Note 4)	Depolarizer mg/in.²	Electrolyte	Current Density ma/in.	Cell Efficiency % to 0.8 v	Cell Emf Volts	Comments
64304-19	Picric Acid(45)	45	1/8" Dynel (5)	5 PVP	D	27.8	Sat'd $AlCl_3$	250	64	1.23	
64304-20	" " "	45	" " "	" "	"	23.8	"	"	61	1.22	
64304-22	" " "	45	" " "	" "	"	26.4	"	750	41	0.92	
64304-23	" " "	45	" " "	" "	"	24.5	"	"	40	0.98	
64304-28	" " "	45	" " "	" "	"	49.4	"	500	54	1.10	
64304-30	" " "	45	" " "	" "	"	50.6	"	"	54	1.10	
64304-26	" " "	45	" " "	" "	"	47.6	"	250			Anode consumed at 51% eff. 1.06 cell voltage
64304-29	" " "	45	" " "	" "	"	55	"	750			Tape did not hold this current
64304-5	" " "	45	" " "	" "	"	39.2	"	250			Anode corroded at 40% eff. and 1.5 cell voltage (8 minutes)
64304-25	" " "	45	" " "	" "	"	39.1	"	"			Same as above
64304-7	" " "	45	" " "	" "	"	77.9	"	500	54	1.26	double thickness anode
64304-15	" " "	45	" " "	" "	"	76.8	"	750	53	1.15	used "
64304-16	" " "	45	" " "	" "	"	83.4	"	"	52	1.20	"
64304-13	" " "	45	" " "	" "	"	77.5	"	250			Stopped at 30% (1.60v) due to anode failure-double anode
64304-18	" " "	45	" " "	" "	"	69.7	"	"			Stopped at 35% (1.30v) due to anode failure-4 layer anode
64309-34	" " "	45	" " "	" "	"	103	"	500	42	1.30	
64309-35	" " "	45	" " "	" "	"	106	"	"	37	1.35	
64309-45	" " "	45	" " "	" "	"	108	"	750	19	0.85	
64309-46	" " "	45	" " "	" "	"	104	"	"	21	0.86	
64309-40	" " "	45	" " "	" "	"	115	"	500	34	1.26	Anode failed-10 min run
64309-43	" " "	45	" " "	" "	"	111.3	"	750	46	1.17	-8.5 min run
64312-51	" " "	45	" " "	" "	"	178.9	"	250	55	1.20	AZ 31B-perforated sheet
64312-56	" " "	45	" " "	" "	"	173	"	"	57	1.15	stock anode
64312-57	" " "	45	" " "	" "	"	199.4	"	500	67	1.15	Electrolyte added to separator only
64312-59	" " "	45	" " "	" "	"	210.7	"	"	50	1.00	Separator wet only-cell ran 26 minutes
64312-58	" " "	45	" " "	" "	"	216.8	"	750	47	0.95	Separator wet only
64312-60	" " "	45	" " "	" "	"	195.5	"	"	48	1.00	Separator wet only
64316-1	" " "	45	" " "	" "	"	61.9	"	"	28	0.85	Separator wet only
64316-2	" " "	45	" " "	" "	"	39.7	"	250	68	1.14	Separator wet only
64316-3	" " "	45	" " "	" "	"	38.9	"	"	67	1.10	Separator wet only

Table A-3 (continued)

PHYSICAL DATA ON CAPSULES PREPARED FOR PERMEABILITY TESTS

Capsule Number	Capsule Material	Liquid	Conditions *	Film Thickness (mils)	Film Weight (g)	Total Weight (g)	Liquid Weight (g)	I. D. (in.)	O. D. (in.)	Flat Width (in.)	Length (in.)	Approximate Thickness (inches)	Surface Area (in.^{2})	Initial Payload Weight (g)
E36	Kel-F 81	2 M $AlCl_3$	C	3.5	-	0.6074	-		0.12		2.25	-	0.88	-
E37	FEP-Teflon	water	A	2	0.2878	1.0780	0.7902			0.36	4.0	0.08	3	73.2
E38	Aclar	2 M $Mg(ClO_4)_2$	C	2	0.7635	3.2884	2.5249			0.56	6.20	0.06	7	76.7
E39	Aclar	2 M $Mg(ClO_4)_2$	C	2	0.7479	2.9872	2.2393			0.56	6.20	0.06	7	75.1
E40	Aclar	2 M $Mg(ClO_4)_2$	B	2	0.7750	3.1044	2.3294			0.56	6.20	0.06	7	75.1
E41	Aclar	2 M $Mg(ClO_4)_2$	B	2	0.7152	2.9883	2.2731			0.56	6.20	0.06	7	76.0
E42	Aclar	2 M $Mg(ClO_4)_2$	A	2	0.7730	3.2693	2.4963			0.56	6.20	0.06	7	76.3
E43	Aclar	2 M $Mg(ClO_4)_2$	A	2	0.7018	3.2358	2.5340			0.56	6.20	0.06	7	78.2
E44	Kel-F 81	water	C	3	0.2733	1.4907	1.2174	0.12			6.0	-	2.36	81.7
E45	Kel-F 81	2 M $Mg(ClO_4)_2$	C	3	0.2674	1.8456	1.5782	0.12			6.0	-	2.36	85.3
E46	Kel-F 81	water	B	3	0.2703	1.5016	1.2313	0.12			6.0	-	2.36	82.1
E47	Kel-F 81	2 M $Mg(ClO_4)_2$	B	3	0.2704	1.8893	1.6189	0.12			6.0	-	2.36	85.6
E48	Kel-F 81	water	A	3	0.2833	1.6218	1.3385	0.12			6.0	-	2.36	82.6
E49	Kel-F 81	2 M $Mg(ClO_4)_2$	A	3	0.2696	1.8540	1.5844	0.12			6.0	-	2.36	85.6
E50	Kel-F 81	2 M $AlCl_3$	A	3	0.2798	1.8033	1.5235	0.12			6.0	-	2.36	84.6
E51	Kel-F 81	2 M $AlCl_3$	B	3	0.2760	1.8123	1.5363	0.12			6.0	-	2.36	84.9
E52	Kel-F 81	2 M $AlCl_3$	C	3	0.2788	1.8166	1.5378	0.12			6.0	-	2.36	84.5
E53	Kel-F 81	2 M $AlCl_3$	C	3	0.2739	1.7376	1.4637	0.12			6.0	-	2.36	84.1
E54	Kel-F 81	37% KOH	A	3	0.2785	1.8743	1.5958	0.12			6.0	-	2.36	85.3
E55	Kel-F 81	37% KOH	A	3	0.2792	1.8506	1.5714	0.12			6.0	-	2.36	84.9

Table A-3 (continued)

PHYSICAL DATA ON CAPSULES PREPARED FOR PERMEABILITY TESTS

Capsule Number	Capsule Material	Liquid	Conditions *	Film Thickness (mils)	Film Weight (g)	Total Weight (g)	Liquid Weight (g)	I. D. (in.)	O. D. (in.)	Flat Width (in.)	Length (in.)	Approximate Thickness (inches)	Surface Area ($in.^2$)	Initial Payload Weight (g)
E56	Kel-F 81	37% KOH	B	3	0.2792	1.8760	1.5968	0.12			6.0	-	2.36	84.9
E57	Kel-F 81	37% KOH	B	3	0.2763	1.8892	1.6129	0.12			6.0	-	2.36	85.3
E58	Kel-F 81	37% KOH	C	3	0.2764	1.8361	1.5597	0.12			6.0	-	2.36	84.8
E59	Kel-F 81	37% KOH	C	3	0.2807	1.8330	1.5523	0.12			6.0	-	2.36	84.8
E60	Kel-F 81	37% KOH	C	3	0.2850	1.9113	1.6263	0.12			6.0	-	2.36	85.2
E61	Kel-F 81	37% KOH	C	3	0.2790	1.8954	1.6164	0.12			6.0	-	2.36	85.1

Table A-4

LABORATORY PROCEDURE FOR CHEMICAL ETCHING OF MAGNESIUM

Degreasing Bath

20 grams Alconox/liter H_2O (dist.)

or

22.5 grams Na_2CO_3
15.0 grams NaOH } /liter H_2O (dist.)

Etching Bath

60 ml conc. HNO_3
150 grams $NaNO_3$ } /liter H_2O (dist.)

Procedure (Batch Method)

1. Clean magnesium in either of the degreasing baths for approximately 5 minutes, sponging or wiping as required. For heavy grease deposits, the Alconox bath is preferred but requires a longer following rinse.

2. Rinse thoroughly in tap water.

3. Etch for approximately 30 seconds to 1 minute for each 1 mil reduction in thickness, monitoring continuously with micrometer as desired thickness is approached. This can be done by removing and rinsing in H_2O bath for a few seconds on each check.

4. Rinse well in tap water.

5. Dry with towelling.

Table A-5

FORMULAS USED FOR COMPRESSION AND EXTRUSION TRIALS

	%Weight	%Volume
	Formula A	
KIO_4	67.91	53.3
Acetylene Black	29.30	42.7
Carbon Fiber	2.37	3.0
Binder	0.42	1.0
	100.00	100.0
	Formula B	
KIO_4	68.05	53.6
Acetylene Black	29.37	42.9
Carbon Fiber	2.37	3.0
Binder	0.21	0.5
	100.00	100.0
	Formula C	
KIO_4	67.33	53.2
Acetylene Black	23.20	34.2
No. 6553 Graphite	6.72	8.6
Carbon Fiber	2.33	3.0
Binder	0.42	1.0
	100.00	100.0
	Formula D	
KIO_4	67.46	53.6
Acetylene Black	23.25	34.3
No. 6553 Graphite	6.74	8.6
Carbon Fiber	2.34	3.0
Binder	0.21	0.5
	100.00	100.0
	Formula E	
KIO_4	68.21	This formula adjusts to formulas A,B,G,or H when binder is added. Used for mixing purposes.
Acetylene Black	29.43	
Carbon Fiber	2.36	
Binder	-	
	100.00	
	Formula F	
KIO_4	60.0	44.5
Acetylene Black	36.5	50.3
Carbon Fiber	2.5	3.0
Binder	1.0	2.2
	100.0	100.0
	Formula G	
KIO_4	67.62	52.8
Acetylene Black	29.20	42.3
Carbon Fiber	2.36	3.0
Binder	0.82	1.9
	100.00	100.0
	Formula H	
KIO_4	67.50	52.5
Acetylene Black	29.03	42.0
Carbon Fiber	2.40	3.0
Binder	1.07	2.5
	100.00	100.0
	Formula J	
KIO_4	62.83	47.5
Acetylene Black	33.83	47.5
Carbon Fiber	2.47	3.0
Binder	0.87	1.9
	100.00	100.0
	Formula K	
KIO_4	63.12	46.9
Acetylene Black	33.83	46.9
(Dynel)	2.00	4.2
Binder	0.87	2.0
	100.00	100.0
	Formula L	
KIO_4	60.66	45.25
Acetylene Black	35.95	49.75
Fiber (Carbon)	2.50	3.00
Binder	0.89	2.00
	100.00	100.00
	Formula M	
	61.21	This formula adjusts to formula L when binder is added. Used for mixing purposes.
	36.27	
	2.52	
	-	
	100.00	

Table A-6

SUMMARY OF TAPE PROCESS RUNS - EXTRUSION AND COMPRESSION

Run No.	Formula Binder *	Solvent +	Adhesive ‡	Adhesion††	Physical Data	Remarks	Elect. Performance**
62463	A- PVF	Chloroform	Chloroform with 25 g/l PVF sprayed on tape	Excel	0.016 in. thick 0.264 g/in.^{2}		Fair (severe sticking)
62465-1	C- PVF	Chloroform w/1.0% Gafac	"	Excel	0.013 in. thick 0.161 g/in.^{2}		Fair-good-up to 0.9 watt/in.^{2} (severe sticking)
62465-2	C- PVF	Chloroform w/0.1% Gafac	"	Excel	0.013 in. thick 0.160 g/in.^{2}		Fair (sticking)
62465-3	C- Styrene	"	"	Excel	0.012 in. thick 0.190 g/in.^{2}	Electrode hydrophobic	Fair up to 0.35 watt/in.^{2} (sticking)
62465-4	B- PVF	Chloroform	None	Poor	0.015 in. thick 0.176 g/in.^{2}	Electrodes were of insufficient strength for general use	Very good-sustain up to 1 watt/in^2 (occasional sticking)
62465-5	B- PVF	"	Sprayed chloroform with unknown strength PVF	Fair	———	Slightly better than above	Good--but less than above
62466-1	A- PVF	Chloroform	Sprayed chloroform w/2.5 g/l PVF	Fair	———		Fair-good-up to 0.9 watt/in^2 (sticking)
62466-2	"	"	Sprayed chloroform w/2.5 g/l styrene	Fair	———		Fair (sticking)
62466-3	"	"	Sprayed H_2O w/1% Gelvatol	Poor	———	H_2O glue solutions caused wavy electrodes on drying	———
62466-4	"	"	Sprayed H_2O w/0.7% CMC	Fair	———		Poor (sticking)
62466-5	C- PVF	Chloroform	Sprayed chloroform w/2.5 g/l PVF	Fair	———		Fair-good-up to 0.88 watt/in.^{2}
62466-6	"	"	Sprayed chloroform w/2.5 g/l styrene	Poor	———		———
62466-8	"	"	Sprayed H_2O with 0.7% CMC	Poor	———	Wavy or rippled	———
62467-1	A	Chloroform with 5 g/l PVF	None	Good	0.015 in. thick 0.210 g/in.^{2} 28% solids		Maintain 0.85 watt/in.^{2} Sticking to collector
62467-2	"	Chloroform with 5 g/l PVB	None	Fair-Good	0.264 g/in.^{2} 38% solids	Electrode hydrophopic	Essentially wetproofed Sustained very little current

See notes at end of table.

Table A-6 (Cont'd)

SUMMARY OF TAPE PROCESS RUNS - EXTRUSION AND COMPRESSION

Run No.	Formula Binder *	Solvent +	Adhesive ±	Adhesion†*	Physical Data	Remarks	Elect. Performance**
62467-3	A	Chloroform with 5 g/l PVF	Prewet with chloroform prior to extruding	Good	——	Short sections	——
62467-4	A	Chloroform with 5g/l PVB	Prewet with chloroform prior to extruding	Good	——	Short sections	——
62468	E	Chloroform with 5 g/l PVB and 5 ml/l Gafac	Prewet with chloroform prior to extruding	Fair-Good	0.015 in. thick 0.230 g/in.^{2}	With binder in solvent formula adjusts to ≈ 2% Vol PVB	Sustain up to 0.44 watt/in.^{2}
62469	F	H_2O with 5 g/l methocel	None	Fair	——	Could not manufacture until nylon netting was inserted between cathode surface and blotting paper	Fair-good-up to 0.95 watt/in.^{2} (severe sticking)
62470-1	B- PVB	Chloroform with 5 ml/l Gafac	Sprayed chloroform w/5 g/l PVF	Poor	——	Adhesive added by drawing tape thru solution prior to extruding	——
62470-2	"	"	Sprayed chloroform w/25 g/l PVF	Fair	0.013 in. thick 0.190 g/in.^{2}	"	Fair up to 0.65 watt/in.^{2} (sticking)
62470-3	"	"	Sprayed chloroform w/5 g/l PVP/VA	Fair	——	"	——
62470-4	"	"	Sprayed chloroform w/25 g/l PVP/VA	Short section- did not determine	——	"	——
62470-5	"	"	Sprayed chloroform w/25 g/l PVF (repeat)	Fair-good	0.013 in. thick 0.185 g/in.^{2} 30% solids	" (2-3 mg binder/in.^{2} on tape)	Fair-maintain 0.70 watt/in.^{2}
62470-6	"	"	Sprayed chloroform w/25 g/l PVP/VA (Repeat)	Poor-fair-some good	0.210 g/in.^{2}	"	——
62471-1	A- PVF	Chloroform with 5 ml/l Gafac	Prewet with chloroform	Poor	0.017 in. thick 0.225 g/in.^{2}	——	Fair-up to 0.76 watt/in.^{2}
62471-2	C- PVF PVP	Chloroform with 5 ml/l Gafac	Prewet with chloroform None	Poor Poor-fair	0.017 in. thick 0.280 g/in.^{2}	—— ——	Fair-up to 0.63 watt/in.^{2}
62472-1	F- PVF	Chloroform	H_2O with 0.7% CMC applied with paint brush	Mix was rubbery could not extrude	——	Carbon black and KIO_4 were not Waring Blended during mixing	——
62472-2	G- PVF	Chloroform	None	"		"	——

See notes at end of table.

Table A-6 (Cont'd)

SUMMARY OF TAPE PROCESS RUNS - EXTRUSION AND COMPRESSION

Run No.	Formula - Binder *	Solvent †	Adhesive ‡	Adhesion††	Physical Data	Remarks	Elect. Performance**
62473-1	G- PVF	Chloroform	None	Fair	0.013 in. thick 0.181 g/in.^{2} 30% solids	This and all following tapes: 1. Adjusted mixing procedure 2. Nylon screen pattern on surface	Good-0.80 watt/in.^{2} sustained (stuck once)
62473-2	F- PVF	Chloroform	None	Fair-good	0.012 in. thick 0.119 g/in.^{2} 23% solids	"	Fair-0.59 watt/in.^{2} (sustained runs without sticking)
62474-1	H- PVF	Chloroform with 0.12 g Nekal BX-78 per 100 g mix	None	Fair	0.018 in. thick 0.310 g/in.^{2} 25% solids	Made with .030 in. extrusion opening	Good-0 86 watt/in.^{2} (sticking)
62474-2	"	"	"	Poor	0.335 g/in.^{2} 28% solids	Made with .040 in. extrusion opening	----------
62474-3	J- PVF	Chloroform	None	Poor-fair	0.025 in. thick 0.280 g/in.^{2} 25% solids	Made with .040 in. extrusion opening	Good--1.1 watt/in.^{2}
62474-4	"	"	"	Fair-good	0.017 in. thick 0.151 g/in.^{2} 21% solids	Made with 0.030 in. extrusion opening	Good-0.79 watt/in.^{2}
62475-1	J- PVF	Chloroform	Prewet with chloro	Poor		This entire series run to test various methods of obtaining good adhesion to tape substrate without masking KIO_4 with excess binder. The insertion of poorly absorbing materials between top blotter and coating was intended to force the excess chloroform (with binder) to the bottom blotter during compression.	----------
62475-2	"	"	Insert 5 mil dynel between top blotter and cathode coating	Fair			----------
62475-3	"	"	Insert Saran Wrap as above	Poor			----------
62475-4	"	"	Prewet top blotter with chloroform	Fair			----------
62475-5	"	"	Prewet tape with chloroform containing 50 g/l PVF	Good	0.016 in. thick 0.177 g/in.^{2} 24% solids approx 6 mg PVF per in.^{2} tape		Fair-0.69 watt/in.^{2}
62477-1	K- PVF (Dynel Fibers)	Chloroform	Fibers	bridged -- Could not extrude		----------	----------
62477-2	K (Dynel Fibers)	Chloroform with required PVF pre-dissolved	"	"	" " "	----------	----------

See notes at end of table.

Table A-6 (Cont'd)

SUMMARY OF TAPE PROCESS RUNS - EXTRUSION AND COMPRESSION

Run No.	Formula - Binder *	Solvent †	Adhesive ‡	Adhesion††	Physical Data	Remarks	Elect. Performance**
62-77-3	J-	Chloroform with required PVF pre-dissolved	None	Good	0.015 in. thick 0.160 g/in.² 22% solids		Good-0.67 watt/in.²
62-77-4	J	Chloroform with 3 g/l PVF pre-dissolved	None	Good	0.015 in. thick 0.156 g/in.² 26% solids	Base tape prefluffed with emery cloth	Good-0.7? watt/in.² (some sticking at higher outputs)
62-77-5	J	"	"	Good (Better than above)	"	Base tape prefluffed with wire brush	————
6247?-1	J	Chloroform with 3.5 g/l	None	Good	————	Base tape fluffed by passing under weighted emery	
62?7?-2 62?7?-3	J	"	None	Good (Better than above)	0.022 in. thick 0.280 g/in.² 27-28% solids	Run in 2 parts with overnight stand in between. Both sections good. Base tape hand fluffed with wire brush.	Good-0.76 watt/in.² (occasional sticking)
62-79	M- (This adjusts to formula "L" when PVF strength is included)	Chloroform with 2.4 g/l PVF	None	Good	0.017 in. thick 0.210 g/in.² 24% solids	Hand fluffed with wire brush. Continuous run of 80 ft.	Good-0.79 watt/in.²

NOTES:

* Formulas shown in Table A-5, do not specify binder. Those chosen for each run are indicated in this column. Formula volume percentages hold for binders whose specific gravity is close to 1.2 (most of those used). Where no binder is indicated, it has been included with the slurry solvent.

† Liquid media used to make slurry. Sometimes will contain binder or wetting agent.

‡ Additional adhesive elements, added to tape prior to extrusion

†† Adhesion ratings as follows: Poor-excessive flake-off of coating; Fair-occasional flake-off of coating, can be discharged dynamically if desired; Good-no flaking but care should be exercised in handling; Excellent-reasonably rugged, adherent coating

** General rating of dynamic discharge characteristics takes into account current efficiency, voltage, current density and output maintenance with time. Sticking to current collector noted where appropriate. See Table A-7 for details.

Table A-7

DYNAMIC TESTS RESULTS WITH TAPES USING POTASSIUM PERIODATE AS CATHODE DEPOLARIZER

P - Primary Mg, no holes
p - Perforated Primary Mg
Ex- Expanded Primary Mg
Tc- Machined Punched Primary Mg
MO- Saturated $AlCl_3$ (2.8 M)
M1- 2M $AlCl_3$ + 1M HCl
M2- 2M $AlCl_3$ + 0.5M HCl
M4- 2M $AlCl_3$ + 0.5M HBF_4
D - Dynel 3.5 mil
DS- Dynel 2.5 mil
N1- Nylon 4 mil
N2- Nylon 2.5 mil
PP- Polypropylene 2.7 mil
Pt- Platinum
G - U.S. Graphite 443
Gp- Graphite powder
Gs- Slotted Graphite
GS- Graphite-Silastic alternating slots
GM- Graphite large slots
Gm- Multiple Slotted Graphite
GW- Graphite 1.5 in. wide
S - Cathode stuck to Collector

			Electrolyte		Collector		Tape Speed	Run Time		Electrolyte Feed Rate	Cathode					Cell		
						Pressure					Wt/thickness	Capacity AM/in.²		Area	Coul. Eff.	V_{av}	I	
Run No.	Tape No.	Anode	Type	Separator	Type	g/in.²	in./min	min	OCV volts	cc/in.²	mg/in.²/mils	Theo.	Dynamic	in.²	%	volts	ma	Comments
66219-1	62453-F	p	MO	D	Pt	220	0.15	38	2.55	0.35	180			1.75		1.60	450	stuck
66219-2	62453-F	p	M2	D + D	Pt	220	0.20	3S	-	-	180			1.75		1.65	480	stuck
66219-3	62453-F	p	MO	D + N1	Pt	180	0.20	8S	2.6	-	180			1.75		1.65	480	coll. area
66220	62453-F	p	MO	D + N1	Gp	180	0.25	14S	2.57	0.30				1.75		1.55	480	coll. area
66221	52779-1	p	M2	D	G	300	0.25	37	2.55	0.5	180/20	4.8	2.2	1.75	47	1.95	560	electrolyte fed into separator
66222	-------	p	M2	PP	G	410	0.15	5S	2.57	-	318			1.75		1.90	870	coating falls off
66223-1	52779-1-2	p	M2	N1	G	220	0.25	24	2.87	0.57				1.75		1.90	660	
66223-2	52779-1-2	p	M2	N2	G	220	0.25	24	-	0.54				1.75		1.83	700	
66224	52779-1-2	p	M2	D	G	220	0.25	24	-	0.51				1.75		1.75	700	
66225	62453-F	p	M2	N1	GS	220	0.25	15S	2.85	0.4				1.75		1.85	600	slotted collector
66227-1	52779-1-3	p	M2	D + PP	GS	220	0.25	13	2.90	0.5				1.75		1.80	600	slotted collector
66227-2	52779-1-3	Ex	M2	D	GS	220	0.25	45	-	0.50				1.75		1.70	700	slotted collector
66229-1	62453-F	p	M1	N1	GS	80	0.25	25	2.67	0.56				1.75		1.90	750	slotted collector
66229-2	62453-F	p	M1	N1	GS	80	0.30	18	-	0.60				1.75		1.80	950	slotted collector
66231-1	62457-W	p	M1	DS	GS	80	0.25	30	2.89	0.65				1.75		1.82	750	foam due to PVP glue
66231-2	62457-X	p	M1	DS + N1	GS	80	0.25	13	2.75	0.58				2.0		1.95	900	
66231-3	62457-X	p	M1	DS	GS	80	0.25	20	-	0.54				2.0		1.94	900	
66234-1	62457-V	p	M1	DS	GS	80	0.30	12	2.75	0.5				2.0		1.88	800	
66234-2	62457-V	p	M4	DS	GS	80	0.30	5	-	0.7				2.0		1.85	1000	
66235-F	62453-F	p	M2	D + N2	Pt	80	0.30	30	-	-				1.75		1.85	700	
66235-R	62453-F	Ex	M2	D + N2	GS	80	0.30	30	2.75	-				2.0		1.85	700	series connected
66236-1	52779-1-4	p	M2	D + N1	GS	220	0.25	13	2.75	0.54				1.75		1.80	800	
66236-2	52779-1-4	P	M2	D + N1	GS	220	0.25	20	-	0.54				1.75		1.85	800	
66237-1	62453-WA	P	M1	D + N1	GS	80	0.25	30	2.25	0.5	174/14	5.7	2.0	1.75	35	1.80	500	
66237-2	62453-WA	P	M1	D	GS	80	0.25	15	-	0.6	174/14	5.7	2.7	1.75	48	1.85	650	
66238-1	62453-WA	p	M1	D + N1	GS	80	0.25	15	2.75	0.6	174/14	5.7	3.4	2.0	59	1.80	850	
66238-2	62453-WA	P	M1	D + N1	GS	80	0.25	26	-	0.7	174/14	5.7	3.4	2.0	59	1.70	850	
66239	52779-3-1	p	M1	D + N1	GS	160	0.25	30	2.8	0.65	148/15	4.3	2.8	2.0	65	1.90	700	
66240	62465-4	p	M1	N1	GS	80	0.25	13	2.92	-	176/15	5.7	3.6	2.0	63	1.95	900	
66241	62453-F	p	M1	N1	GS	40	0.25	28S	2.82	0.6	176/15	5.7	4.0	2.0	69	2.0	1000	
66243	62462	p	M1	N1	GS	80	0.25	55	2.75	-	238/16	7.8	3.6	2.0	47	1.8	900	
66244	62453-F	p	M1	N1	GS	60	0.25	35	2.9	0.5	176/15	5.7	4.0	2.0	69	2.0	1000	
66245	62453-F	p	M1	N1	GS	80	0.25	5S	2.88					2.0		2.0	950	stuck after 5 min.
66246	62465-1	p	MO	N1	GS	40	0.25	2S	2.60					2.0		2.0	900	stuck immediately
66247	62465-2	p	M1	N1	GS	40	0.25	1S	2.60					2.0				stuck immediately
66248	62465-3	p	M1	N1	GS	40	0.25	6S	2.60									stuck after 6 min.
66249	52781-6	p	M1	N1	GS	320	0.25	56	2.90	0.62	231/18	6.6	4.0	2.0	61	1.85	1000	
66250	62465-3	p	M1	N1	GS	40	0.30	12S	2.60		190/13			2.0		2.0	700	sticks repeatedly
66251	62464-A	p	M1	N1	GS	40	0.25	5S	2.80		264/20			2.0				thru C all stick after 2 to 5 min. operation
66252	62467-2	p	M1	N1	GS	40	-							2.0		1.5	300	will not wet out
66253	62467-1	sticks repeatedly, Ir free meas. shows 0.2v drop in cell at 1000 ma.									205/15			2.0		1.9	700	

Table A-7 (Cont'd)

P- Primary Mg, no holes
p- Perforated Primary Mg
Ex-Expanded Primary Mg
Tc-Machined Punched Primary Mg
MO-Saturated $AlCl_3$ (2.3 M)
M1-2M $AlCl_3$ + 1M HCl

M2- 2M $AlCl_3$ + 0.5M HCl
M4- 2M $AlCl_3$ + 0.5M HBF_4
D - Dynel 5.5 mil
DS- Dynel 2.5 mil
N1- Nylon 4 mil
N2- Nylon 2.5 mil

PP- Polypropylene 2.7 mil
Pt- Platinum
G - U. S. Graphite 443
Gp- Graphite powder
Gs- Slotted Graphite
GS- Graphite-Silastic alternating slots

GM- Graphite large slots
Gm- Multple Slotted Graphite
GW- Graphite 1.5 in. wide
S - Cathode stuck to collector

Run No.	Tape No.	Electrolyte Anode	Type	Separator	Type	Collector Pressure #/in.²	Tape Speed in./min	Run Time min.	OCV volts	Electrolyte Feed Rate #/in.²	Cathode Wt/Thickness mg/in.²/mils	Capacity AN/in.² Theo.	Capacity AN/in.² Dynamic	Area in.²	Coul. Eff. %	Coll. V_{ave} volts	Coll. I ma	Comments
66254-1	62477-1	p	M1	N1	GS	40	0.25	40	2.57	0.5	211/15	6.8	2.8	2.0	41	1.95	700	
66254-2	62477-1	same as above but sticks at a higher output									211/15	6.8	3.6	2.0	52	1.94	900	
66255	62477	will not wet out well, IR free meas. shows 0.4v drop at 1000 ma.												2.0		1.5	600	
66256	62479	sticks to collector firmly												2.0		1.94	1000	
66257	62477-1	p	M1	N1	GM	80	0.25	40S	2.61	0.66	211/15	6.8	3.6	2.0	52	1.85	900	
66258	62470-4	p	M1	N1	GS	140	0.25	24S	2.7	0.5	190/13	6.0	2.8	2.0	47	1.85	700	
66259	62470-4	Tc	M1	N1	GS	100	0.25	71	2.55	0.4	190/13	6.0	2.8	2.0	47	1.9	700	
66260	52781-7	Tc	M1	N1	GM	180	0.25	24	2.9	0.65	220/18	6.1	4.0	2.0	65	2.02	1000	
66261	62470-5	Tc	M1	N1	GM	60	0.25	100	2.75	0.5	190/13	6.0	2.8	2.0	47	2.0	700	
66263-1	62471-2	Tc	M1	N1	GM	80	0.25	12	2.82		280/18			2.0		1.7	740	
66263-2	62471-1	Tc	M1	N1	GM	80	0.25	14	2.93	0.45	225/17			2.0		1.9	800	
66264-2	62472-3	Tc	M1	N1	GM	40	0.25	4S	2.95					2.0		2.0	800	
66265	52781-7	p	M1	N1	GM	140	0.25	35	2.89		227/31	6.6	4.0	2.0	60	1.96	1000	Temp. cathode 120°F
66266	52781-7	Tc	M1	N1	GW	160	0.25	52	2.95	0.8	260/31	7.5	4.8	3.75	64	1.85	1800	Temp. anode 145°F
66267	62473-1	Tc	M1	N1	GM	40	0.25	24	2.95		180/13	5.8	3.2	2.0	56	2.02	800	
66268	62473-2	Tc	M1	N1	GW	40	0.25	32S	2.93	0.67	119/12	3.5	3.0	3.75	85	1.93	1120	
66269	62473-2	Tc	M1	N1	GW	40	0.25	64	2.91	0.54	119/12	3.5	2.95	3.75	83	2.02	1100	
66272-1	62474-4	Tc	M1	N1	GW	40	0.25	20	2.90	0.50	151/12	4.5	3.9	3.75	85	2.03	1450	
66272-2	62474-3	Tc	M1	N1	GW	40	0.25	20	2.92	0.77	280/23	8.5	5.3	3.75	63	1.95	2000	
66273	62474-1	Tc	M1	N1	GW	20	0.25	13S	2.85		310/18	10.1	4.6	3.75	46	1.90	1700	
66274	62475-5	Tc	M1	N1	GW	40	0.25	18	2.75	0.55	177/16	5.3	3.7	3.75	69	1.95	1400	
66276	62477-3	Tc	M1	N1	GW	40	0.25	40	2.78	0.54	155/16	4.6	3.3	3.75	75	2.0	1250	
66277	62477-4	Tc	M1	N1	GW	40	0.25	50	2.90	0.55	188/16	5.7	3.7	3.75	65	2.0	1400	sticks at 1.5 amp
66279-1	62478-2	Tc	M1	N1	GW	40	0.25	40S	2.92	0.67	227/20	6.8	3.9	3.75	57	1.95	1450	
66279-2	62478-2	Tc	M1	N1	GW	20	0.125	44		1.0	227/20	6.8	4.0	3.75	58	2.13	750	
66279-3	62478-2	Tc	M1	N1	GW	40	0.125	9		1.0	227/20	6.8	4.8	3.75	71	2.04	900	
66280	62477-4	Tc	M1	N1	GW	20	0.125	11S	2.92		188/16	5.7	4.0	3.75	69	2.17	750	sticks
66281	62479	Tc	M1	N1	GW	20	0.25	48	2.90	0.58	170/16	4.8	4.0	3.75	83	1.96	1500	
66282-F	62479	Tc	M1	N1	GW	20	0.25	76	2.85	0.65	175/17	5.1	3.7	3.75	73	1.93	1400	series connected
66282-R	62479	Tc	M1	N1	GW	20	0.25	76	2.75	0.67	175/17	5.1	3.7	3.75	73	1.82	1400	series connected
66285-F	62479	Tc	M1	N1	GW	20	0.25	24	2.85	0.9	175/16	5.1	4.0	3.75	79	1.98	1500	series connected
66285-R	62479	Tc	M1	N1	GW	20	0.25	24	2.88	0.8	177/17	5.1	4.0	3.75	79	1.60	1500	series connected

Note: Tape numbers in 52,000 series were hand cast, those in 62,000 series were machine made. Cathode coulombic efficiencies were based on KIO_4 makeup weights and a theoretical capacity of 49 A-M/g KIO_4. Analyses of KIO_4 in completed tapes was usually a few percent below the makeup value.

Table A-8

STORAGE STABILITY TEST SUMMARY
FOR KIO_4-Mg SYSTEM

	Weight Change in 30 Days		
	Conditions		
Magnesium	Ambient($25°C$, 50% RH)	Vacuum (0% R.H.)	88% R.H., 25°C
Primary Mg	No change	No change	+0.4%
AZ31B	No change	No change	+0.08%
KIO_4-Mg Tape	No change	-0.2%	+40%

APPENDIX B

ENCAPSULATION OF ELECTROLYTES FOR FUEL CELLS

by E. C. Martin and W. W. Harlowe

Southwest Research Institute
San Antonio, Texas

Prepared under Subcontract to
Monsanto Research Corporation
Everett, Mass.

APPENDIX B

ENCAPSULATION OF ELECTROLYTES FOR FUEL CELLS

by E. C. Martin and W. W. Harlowe

Southwest Research Institute
San Antonio, Texas

I. INTRODUCTION

Fuel cells or batteries that are being manufactured at the present time have a limited shelf-life and as a result are not applicable to space travel, since several years may pass before the cell is used for current production. In order to eliminate the limited storage life of the cell, it is necessary to keep the components of the cell separated. One approach under investigation is to have the dry elements of the cell in the form of a tape. As the tape is advanced for use, the electrolyte is introduced at the advanced section of the tape to moisten it.

The objective of this program is to investigate the feasibility of encapsulating various electrolytes. The capsules can be imbedded in the tape. As the tape is advanced, the capsules will be crushed to release the electrolyte and form an activated cell.

The electrolytes suggested for encapsulation were both aqueous and organic systems. One aqueous system was 2 M lithium chloride. The organic systems were butyrolactone, butyronitrile, acetonitrile, dimethylformamide, dimethylsulfoxide, propylene carbonate, and dioxane.

For the purposes of this feasibility study, capsules having a size range of 500 to 1000 microns were considered acceptable; however, it is anticipated that the optimum capsule must be 500 microns or less.

II. EXPERIMENTATION

A. Equipment

The extrusion equipment for the encapsulation of liquids was used to prepare capsules during this program. This equipment consists of a steam jacketed encapsulation nozzle having concentric tubes. For the encapsulation of electrolytes using polymer solutions as the shell formulation, the inner tube had a 0.010-inch ID and a 0.018-inch OD. The outer orifice was 0.045-inch in diameter.

When hot melts were used to encapsulate the electrolytes, the polymer reservoir, pump assembly and the extrusion encapsulation equipment were placed in a constant temperature oil bath in order to keep the molten polymer and the filler at a uniform temperature. During the initial experiments, the inner tube had a 0.016-inch ID and a 0.028-inch OD, and the outer orifice was 0.625-inch in diameter. This combination of orifices produced capsules in the range of 1000 microns. When the inner tube was decreased to 0.007-inch ID and 0.014-inch OD and the outer orifice was decreased to 0.018-inch, the resulting capsules were less than 600 microns in diameter.

B. Encapsulation of Aqueous Electrolytes Using Polymer Solutions

The initial experiments were made using a polymer blend as the shell material. The polymers used were Elvax 250 (an ethylene-vinyl acetate copolymer manufactured by du Pont), Nevindene R-7 (a coumarone indene resin produced by Neville Chemical Co.), Parlon S-10 (a chlorinated rubber produced by Hercules Powder Co.), and Sunoco 4412 (a hydrocarbon wax manufactured by Sun Oil Company).

In run number 1-3 as listed in Table 1, the shell material consisted of 34.2 weight percent Elvax 250, 29.0 weight percent Nevindene R-7, 22.2 weight percent Parlon S-10 and 14.6 weight percent Sunoco 4412 wax. The solvent system for the shell materials was a 50:50 mixture of benzene and toluene, and the hardening bath was methanol containing 0.01 weight percent Tween 80, a nonionic surfactant manufactured by Atlas Powder Company. Using a shell solution having a total solids concentration of 35 weight percent and water as the filler, capsules were obtained having a diameter of 2000 microns. Analysis showed that the capsules had a payload of 60.1 weight percent. The payload was determined by crushing a weighed quantity of capsules, washing with methanol

and then drying the residual shells in a vacuum desiccator. The payload was readily determined after weighing the dried shell material.

A storage test was made on all of the capsules produced during this investigation. The test consisted of taking approximately 1.0 gram of capsules and permitting them to air-dry for 24 hours. The capsules were then weighed and placed in a room maintained at 77°F and a relative humidity of 50 percent. Figure 1 shows the plot obtained using the capsules prepared in run number 1-3. It can be noted that the capsules lost 12 weight percent water in the first twelve days. Since the stability test was started 24 hours after the capsules were prepared, this weight loss is probably high since there was some residual solvent in the shell.

In run number 1-7, the Elvax and Nevindene concentrations were increased, and the Parlon and wax were decreased. The total solids in the shell solution was 30 weight percent, and the filler was water. This system produced capsules having a size range of 840 to 1000 microns. Analysis of the capsules showed them to contain 74.9 weight percent water. The storage test, as shown in Figure 1, revealed that the capsules lost 90 weight percent of the water in 20 days.

In run number 1-10, 0.01 weight percent Triton X-100, a nonionic surfactant manufactured by Rohm and Haas, was added to the water. The shell formulation was the same as was used in run number 1-7. Figure 1 shows that these capsules also had a high weight loss during the storage tests. This high weight loss is probably due to the fact that the filler in some of the capsules was off-center. This causes the capsules to have a thin film on one side and produces a higher permeation rate.

Initially, there was some interest in encapsulating an electrolyte that would function over a wide temperature range. In view of this, several runs were made in which the filler was 40 volume percent glycerol and 60 volume percent water. The composition of the shell material is listed in run number 1-14 in Table 1. These capsules had an average size range of 590 to 840 microns, and the payload was 47.0 weight percent. The results of the storage test for these capsules are presented in Figure 2. In 47 days, the capsules had lost only 20 weight percent of the filler. The high initial weight loss is probably caused by the residual solvent in the shell.

When the solids content of the polymer solution was increased to 35 weight percent (run number 1-23), the resulting capsules had a payload of 43.9 weight percent. The size of these capsules were from 1000 to 1300 microns. Figure 2 shows that the capsules lost 15 weight percent of the filler when stored for 32 days at 77°F and 50 percent relative humidity.

In run number 1-25, the polymer solution was the same as was used in run number 1-23. The resulting capsules were slightly larger (1400 to 1600 microns); however, the storage test results were essentially the same as were obtained in run number 1-23. This shows that the formulation is reproducible.

Another system of interest for encapsulation was a 2 M aqueous solution of lithium chloride. In run number 1-26 as listed in Table 1, the shell consisted of Elvax 250, Nevindene R-7, Parlon S-10 and Sunoco 4412 wax. With a total solids content of 35 weight percent in the shell solution, the resulting capsules had a payload of 44.7 weight percent and a size range of 1000 to 1200 microns. The plot of the storage test (Figure 3) shows that the capsules lost 75 percent of the fill in 30 days.

In run number 1-29, the feed rates were adjusted and increased in order to obtain smaller capsules with a higher payload. The dried capsules had a 72.2 weight percent payload and a size range of 700 to 900 microns. The storage test showed that the capsules lost 22 weight percent of the filler during the 32 day test. The plot also shows that the weight lost per day would be much lower if the test had been conducted over a longer period of time because the greatest loss occurs during the first few days of the test.

C. Encapsulation of Aqueous Electrolytes Using Hot Melts

The second approach undertaken for the encapsulation of electrolytes was to melt the polymer blend and use the molten mixture in place of a solution. This technique has an advantage over the preceding technique in that no solvents are used.

In run number 1-33a as listed in Table 2, the polymer blend consisted of 15.0 weight percent Elvax 240 and 85 weight percent Sunoco wax 4412. The shell materials were held at 160°F while encapsulating water. The resulting capsules contained 56.5 weight percent water and had a size range of 1190 to 1410 microns. These capsules, when stored for 25 days at 77°F and 50 percent relative humidity, lost 14.0 weight percent of the water (Figure 4).

In an effort to increase the payload, the above run (run number 1-33a) was repeated. In this run (run number 1-33b), the feed rate of water was increased. This experiment produced capsules having a

payload of 62.9 weight percent and a size range of 1410 to 1680 microns. Results of the storage test as plotted in Figure 4 show that the weight loss was the same as was obtained with the capsules made in run number 1-33a.

Several experiments were made in an effort to encapsulate a 2 M aqueous solution of lithium chloride. In run number 1-33d, the shell consisted of 15 weight percent Elvax 240 and 85 weight percent Sunoco wax 4412. Tween 80 (0.01 weight percent), a nonionic surfactant manufactured by Atlas Powder Company, was added to the filler to aid in droplet formation. This system produced capsules having a 39.3 weight percent payload and a size range of 1680 to 2380 microns. These capsules lost 11.0 weight percent of the water over 25 days storage. The rate of weight loss per day is shown in Figure 5.

A series of runs was also made using Elvax 210 in place of Elvax 240. The Elvax 210 is a lower molecular weight polymer and has improved barrier properties. In run number 1-39, a 2 M aqueous lithium chloride solution was encapsulated using a polymer blend consisting of 21.0 weight percent Elvax 210 and 79.0 weight percent Sunoco wax 4412 as the shell material. The capsules contained 52.2 weight percent water and had a size range between 1200 and 1300 microns. Results of the storage test are shown in Figure 7. It can be noted that the test lasted only 17 days. During this time the capsules lost 8.0 weight percent of the filler.

In run number 1-41, the Elvax 210 concentration was decreased to 15.0 weight percent and the Sunoco wax 4412 concentration was increased to 85 weight percent. These capsules contained 40.4 weight percent 2 M aqueous lithium chloride. Over the 15 days storage test, the capsules lost 12 weight percent of the filler.

In run number 1-43, a blend of Elvax 210 and candelilla wax was used to encapsulate the aqueous lithium chloride. These capsules had a payload of 38.6 weight percent and a size range of 1300 to 1500 microns. Figure 6 indicates that 5.0 weight percent of the filler was lost during the 14 day storage test. The plot indicates that if the storage test had continued, a lower average weight loss/day would be obtained.

Since smaller capsules were desired, the inner tube of the encapsulation equipment was decreased to 0.014-inch OD, 0.007-inch ID, and the outer orifice was decreased from 0.625-inch to 0.018-inch. A description of this equipment appeared in a previous section. In run number 1-45, aqueous 2 M lithium chloride was encapsulated using

the above equipment. The shell material was again the Elvax 210-Sunoco wax 4412 blend. The capsules produced in this experiment were less than 595 microns in diameter and had a 68.4 weight percent payload. Figure 7 shows that the capsules lost 17.0 weight percent of the filler in the 10 day storage test. The plot also shows that the loss in weight had started to level off. This indicates that a much lower average weight loss/day would be obtained had the storage test extended over a longer period of time.

D. Encapsulation of Organic Electrolytes Using Hot Melts

In addition to the aqueous electrolyte systems, attempts were made to encapsulate several organic electrolytes. The organic electrolytes under consideration were propylene carbonate, butyrolactone, and dioxane. The initial screening tests showed these compounds to be water-miscible and miscible with most organic solvents normally used to dissolve various polymers. In fact, these compounds are excellent solvents for many polymers. However, it was learned that these electrolytes are immiscible with a molten mixture consisting of 15.0 weight percent Elvax 210 and 85 weight percent Sunoco wax 4412.

In run number 2-2, the aforementioned polymer blend was used to encapsulate propylene carbonate. The resulting capsules had a payload of 57.4 weight percent. The size range of the capsules was from 595 to 1000 microns. The capsules were sieved, and the fraction between 840 and 1000 microns was used in the storage tests. A plot of the results of the storage test is shown in Figure 8. The total weight loss over the 9-day storage test was 4.0 weight percent. The plot shows that, had the test continued, a much lower loss rate would have been obtained.

In run number 2-7, the same polymer blend was used to encapsulate butyrolactone. Figure 9 indicates that the butyrolactone was rapidly permeating the shell; however, the storage test was very short and as a consequence, no definite conclusions can be made.

In run number 2-9, the Elvax-wax blend was used to encapsulate dioxane. After 24 hours, it was noted that the capsule shells had collapsed. This is caused by the dioxane permeating through the shell faster than air can permeate into the capsule. The possibility exists that a different ratio of Elvax to wax, a different Elvax and wax, or a different polymer system is needed to satisfactorily contain the dioxane.

III. CONCLUSIONS

The results obtained during this program show that both aqueous and organic electrolytes can be successfully encapsulated. No attempt was made to optimize the shell formulation or the equipment since the major effort was directed toward encapsulating as many of the potential electrolytes as possible. Because of the short duration of the storage tests, many of the reported weight losses are exceptionally high. Examination of the plots indicates that, in many instances, the filler loss rate would be much lower if the tests had continued over an extended period of time.

It is believed that the high initial weight losses are caused by several factors. When polymer solutions are used to prepare the capsules. the residual solvents in the shell will produce high initial weight losses by two mechanisms. One is the continued evaporation of the residual solvents. The second is that the residual solvents in the shell will cause a high diffusion rate of the filler. As the solvents evaporate, the wax content of the shell will crystallize, retarding the diffusion rate.

When hot melts are used to encapsulate the electrolytes, the shell is rapidly cooled. This causes the wax content of the shell to solidify in an amorphous form. This random molecular structure will permit the filler to have a high diffusion rate. With time, the wax molecules will orient themselves and form crystals. In this oriented form the wax has a very low diffusion rate. Various techniques can be employed to increase the crystallization rate of the wax. One technique is to warm the capsules in order to increase the molecular orientation process. Slow cooling will cause the wax to assume the crystalline form.

TABLE I

ENCAPSULATION OF AQUEOUS SYSTEMS USING VARIOUS POLYMER SOLUTIONS

Solvent System : 50 50 Benzene-Toluene
Hardening Bath : Methanol containing Tween 80

Run No.	Shell Composition, Wt. Percent				Total Solids Wt %	Filler	Payload Wt %	Capsule Size, Microns
	Elvax 250[1]	Nevindene R-7[2]	Parlon S-10[3]	Sunoco 4412 Wax[4]				
1-3	34.2	29.0	22.2	14.6	35	HOH	60.1	2000
1-7	36.2	31.4	20.8	11.6	30	HOH	74.9	840-1000
1-10	36.2	31.4	20.8	11.6	30	HOH[5]	56.7	500-700
1-14	35.0	30.0	20.0	15.0	20	40% Glycerol 60% HOH	47.0	590-840
1-23	35.0	30.0	20.0	15.0	35	40% Glycerol 60% HOH	43.9	1000-1300
1-25	35.0	30.0	20.0	15.0	35	40% Glycerol 60% HOH	43.8	1400-1600
1-26	35.0	30.0	20.0	15.0	35	2 M LiCl in HOH	44.7	1000-1200
1-29	35.0	30.0	20.0	15.0	35	"	72.2	700-900

(1) Elvax 250. A copolymer of ethylene and vinyl acetate (du Pont)
(2) Nevindene R-7. A coumarone-indene resin (Neville Chemical Co)
(3) Parlon S-10. A chlorinated rubber (Hercules Powder Co.)
(4) Sunoco 4412 Wax A hydrocarbon wax (Sun Oil Co.)
(5) 0 01 wt % Triton X-100 (Rohm & Haas) was added to the water.

TABLE 2

ENCAPSULATION OF VARIOUS ELECTROLYTES USING HOT MELTS

Temperature of System : 160°F
Hardening Bath : Methanol containing .01 wt % Tween 80

Run No.	Shell Composition		Filler	Payload Wt %	Capsule Size, Microns
	Material	Wt %			
1-33a	Elvax 240 Sunoco wax 4412	15 85	HOH	56.5	1190-1410
1-33b	Elvax 240 Sunoco wax 4412	15 85	HOH	62.9	1410-1680
1-33c	Elvax 240 Sunoco wax 4412	15 85	HOH	59.6	>1680
1-33d	Elvax 240 Sunoco wax 4412	15 85	2 M aq. LiCl .01 wt % Tween 80	39.3	1680-2380
1-37	Elvax 240 Sunoco wax 4412 Triton X-15	15 84.99 0.01	HOH 0.01 wt % Triton X-15	--	No capsules were formed.
1-38	Elvax 210 Carnauba wax No. 3	15 85	HOH	--	No capsules were formed.
1-43	Elvax 210 Candelilla wax	15 85	2 M aq. LiCl	38.6	1300-1500
1-39	Elvax 210 Sunoco wax 4412	21 79	2 M aq. LiCl	52.2	1200-1300

TABLE 2 (Cont'd)

ENCAPSULATION OF VARIOUS ELECTROLYTES USING HOT MELTS

Temperature of System : 160°F
Hardening Bath : Methanol containing .01 wt % Tween 80

Run No.	Shell Composition		Filler	Payload Wt %	Capsule Size, Microns
	Material	Wt %			
1-41	Elvax 210 Sunoco wax 4412	15 85	2 M aq. LiCl	40.4	1200
1-45	Elvax 210 Sunoco wax 4412	15 85	2 M aq. LiCl	68.4	<595
2-2	Elvax 210 Sunoco wax 4412	15 85	Propylene Carbonate	57.4	595-1000
2-7	Elvax 210 Sunoco wax 4412	15 85	Butyrolactone	58.2	595-1410
2-9	Elvax 210 Sunoco wax 4412	15 85	Dioxane	--	Capsules collapsed after 24 hours.

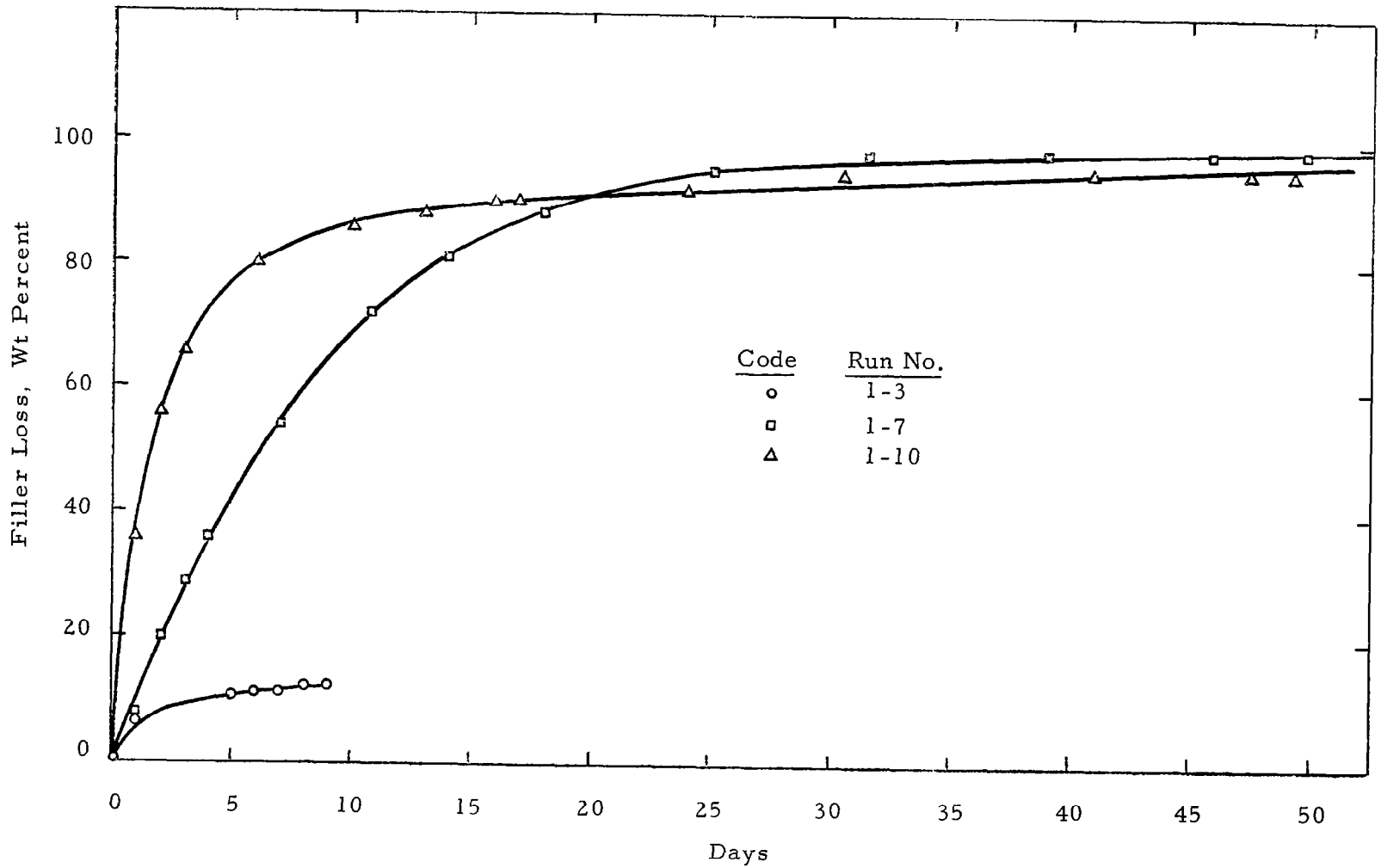

FIGURE 1
STORAGE TESTS ON ENCAPSULATED WATER

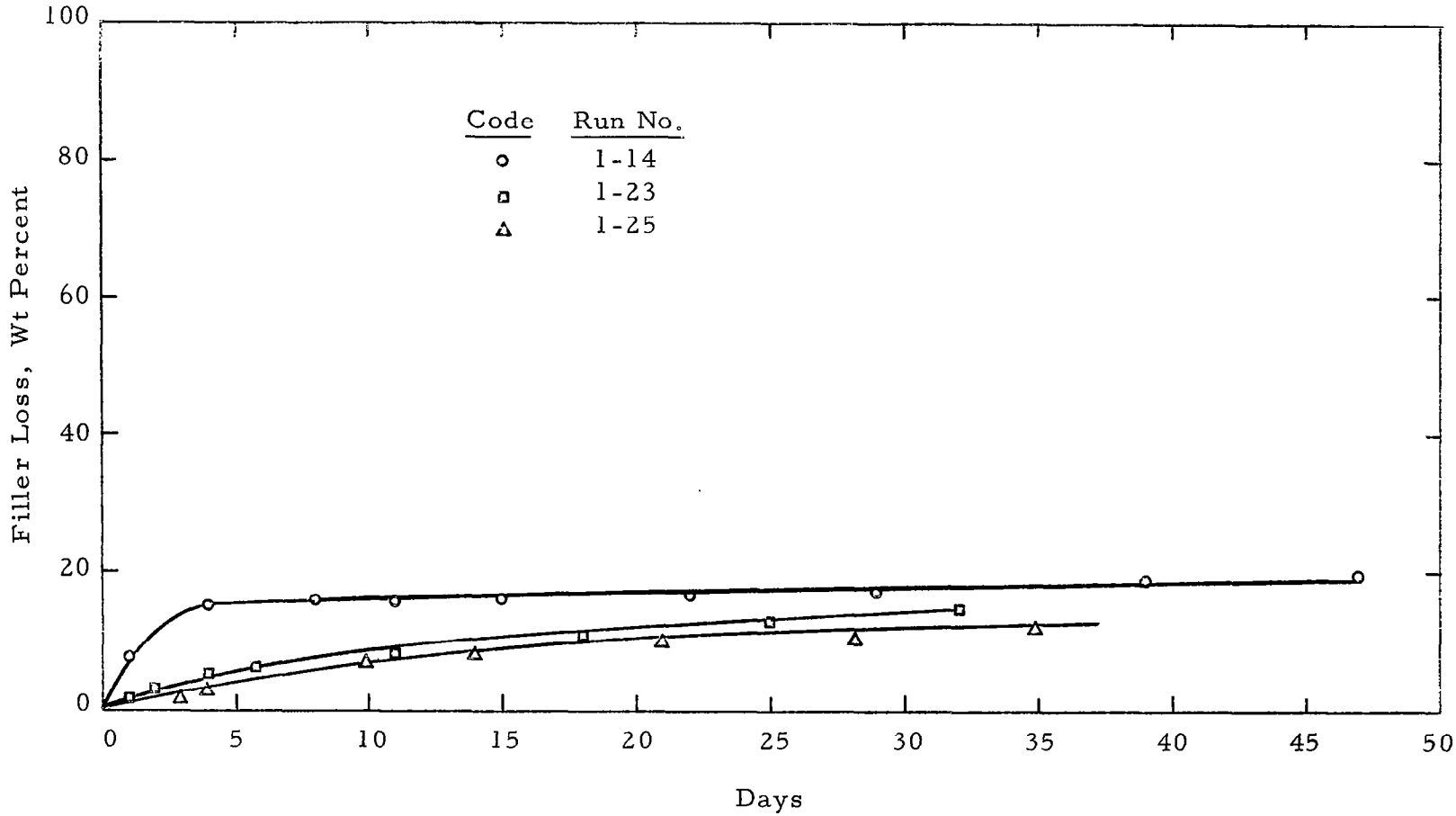

FIGURE 2
STORAGE TESTS ON ENCAPSULATED GLYCEROL-WATER MIXTURES

Filler: 40 Volume Percent Glycerol
60 Volume Percent Water

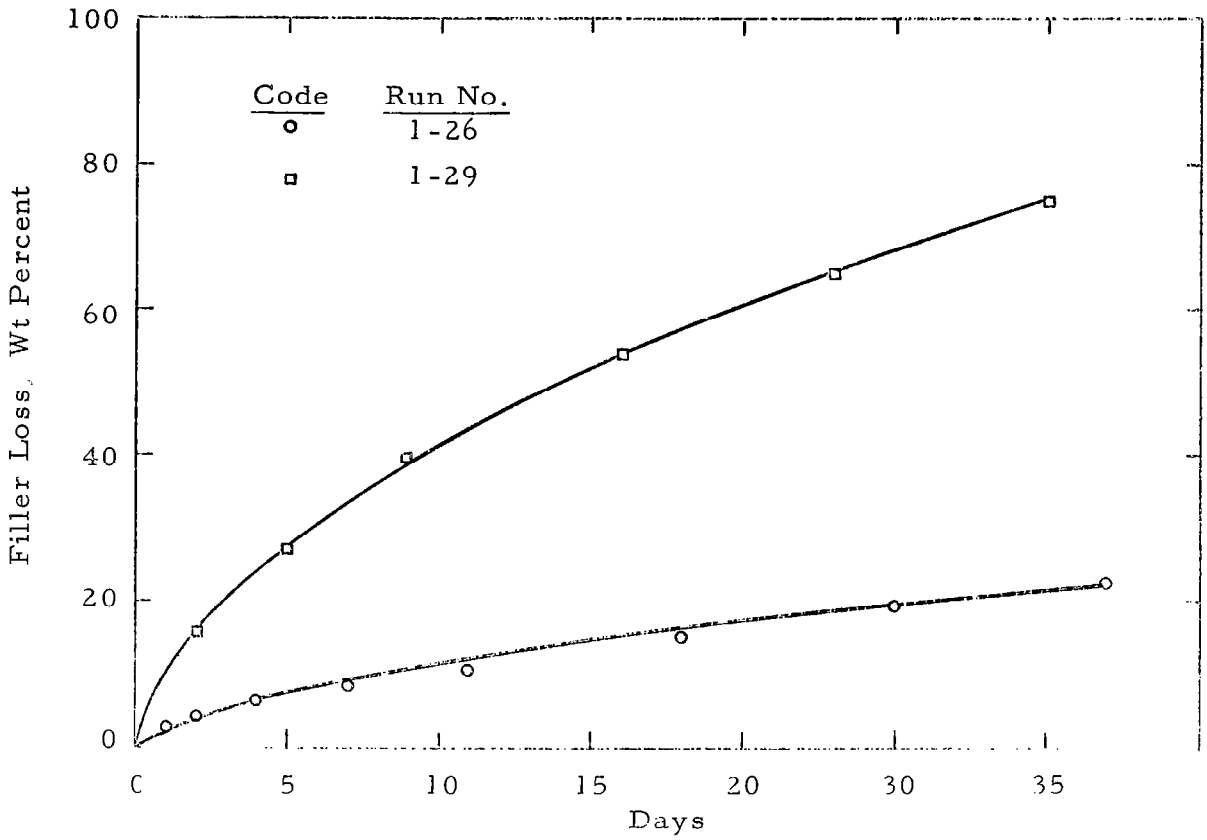

FIGURE 3
STORAGE TESTS ON ENCAPSULATED 2M AQUEOUS LiCl

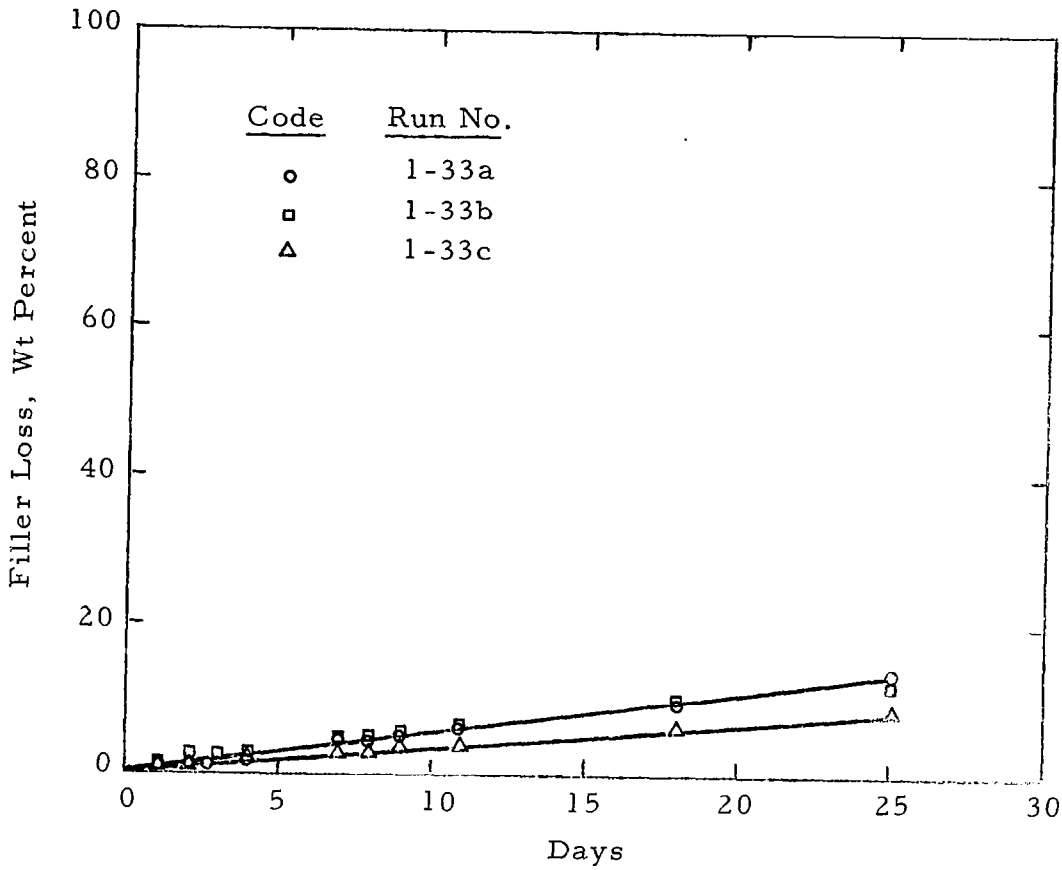

FIGURE 4
STORAGE TESTS ON ENCAPSULATED WATER USING HOT MELTS

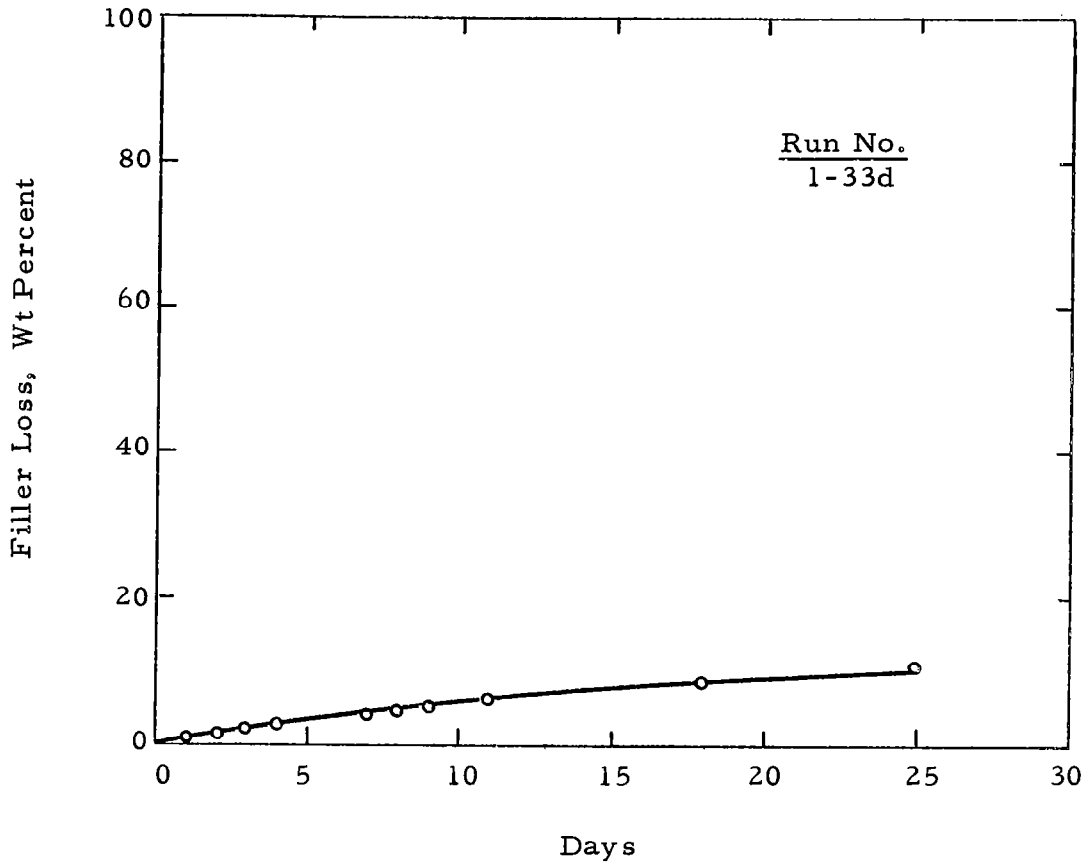

FIGURE 5
STORAGE TEST ON ENCAPSULATED AQUEOUS
2M LiCl-SURFACTANT MIXTURE
USING HOT MELT

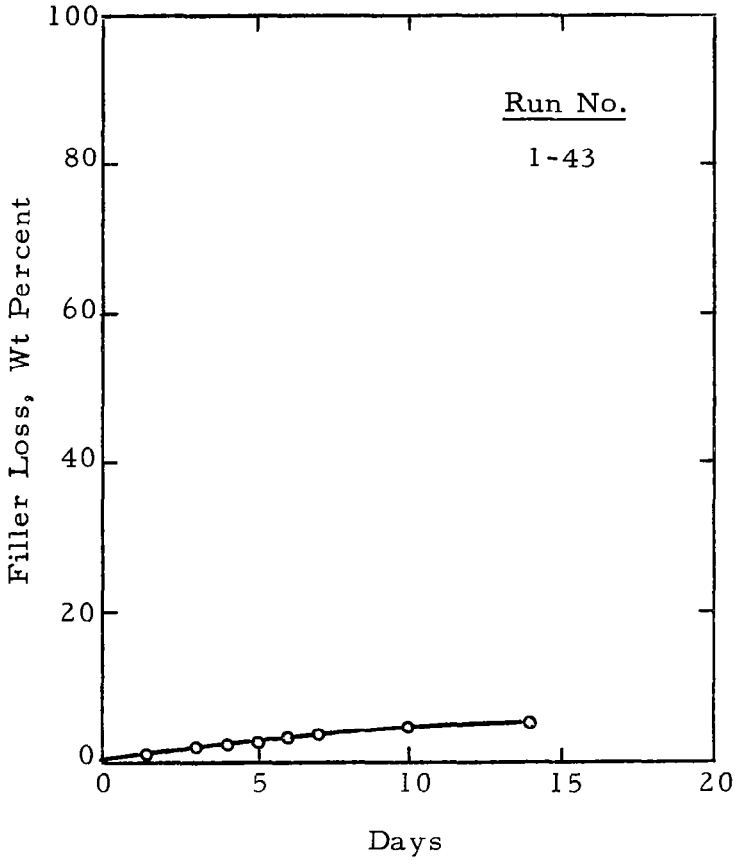

FIGURE 6
STORAGE TEST ON AN ENCAPSULATED AQUEOUS
2M LiCl SOLUTION USING HOT MELT

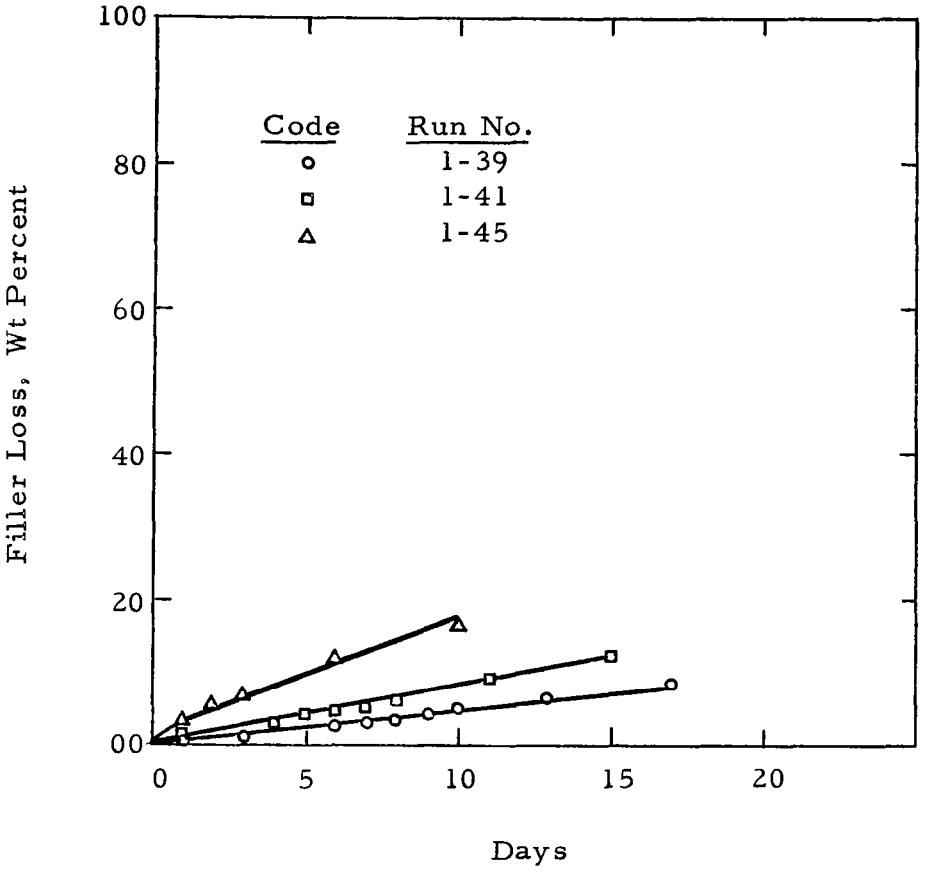

FIGURE 7
STORAGE TESTS ON ENCAPSULATED AQUEOUS
2M LiCl USING HOT MELTS

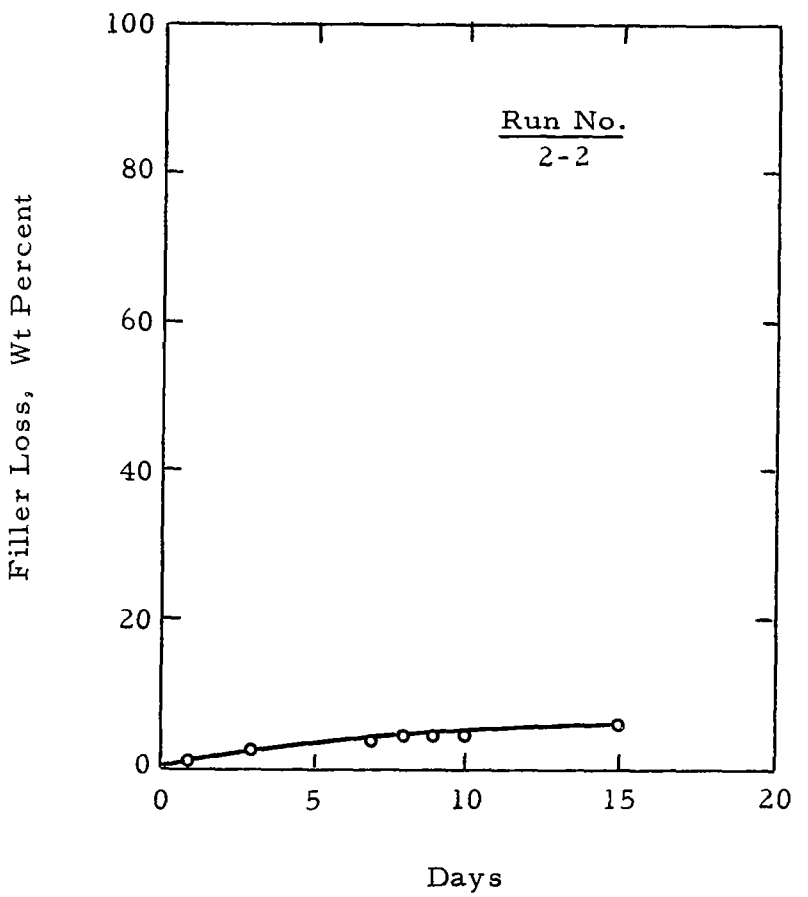

FIGURE 8
STORAGE TEST ON ENCAPSULATED PROPYLENE CARBONATE USING HOT MELT

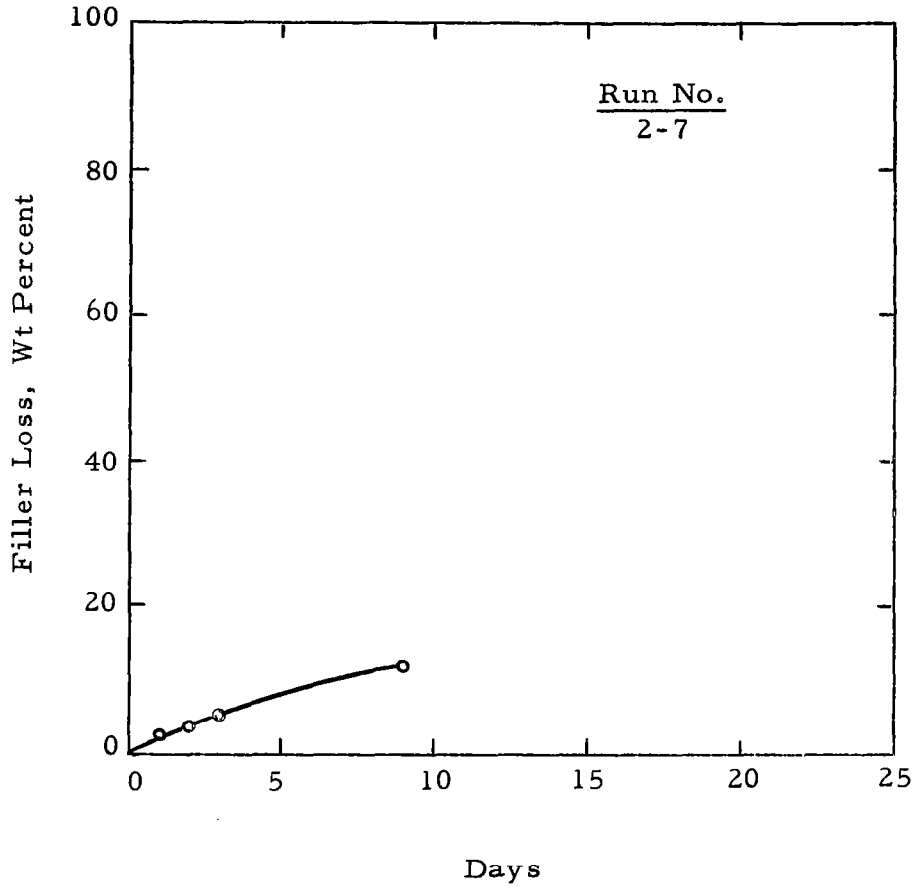

FIGURE 9
STORAGE TEST ON ENCAPSULATED BUTYROLACTONE USING HOT MELT